Metal-Catalyzed Carbenoid Cascade Reactions Involving a C–H Insertion/Annulation — Applications in the Synthesis of Carbo- and Heterocycles

by

© Aabid H. Bhat

A thesis submitted to the

School of Graduate Studies

in partial fulfillment of the requirements

for the degree of Doctor of Philosophy

Department of Chemistry

Memorial University of Newfoundland

May 2023

St. John's Newfoundland

To Al-Wadūd "The affectionate"

Abstract

Cascade reactions have gained significant importance in the pursuit of efficient and elegant synthetic chemistry. These processes offer environmental friendliness, atom economy and enable the synthesis of highly complex molecules. This thesis covers the general topic of tandem reactions based on metallocarbene insertion into C–H bonds and subsequent trapping of carbanion intermediate *via* annulation chemistry in a cascade manner to access various hetero- and carbocyclic frameworks. Three related projects illustrate this strategy; the last project is based on the pericyclic cascade strategy.

In Chapter 2 of this thesis, a Rh(II)-catalyzed acceptor/acceptor diazo carbene insertion/annulation strategy will be discussed. A series of *N*-alkylated indoles contain an alkyne electrophile were prepared for this study. These indoles were reacted with diazo reagents under Rh(II) catalysis to achieve tandem C(sp^2)–H carbene insertion and subsequent Conia-ene annulation for the synthesis of pyrroloindoles.

Chapter 3 of this thesis discusses a Cu(II)-catalyzed C(sp^2)–H insertion/Michael annulation cascade between α-diazocarbonyls and appropriately functionalized indoles containing alkynyl-ester electrophiles to access a variety of fused indole scaffolds in a stereoselective manner. Advancements of this reaction manifold to include alkenyl-esters as electrophiles were also explored allowing access to a range of new indole frameworks. By extending the reaction protocol to donor/acceptor diazocarbonyls, an additional synthetic value was achieved.

Chapter 4 of this thesis presents a preliminary study on the Rh(III)-catalyzed pyrimidine-directed C–H activation of indole, followed by coupling with Meldrum's acid-derived α-diazocarbonyls through a migratory carbene insertion pathway. The resulting intermediate, upon the elimination of acetone and carbon dioxide, undergoes a Dieckmann condensation with a

pendant ester moiety, leading to the formation of a carbazole core. The progress made in this study, as well as the planned future work, regarding the application of this novel reaction in the synthesis of various carbazole-based natural products, will be discussed in detail.

Finally, Chapter 5 of this thesis discusses a pericyclic cascade towards the synthesis of citridone A and tersone D natural products. The key transformation involves a domino Knoevenagel condensation between branched conjugated dienals and pyridone-type 1,3-dicarbonyl substrates followed by an oxa-6π electrocyclic ring-closure cascade to construct a cyclopenta[*b*]furopyridone framework. This project was completed in collaboration with the Rivera Group of Rosario Institute of Chemistry-IQUIR and for simplicity, only our total synthesis efforts will be discussed.

Acknowledgement

I would like to express my sincere gratitude to the following individuals for their unwavering support throughout this journey:

My deepest gratitude to Dr. Huck Grover, my supervisor, for his unwavering support and invaluable guidance throughout my Ph.D. program. Not only did he provide me with guidance on my research, but he also went above and beyond by guiding me through chemistry courses, helping me prepare for the Ph.D. comprehensive exam, and supporting me through the rough road to finishing this thesis. His unwavering commitment to my success was truly remarkable, and I am grateful for his invaluable guidance every step of the way. My success as a chemist so far, and the accomplishments I will achieve in the future, are owed to his significant contribution in my life.

The Grover group, both past and present, for their invaluable contributions to my research. I am grateful to Sima Alavi and Nathan Tucker, whose contribution was critical to the success of my work.

The members of my thesis committee, Dr. Chris Kozak and Dr. Sunil Pansare for their insightful comments, suggestions, and feedback. I also appreciate Prof. Yuming Zhao for providing insightful comments and suggestions on my research work. I would like to acknowledge the other faculty members and staff of the Department of Chemistry at Memorial University for their support.

Prof. Graham Bodwell and his group "Bodwell Group", both past and present members, for their invaluable contributions to my knowledge of chemistry. Their significant input during group meetings and general chemistry discussions have helped me gain a deeper understanding of my field and have inspired me to explore new areas of research.

Dr. Martin J. Riveira and his group from the Instituto de Química Rosario in Argentina, who offered the opportunity to work in collaboration on total synthesis project. I am grateful for the time he spent sharing his expertise and knowledge, which greatly contributed to my success of synthesizing two natural products. This collaboration has not only enriched my research experience but has also broadened my perspectives and allowed me to develop new skills.

The Blackmore family - Margie, Cherish, Linda, and Elizabeth - from Newfoundland, who welcomed me into their home with open arms and made me feel like a part of their family. Their warmth, kindness, and generosity have made my international graduate school experience all the more special, and I am honored to have had the opportunity to get to know them. I will always cherish the memories we have shared, and I am grateful for their hospitality and friendship.

I express my sincere appreciation to my family and friends for their unwavering love and support throughout my academic journey. I would like to extend a special acknowledgment to my late grandfather, Ghulam Ahmad Bhat, who regrettably passed away prior to the commencement of my higher educational pursuits. His remarkable work ethic, which I witnessed firsthand during my formative years, has remained a constant source of inspiration for me. I am confident that he would have taken great pride in witnessing my achievements.

Lastly, my greatest blessing in life, my daughter Lilya. Thank you for bringing immense joy and love into my life. Despite the challenges of balancing the demands of research work with those of fatherhood, you have been a true inspiration to me. Your presence has given me the strength, and your infectious laughter has brought a smile to my face even on the most difficult days. I am immensely proud to be your dad.

Table of Contents

List of Figures

List of Schemes

List of Tables

List of Abbreviations and Symbols

Å	Angstrom(s)
A	acceptor group
AA	acceptor-acceptor group
Ac	acetyl
APPI	atmospheric pressure photo ionization
°C	degree centigrade
^{13}C	carbon 13, isotope
ca.	*Circa*
calcd	calculated
cm	centimeter(s)
d	doublet
D	donor group
DA	donor-acceptor
DBU	1,8-diazabicyclo[5.4.0]undec-7-ene
DCE	1,2-dichloroethane
DIBAL-H	diisobutylaluminum hydride
DDQ	2,3-dichloro-5,6-dicyano-1,4-benzoquinone
DFT	density functional theory
DMF	*N*,*N*-dimethylformamide
DMSO	dimethyl sulfoxide
ee	enantiomeric excess
Et	ethyl
EWG	electron withdrawing group
EDG	electron donating group
equiv	equivalent(s)
g	gram(s)

h	hour(s)
Δ	heat
^{1}H NMR	proton nuclear magnetic resonance
HPLC	high performance liquid chromotography
HRMS	high-resolution mass spectroscopy
Hz	hertz
J	coupling constant (Hz) (in NMR)
kcal	kilocalorie
LDA	lithium diisopropylamine
LAH	lithium aluminum hydride
LiHMDS	lithium hexamethyldisilazide
MS	molecular sieves
m	multiplet
m-	meta
mg	milligram(s)
mL	milliliter(s)
mmHg	millimetres of mercury
min	minute(s)
mp	melting point
Me	methyl
MO	molecular orbital
mol	mole(s)
MHz	megahertz
m/z	mass to charge ratio
n-Bu	*n*-butyllithium
nm	nanometer(s)
NMR	nuclear magnetic resonance
Nu	nucleophile

NR	no reaction
p-	para
PCC	pyridinium chlorochromate
Pd/C	palladium/charcoal
Ph	phenyl
$PhCF_3$	trifluorotoluene
pKa	acid dissociation constant at logarithmic scale
ppm	parts per million
rt	room temperature
q	quartet
R_f	retention factor
rt	room temperatures
s	singlet
S_N1	unimolecular nucleophilic substitution
S_N2	biomolecular nucleophilic substitution
TLC	thin-layer chromatography
Ts	4-toluenesulfonyl or tosyl
THF	tetrahydrofuran
tfacac	trifluoroacetylacetonate
TFA	trifluoroacetic acid
UV/vis	ultraviolet visible
TEA	triethylamine
δ	chemical shift
$\Delta\delta$	difference in chemical shift
μW	microwave irradiation

Chapter 1: Introduction

1.1 A Cascade Synthesis

A cascade reaction, also called a tandem or domino reaction, is a chemical process wherein a minimum of two sequential chemical transformations occur in a single reaction apparatus.[1] Moreover, each transformation that takes place in the sequence can only occur as a result of structural functionality generated in the previous step and not through the addition of subsequent reagents or catalysts. This distinct difference separates cascade reactions from classic telescoped reactions,[2] which involve the continual addition of new material to the reaction apparatus after each transformation has occurred (Scheme 1.1)

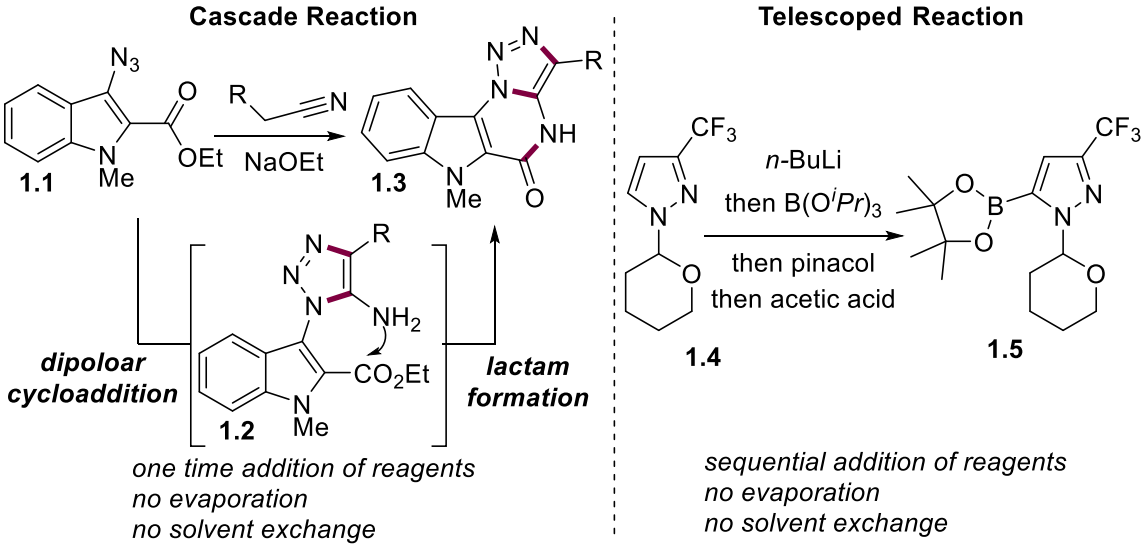

Scheme 1.1: A comparison between a cascade and a telescoped reaction.

The area of research in organic chemistry devoted to the development and application of cascade protocols has become a cornerstone topic in synthetic chemistry over the last several decades.[3] It represents a particularly attractive avenue for the rapid construction of molecular complexity. From a synthetic design perspective, there are several important benefits to utilizing

cascade reaction approaches in comparison to traditional (step-by-step) synthetic approaches. A simplified example of this concept is highlighted in Figure 1.1. One of the major appeals to utilizing cascade reactions is that they avoid the multiple reaction work-up and purification steps required in traditional synthetic approaches (**1.6** to **1.11**) (Figure 1.1). Not only does this save time by reducing the number of "hands-on" manipulations required in a particular synthesis but it also has the added advantage of utilizing reactive intermediates **1.8** in subsequent steps (**1.8** to **1.11**). This alleviates the requirement of regenerating these intermediates, which might otherwise be difficult or expensive to construct.

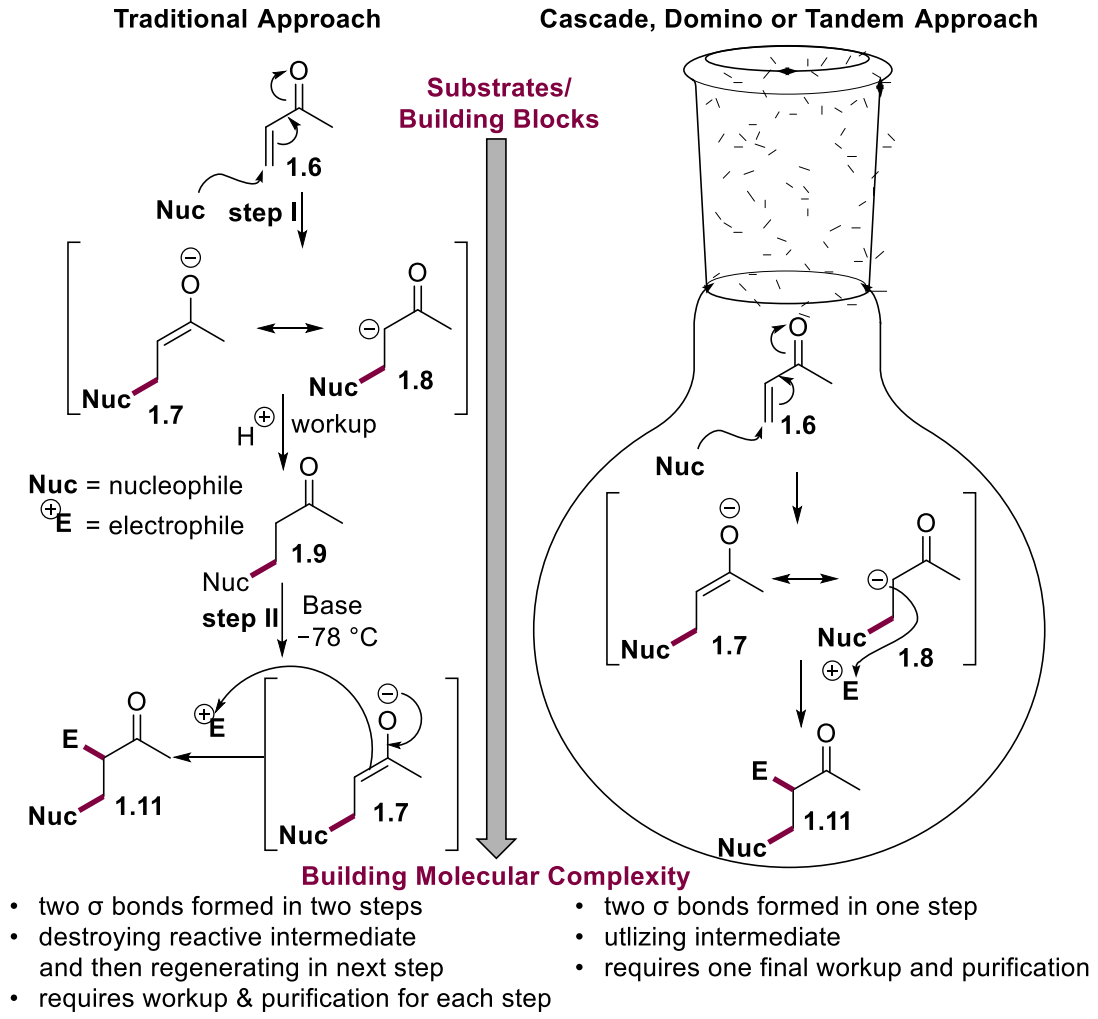

Figure 1-1: Cascade *vs.* multistep approach for building molecular complexity.

Ultimately, in addition to their aesthetic appeal, cascade reactions can be cost-saving in terms of limiting the number of reagents, catalysts, and solvents, as well as the time and effort required to complete a synthesis. Therefore, the utilization of cascade reactions can be considered a green approach to synthesis and the construction of organo-materials, pharmaceuticals, and fine chemicals.[4] In fact, employing cascade reactions in the design of target-specific molecules containing considerable structural and stereochemical complexity has elegantly and routinely been adopted by the total synthesis community as a fascinating method of solving some of today's most significant synthetic challenges.[5]

1.2 Classifications of Cascade Reactions

In 2006, Nicolaou and colleagues published an excellent review on cascade reactions in total synthesis.[6] This review presents a collection of various synthetic strategies where cascade reactions of different types have played a critical role in building molecular complexity. In their study, the authors point out how multistep cascade transformations can complicate the classification of cascade reactions. As many cascade reactions can involve several different classes of reaction in one sequence, a generally accepted means of categorizing cascades relies on identifying the "key" bond-forming step(s) of the overall sequence. For simplicity, a variation of the characterization developed by Nicolaou and colleagues is used herein, which classifies cascade reactions into four distinct categories: ionic (nucleophilic/electrophilic), radical-based, pericyclic, and transition metal-catalyzed cascades. For a more detailed study of each category, which is beyond the scope of this thesis, readers are referred to the Nicolaou review.[6] The discussion here will be limited to transition metal-based cascades and pericyclic cascades.

1.2.1 Transition Metal-Catalyzed Cascades

The discovery, advancement, and application of transition metal-catalyzed processes have had a tremendous impact in the area of organic synthesis.[7] The development of this area of research has provided the synthetic chemists with countless avenues of generating molecular complexity, and in fact, many catalytic processes—for example, the olefin metathesis reactions[8] and the palladium-catalyzed cross-coupling[9] reactions are in essence, cascade reactions. More specifically, cascade reactions involving a transition metal-promoted step followed by a subsequent annulation process have emerged as a powerful tool in the construction of cyclic and polycyclic structures.[10] A prominent example of this category of cascades in the literature is transformations involving the Heck reaction. For example, the Werz group described an efficient enantioselective synthesis of (+)-lysergol, which required 12 steps with a 13% overall yield.[11] The key step (**1.16** → **1.17**) relies on a domino reaction containing a formal *anti*-carbopalladation, which is terminated by a β-silyl-directed Heck reaction (Scheme 1.2). As a result of this transformation, two six-membered rings of the ergot alkaloid scaffold are formed in a completely stereospecific manner.

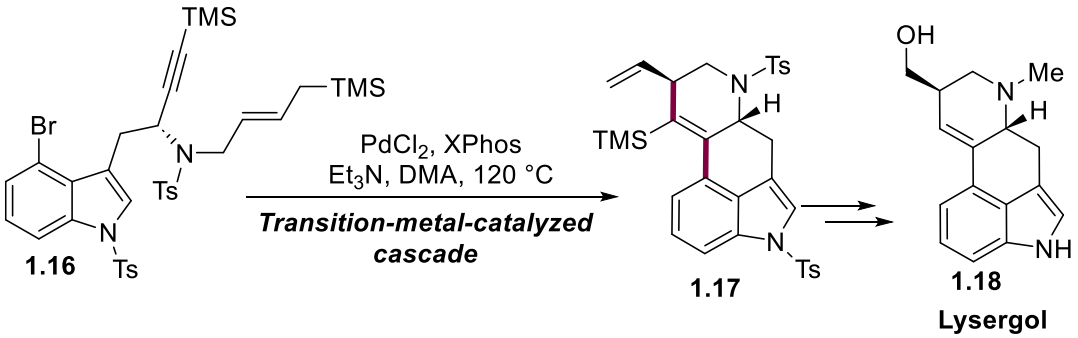

Scheme 1. 2: Synthesis of a key indole intermediate (**1.17**) in the synthesis of (+)-lysergol by Werz and coworkers.

1.2.2 Pericyclic Cascades

Pericyclic cascades, which include cycloadditions, electrocyclic reactions, and sigmatropic rearrangements, are particularly valuable because of their often-predictable stereochemical

control.[12] Moreover, tandem pericyclic reactions are becoming increasingly popular in the biomimetic synthesis of complex natural diterpenes. A representative example of a pericyclic cascade is the synthesis of the alkaloid benzosimuline reported by the Rivera group in 2016. The key transformation involves an oxa-6π electrocyclic ring-opening/hetero-Diels-Alder pericyclic cascade (Scheme 1.3).[13] As a result, natural product benzosimuline **1.24** was synthesized in 4 steps from commercially available citral **1.20** and 4-hydroxy-1-methyl-2(1*H*)-quinolone (**1.19**) with a 34% overall yield.

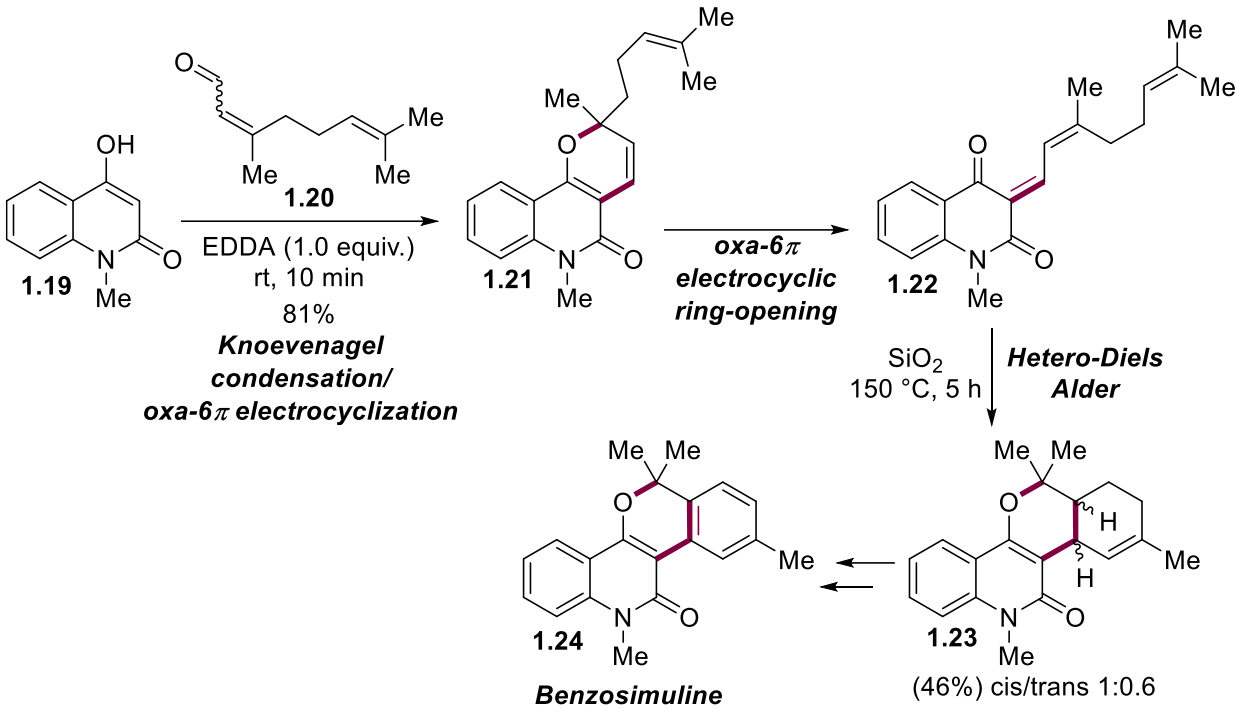

Scheme 1.3: Synthesis of alkaloid benzosimuline (**1.24**) by the Rivera group.

A myriad of other types of cascades have been developed, a related class of catalytic cascades has gathered significant interest over the last two decades involving the use of carbene intermediates.[14] Generally, this class of cascade is characterized by the formation of a metal carbenoid (**1.26**), from a carbene precursor (**1.25**) with a catalytic metal, which can then undergo

a variety of cascade processes (Figure 1.2). Catalytic cascade reaction involving metal carbenes, commonly referred to as carbene or carbenoid cascades are the focus of this thesis.

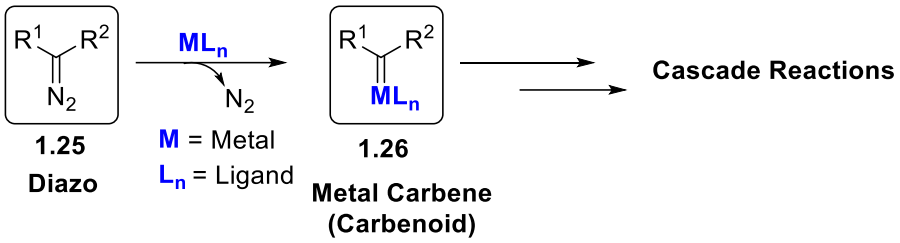

Figure 1.2: Metal carbene-based cascades.

1.3 Carbenes

Carbenes are highly reactive carbon intermediates containing six valence electrons. Carbenes can either be in the singlet or triplet form depending on whether their unshared electrons are in the same or different orbitals. When both unshared electrons are in one orbital (σ orbital) and the p orbital is empty, a carbene is referred to as a singlet carbene, while if they are shared between the p and σ orbitals, a carbene is referred to as a triplet carbene (Figure 1.3). A singlet carbene is ambiphilic as it resembles a carbocation and carbanion on the same carbon, so it has both nucleophilic and electrophilic characteristics.[15]

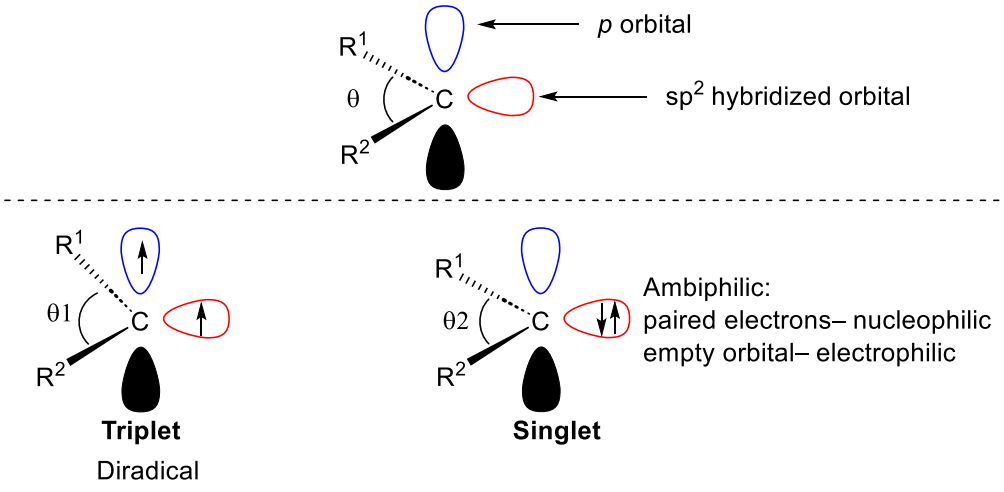

Figure 1. 3: Structure of carbene.

1.4 Diazocarbonyl Compounds as Carbene Precursors

Since Curtius prepared ethyl diazoacetate in 1883,[16] α-diazocarbonyl compounds have been extensively studied and are considered a principal class of carbene precursors.[17] Before transition metal-mediated methods became available, carbenes were produced through the photochemical or thermal decomposition of diazo compounds (Scheme 1.4). However, controlling the reactions of these carbenes **1.27** was challenging due to their high reactivity, resulting in low selectivity. In contrast, carbenes generated by transition metals, known as metal carbenoids **1.29**, are usually more stable and exhibit predictable reactivity.

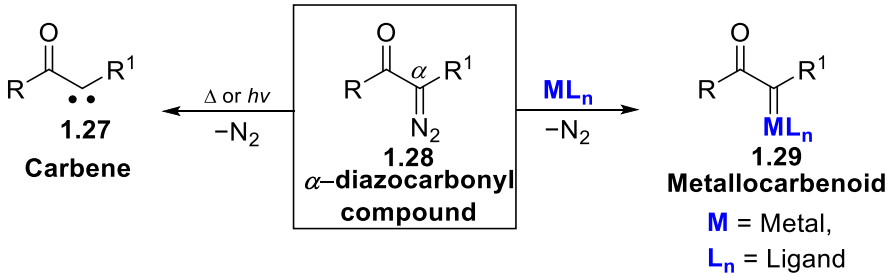

Scheme 1.4: Decomposition methods of α-diazocarbonyl compounds.

The reactivity of a metal carbenoid can be influenced by changing the electronics of the substituents connected to the carbenoid carbon.[18] The resulting metal-carbenoids with different combinations of the acceptor (electron withdrawing group) and donor (electron donating group) substituents on diazo-bearing carbon can be classified into three primary categories (Figure 1.4), the acceptor/acceptor carbenoids **1.30**, the acceptor carbenoids **1.31** and the donor/acceptor carbenoids **1.32**. Generally, an acceptor substituent makes the carbenoid species more electrophilic and more reactive, whereas a donor group makes the carbenoid more stable and thus more selective in a reaction it participates in.[19]

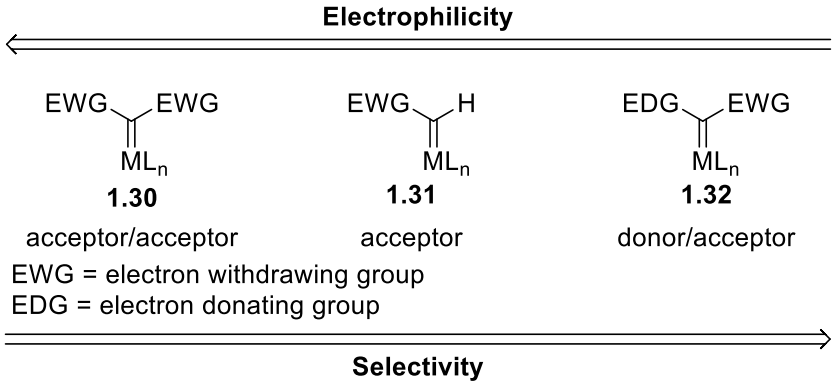

Figure 1.4: Classification of metal carbenoid intermediates.

1.5 Reactions of *α*-Diazocarbonyl Compounds

Diverse types of diazocarbonyl carbene transfer reactions can be accomplished depending on the type of catalyst, and reagents employed.[20] Upon activation of **1.28**, the carbene generated (**1.33**) can undergo transformations including Wolff rearrangement to generate ketene **1.34** which can be trapped with nucleophiles to furnish **1.35** or undergo [2+2] cycloadditions with alkenes to generate cyclobutenes **1.36** (Scheme 1.5). Alternatively, metal carbenoid **1.29** can undergo benchmark carbene transfer reactions, such as C–H and X–H (X = O, N, S, etc.) insertions to furnish carbene insertion products **1.37**. Metal carbenoids can also undergo reactions with alkenes to generate cyclopropanes **1.38**, or with alkynes to form cyclopropenes **1.39**. From these applications of *α*-diazocarbonyl compounds, this thesis will focus on C–H and X–H insertion reactions.

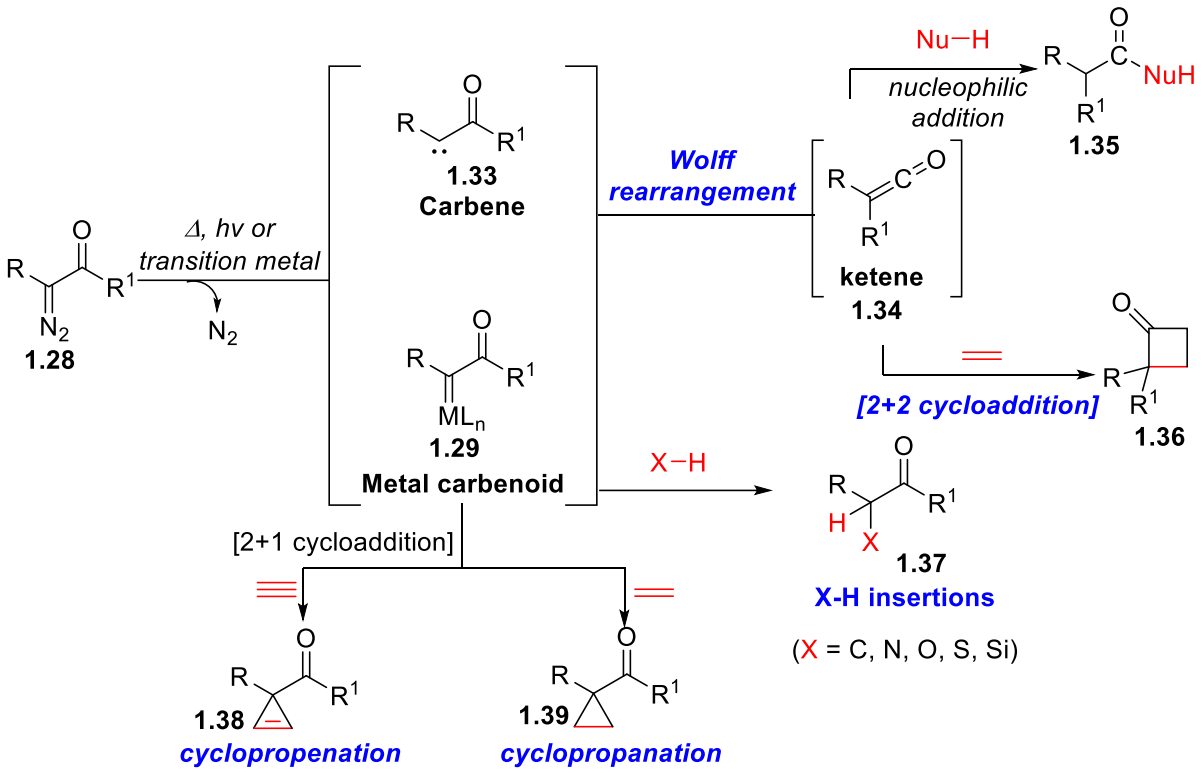

Scheme 1.5: Common reactions of carbenoids derived from α-diazocarbonyl compounds.

1.6 Carbene Cascades Involving a Heteroatom–H Bond Insertion

The carbon–heteroatom bond is a ubiquitous motif in both natural and synthetic molecules. Methods for constructing these types of bonds have played a significant role in the field of chemical synthesis. Metal carbenoids, usually derived from diazo compounds, have been proven as valuable intermediates in the construction of these bonds.[21] For example, in a X–H (X = N, O, S, etc.) insertion reaction, a metal–carbenoid **1.26** reacts with an X–H reactant to deliver, either in a concerted (**path a**) or stepwise fashion (**path b**), a product that contains one new carbon–heteroatom bond **1.42** (Scheme 1.6). While two main mechanistic pathways to this product exist, in most cases, the evidence suggests a stepwise ylide formation mechanism **1.43** (**path b**).[22] Mechanistically, this pathway proceeds by nucleophilic addition of a heteroatom **1.40** to the electrophilic metal-carbenoid species **1.26** to generate a transition metal-associated or free ylide

intermediate **1.43**. The ylide species can undergo a 1,2-proton shift to yield the net insertion product **1.42**.

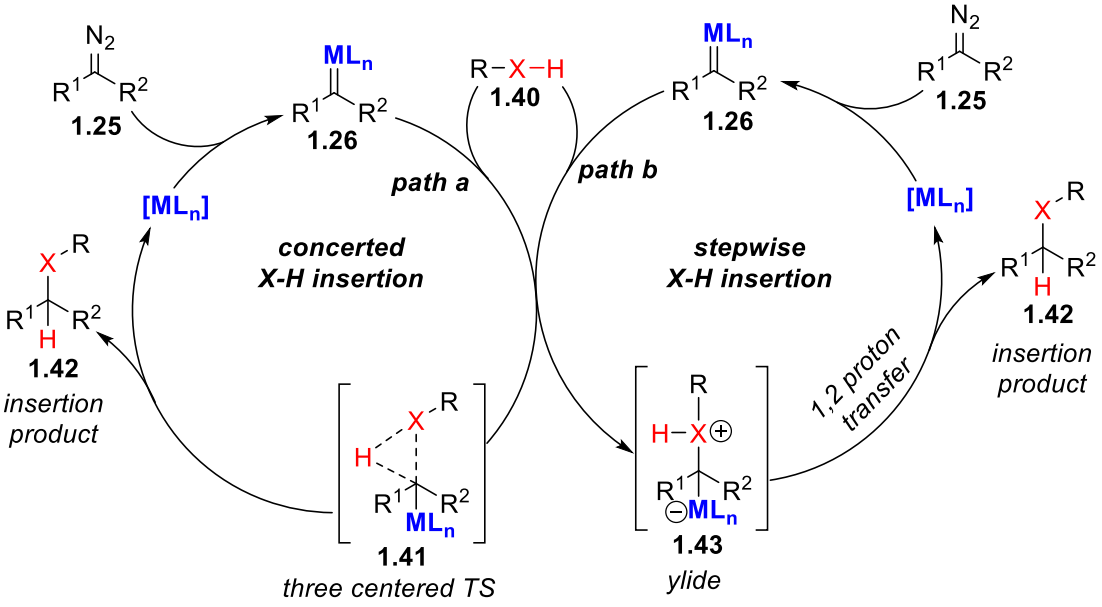

Scheme 1.6: Stepwise and concerted mechanism of X–H insertion.

In general, X–H insertion reactions are well established, with many advancements devoted to catalyst design, asymmetric control, and heteroatom scope. One interesting advancement of this chemistry, which supports the stepwise mechanism proposed in Scheme 1.6, is the trapping of the ylide **1.45** with various electrophiles (Scheme 1.7). Overall, the process forms two new non-hydrogen sigma bonds to the carbene carbon in a cascade fashion. These types of reactions are also well established and can be performed intermolecularly when the nucleophilic reagent contains no electrophilic sites, e.g., the formation of **1.46**, or intramolecularly when the nucleophilic component contains a compatible electrophile. The latter process provides expedient access to various substituted heterocycles **1.47**.

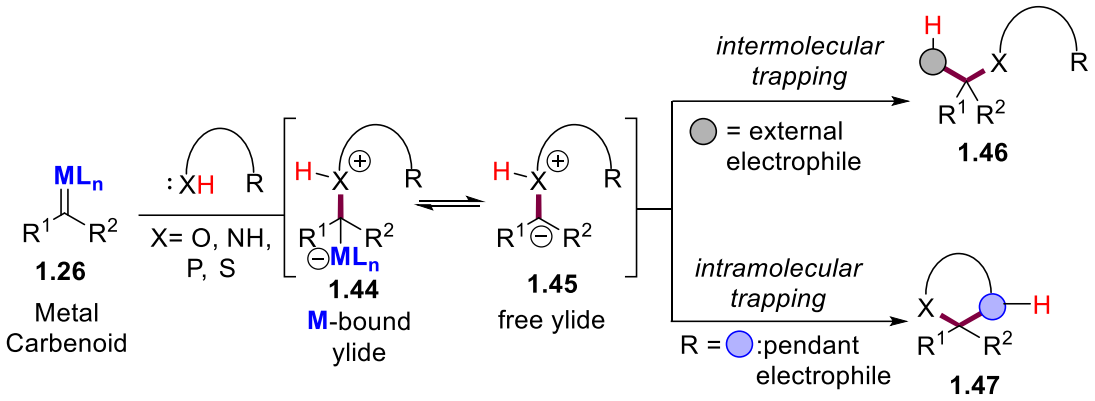

Scheme 1.7: Inter– and intramolecular trapping of ylide with electrophiles.

Intramolecular cascade processes have shown great versatility in organic synthesis, in particular through the use of formal insertion/annulation chemistry to access cyclic compounds. This general reaction manifold has been applied to the synthesis of various fused heterocycles. For example, *α,β*–unsaturated carbonyls **1.48** have been used as the pendant electrophile in these reactions providing **1.53** *via* a conjugate addition annulation (Scheme 1.8).[23] Additionally, both carbonyls **1.49** and imines **1.51** have been studied as the electrophile through intramolecular aldol[24] and Mannich[25] type reactions providing **1.54** and **1.56,** respectively. Recently, alkyl halides **1.50** have proved effective as electrophiles furnishing **1.55** *via* an S_Ni reaction.[26] Finally, alkynes have also been explored as carbon-based electrophiles to provide **1.57** *via* a Conia-ene annulation.[27]

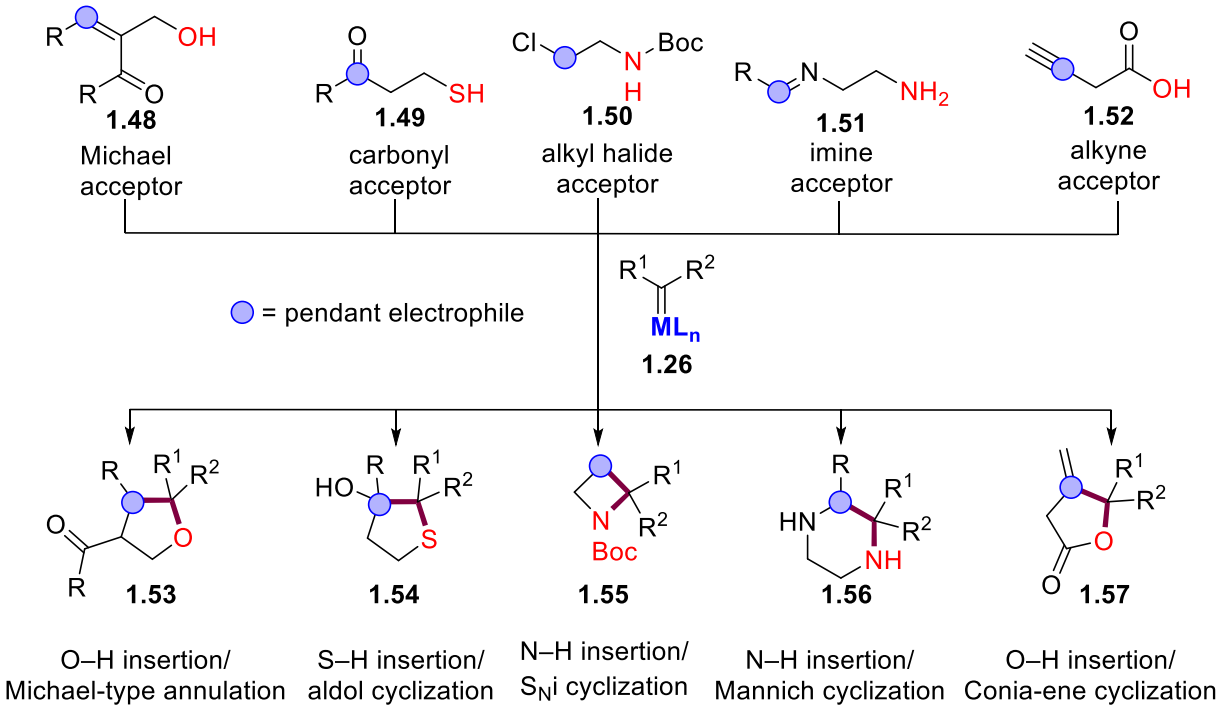

Scheme 1.8: Selected examples of heteroatoms and electrophiles in a carbene insertion/annulation reaction.

1.7 Carbene Cascades Involving a Formal C–H Bond Insertion

The synthesis of complex natural products and pharmaceutical targets has been revolutionized by C–H functionalization.[28] Among the many methods that exist to functionalize a C–H bond, one promising approach that has received much attention over the last several decades is through a formal carbene C–H insertion process.[29] Similar to formal carbene X–H insertion reactions, these types of reactions are known to proceed *via* (*i*) an electrophilic addition of a metal carbene with a nucleophile coupling partner (**1.58** → **1.66**) or (*ii*) a migratory insertion *via* a metal-catalyzed C–H activation step (**1.60** → **1.66**), or (*iii*) a concerted C–H bond insertion (**1.62** → **1.66**) (Scheme 1.9).

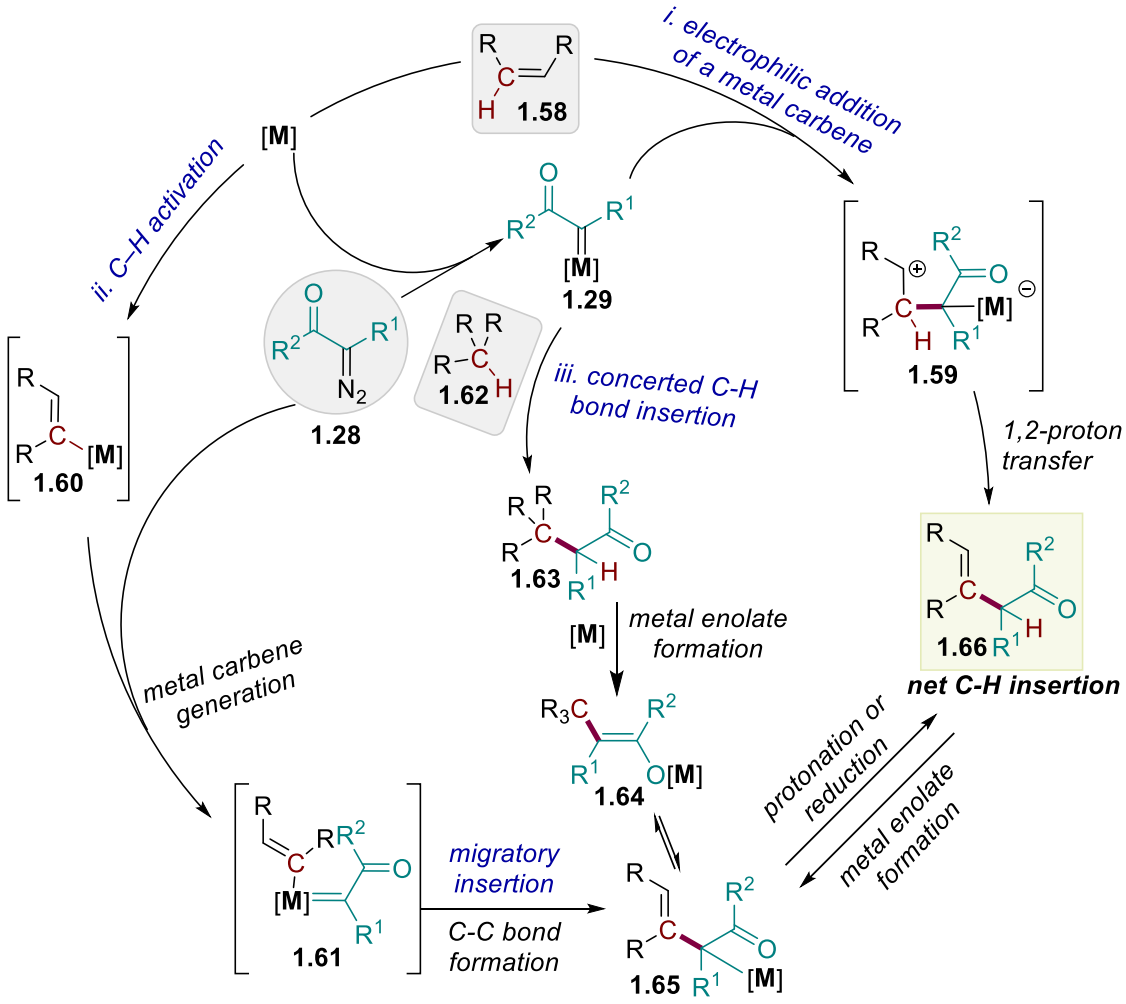

Scheme 1.9: Mechanistic pathways for formal carbene C–H insertion.

In contrast to carbene X–H insertion the advancements in carbene C–H insertion chemistry to include C–H insertion/annulation cascades in which two new carbon–carbon sigma bonds are formed to the carbene carbon in the product (i.e., the synthesis of a carbocycle) are limited, even though similar ylides **1.59** or enolates (**1.64** and **1.65**) can be generated upon the insertion event. One primary reason for this may be the site selectivity issues associated with the C–H insertion process. A typical organic substrate will have many different C–H bonds; thus, the challenge becomes developing a method to control which specific C–H bond the carbene will insert into. Moreover, another hurdle in developing a cascade sequence is having a compatible electrophile

for the annulation event. Despite these challenges in carbene C–H insertion, a few successful approaches to achieve these types of cascades have been reported including Type I – Migratory insertion by a metal-catalyzed C–H activation, Type II – Nucleophilic arene couplings, and Type III – Intramolecular C–H functionalization cascades.

1.7.1 Type I – Migratory Insertion by a Metal-Catalyzed C–H Activation

One way to overcome the problem of site selectivity is through the assistance of directing groups (DGs) on a substrate.[30] In this strategy, a coordinating moiety (an "internal ligand") on the substrate **1.67** (Scheme 1.10) directs a metal catalyst into the proximity of a particular C–H bond in the molecule, leading to its selective activation and generation of organometallic intermediate **1.68**. Upon reaction with diazocarbonyl **1.25** results in the generation of metal carbene **1.69,** and subsequent migratory insertion forms the first C–C bond **1.70**. In the case where the directing group serves a dual purpose and can also react as an electrophile in a subsequent step, the formal insertion product **1.70** (or the metal bond intermediate) can be trapped in a cascade process to form cyclic product **1.71**.

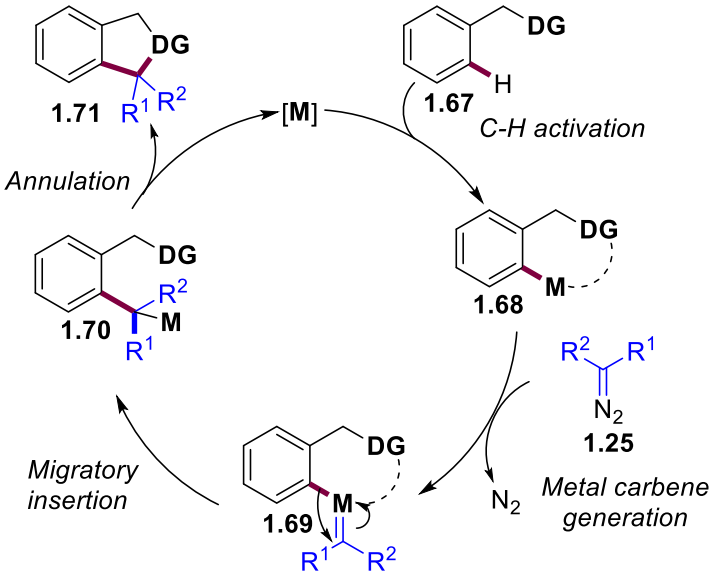

Scheme 1.10: Mechanism of C–H functionalization *via* carbene migratory insertion.

Li and coworkers[31] were among the first to explore this type of reaction manifold by developing a C−H activation of phenacyl ammonium salts **1.72** with α-diazomalonates, in which the alkyl ammonium moiety served as a directing group (Scheme 1.11). The transformation involves Rh(III)-catalyzed *ortho* C−H activation event, assisted by the polar C−N bond, followed by a reaction with diazo substrate **1.25** to generate a metal carbene which undergoes migratory insertion to form the C–C bond in intermediate **1.73**. The subsequent annulation *via* S_N2 on the C–N bond which also acts as an electrophile allows the synthesis of carbocycle **1.74**. This method highlights a broad substrate scope, and the reactions proceed with high efficiency and good functional group tolerance.

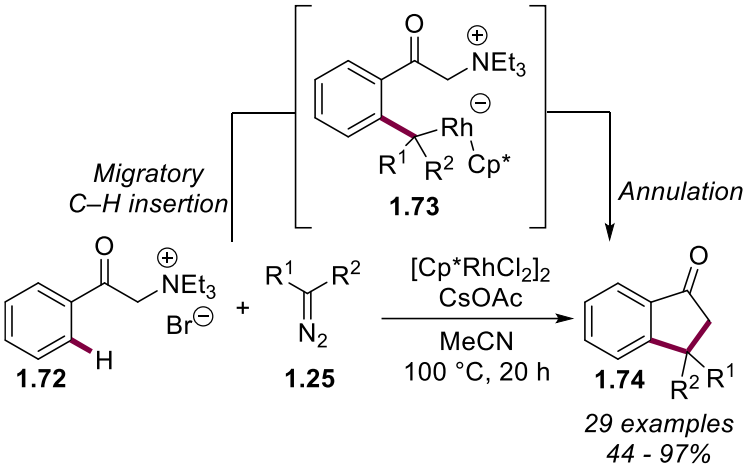

Scheme 1.11: Synthesis of benzocyclopentanones (**1.74**) by Li and coworkers.

Using similar Rh(III) catalysis, the Chang group reported the *ortho*-C–H functionalization of nitrones **1.75** with diazo compounds for the synthesis of *N*-hydroxyindolines (Scheme 1.12).[32] The transformation proceeds through a directed C–H activation using nitrone as a directing group. Upon C–H activation, reaction with diazo **1.25** generates a metal carbene, which undergoes migratory insertion to form the first C–C bond in intermediate **1.76** and subsequent Mannich-type cyclization with the polarized C=N bond of the nitrone, which also acts as an electrophile, provides indoline **1.77** *via* the formation of the second C–C bond.

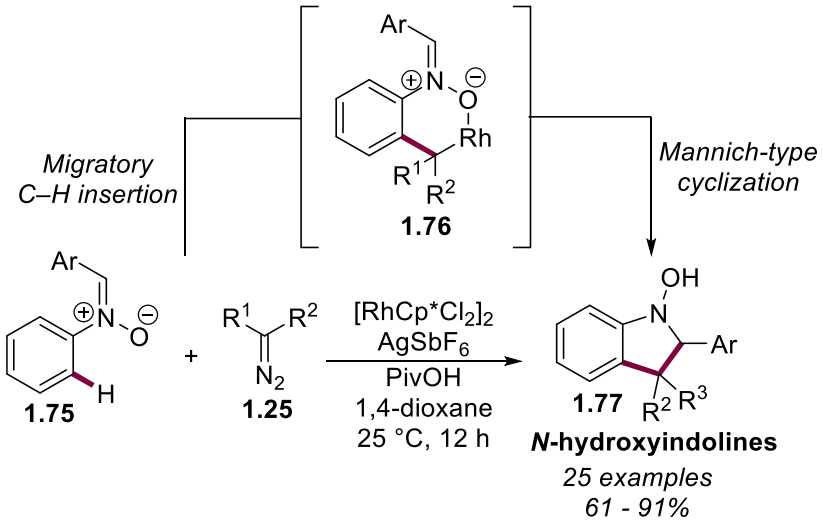

Scheme 1.12: Synthesis of *N*-hydroxyindolines (**1.84**) by Chang and coworkers.

The groups of Chen and Zhou have reported Rh(III)-catalyzed directed C-2–H functionalization of indoles with diazo compounds. The transformation proceeds through a pyrimidine-directed C–H activation, metal carbene generation, migratory insertion, and finally, intramolecular aldol cyclization for the synthesis of 2,3-fused indoles (Scheme 1.13).[33] Unlike previous methodologies in this area of research, this work utilizes a remote electrophile to trap the intermediate **1.79** instead of the directing group. This method also highlights the compatibility with both acceptor/acceptor and donor/acceptor diazo compounds providing various 2,3-fused indoles. Notably, a selective C–H dialkylation reaction at C-2 and C-7 positions of indoles has also been developed by simply changing the reaction conditions. While CsOAc as an additive afforded **1.80** as the sole product in 92% yield, $Cu(OAc)_2$ as the additive furnished bis-functionalized indole **1.81** in 82% yield.

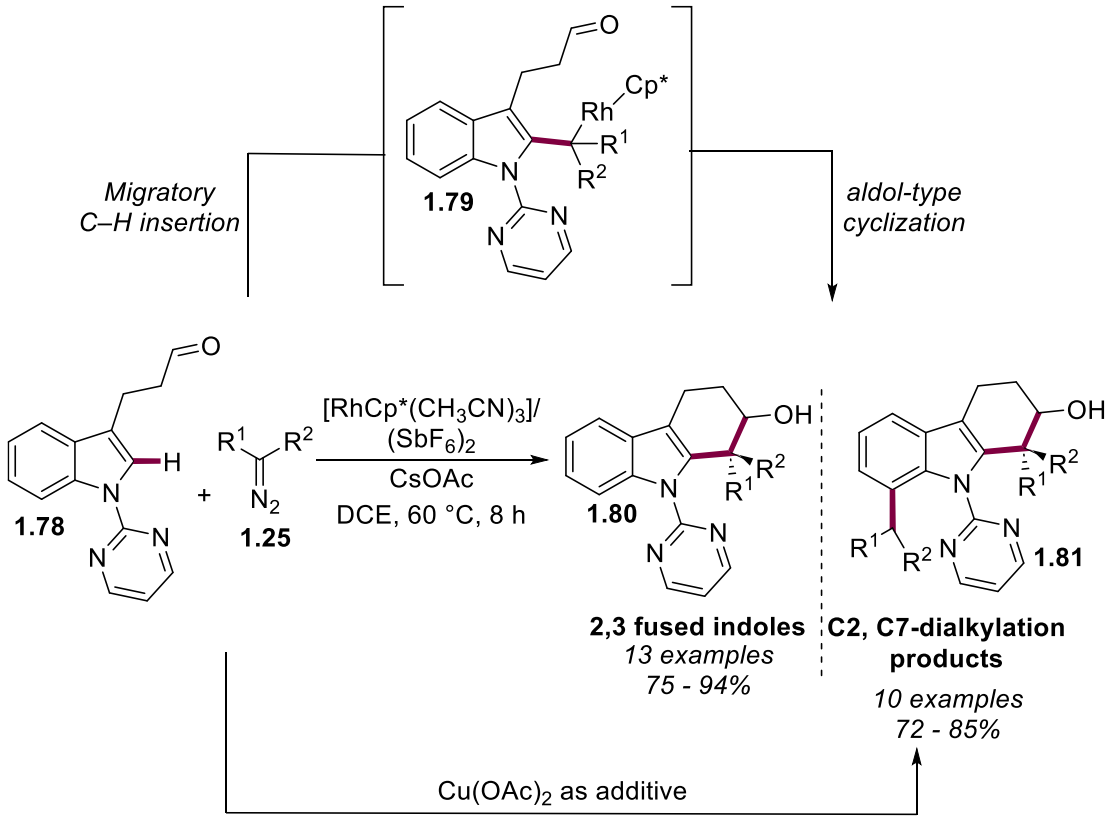

Scheme 1.13: Synthesis of 2,3-fused indoles (**1.87**) by Chen, Zhou, and coworkers.

Outside of these three diverse examples there have been several other advances in this type of directed C–H activation/migration-carbene-insertion then annulation protocol in recent years. Researchers including Zhou[34], Fan[35], Huang[36], Xiao[37] and a few others[38] have significantly contributed to this area of research. Most advances in this area have focused on exploring various substrates that contain different directing group compatibility of controlling the site selectivity of C–H insertion event and then participating as the electrophile.

1.7.2 Type II – Nucleophilic Arene Couplings

Alternatively, complementary methods of controlling the regioselectivity of the carbene C–H insertion based on a substrate-controlled approach have been less explored in this area of research. Nucleophilic arene coupling partners provide inherent regioselectivity and obviate the need for the use of external directing groups. Metal-bound carbenoids **1.26** react readily with electron-rich aromatics and heteroaromatics **1.82** to provide formal C–H insertion products *via* intermediate **1.83** (Scheme 1.14). When the reactive intermediate is trapped intramolecularly by an appropriate pendant electrophile, annulation product **1.84** can be constructed.

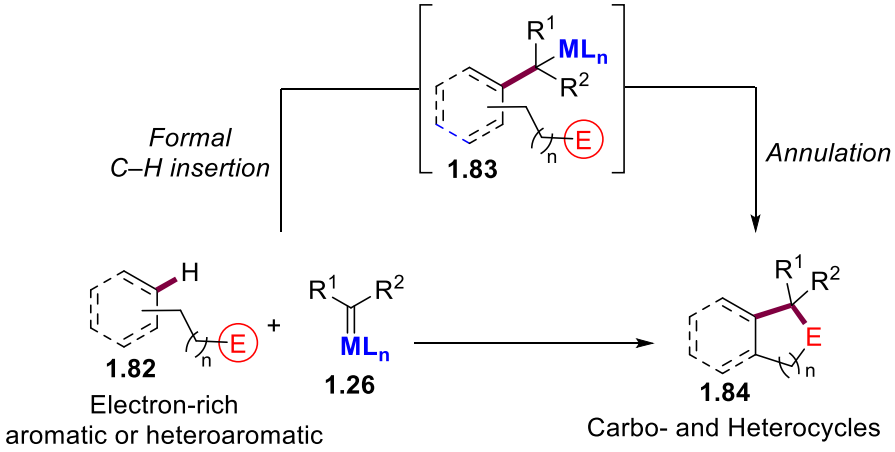

Scheme 1.14: Nucleophilic arene coupling followed by annulation with α-diazocarbonyls.

Zhang, Liu, and co-workers established a gold(I)-catalyzed C–H functionalization/carbocyclization reaction of *o*-alkynylaryl α-diazoesters **1.85** with electron-rich aromatics **1.86** (Scheme 1.15).[39] The transformation proceeds by gold-catalyzed formation of the zwitterionic intermediate **1.87** *via* arene coupling, followed by an intramolecular *5-endo-dig* cyclization with pendant alkyne moiety to obtain carbocyclic indene derivatives **1.88**. The authors also carried out an experiment for asymmetric version of this reaction and when the chiral binuclear gold catalyst was used, the indene derivatives **1.88** was obtained in moderate yield (52%) with low enantioselectivity (25% ee).

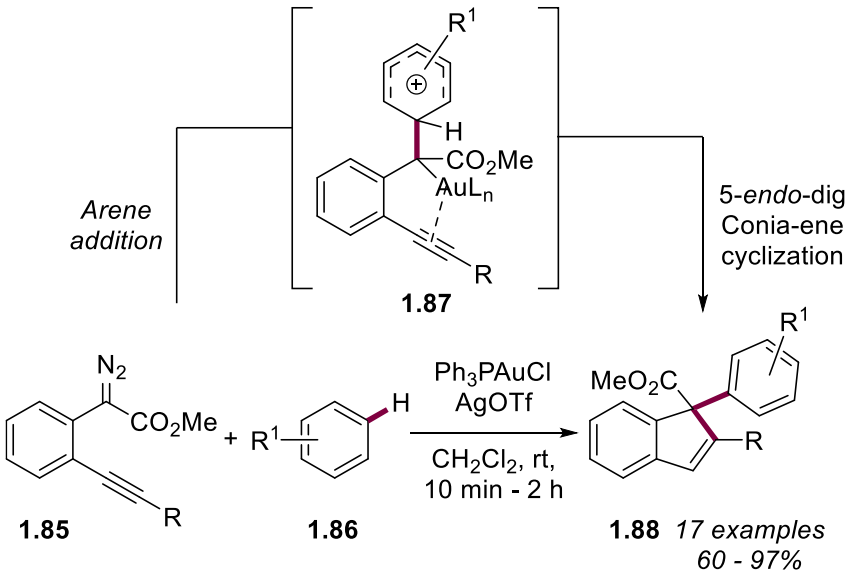

Scheme 1.15: Synthesis of indene derivatives (**1.88**) by Zhang, Liu, and coworkers.

Hu and co-workers have reported a simple, mild, and efficient rhodium-catalyzed reaction of α-phenoxyketones **1.89** and 3-diazooxindoles **1.90** for the synthesis of functionalized spiro[chroman-4,3′-oxindoles] **1.92** in high yields and stereoselectivities.[40] The optimized transformation protocol tolerates differently substituted aryl groups (electron-donating or electron-withdrawing as well as heterocyclic) on the α-phenoxyarylethanones. It provides access to the desired products in excellent yields and diastereoselectivities, even with bulky aryl groups such as naphthyl. The transformation involves rhodium-catalyzed formation of the zwitterionic intermediate **1.91** through arene coupling and subsequent intramolecular aldol-type cyclization (Scheme 1.16).

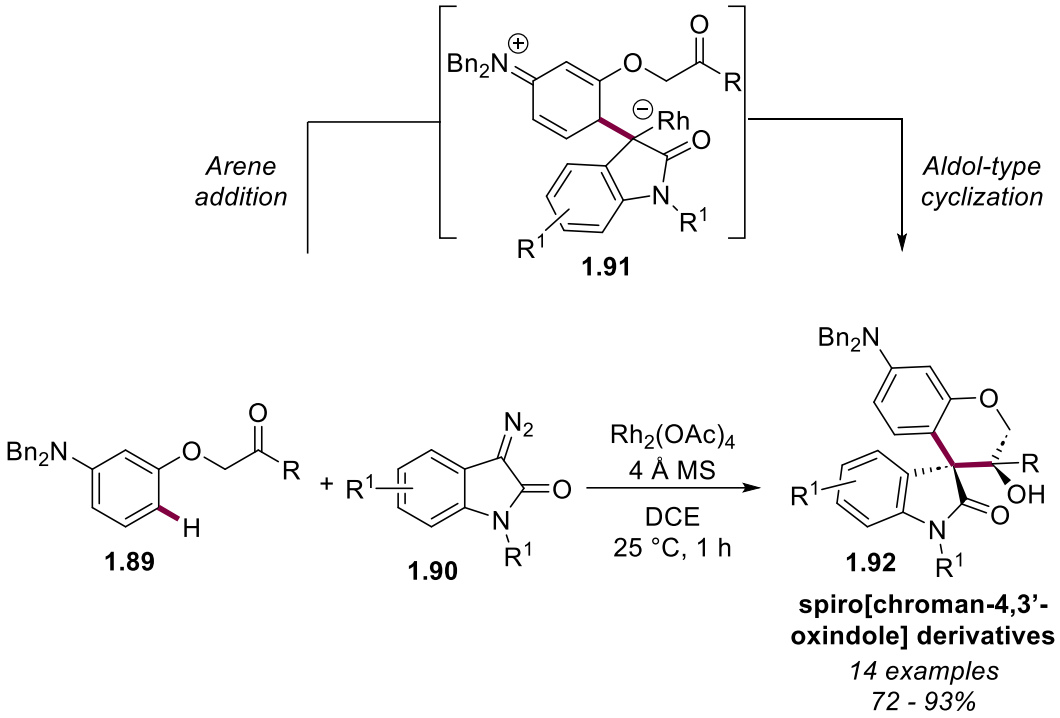

Scheme 1.16: Synthesis of functionalized spiro[chroman 4,3'-oxindole] derivatives (**1.92**) by Hu and coworkers.

The Xu group reported a copper-catalyzed [4+1]-annulation of 2-vinylindoles **1.93** with *α*-aryldiazoacetates **1.94** in the synthesis of substituted dihydrocyclopenta[*b*]indoles **1.96**.[41] This transformation proceeds through copper-catalyzed arene coupling followed by a *5-endo-trig* cyclization onto an alkene through a zwitterionic intermediate **1.95** (Scheme 1.17). In the case of mono-EWG-substituted 2-vinylindoles (EWG = -CO_2R, -CN, and -COR) mainly the C–H insertion products **1.97** were observed (67–81%) with little to no production of the desired annulation product.

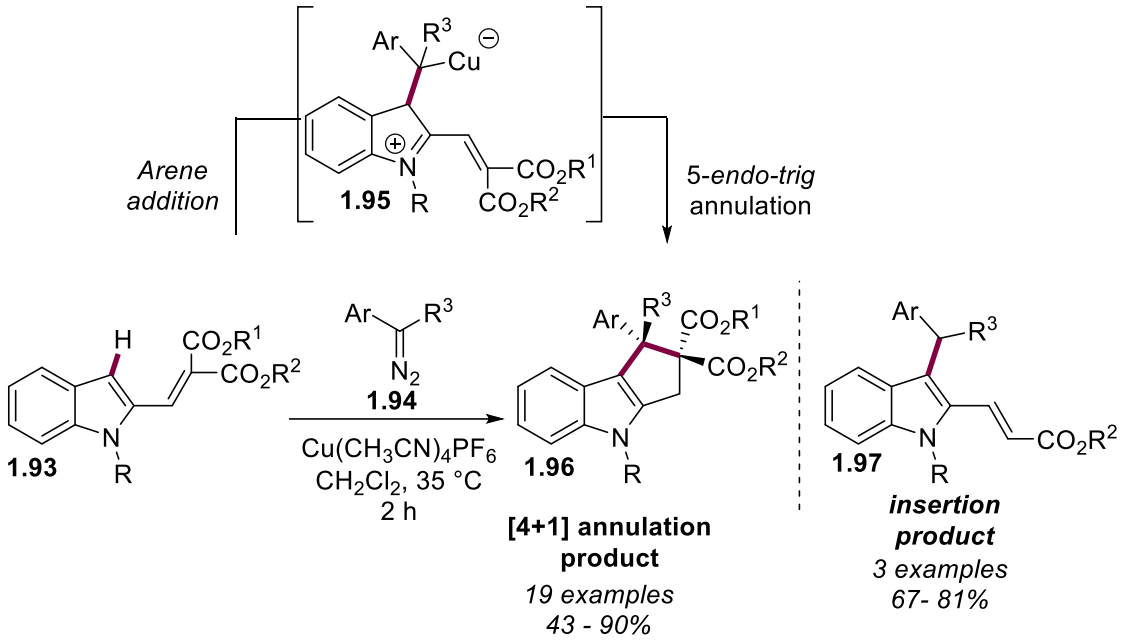

Scheme 1.17: Synthesis of substituted dihydrocyclopenta[*b*]indoles (**1.96**) by Xu and coworkers.

Despite the fact that carbene insertion into a nucleophilic arene molecule can bias regioselectivity, it still poses a challenge because it can undergo multiple types of carbene transfer reactions, including cyclopropanation.[42] Therefore, it is necessary to overcome competition and side reactions in order to functionalize non-activated arene C–H bonds through carbene insertion.

1.7.3 Type III – Intramolecular C–H Functionalization Cascades

The early research on carbene C–H insertion was mainly focused on intramolecular reactions because of the challenges associated with regioselectivity. The metal carbene and the reacting C–H bond, being connected through a suitable tether, allow for a regioselective transformation to be achieved, driven by the preferential formation of 5-membered rings.[43] This method of controlling the site selectivity of the C–H functionalization has been utilized once in a carbene C–H bond insertion/annulation process.

Sharma and coworkers have reported Rh(II)/Au(I)-catalyzed carbene cascade approach for the stereoselective synthesis of diverse spirocarbocycles. The cascade reaction involves a rhodium

carbene initiated arene coupling to provide oxindole intermediate **1.99**, followed by Au(I) activated *exo-dig* Conia-ene cyclization between the corresponding enolate and the pendant alkyne to provide spirocarbocycle **1.100** (Scheme 1.18).[44] In addition, an extension of the carbon skeleton of the diazo precursor has successfully allowed access to 6- and 7-membered spirocycles. This is the first report of combining entropically favored intramolecular C–(sp^2)–H carbene insertion and Conia-ene annulation in a cascade manner. A combination of three complexes (RhII/AuI/CuI) was used to achieve this intramolecular aryl C–(sp^2)–H functionalization by diazo carbene insertion/Conia-ene cascade for the synthesis of spirocarbocycles. The role of Cu(I) triflate is to activate Au(I) salt to form a stable cationic Au(I) complex at an elevated temperature.

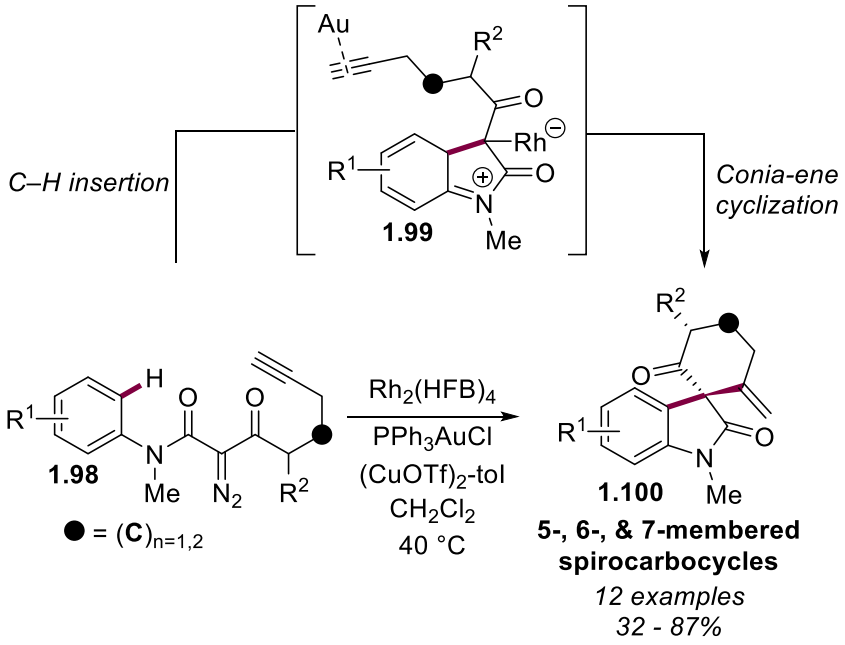

Scheme 1.18: Synthesis of diverse spirocarbocycles (**1.100**) by Sharma and coworkers.

The feasibility of forming C–C bonds by insertion of a carbene into a C–H bond has attracted considerable attention over the last four decades. Since significant progress has been made in developing and understanding carbene C–H insertion reactions, selectivity has significantly improved, making this an essential tool in synthetic chemistry.

In this thesis, the continuation of efforts to address the challenges of selectivity associated with the C–H insertion of carbenes derived from α-diazocarbonyl compounds is demonstrated. Our primary research objective was to conduct transition metal-mediated C–H bond functionalization (*via* either concerted or migratory carbene C–H insertion) on an electron-rich arene coupling partner containing a tethered electrophile. As a result, this insertion event will allow the formation of the first C–C bond and simultaneously generate a highly reactive carbanion intermediate that triggers a subsequent cascade reaction. In a subsequent intramolecular annulation event, an appropriate electrophile will intercept the carbanion intermediate, leading to the formation of a second C–C bond, allowing efficient construction of cyclic frameworks. This overall tandem process avoids multiple reaction setups, work-up, and purification steps, thus making it an efficient synthetic route to access molecular complexity. Furthermore, using electron rich indoles as coupling partners to carbenoids allows synthesis of medicinally important indole-based frameworks.

1.8 References

1. Ciulla, M. G.; Zimmermann, S.; Kumar, K. *Org. Biomol. Chem.* **2019**, *17*, 413.
2. Hayashi, Y. *Chem. Sci.* **2016**, *7*, 866.
3. Feng, C.-N.; Hsieh, Y.-C.; Wu, Y.-T. *Chem. Rec.* **2015**, *15*, 266.
4. Schrittwieser, J.H.; Velikogne, S.; Hall, M.; Kroutil, W. *Chem. Rev.* **2018**, *118*, 270.
5. Tietze, L. F. *Chem. Rev.* **1996**, *96*, 115.
6. Nicolaou, K. C.; Edmonds, D. J.; Bulger, P. G. *Angew. Chem. Int. Ed.* **2006**, *45*, 7134.
7. Yorimitsu, H.; Kotora, M.; and Patil, N.T. *Chem. Rec.*, **2021**, *12*, 3335.
8. Nicolaou, K. C.; Bulger, P. G.; Sarlah, D. *Angew. Chem. Int. Ed.* **2005**, *44*, 4442.
9. Han, J. C.; Li, C. C. *Synlett* **2015**, *26*, 1289.
10. Song, L.; Eycken, E. V. D. *Chem. Eur. J.* **2021**, *27*, 121.
11. Milde, B.; Pawliczek, M.; Jones, P. G.; Werz, D. B. *Org. Lett.* **2017**, *19*, 1914.
12. Roche, S. P. *Organics* **2021**, *2*, 376.
13. Riveira, M. J.; La-Venia, A.; Mischne, M. P. *J. Org. Chem.* **2016**, *81*, 7977.
14. Xiang, Y.; Wang, C.; Ding, Q.; Peng, Y., *Adv. Synth. Catal.* **2019**, *361*, 919.
15. Schoeller, W.; Brinker. H. *Z. Naturforsch., B: Anorg. Chem., Org. Chem.* **1980**, *35*, 475.
16. Curtius, T. *Ber. Dtsch. Chem. Ges.* **1883**, *16*, 2230.
17. Zhang, Z.; Wang, J. *Tetrahedron* **2008**, *64*, 6577.
18. Davies, H. M. L.; Manning, J.R. *Nature* **2008**, *451*, 417.
19. (a) Padwa, A; Krumpe, K. E. *Tetrahedron* **1992**, *48*, 5385. (b) Davies, H. M. L.; Morton, D. *Chem. Soc. Rev.* **2011**, *40*, 1857.
20. Ford, A.; Miel, H.; Ring, A.; Slattery, C. N.; Maguire, A. R.; McKervey, M. A. *Chem. Rev.* **2015**, *115*, 9981.

21. Gillingham, D.; Fei, N. *Chem. Soc. Rev.* **2013**, *42*, 4918.

22. Thumar, N. J.; Wei, Q.; Hu, W. *Adv. Organomet. Chem.* **2016**, *66*, 33.

23. Alavala, G. K. R.; Sajjad, F.; Shi, T.; Kang, Z.; Ma, M.; Xing, D.; Hu, W. *Chem. Commun.* **2018**, *54*, 12650.

24. Jing, C.; Xing, D.; Gao, L.; Li, J.; Hu, W. *Chem. Eur. J.* **2015**, *21*, 19202.

25. Xu, X.; Zavalij, P. Y.; Doyle, M. P. *Angew. Chem. Int. Ed.* **2012**,*51*, 9829.

26. (a) Davis, O. A.; Bull, J. A. *Angew. Chem. Int. Ed.* **2014**, *53*, 14230. (b) Davis, O. A.; Bull, J. A. *Synlett* **2015**, *26*, 1283.

27. Hunter, A. C.; Schlitzer, S. C.; Sharma, I. *Chem. Eur. J.* **2016**, *22*, 16062.

28. Abrams, D. J.; Provencher, P. A.; Sorensen, E. J. *Chem. Soc. Rev.* **2018**, *47*, 8925.

29. He, Y.; Huang, Z.; Wu, K.; Ma, J.; Zhou, Y. – G.; Yu, Z. *Chem. Soc. Rev.* **2022**, *51*, 2759.

30. Hu, F.; Xia, F.; Ma, C.; Zhang, Y.; Wang, J. *Chem. Commun.* **2015**, *51*, 7986.

31. Yu, S.; Liu, S.; Lan, Y.; Wan, B.; Li, X. *J. Am. Chem. Soc.* **2015**, *137*, 1623.

32. Dateer, R. B.; Chang, S. *Org. Lett.* **2016**, *18*, 68.

33. Gao, M.; Yang, Y.; Chen, H.; Zhou, B. *Adv. Synth. Catal*. **2018**, *360*, 100.

34. Yang, Y.; Wang, X.; Li, Y.; Zhou, B. *Angew. Chem.* **2015**, *127*, 15620.

35. Guo, S.; Sun, L.; Liu, Y.; Ma, N.; Zhang, X.; Fan, X. *Org. Lett.* **2019**, *1*, 4082.

36. Wu, J.-Q.; Yang, Z.; Zhang, S.-S.; Jiang, C.-Y.; Li, Q.; Huang, Z.-S.; Wang, H. *ACS Catal.* **2015**, *5*, 6453.

37. Lou, J.; Han, W.; Liu, Z.; Xiao, J. *Org. Chem. Front.* **2021**, *8*, 1447.

38. (a) Yanagawa, M.; Harada, S.; Hirose, S.; Nemoto, T. *Adv. Synth. Catal.* **2021**, *363*, 2189. (b) Harada, S.; Yanagawa M.; Nemoto, T. *ACS Catal.*, **2020**, *10*, 11971. (c) Ma, B.; Wu, P.; Wang, X.; Wang, Z.; Lin, H. X.; Dai, H. X. *Angew. Chem. Int. Ed.* **2019**, *58*, 13335.

39. Ma, B. Wu, Z. Huang, B. Liu, L. Zhang, J. *Chem. Commun.* **2016**, *52*, 9351.

40. Jia, S.; Lei, Y.; Song, L.; Krishna Reddy, A. G.; Xing, D.; Hu, W. *Adv. Synth. Catal.* **2017**, 359, 58

41. Dong, K.; Pei, C.; Zeng, Q.; Qiu, L.; Hu, W.; Qian Y.; Xu, X. *Chem. Commun.* **2019**, *55*, 6393.

42. Doyle, M. P.; Duffy, R.; Ratnikov, M.; Zhou, L. *Chem. Rev.* **2010**, *110*, 704.

43. Caballero, A.; Díaz-Requejo, M. M.; Fructos, M. R.; Olmos, A., Urbano, J.; Pérez, P. J. *Dalton Trans.* **2015**, *44*, 20295.

44. Hunter, A. C.; Chinthapally, K.; Bain, A.; Steven, J. C.; Sharma, I. *Adv. Synth. Catal.* **2019**, *361*, 2951.

Chapter 2: Tandem Carbenoid C–H Functionalization/Conia-ene Cyclization of *N*-Propargyl Indoles Generates Pyrroloindoles Under Cooperative Rh(II)/Zn(II) Catalysis

With the publisher's permission, this chapter was adapted from the original manuscript: Bhat, A. H.; Alavi, S.; Grover, H. K. *Org. Lett.* **2020**, *22*, 224−229.

Statement of Co-Authorship

Aabid H. Bhat (listed as 1st author): Performed the synthetic work, data collection, data analysis, and contributed significantly to the preparation of the manuscript and supporting information.

Sima Alavi: Synthesized, characterized, and collected data of starting materials for compounds **4r**, **4s**, and **4w** and contributed to the preparation of the supporting information.

Huck K. Grover: Principal investigator (PI) of the work, who led the project and majorly contributed to the interpretation/analysis of data and writing of the manuscript.

The article has been reproduced in this Chapter in a modified form that includes the contributions of all the co-authors for the purpose of a complete discussion.

1.9 Introduction

1.9.1 Indole Core

Benzo[*b*]pyrrole, or as it is commonly called, indole, is a prominent heterocycle comprised of a benzene ring fused to the 2,3 positions of the pyrrole nucleus. Indole is perhaps the most essential and ubiquitous nitrogen-containing heterocycle and, therefore one of the most studied. Indole is the main metabolite produced by gut bacteria during tryptophan metabolism and plays several important roles in intercellular communication. There are countless derivatives of indole that play an integral role in many aspects of our lives.[1]

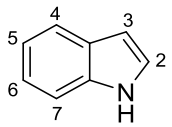

2.1

Figure 0-1: Structure and numbering of indole.

1.9.2 Reactivity of Indole

Indole possesses a conjugated π-electron system, extending over both the benzene ring and the five-membered heterocyclic ring. This conjugation in indole enables the delocalization of electrons throughout the entire system, leads to its aromaticity. It contains ten π electrons (eight electrons from eight carbons and two lone pair electrons from nitrogen). The participation of the nitrogen lone electron pair in the aromatic ring indicates that the indole nitrogen is weakly basic, and it does not behave like a simple aliphatic amine. In fact, indole is a π-excessive (electron-rich) heterocycle, and as such the chemistry of this heterocycle is mostly dominated by electrophilic substitution reactions.[2]

1.9.3 Electrophilic Aromatic Substitution on Indole

The pyrrole ring in indole is more electron-rich in comparison to the benzene ring. Therefore, electrophilic attack generally occurs on the five-membered ring, except in special circumstances. In electrophilic substitution, the C-3 position is the preferred site of substitution since the Wheland intermediate cation formed by the C-3 attack **2.3** is more stable than the one formed by a C-2 attack **2.6** (Scheme 2.1). The electrophilic substitution at C-2 occurs when C-3 is occupied. Since the pyrrole ring is the most reactive portion of indole, electrophilic substitution of the carbocyclic (benzene) ring can take place only after N-1, C-2, and C-3 are substituted.[3]

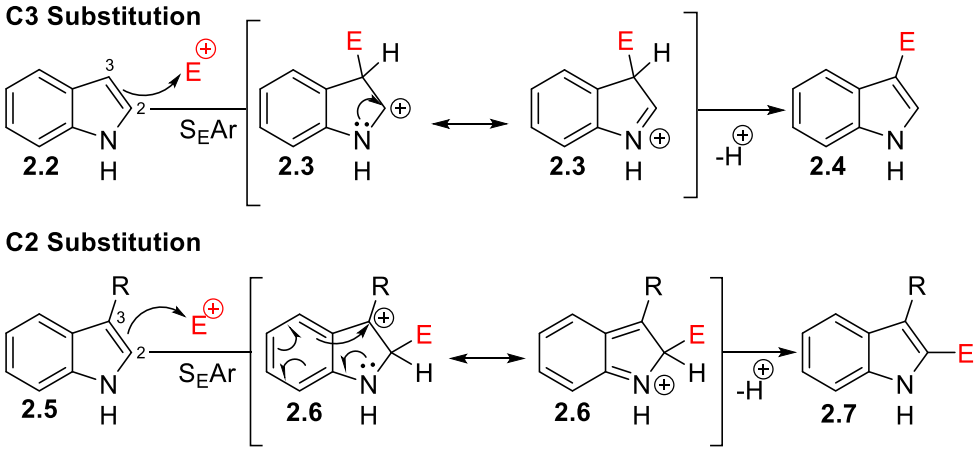

Scheme 0.1: Electrophilic aromatic substitution on C-2 and C-3 positions of indole.

1.10 C–H Functionalization of Indoles With Metal Carbenoids

Indoles are present in a wide variety of biologically interesting natural products and pharmaceutical targets.[4] Consequently, the development of mild and efficient protocols for the synthesis of functionalized indoles remains a field of intensive research. One of these strategies involves the selective functionalization of indole with metal carbenoids derived from α-diazocarbonyl compounds.[5] Wenkert and coworkers at Indiana University in 1977 demonstrated the reaction of methylated indole substrates with ethyl diazoacetate (EDA) using copper bronze as a catalyst (Scheme 2.2). Their research highlighted that 1-methylindole **2.8** (R^1=R^2=H) and 1,2-

dimethylindole **2.9** (R^1=H, R^2=Me) both react selectively with EDA **2.11** in the presence of copper bronze to provide the corresponding ethyl (indol-3-yl) acetate derivatives **2.12** and **2.13**. However, only 4% of the indol-2-yl acetate **2.14** derivative was produced by the reaction of EDA with 1,3-dimethylindole **2.10** (R^1=Me, R^2=H).[6]

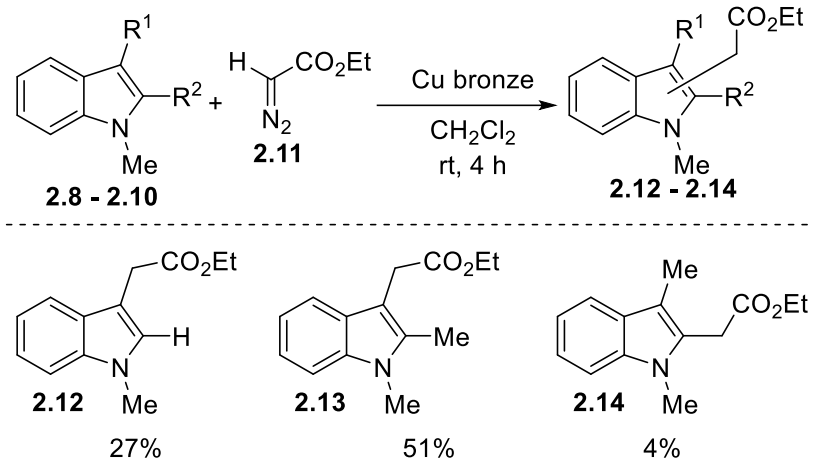

Scheme 0.2: Cu catalyzed C-2, C-3 insertion of ethyl diazoacetate on indole.

Kerr and coworkers reported the $Rh_2(OAc)_4$-catalyzed carbenoid insertion reactions of indoles with α-diazomalonates in 2002, in which C-3 (**2.17**), C-2 (**2.19**), and/or *N*-alkylated (**2.20**) products were formed in modest to excellent yields (Scheme 2.3A/B). This study demonstrated the importance of indole *N*-substitution as a requirement to achieve high levels of C-3 or C-2-selective carbenoid functionalization. Additionally, if positions 1-3 were all substituted (Scheme 2.3C), insertion was shown to take place at the 6-position (**2.22**) on the indole.[7]

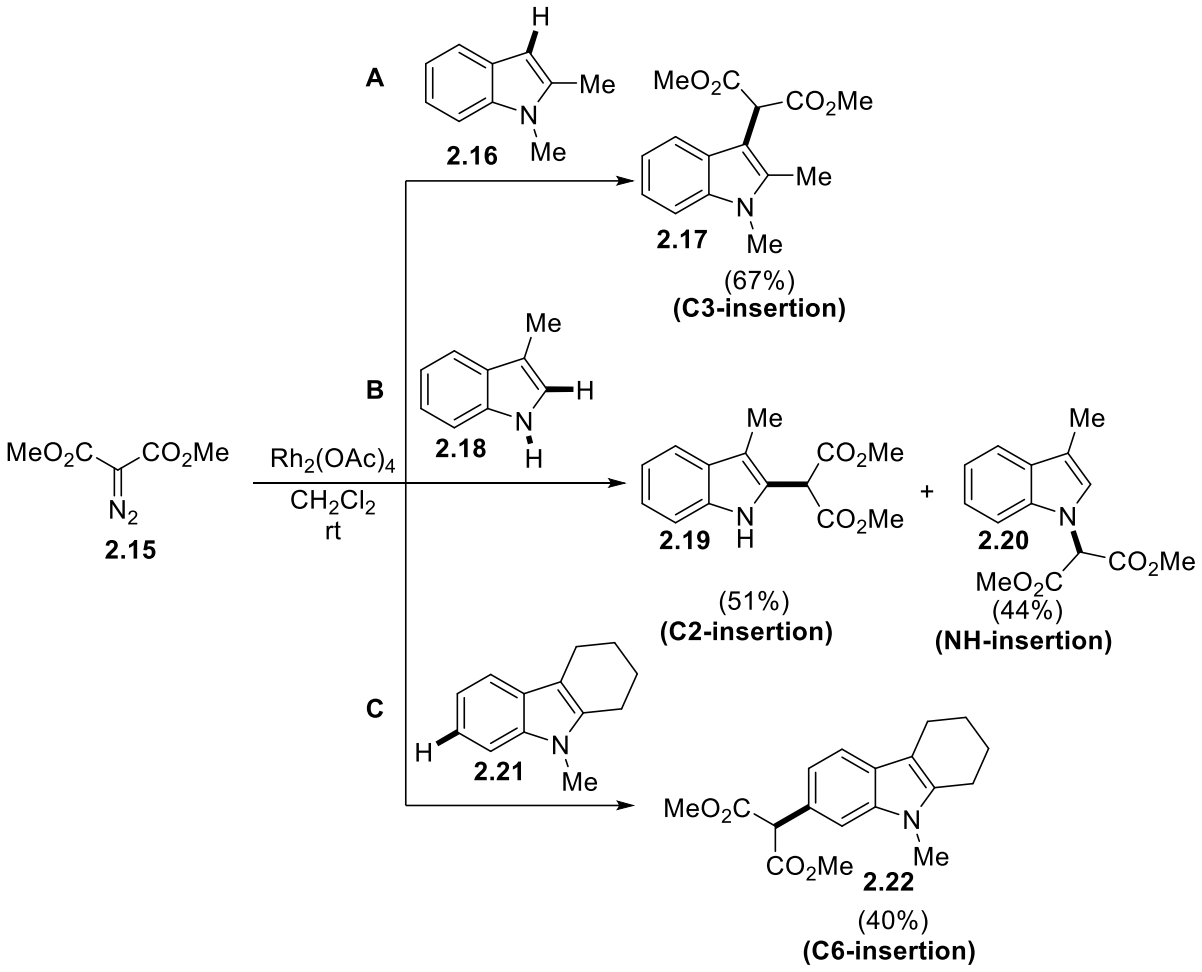

Scheme 0.3: Rh(II)-catalyzed carbenoid insertion reactions of indoles with α-diazomalonates.

In 2010, the Kerr group developed $Cu(acac)_2$-catalyzed conditions for the malonyl carbenoid insertion into indole substrates (Scheme 2.4).[8] This study demonstrated better yields for a variety of substitution patterns and functional groups compared to their previous report in 2002. The method highlights a high degree of regiocontrol, and the reaction can be accelerated under microwave irradiation conditions. The authors surveyed different substituents at the various positions of the indole ring system, and in general, the desired malonyl indoles were obtained in excellent yields except in a few examples where lower yields were observed. Indoles starting materials containing a *N*-alkyl group (methyl or benzyl) worked well under the copper-catalyzed reaction conditions providing **2.17** and **2.25** in excellent yields, but the use of electron-withdrawing

Boc or Ts groups diminished the reaction efficiency. A low yield was also observed for a substrate bearing an electron-withdrawing ester group (CO_2Me) at the C-2 position of indole **2.28**. Observing the outcome of the substitution pattern on indole, it is evident that any functional group that withdraws electrons from the pyrrole ring decreases its nucleophilicity rendering carbene insertion less efficient.

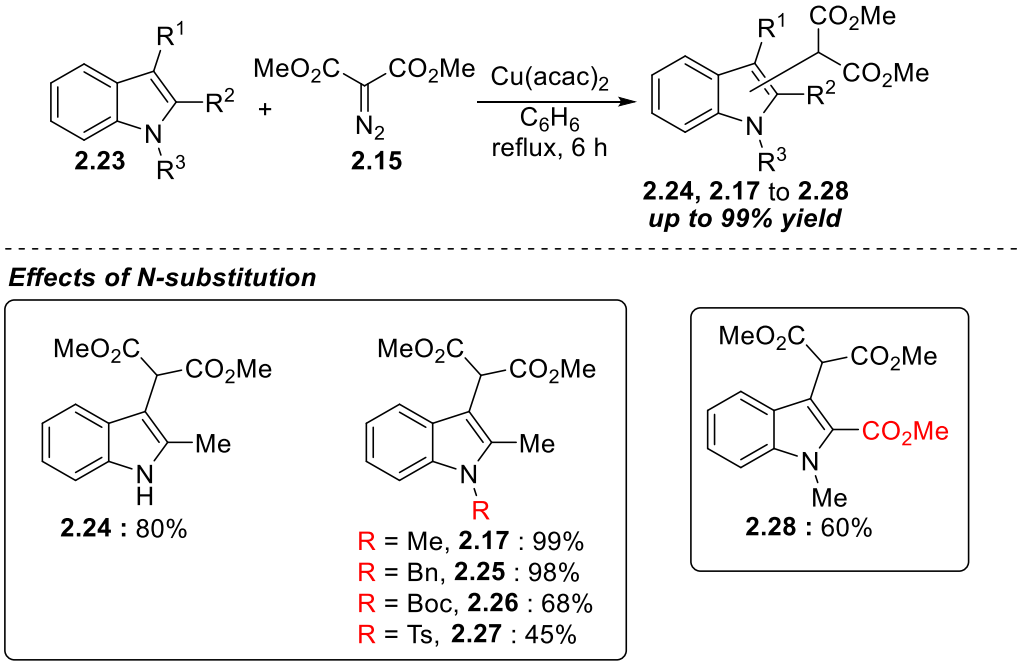

Scheme 0.4: Cu-catalyzed carbenoid insertion of α-diazomalonates on indole.

The literature cited above suggests that metal-stabilized carbenoids react well with indoles, and substrate-controlled site-selective C–H insertion on indoles can be achieved in high yields. The authors described a plausible mechanism for this regioselective alkylation on indole which proceeds *via* intermediate cyclopropylindoline **2.29** (Scheme 2.5). The intermediate **2.29** could conceivably collapse to two regioisomeric products giving either the 2-alkyl **2.30** or 3-alkyl **2.31** product. If there is no substituent on the C-3 position of indole, a loss of a proton from the benzylic position and dissociation of the cyclopropane bond will lead to 3-alkylation (compound **2.31** *via* path a). However, if there is a substituent on the C-3 position of indole, then a loss of a proton α

to the nitrogen atom and dissociation of a cyclopropane bond leads to 2-substitution (compound **2.30** *via* path b).

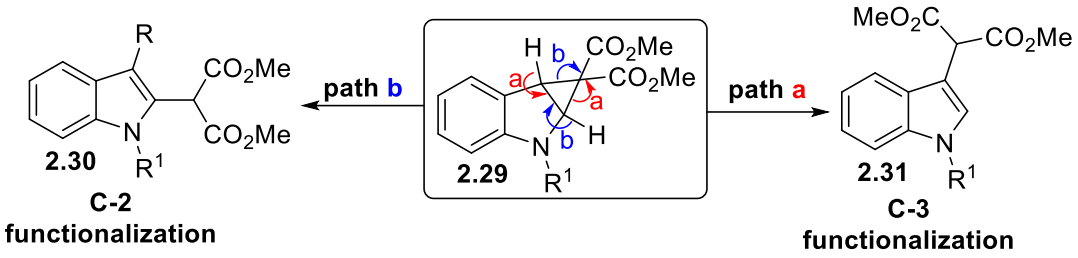

Scheme 0.5: Regioselective C-2, C-3 malonyl insertion on indoles *via* intermediate cyclopropylindoline.

1.11 The Conia-ene Reaction

Jean-Marie Conia, a French chemist at Paris-Sud University, was studying carbocyclic molecules formed by ene-type reactions with carbonyls in the late 1960s, a discovery he published in a 1975 review with colleague P. Le Perchec titled "The Thermal Cyclization of Unsaturated Carbonyl Compounds."[9] The Conia-ene reaction originally was an intramolecular thermal cyclization reaction of the enolizable carbonyls (aldehyde or ketone) **2.32** wherein an enol tautomer would react with a pendant alkyne/alkene at high temperature to form a C–C bond, resulting in the formation of cyclopentanes **2.34** (Scheme 2.6).

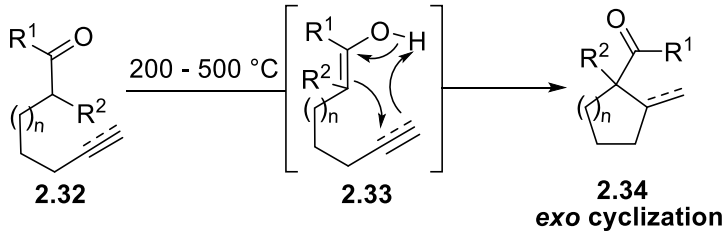

Scheme 0.6: Thermal Conia-ene reaction.

1.11.1 Advancements in Catalyst and Asymmetric Synthesis

The Conia-ene reaction at its inception had limited applicability in synthesis as molecules with heat-labile functional groups were often incompatible with the elevated temperature

conditions required for this reaction. Additionally, regio- and diastereoselectivity was entirely substrate dependent, offering little to no control over the orientation of the product. In general, commonly employed substrates for the Conia-ene reaction provide two different sites for activation: the nucleophilic enol, originating from the carbonyl moiety, and the alkyne or alkene as an electrophilic moiety (Figure 2.2).

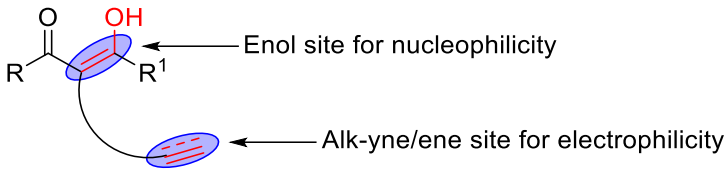

Figure 0-2: Typical substrate for Conia-ene reaction with two sites of activation.

Over the past 50 years, the Conia-ene reaction has evolved to include milder reaction conditions which employ main-group Lewis acids to promote the cyclization.[10] Additionally, these advancements have led to the identification of different modes of activation based on the choice of metal(s) used to promote the Conia-ene reaction. In a 2008 report, Nakamura proposed five distinct modes of activation mechanism for the metal-mediated Conia-ene cyclization (Figure 2.3).[11] The first mode of activation is to enhance the reactivity of the nucleophilic component in the reaction by means of a metal enolate formation by hard metals such as sodium, tin, and lithium (enolate activation - Figure 2.3**A**). In contrast, it is also possible to enhance the electrophilicity of alkynes by coordination with a soft carbophilic Lewis acids like gold, silver, and platinum, thereby increasing susceptibility to enol attack (alkyne activation -Figure 2.3**B**). Alternatively, a single metal such as nickel, cobalt, and rhenium can activate both the enol and alkyne moiety by coordination of the π bonds of each functional group to facilitate the annulation (ene-yne activation - Figure 2.3**C**). Similarly, other metals like iron, zinc, and copper can activate both the nucleophilic and electrophilic components coordinating the alkyne as well as the enolate oxygen (one-metal double activation - Figure 2.3**D**). On the other hand, dual activation can be achieved by two

different metals, one associated with the enolate and the other activating the alkyne site (double activation by two metals - Figure 2.3**E**).

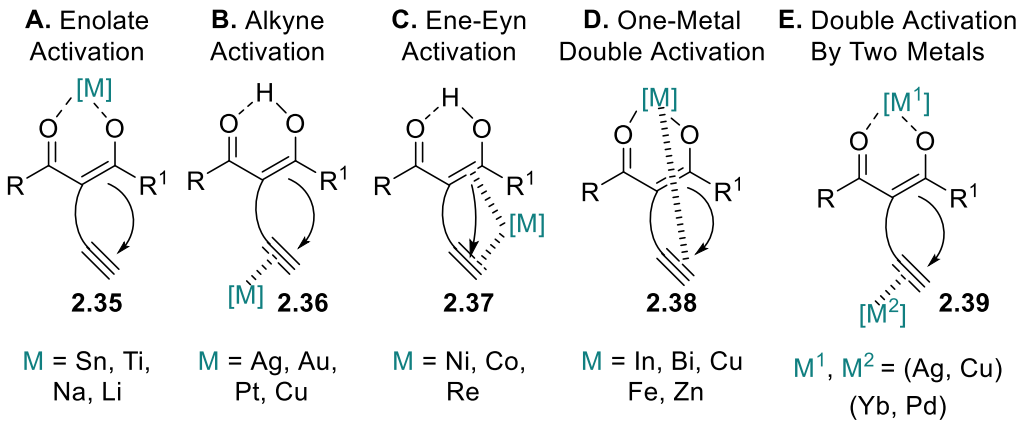

Figure 0-3: Proposed activation modes for Conia-ene reaction by Nakamura.

1.12 Tandem Reactions Involving Conia-ene

Due to the mild Lewis-acid catalyzed reaction conditions developed for the Conia-ene reaction, this type of cyclization has found a common place in tandem transformations. In particular, the reaction pathways involve the initial formation of a reactive enol or enolate intermediate, which subsequently can then be intercepted by the alkene or alkyne-based electrophiles. Prominent examples of this type of cascade are initiated by Michael addition and cyclopropane ring-opening reactions. For example, the Nakamura group has reported Zn(II)-catalyzed tandem Michael-addition/Conia-ene protocol for the synthesis of tetrahydrofurans **2.43** (Scheme 2.7A).[12] The transformation involves Michael addition between propargyl alcohol **2.41** and alkylidene malonate (Michael acceptor) **2.40** followed by Conia-ene cyclization *via* zinc enolate intermediate **2.42.** The method highlights mild reaction conditions and the synthesis of a variety of substituted 3-methylene tetrahydrofurans. In a similar tandem protocol, the Kerr group reported a Zn(II)-catalyzed reaction of benzyl-protected propargyl amines **2.45** and donor-acceptor cyclopropanes **2.44** for the synthesis of highly functionalized piperidines (Scheme 2.7B).[13] The

reaction proceeds by a nucleophilic cyclopropane ring-opening by the amine followed by a Conia-ene cyclization *via* intermediate zinc enolate **2.46** to give piperidine **2.47**.

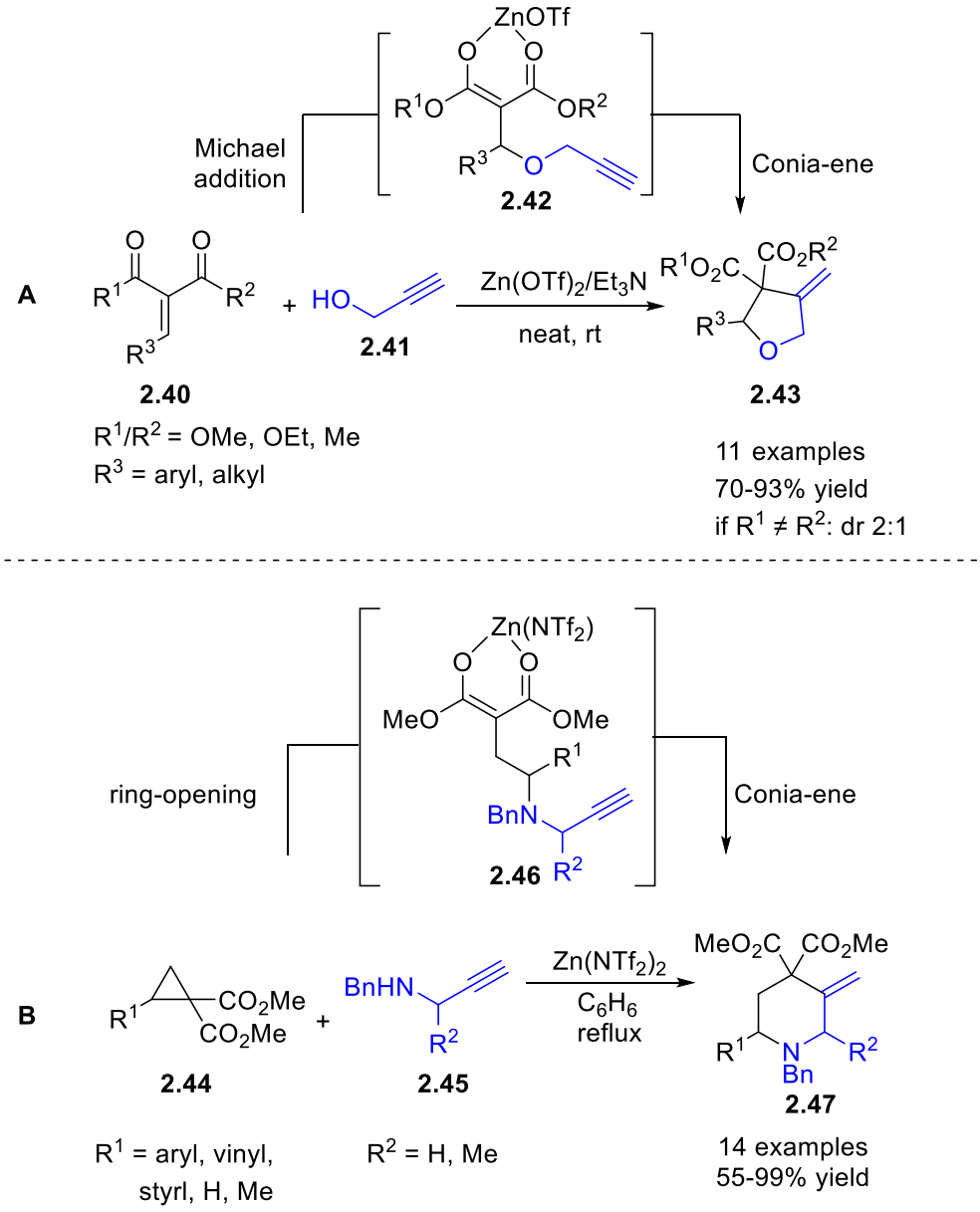

Scheme 0.7: (**A**) Tandem Michael-addition/Conia-ene cyclization for the synthesis of tetrahydrofurans (**2.43**) by Nakamura (**B**) Tandem ring-opening/Conia-ene cyclization for the synthesis of piperidines (**2.47**) by Kerr.

While both the insertion of metal carbenoid compounds into heteroatom–H bonds and the Conia-ene annulations are well established reactions in the literature, the combination of these two

processes in a tandem/cascade event was unknown until 2014. Hatakeyama *et al.* were the first to explore this unique reaction manifold through the reaction of homopropargyl alcohols **2.48** with *α*-diazocarbonyl **2.49** as carbene precursors (Scheme 2.8). The authors successfully developed a tandem carbenoid O–H insertion followed by a subsequent Conia-ene cyclization to access various substituted tetrahydrofurans **2.51** in modest to excellent yields under a rhodium/zinc dual catalyst system (Scheme 2.9). The requirement of the dual catalyst system in this transformation was explored, and it was noted that while O–H insertion was efficient under rhodium catalysis leading to ether intermediate **2.50**, the subsequent annulation was sluggish. Thus the presence of the Lewis acid $ZnCl_2$ was identified as an appropriate compatible co-catalyst to promote the cyclization.[14]

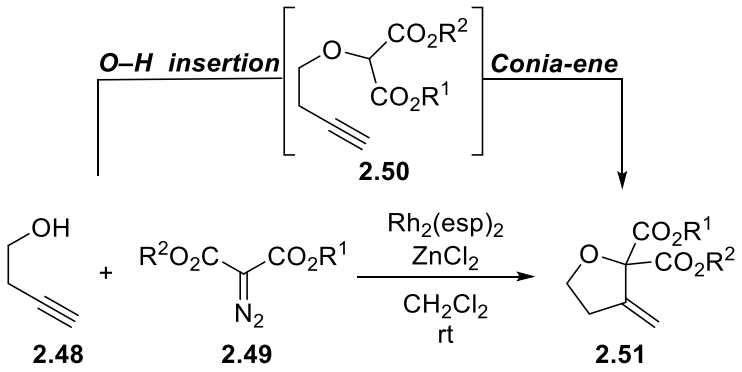

Scheme 0.8: Synthesis of tetrahydofurans *via* O–H insertion/Conia-ene cyclization.

Shortly after the work of Hatakeyama, in 2015, Sun *et al.* reported a similar protocol for the rhodium-catalyzed tandem carbenoid N–H insertion/Conia-ene cyclization of diazo compounds with aminoalkynes **2.52** to synthesize 3-methylene pyrrolidines **2.55** (Scheme 2.9 path a).[15] Like Hatakeyama, they noted that $ZnCl_2$ as an additive was required to promote the cyclization event. In addition to the development of the tandem N–H insertion/Conia-ene reaction, the authors also described the stereodivergent synthesis of **2.57** and **2.58** from the same starting materials (**2.52** and **2.53**) under copper-catalysis (Scheme 2.10 path b). Although the process is

outside the scope of heteroatom–H bonds insertion/Conia-ene annulation reactions of metal carbenoids, the generation of allenoates from α-diazocarbonyl compounds and terminal alkynes under copper catalysis followed by intramolecular hydroamination represents another interesting class of carbene cascades.[16]

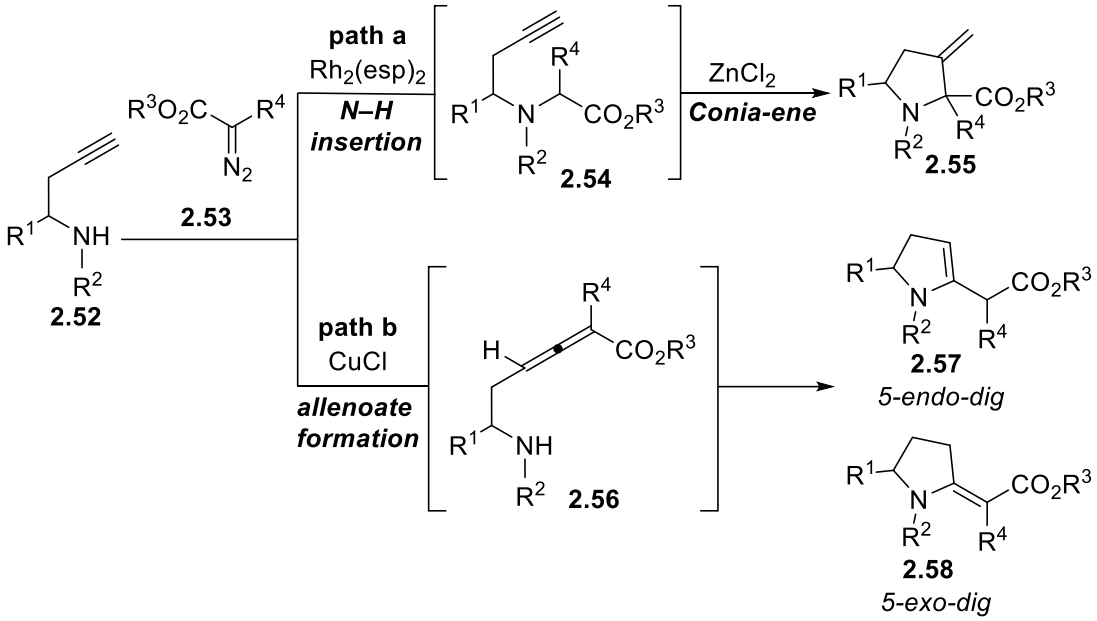

Scheme 0.9: Synthesis of pyrrolidines (**2.55**) *via* tandem N–H insertion/Conia-ene cyclization by Sun group.

The Sharma research group at the University of Oklahoma, with extensive research interests in diazo chemistry, has published multiple reports on the synthesis of heterocyclic frameworks *via* tandem heteroatom–H insertion/Conia-ene cyclization. In 2016, they reported the insertion/Conia-ene cascade cyclization reaction of homopropargylic acids **2.59** with diazocarbonyl compounds **2.60** for the synthesis of γ-butyrolactones **2.62** (Scheme 2.10A).[17] Moreover, in 2018, they reported O–H insertion/Conia-ene cyclization of homopropargylic alcohols **2.63** with diazocarbonyls **2.64** for the synthesis of diverse spiroethers **2.66** under synergistic Rh/Au-catalysis (Scheme 2.10B).[18] In the same year, they also developed a convergent approach for synthesizing diverse *N*-heterocycles. The reaction involves a Rh(II)-catalyzed insertion reaction of aminoalkynes **2.67** with donor/acceptor diazo compounds **2.68**, followed by

subsequent trapping of gold-activated aminoalkyne intermediate **2.70** *via* Conie-ene cyclization (Scheme 2.10C).[19] Unlike Sun's work which was mostly limited to acceptor/acceptor diazo compounds, Sharma showed that both donor/acceptor and acceptor/acceptor diazocarbonyls worked efficiently under the rhodium/gold dual catalyst system.

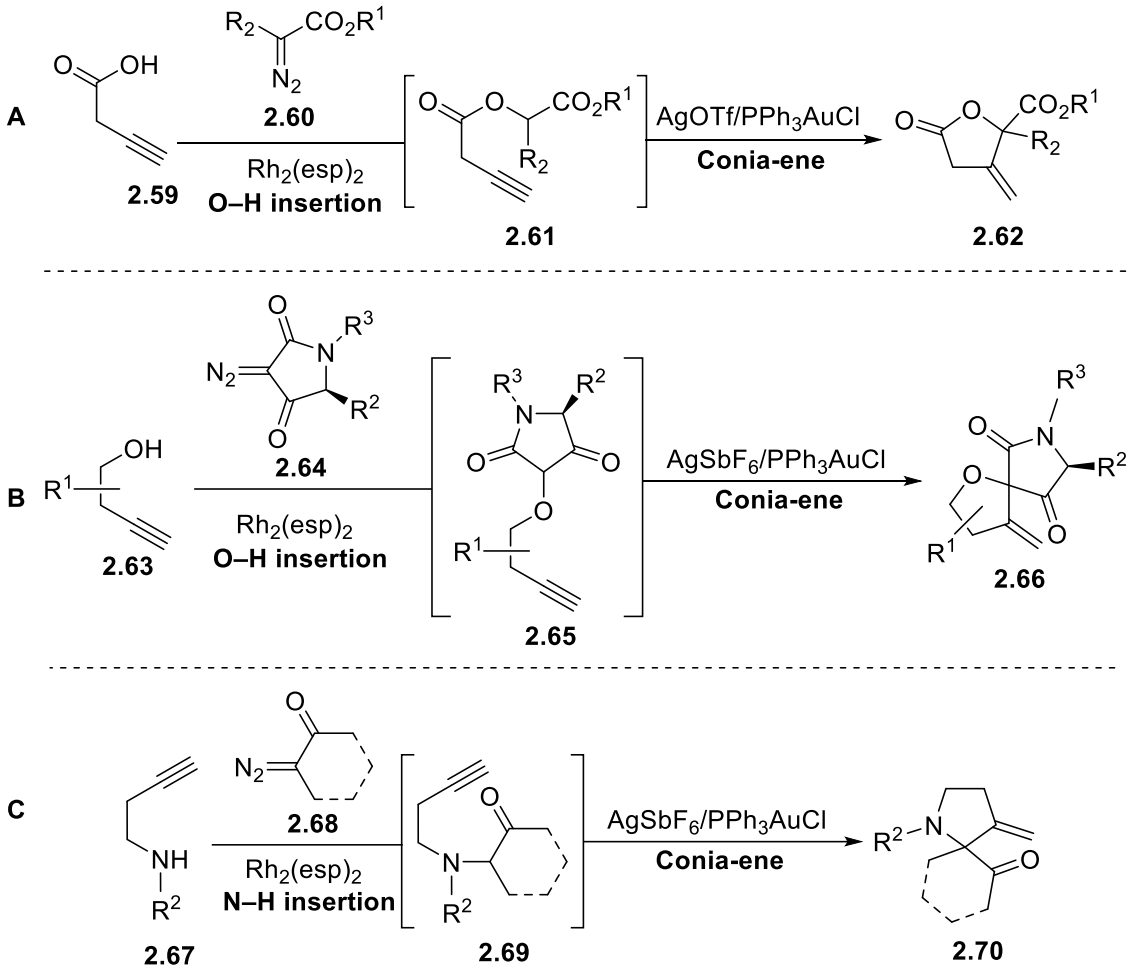

Scheme 0.10: Synthesis of hetero- and spirocycles *via* X–H insertion/Conia-ene cyclization cascades.

1.13 **Hypothesis**

With literature precedent limited to carbenoid heteroatom–H insertion/annulation, we hypothesized a novel approach involving an intermolecular carbenoid insertion into a C(sp^2)–H bond to generate a carbanion intermediate **2.73** (Scheme 2.11). The resulting intermediate (**2.73**) can be subsequently intercepted by a carbon-based electrophile *via* Conia-ene cyclization resulting

in the construction of various heterocyclic systems in a cascade manner. To the best of our knowledge, the proposed research would represent the first intermolecular C–H bond insertion/Conia-ene cascade.

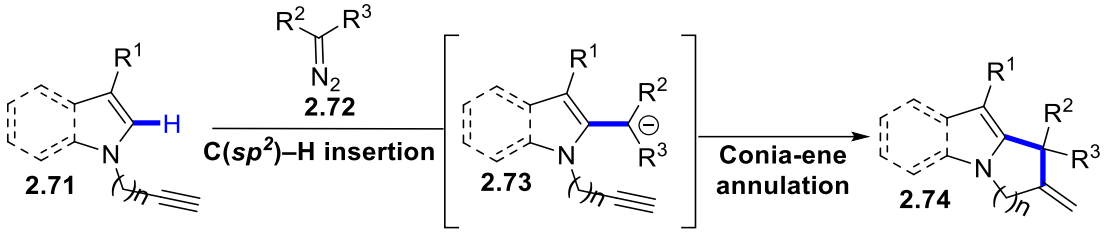

Scheme 0.11: Proposed objective involving C(sp^2)–H insertion/Conia-ene cyclization cascade.

Furthermore, it was hypothesized that utilizing indole as the C–H bond containing starting material would be advantageous for a variety of reasons. Firstly, the reactivity of carbenoids with indoles has been highlighted as an attractive method of regioselective C–H functionalization.[20] Secondly, the indole ring system is one of nature's most abundant and important heterocycles. The indole scaffold is present in a variety of biologically significant natural compounds, including neurotransmitter serotonin, complex alkaloids and pharmaceuticals such as anticancer and antimalarial drugs.[21] Also, our proposed cascade transformation will result in the synthesis of pyrrolo[1,2-*a*]indoles **2.75**. Some notable examples containing this scaffold include antimalarial agent flinderole C **2.76**, protein kinase inhibitor JTT-010 **2.77** and anti-cancer compound mitomycin III **2.78** (Figure 2.4). Finally, indole is an abundant, readily available, and inexpensive nitrogen-containing heterocycle, thus making it an ideal substrate for the time- and cost-effective study of cascade reactions.

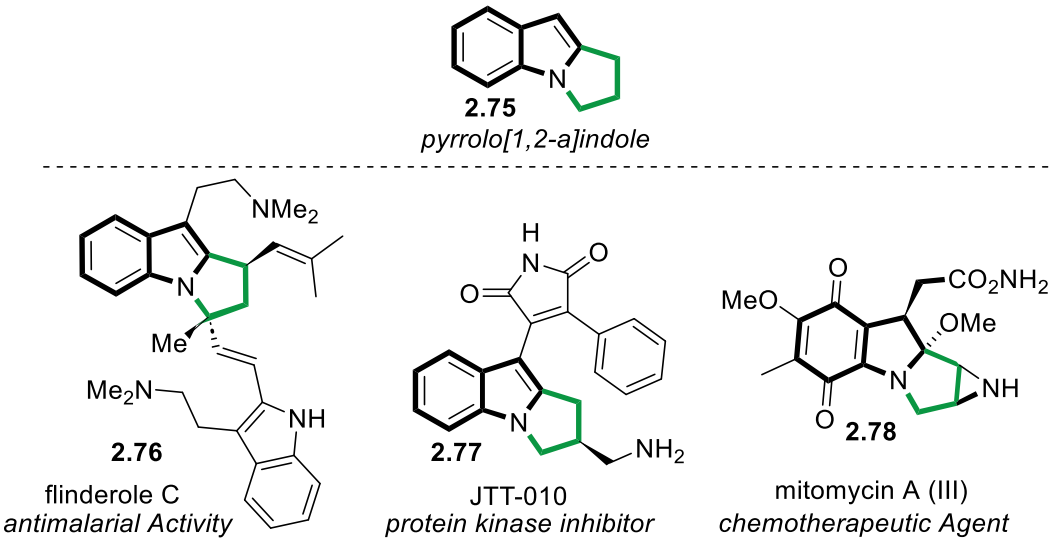

Figure 0-4: Notable examples of biologically important pyrroloindole containing compounds.

1.14 Results and Discussion — Synthesis of Starting Materials

We initiated our work towards the synthesis of *N*-propargylskatole **2.81** from commercially available 3-methylindole **2.79**. Using classical *N*-alkylation conditions, which utilize sodium hydride and propargyl bromide **2.80** in DMF, **2.81** was isolated in 75% yield (Scheme 2.12A). Having the indole substrate in hand, we next synthesized the diazocarbonyl component through the Regitz diazo transfer method (Scheme 2.12B).[22] Diethyl malonate **2.82** was treated with freshly prepared tosyl azide in the presence of triethylamine to provide diazo malonate **2.83** in 85% yield. (Scheme 2.12B).

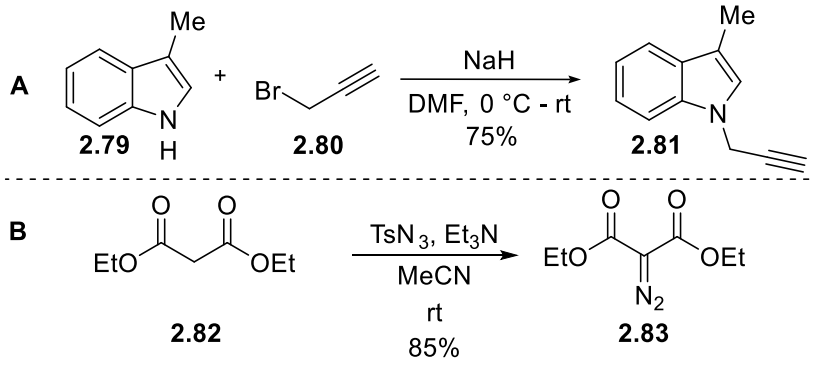

Scheme 0.12: Synthesis of *N*-propargylskatole **2.84** and diethyl diazomalonate **2.86**.

1.15 Optimization and Scope

To begin testing our hypothesis and the aim of identifying a single catalyst system capable of promoting the tandem transformation, copper-based systems were examined due to their known reactivity toward α-diazodicarbonyl compounds[23,8] and utilization in the Conia-ene cyclization.[24] Subjecting *N*-propargylskatole **2.81** and diethyl diazomalonate **2.83** to $Cu(acac)_2$ in benzene at room temperature (Table 2.1, entry 1), the expected cascade transformation for the synthesis of pyrroloindole **2.84** did not occur; however, C-2 functionalized product **2.85** was obtained in 15% yield. Next, elevating the temperature (Table 2.1, entry 2) resulted in increased yield in the insertion product **2.85**; however, no desired cyclization product **2.84** was observed, even after prolonged reaction times. Further attempts to increase the yield of **2.85** or promote the cyclization by varying the copper catalyst and temperature were all unsuccessful. A potential reason for this could be that copper as carbophilic Lewis acid is known to involve double activation of enolate and alkyne electrophile (Figure 2.3D). In our reaction conditions, a copper catalyst appears to have primarily been involved in alkyne coordination rather than in the formation of metal carbenoid for C–H insertion, which is a prerequisite step for subsequent cyclization.

Table 0.1: Screening of copper catalysts for the synthesis of **2.84**

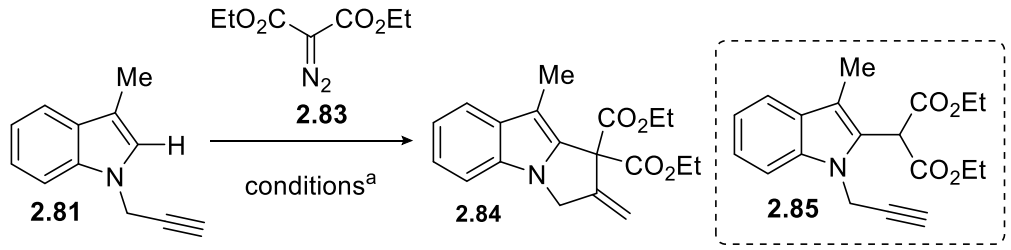

Entry	Catalyst	Solvent	Temp	Result	
				2.84	**2.85**
1	$Cu(acac)_2$	C_6H_6	rt	0	15%
2	$Cu(acac)_2$	C_6H_6	reflux	0	34%
3	$Cu(OTf)_2$	C_6H_6	rt-reflux	0	trace[b]
4	$Cu(tfaca)_2$	C_6H_6	rt-reflux	0	trace[b]

[a] Reaction conditions: **2.81** (1.2 equiv), **2.83** (1.0 equiv), cat. (10 mol%), solvent (0.2 M), time (2 -12 h). [b]trace: visible just above baseline by crude NMR.

Switching from copper to the rhodium(II)acetate dimer catalyst at room temperature resulted in a slight increase in the yield of **2.85** (Table 2.2, entry 1) and provided the desired cyclized product **2.84** in 2% yield. Elevating the temperature (Table 2.2, entry 2) resulted in a slight increase in yield of **2.85** and **2.84** with some diazo reagent **2.83** unconsumed. To increase the solubility of the catalyst, the reaction solvent was changed to dichloromethane and the reaction was preformed at varying temperatures (entry 3 and 4) leading to an overall decreased reaction time (complete consumption of **2.83**) and increased yield of **2.84**. Additional attempts (varying catalyst and temperature) to fully promote the cyclization using a single catalyst were ultimately met with low yields. It was observed that when $Rh_2(esp)_2$ was used (entries 5 and 6), rapid decomposition of the diazo compound occurred at room temperature as indicated by the immediate generation of N_2 gas bubbles and a color change in the reaction flask. Further decreasing the

temperature also resulted in complete consumption of the diazo reagent **2.83**, but provided no discernible products and near complete recovery of the indole starting material **2.81**.

Table 0.2: Screening of rhodium catalysts for the synthesis of **2.84**.

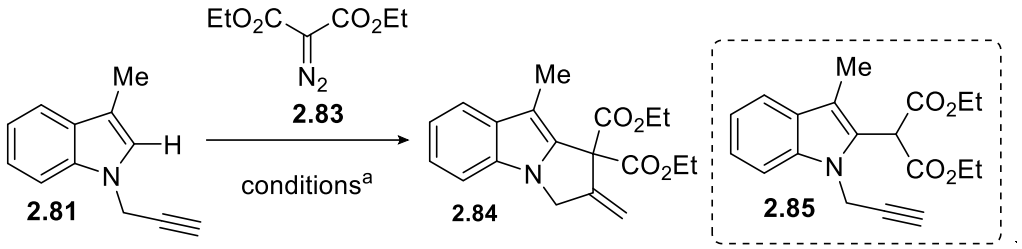

Entry	Catalyst	Solvent	Temp	Result	
				2.84	**2.85**
1	$Rh_2(OAc)_4$	C_6H_6	rt	2%	37%
2	$Rh_2(OAc)_4$	C_6H_6	reflux	7%	38%
3	$Rh_2(OAc)_4$	CH_2Cl_2	rt	9%	30%
4	$Rh_2(OAc)_4$	CH_2Cl_2	reflux	12%	34%
5	$Rh_2(esp)_2$	CH_2Cl_2	rt	Decomposition	
6	$Rh_2(esp)_2$	CH_2Cl_2	-10 °C	Decomposition	
7	$Rh_2(oct)_4$	CH_2Cl_2	reflux	trace[b]	20%
8	$Rh_2(tfa)_4$	CH_2Cl_2	reflux	5%	20%

[a] Reaction conditions: **2.81** (1.2 equiv), **2.83** (1.0 equiv), cat. (2 mol%), solvent (0.2 M), time (2 -3 h). [b]trace: visible just above NMR spectrum baseline.

Next, we focused on the development of a dual catalyst system capable of promoting both C-2 functionalization and Conia-ene cyclization. With $Rh_2(OAc)_4$ as the catalyst we examined several Lewis acid co-catalysts known to promote the cyclization event (Cu, Ag, Zn).[25] To our satisfaction, some of them produced **2.84** as the major isolable product (Table 2.3, entries 3 and 6), with $ZnBr_2$ providing the highest yield at 47% (Table 2.3, entry 10). It is noteworthy that the 5-*exo*-cyclization product **2.84** is the sole cyclization product formed with copper or zinc co-catalysis, but the 6-*endo*-cyclization product **2.86** was also formed with silver salts as a co-catalyst

(Table 2.3, entries 4 and 5). Conia-ene reaction generally proceeds with *exo-dig* regioselectivity to create the smaller ring; however, several catalysts with different modes of activation can dictate the outcome for the Conia-ene cyclization (Section 2.3.1, Figure 2.3). We believe the 6-*endo* product **2.86** comes either from π-activation of the alkyne by Ag (soft carbophilic Lewis acid) through the two-metal double activation mode of Conia-ene reaction (Figure 2.3E) or alkyne activation when a soft carbophilic Lewis acid coordinates to alkyne moiety and enhances its electrophilicity (Figure 2.3B).

Table 0.3: Survey of dual catalyst system for the synthesis of **2.84**.

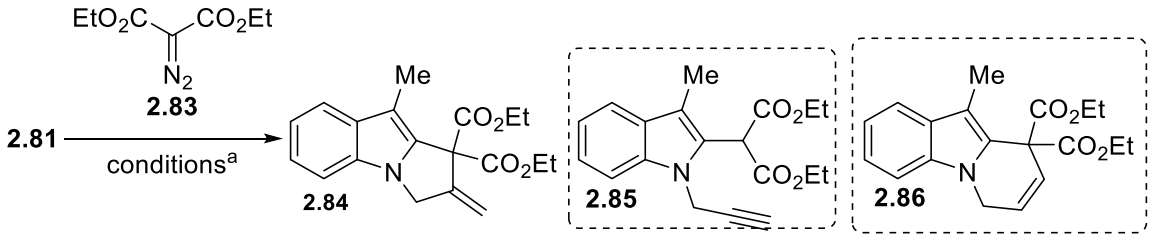

Entry	Catalyst	Co-Catalyst	Solvent	Temp	Result		
					2.84	**2.85**	**2.86**
1	$Rh_2(OAc)_4$	$Sc(OTf)_3$	CH_2Cl_2	reflux	4%	44%	0
2	$Rh_2(OAc)_4$	$Cu(acac)_2$	CH_2Cl_2	reflux	28%	24%	0
3	$Rh_2(OAc)_4$	$Cu(OTf)_2$	CH_2Cl_2	reflux	47%	5%	0
4	$Rh_2(OAc)_4$	$AgBF_4$	CH_2Cl_2	reflux	24%	4%	20%
5	$Rh_2(OAc)_4$	Ag(OAc)	CH_2Cl_2	reflux	9%	20%	1%
6	$Rh_2(OAc)_4$	$Zn(OTf)_2$	CH_2Cl_2	reflux	30%	10%	0
7	$Rh_2(OAc)_4$	$ZnCl_2$	CH_2Cl_2	reflux	23%	35%	0
8	$Rh_2(OAc)_4$	$ZnCl_2/MgSO_4$[b]	CH_2Cl_2	reflux	10%	30%	0
9	$Rh_2(OAc)_4$	$ZnCl_2$/4 Å MS[b]	CH_2Cl_2	reflux	12%	27%	0
10	$Rh_2(OAc)_4$	$ZnBr_2$	CH_2Cl_2	reflux	47%	0	0

[a] Reaction conditions: **2.81** (1.2 equiv), **2.83** (1.0 equiv), cat. (2 mol%), co-cat. (10 mol%) solvent (0.2 M), [b]loading (50 mol%).

The application of cooperative catalysis (entry 10) resulted in partial success in terms of achieving the desired transformation. However, the yield under 50% was not satisfactory. Initially, dimerization of the limiting reagent diazo compound seemed to be a possible reason for lower yields. In literature, diazocarbonyl compounds are known to undergo dimerization reactions.[26] To circumvent diazo dimerization, the dual catalyst reaction conditions (entry 10) were replicated while adding diazo reagent **2.83** slowly (over 2 to 6 h) using a syringe pump. However, this modification did not lead to any noticeable change in the overall yield. It is essential to note that during optimization, the formation of a byproduct was identified by TLC analysis (Figure 2.5). Unfortunately, the identification of this material by NMR analysis was inconclusive because of the complexity of the spectra, which indicated multiple byproducts. Moreover, this byproduct mixture was inseparable through both column and preparative TLC purification techniques in various solvent systems.

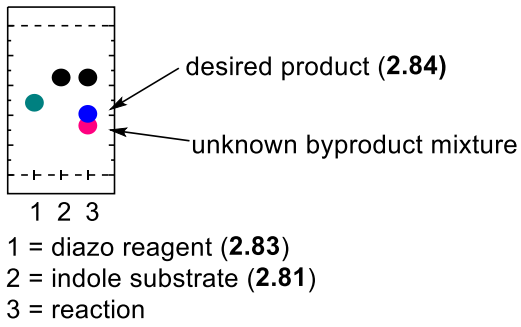

Figure 0-5: TLC analysis of the reaction of **2.81** with **2.83.**

Although complete elucidation of the unknown mixture (Figure 2.5) was not possible by ^{1}H NMR, it was clear by the presence of aromatic and ethyl ester proton resonances that both the diazo and indole components were incorporated in this material. It was hypothesized that there might be a selectivity issue with the carbene C–H insertion step of the reaction, and thus, it was decided to explore a comparatively less reactive diazomalonate reagent, in hopes of achieving

higher levels of selectivity. To this end, bis(2,2,2-trifluoroethyl) malonate (**2.90**) was synthesized through acid-catalyzed esterification of malonic acid **2.87** and trifluoroethanol **2.88** (Scheme 2.13). Trifluoroethyl malonate **2.89** was then subjected to Regitz diazo transfer reaction conditions and this provided bis(2,2,2 trifluoroethyl)-2-diazomalonate (**2.90**) in a 70% overall yield.

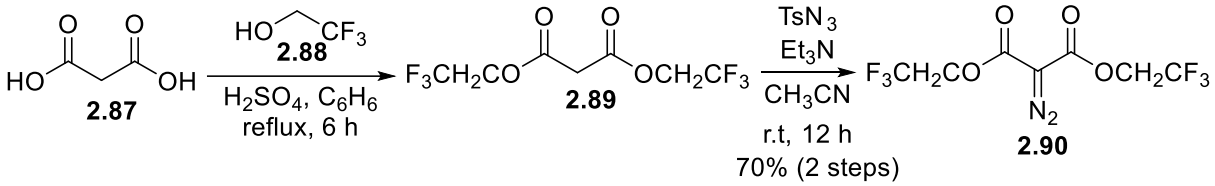

Scheme 0.13: Synthesis of bis(2,2,2-trifluoroethyl)2-diazomalonate **2.90**.

Under the previously optimized conditions, $Rh_2(OAc)_4$, $ZnBr_2$, CH_2Cl_2, the change in the reagent to bis(2,2,2-trifluoroethyl)2-diazomalonate **2.90** resulted in an increase in yield of the desired cyclization product **2.91** to 57% (Table 2.4, entry 1) but the byproduct spot persisted as observed from TLC analysis. A further solvent screen was then performed (Table 2.4, entry 2-7), revealing improved reaction conditions (entry 7), which provided a 64% yield of desired pyrroloindole **2.91**. Interestingly, no reaction occurred when acetonitrile was used as the solvent. Upon addition of $Rh_2(OAc)_4$ to the reaction mixture, there was an immediate color change from light greenish to a dark purple, presumably indicating ligand exchange of acetate with acetonitrile and halting the reaction.[27]

Table 0.4: Optimization using bis(2,2,2-trifluoroethyl)2-diazomalonate **2.90**.

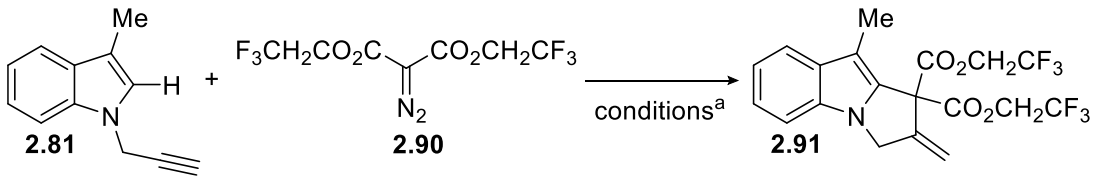

Entry	Catalyst	Co-Catalyst	Solvent	Temp	Result (yield)
1	$Rh_2(OAc)_4$	$ZnBr_2$	CH_2Cl_2	reflux	57%

2	$Rh_2(OAc)_4$	$ZnBr_2$	toluene	reflux	45%
3	$Rh_2(OAc)_4$	$ZnBr_2$	1,4-dioxane	reflux	35%
4	$Rh_2(OAc)_4$	$ZnBr_2$	EtOAc	reflux	37%
5	$Rh_2(OAc)_4$	$ZnBr_2$	MeCN	reflux	NR
6	$Rh_2(OAc)_4$	$ZnBr_2$	C_6F_6	70 °C	52%
7	$Rh_2(OAc)_4$	$ZnBr_2$	$PhCF_3$	90 °C	64%

[a] Reaction conditions: **2.81** (1.2 equiv), **2.90** (1.0 equiv), cat. (2 mol%), co-cat. (10 mol%), solvent (0.2 M), time (2 - 3 h), NR = no reaction.

In order to elucidate the structure of the byproduct formed in the reaction, different solvent combinations for TLC analysis were examined. Fortunately, by changing the diazo reagent from **2.83** to **2.90** (Table 2.4), a separation of the byproduct mixture in 20% acetone in hexane solvent system was observed. Notably, the same solvent system showed no separation of the byproduct mixture produced from the reaction with the diethyl diazomalonate **2.83** (Table 2.3). After a traditional TLC analysis (Figure 2.6A) showed two different spots with different retention factors, a preparative TLC purification (Figure 2.6B) using a 20% acetone in hexanes solvent system, was performed. Interestingly after developing the TLC plate one time in the acetone/hexanes mixture, three bands were visible, and after running the same plate two more times, a fourth band was revealed.

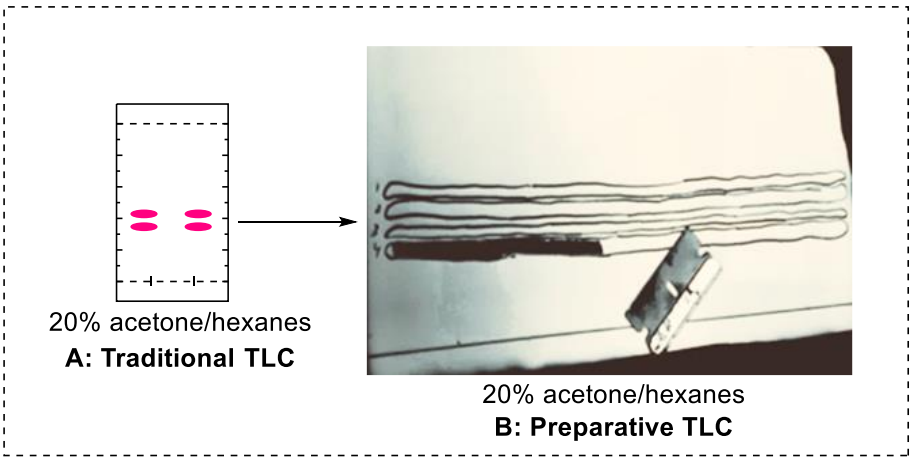

Figure 0-6: Preparative TLC separation of byproduct mixture.

NMR analysis of the four different bands revealed four products that result from competing benzenoid insertions (Scheme 2.14). Among these byproducts, two were the result of insertion on the benzenoid ring leading to the C-5 insertion product **2.92** and the C-6 insertion product **2.93**. The other two byproducts had undergone the desired C-2 insertion/annulation along with a second insertion on the benzenoid ring providing **2.94** and **2.95**. To the best of our knowledge, this is the first example of indole benzenoid functionalization by means of an α-diazodicarbonyl without using a directing group; presumably, the methyl blocking group at the C-3 position of indole and the increased steric interactions created by the nitrogen substituent around the C-2 position lead to a such unique outcome.

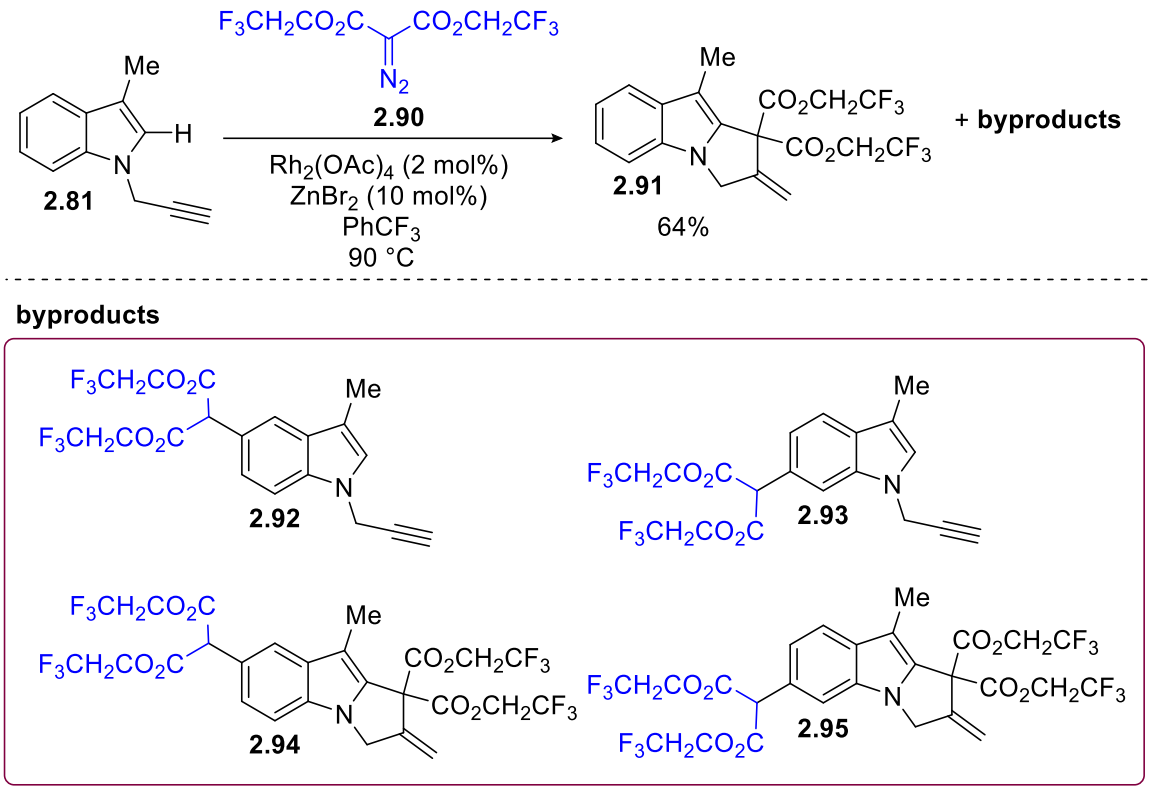

Scheme 0.14: Products of competing benzenoid insertions.

Using the conditions listed in entry 1 (Table 2.4), we conducted a new experiment to determine the yield of benzenoid insertion products. The yield of byproducts **2.92** and **2.93** were 8% and 3%, respectively. A similar experiment was conducted using the conditions outlined in entry 7 (Table 2.4). In addition to the 64% yield of desired product, byproducts **2.92** and **2.93** contributed 9% and 7%, respectively. In both repeated experiments above, byproducts **2.94** and **2.95** were only observed in trace amounts through ^{1}H NMR analysis; thus, yields could not be accurately determined.

Considering the competitive carbene C–H insertion onto the benzenoid ring of indole, we predicted that adding a substituent to the C-5/6 position of the starting material would prevent the competing reaction, allowing the limiting reagent diazo **2.90** to couple to the indole substrate at the desired site. As an experiment to test this hypothesis, 5-methoxy-*N*-propargylskatole **2.96** was

reacted with **2.90** under optimized reaction conditions (Scheme 2.15). As expected, pyrroloindole **2.97** with a C-5 methoxy substituent was obtained in a higher yield (76%) than its unsubstituted counterpart **2.91** (64%).

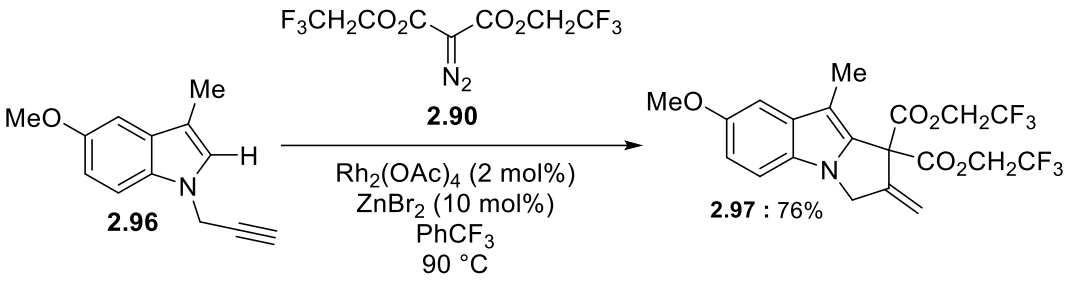

Scheme 0.15: Incorporation of a blocking group at the C-5 position on indole for the synthesis of **2.97**.

Next, we evaluated the tolerance of different α-diazocarbonyl compounds to our optimized dual catalyst reaction conditions (Scheme 2.16). Upon treatment of indole **2.96** with diazo reagents containing different substituents, diethyl (**2.100**, 65%) and dimethyl (**2.101**, 58%) derivatives produced slightly lower yields as compared to **2.97** (Scheme 2.15, 76%) produced from the use of the diazo-bis(2,2,2-trifluoroethyl) malonate **2.90**. The use of more reactive α-diazoketoesters (**2.99**) or α-diazodiketone (not shown in scheme 2.16) provided low yields (**2.102**) or failed to deliver the desired product, and the indole starting material was recovered almost entirely. Potentially, under the current conditions, these types of acceptor/acceptor diazo reagents may be more prone to dimerization and other side reactions compared to the diazomalonates.[26] Additionally, donor/acceptor ethyl α-diazobenzeneacetate compound (not shown) was found to be consumed under the optimal reaction conditions, but led only to intractable product mixtures with no evidence of pyrroloindole ring formation.

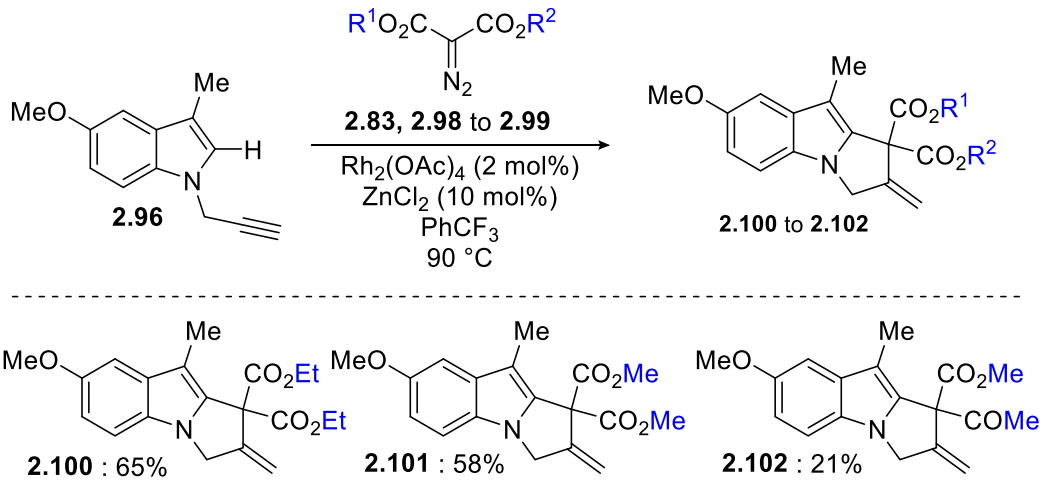

Scheme 0.16: Exploring the influence of diazo substituents on the synthesis of pyrroloindoles.

Having identified a suitable diazo reagent **2.90**, we next explored the tolerance of our reaction conditions to varying substituents at the C-5 and C-6 positions of the indole starting material (Scheme 2.17). It was observed that under optimal reaction conditions, strong electron-donating groups (OMe) and alkyl substituents were tolerated and produced the desired pyrroloindoles **2.97** (5-OMe), **2.119** (6-OMe), and **2.120** (6-Me) in moderate yields. The substrates with halogen substituents produced the highest yields (**2.113**, **2.114**, and **2.121**). The tandem reaction was successful with indoles bearing several reactive functional groups such as esters, additional aromatics, and *α,β*-unsaturated olefins, giving the pyrroloindoles **2.115**, **2.116**, and **2.117**, in yields of 80%, 82%, and 79% respectively. Notably, when indole was substituted with a strong electron-withdrawing group (NO_2), a sharp decline in reactivity was observed, as illustrated by the 21% yield of pyrroloindole **1.118**. The result is not unexpected since it has been demonstrated that the deactivating nature of the nitro group (and other EWGs) at the C-5 position makes the indole core electron deficient and less likely to undergo coupling with the electrophilic metal carbenoid.[8]

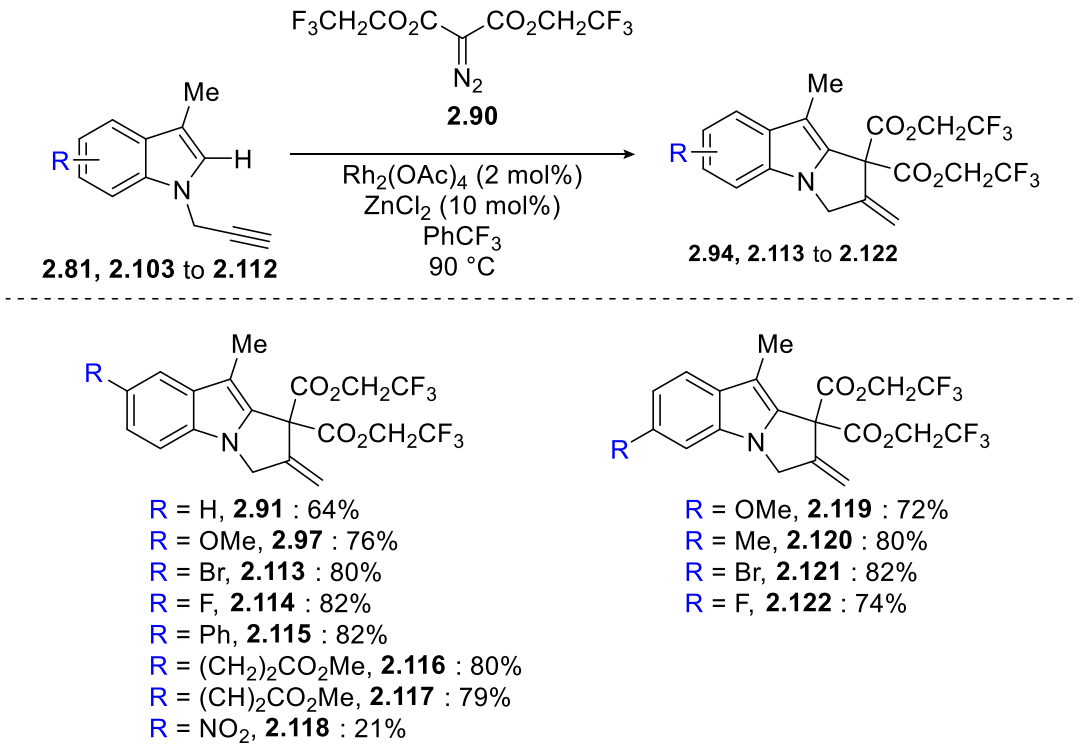

Scheme 0.17: C-5, C-6 substituted indole substrate scope.

Interestingly, when a nitrile group is placed on the indole, it also leads to the formation of pyrroloindole **2.123** (13%) in low yields (Scheme 2.18A). However, this product was also isolated with byproducts oxazole **2.125** in a 23% yield (formed through a [3 + 2] cycloaddition between the in situ generated rhodium carbene and the nitrile group)[28]and the bis-functionalized product **2.126** in a 15% yield. Inspired by this outcome, we envisioned that if the diazo reagent was used in excess, the bis-functionalized product could be obtained as the major product of the reaction. As a result of adding an excess of diazo reagent **2.90** to the nitrile skatole **2.123** portion-wise, bis-functionalized product **2.126** was synthesized in 56% yield (Scheme 2.18B).

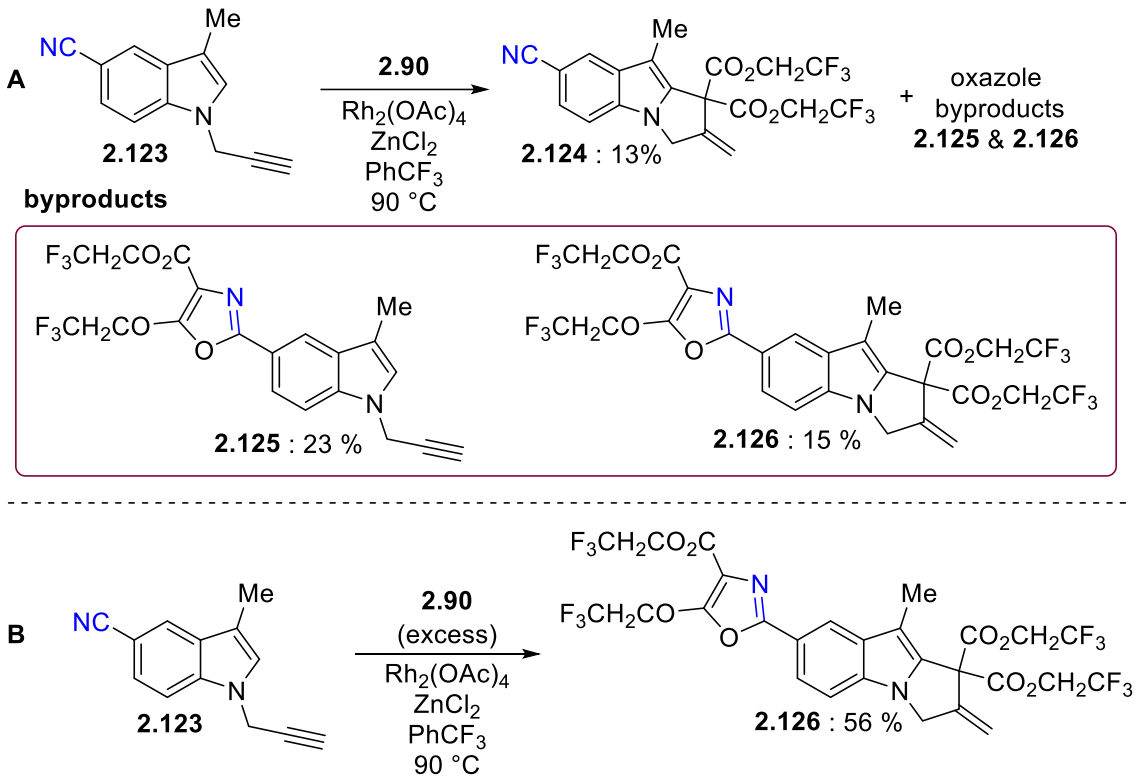

Scheme 0.18: (**A**) Synthesis of pyrroloindole **2.124** and oxazole **2.125** and (**B**) Synthesis of bis-functionalized product **2.126**.

Exploring the scope of this reaction by investigating indole starting materials containing various substituents at the C-3 position led to a series of noteworthy observations (Scheme 2.19). First, as expected, due to the intrinsic electronic nature of indole, an absence of substitution at the C-3 position (**2.133**, where R^1 = H) leads to selective C-3 functionalization (**2.140**, 88%) and, thus, no pyrroloindole. Secondly, when the C-3 methyl group is replaced with a longer alkyl group, the isolated yield of the desired compound decreases substantially. For example, alkyl-substituted indoles **2.127** and **2.129** afford the corresponding pyrroloindoles **2.134** and **2.136** in 38% and 30% yield, respectively. While this outcome was disappointing, adding a methoxy group to the benzenoid ring, the C-3 substituted starting materials cleanly converted to pyrroloindoles **2.135** (74%) and **2.137** (57%) in modest to good yields, confirming the significance of blocking group

to avoid the competing benzenoid insertion. However, this approach is only applicable to certain types of C-3 substituents, as we noticed a drop in yield when the electronics or size of the substituent group were changed (e.g., **2.138** and **2.139**). Most likely, this decrease in yield occurs because the electron withdrawing groups render indole electron deficient. In addition, the bulky substituents create steric hindrance during the C–H functionalization step of the reaction process, thereby preventing indole reactivity.

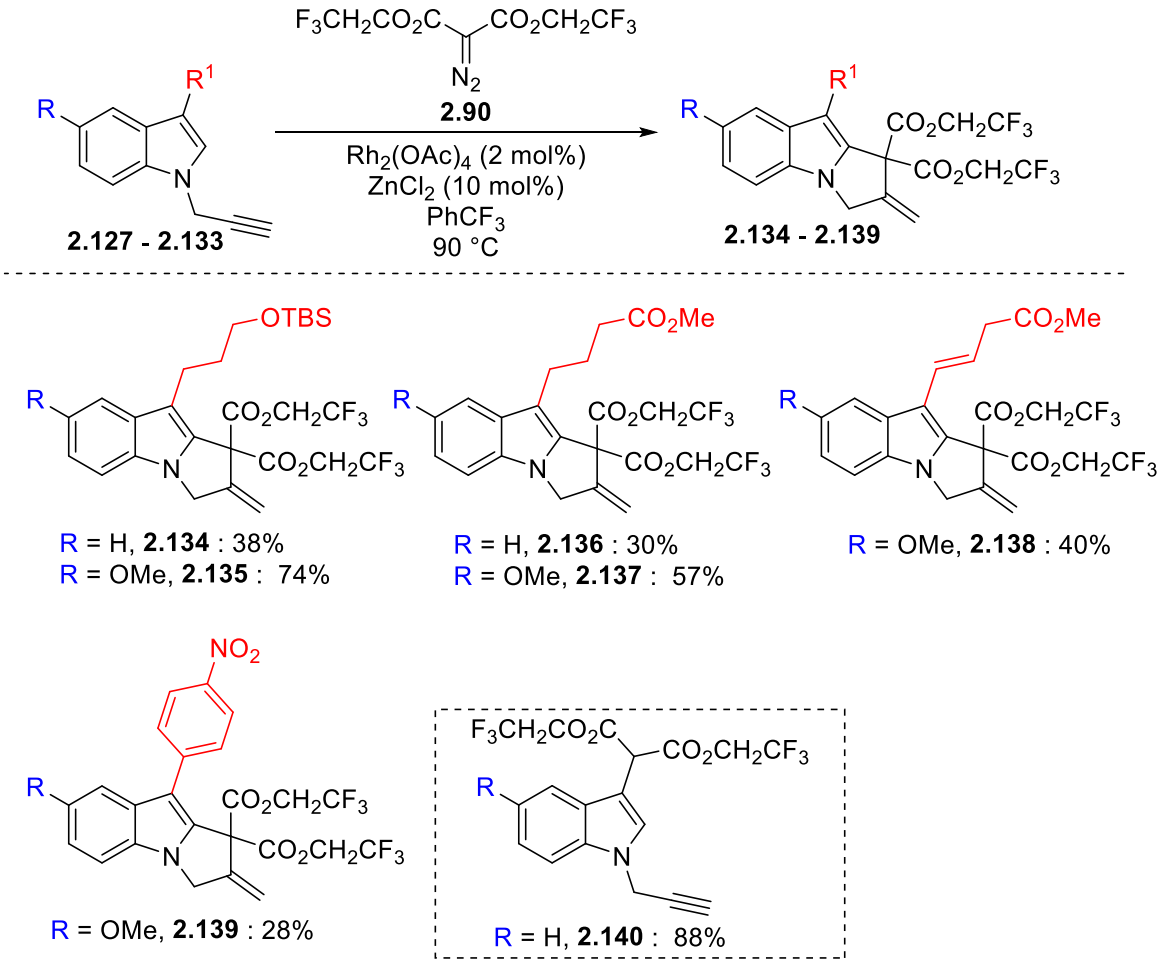

Scheme 0.19: Indole C-3 substitution scope.

The next step was to extend the pendant alkyl chain substituted on the indole nitrogen of the starting material in order to target larger ring systems *via* Conia-ene cyclization. It was challenging to synthesize longer chain *N*-alkylated indole substrates using classical conditions,

which use sodium hydride and alkyl halides in DMF (Scheme 2.20, path a). This was likely due to the decreased electrophilic nature of 4-bromo-1-butyne **2.142** in comparison to the propargyl bromide **2.80** used previously as the alkylating agent. Initially, we tried halide exchange with KI to create the more reactive alkyl iodide before reacting with indole (Scheme 2.20, path b), but this experiment also failed. To resolve this problem, indole was reduced to the more basic nitrogen derivative, indoline **2.144**, with sodium cyanoborohydride in glacial acetic acid (Scheme 2.20, path c). Finally, reaction with alkyl iodide furnished **2.145,** and then oxidation under chloranil in methyl tert-butyl ether conditions produced *N*-alkylated indole products **2.143 – 2.146**.

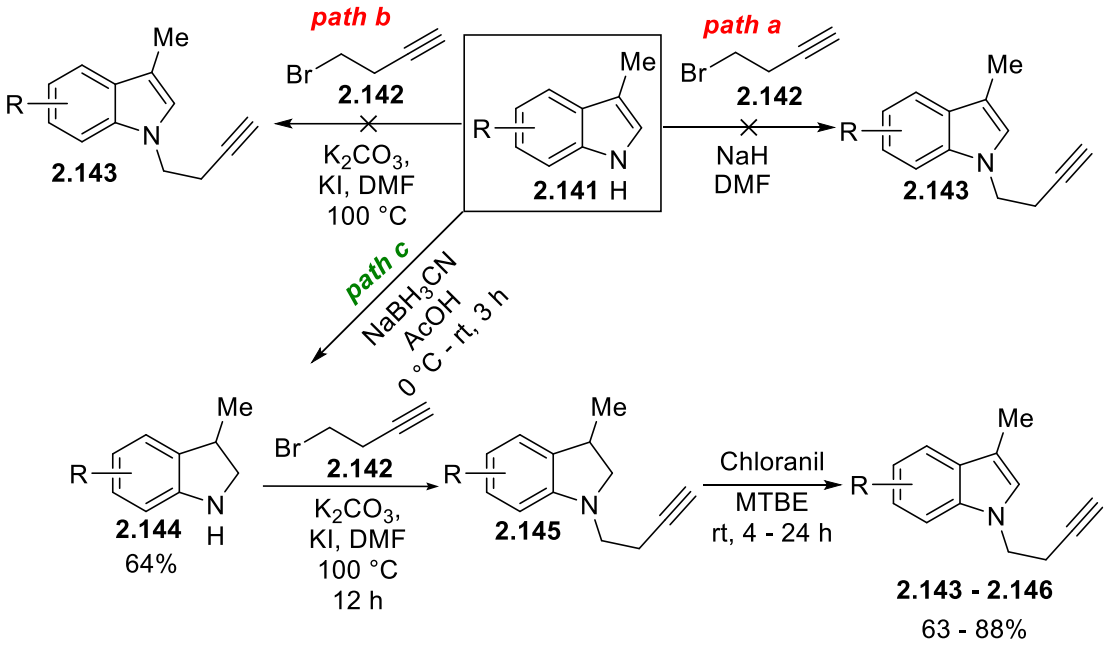

Scheme 0.20: Synthetic pathways for the synthesis of **2.143** – **2.146**.

Similarly to *N*–propargylskatoles, the one carbon homologue series (*N*–butynylskatoles) all undergo the tandem C−H functionalization/6-*exo* Conia-ene cyclization with diazo **2.90** to provide tetrahydropyrido[1,2-*α*]indoles (pyridoindoles: **2.148** to **2.151**) in modest to good overall yields (Scheme 2.21). Moreover, the pyrido[1,2-*α*]indole system and its analogs are found in a large variety of natural compounds and pharmaceuticals, for example, neuronal stem cell

proliferation promoter alstoscholarisine *A* **2.152**.[29] This tandem approach may prove to be an efficient route for synthesizing related targets in the future.

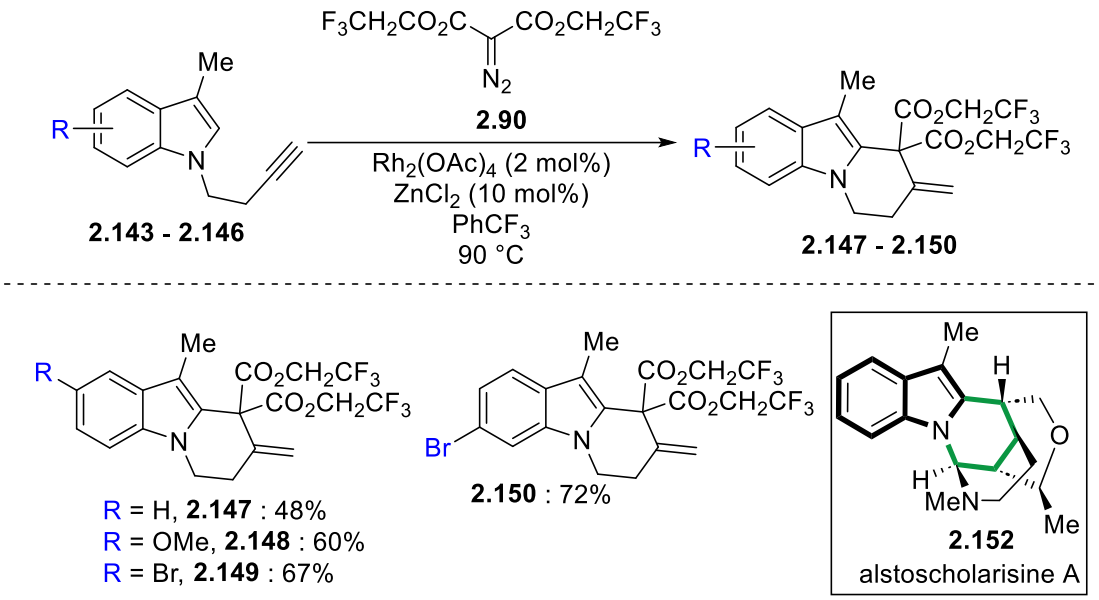

Scheme 0.21: Synthesis of tetrahydropyrido[1,2-*a*]indoles **2.148** – **2.151** from *N*–butynylskatoles; alstoscholarisine A (**2.152**) a notable pyrido[1,2-*a*]indole natural product.

Inspired by the success in the synthesis of the pyridoindole ring system *via* the tandem transformation, a further extension of the pendant alkyne chain on indole nitrogen of the starting material was investigated to determine if larger ring systems could be accessed. When the chain length was extended by one more carbon (*N*–pentynylskatoles **2.153**) azepinoindole (**2.155**), which is a result of 7-*exo-dig* cyclization, was obtained in 28% yield (Scheme 2.22). Although **2.155** was only isolated in low overall yield, its formation marks an uncommon ring size resulting from Conia-ene chemistry and was isolated as the sole cyclization product with no indication of the 8-*endo-dig* product being observed. Unfortunately, the 7-membered ring seems to be the largest system possible under current conditions. A further increase in chain length between the indole

nitrogen and the alkyne (*N*–hexynylskatole **2.154**) yielded only the C-2 functionalization product **2.156** in 50% yield.

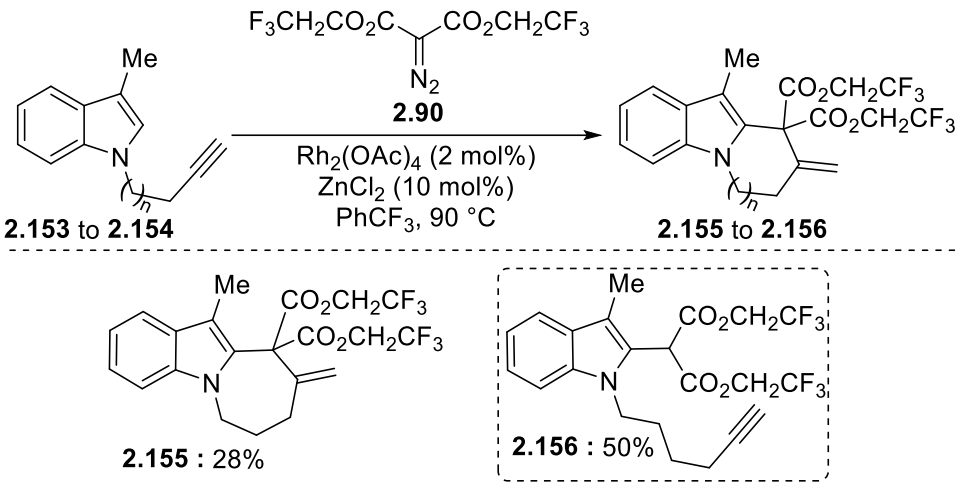

Scheme 0.22: Synthesis of azepinoindole **2.155** and **2.156** from *N*–pentynylskatole.

Finally, as we had observed during our optimization experiments, that apart from the competing formation of C-5/6 benzenoid insertion (**2.92** and **2.93**), there was the formation of bis-functionalized products **2.94** and **2.95** (Scheme 2.23). As a result of this finding, we envisioned that using excess diazo reagent **2.90**, our standard reaction conditions could be effective for the synthesis of bis-functionalized pyrroloindoles from **2.81**. Thus, subjecting skatole **2.81** to the optimized reaction conditions with an excess of diazo **2.90** produced a 56% combined yield of **2.94** and **2.95** (ca. 2:1 mixture). These results demonstrate the potential of this tandem approach in efficiently accessing molecular complexity.

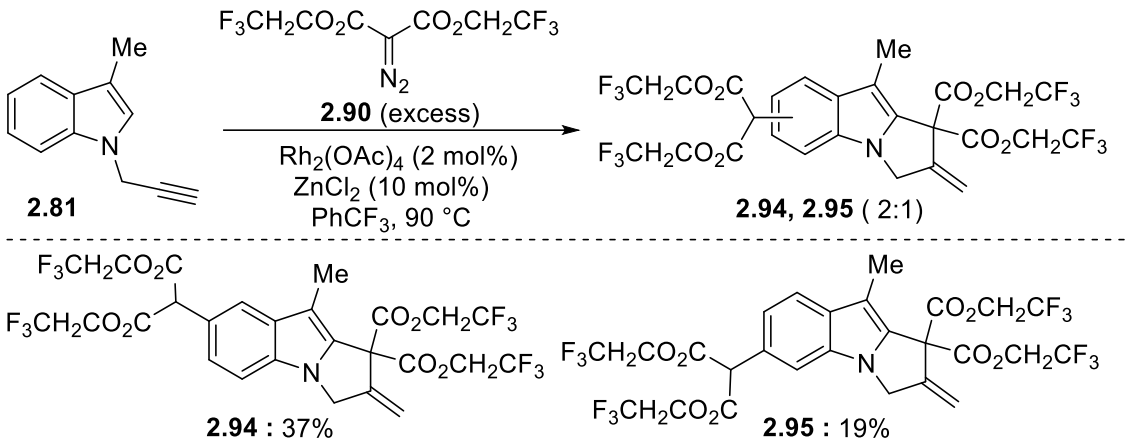

Scheme 0.23: Synthesis of bis-functionalized pyrroloindoles **2.94** and **2.95** using excess diazo **2.90**.

1.16 Summary and Future Outlook

In summary, we have developed a novel synthetic method based on tandem intermolecular C(sp^2)–H insertion and Conia-ene cyclization. This tandem approach provides access to various pyrroloindoles from *N*-propargylindoles and α-diazocarbonyl compounds using Rh(II)/Zn(II) dual catalysis. The method allows for the construction of larger ring systems such as pyridoindoles and azepinoindoles. In addition, various functional groups on the parent indole substrate were well tolerated and produced high yields. By varying the substrate stoichiometry, this method can also be used to synthesize bis-functionalized pyrroloindoles. The future efforts in this methodology can be directed towards exploring compatible silver salts with rhodium to exclusively target 6-*endo-dig* cyclization *via* Conia-ene annulation chemistry, as seen in Table 2.3 (entries 5 and 6). Further, this methodology could be extended to other nucleophilic substrates like glycals (1,2-unsaturated sugar derivatives) (Scheme 2.24A). An alternative area worth investigating involves the exploration of the Thorpe-Ingold effect (angle compression effect)[30] on tethered alkynes. This approach aims to bring the enol moiety and the tethered alkyne into closer proximity, enabling annulation through Conia-ene chemistry. By leveraging this strategy, it may be possible to

overcome the limitation of forming only 7-membered rings within this methodology. (Scheme 2.24B).

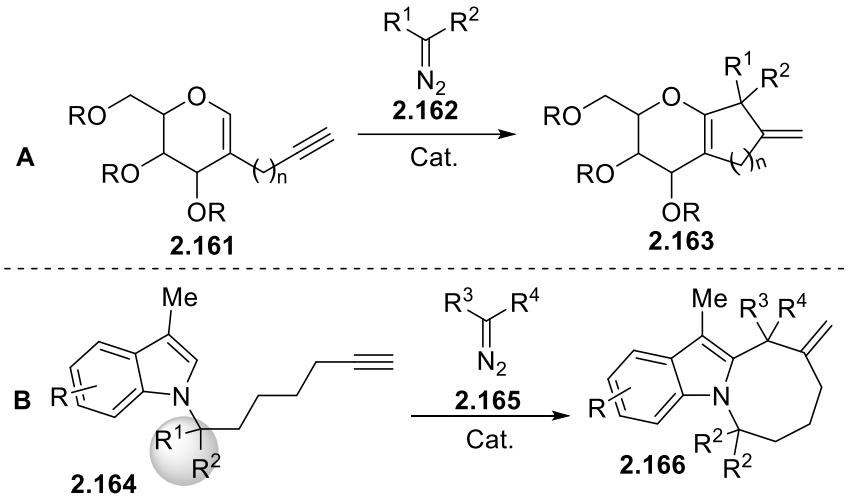

Scheme 0.24: Future outlook for the synthesis of **2.163** and **2.166** using tandem insertion/annulation approach.

1.17 Experimental Section

General Procedures

Unless stated otherwise, all reactions were performed in flame-dried glassware under an atmosphere of dry nitrogen. Dry trifluorotoluene ($PhCF_3$) and *N*,*N*-dimethylformamide (DMF) were obtained from Sigma Aldrich SureSeal™ bottles. Dry methyl *tert*-butyl ether (MTBE) was obtained from Alfa Aesar™. All other reagents were used as received from commercial sources unless stated otherwise. When indicated, solvents or reagents were degassed by sparging with nitrogen for 10 min in an ultrasound bath at 25 °C. For reactions conducted above room temperature, oil bath heating was used as the heat source. Reactions were monitored by thin layer chromatography (TLC) on Silicycle Siliaplate™ glass-backed TLC plates (250 μm thickness, 60 Å porosity, F-254 indicator) and visualized by UV irradiation or development with an anisaldehyde. Volatile solvents were removed under reduced pressure with a rotary evaporator. All flash column chromatography was performed using Silicycle SiliaFlash® F60, 230-400 mesh

silica gel (40-63 μm). ^{1}H NMR and ^{13}C NMR spectra were recorded with Bruker AV, spectrometers operating at 300 or 500 MHz for ^{1}H (75 or 125 MHz for ^{13}C) in $CDCl_3$ or acetone-D_6. Except when noted otherwise, chemical shifts are reported relative to the residual solvent signal (^{1}H NMR: δ = 7.26 ($CDCl_3$), δ = 2.05 (acetone-D_6); ^{13}C NMR: δ = 77.16 ($CDCl_3$)). NMR data are reported as follows: chemical shift (multiplicity, coupling constants where applicable, number of hydrogens). Splitting is reported with the following symbols: s = singlet, bs = broad singlet, d = doublet, t = triplet, app t = apparent triplet, dd = doublet of doublets, ddd = doublet of doublet of doublets, dddd = doublet of doublet of doublet of doublets, m = multiplet. Infrared (IR) spectra were recorded using neat samples on a Bruker Alpha spectrometer. High resolution mass spectrometry (HRMS) data were obtained using an Agilent 6200 series instrument employing a TOF mass analyzer. Melting points (M.P.) were obtained on an OptiMelt instrument (a digital apparatus) produced by Stanford Research Systems by scanning temperature ranges from 40 - 150 °C at a rate of 3 °C/s.

Synthesis and Characterization of Substituted Indole Starting Materials

Scheme 2.25: General Synthetic Scheme for the Synthesis of Substituted *N*-Propargyl Indole Compounds

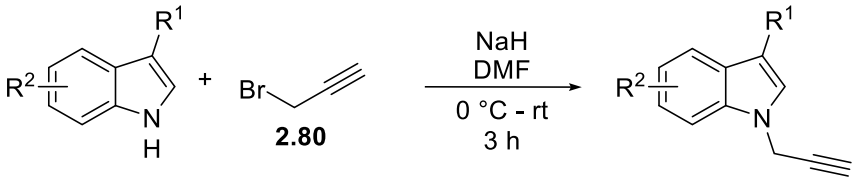

2.79, **2.167** to **2.184** — **2.80** — **2.81**, **2.96**, **2.103** to **2.112**

General Experimental Procedure A:

Substituted indole **2.79**, **2.167 – 2.184** (1 equiv) was added to a round-bottom flask equipped with a magnetic stir bar and dissolved in DMF (2.5 mL/mmol of indole) under a N_2 atmosphere. The solution was cooled to 0 °C and NaH (60 % dispersion in mineral oil, 2.0 equiv) was added. The resulting slurry was stirred for 1 h at 0 °C, followed by the dropwise addition of propargyl bromide (80 wt. % solution in toluene, 2.0 equiv). The reaction mixture was then warmed to room temperature and stirred for 2 h. When the reaction was considered complete as determined by TLC analysis, the mixture was slowly quenched with H_2O, extracted three times with ethyl acetate, washed twice with H_2O, washed once with brine, dried over anhydrous Na_2SO_4, and concentrated *in vacuo*. The resulting residue was purified by silica gel flash column chromatography using a hexanes/EtOAc gradient to yield the substituted *N*-propargyl indole **2.81, 2.96, 2.103 – 2.112**. Note: Substituted indole starting materials (**2.79, 2.167 – 2.184**) were used directly from commercial sources or synthesized following known literature procedures.[31] and detailed experimental procedure can be found in published supporting information available at https://pubs.acs.org/doi/10.1021/acs.orglett.9b04210.

Note: In the ^{1}H-NMR spectra of N-propargylindole starting material compounds, the methyl group at the C-3 position on the indole moiety exhibits coupling with the C-2 hydrogen, resulting in a characteristic "doublet" pattern. However, interestingly, in the reverse scenario, the C-2 hydrogen does not manifest as a "quartet" as expected but rather appears predominantly as a broad rounded "doublet" or, in some cases, as a broad rounded "singlet".

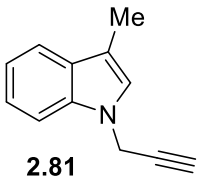

2.81

^{1}H NMR (300 MHz, $CDCl_3$): δ 7.57 – 7.53 (m, 1H), 7.30 (dd, *J* = 8.2, 1.0 Hz, 1H), 7.25 – 7.17 (m, 1H), 7.12 (ddd, *J* = 7.9, 7.0, 1.1 Hz, 1H), 6.90 (d, *J* = 1.1 Hz, 1H), 4.71 (d, *J* = 2.5 Hz, 2H), 2.33-2.26 (m, 4H). ^{13}C NMR (75 MHz, $CDCl_3$): δ 136.3, 129.3, 124.9, 121.9, 119.3, 111.5, 109.3, 78.3, 73.2, 35.5, 9.7. (*one carbon missing due to overlap at 119.3)* IR (neat): 3285, 2885, 1480, 1328, 924, 735 cm^{-1} HRMS (APPI+): calc'd for $C_{12}H_{11}N$ $[M+H]^+$ 170.0964, found 170.0960.

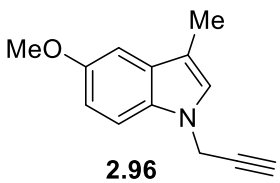

2.96

^{1}H NMR (300 MHz, $CDCl_3$): δ 7.24 (d, *J* = 8.8 Hz, 1H), 7.00 (d, *J* = 2.3 Hz, 1H), 6.93 (d, *J* = 0.7 Hz, 1H), 6.89 (dd, *J* = 8.8, 2.5 Hz, 1H), 4.76 (d, *J* = 2.5 Hz, 2H), 3.86 (s, 3H), 2.34 (t, *J* = 2.5 Hz, 1H), 2.28 (d, *J* = 1.0 Hz, 3H). ^{13}C NMR (75 MHz, $CDCl_3$): δ 154.2, 131.6, 129.7, 125.7, 112.1, 111.1, 110.1, 101.4, 78.3, 73.2, 56.1, 35.8, 9.8. IR (neat): 3257, 2918, 1490, 1227, 1045, 786 cm^{-1} HRMS (APPI+): calc'd for $C_{13}H_{13}NO$ $[M+H]^+$ 200.1070, found 200.1061.

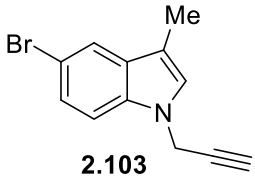

2.103

^{1}H NMR (300 MHz, $CDCl_3$): δ 7.67 – 7.65 (m, 1H), 7.27 (dd, *J* = 8.7, 1.8 Hz, 1H), 7.16 (d, *J* = 8.6 Hz, 1H), 6.90 (d, *J* = 0.9 Hz, 1H), 4.70 (d, *J* = 2.5 Hz, 2H), 2.34 (t, *J* = 2.5 Hz, 1H), 2.24 (d, *J* = 1.1 Hz, 3H). ^{13}C NMR (75 MHz, $CDCl_3$): δ 134.9, 131.1, 126.2, 124.7, 122.0, 112.7, 111.2, 110.8, 77.8, 73.6, 35.8, 9.6. IR (neat): 3410, 2916, 1444, 1354, 1227, 867, 790, 580 cm^{-1} HRMS (APPI+): calc'd for $C_{12}H_{10}BrN$ $[M+H]^+$ 248.0069, found 248.0065

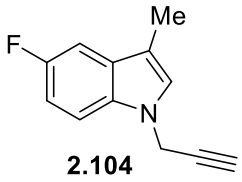

2.104

^{1}H NMR (300 MHz, $CDCl_3$): δ 7.25 (dd, *J* = 9.1, 4.0 Hz, 1H), 7.20 (dd, *J* = 9.5, 2.4 Hz, 1H), 7.01 – 6.93 (m, 2H), 4.79 (d, *J* = 2.5 Hz, 2H), 2.37 (t, *J* = 2.5 Hz, 1H), 2.27 (d, *J* = 1.0 Hz, 3H). ^{13}C NMR (75 MHz, $CDCl_3$): δ 158.0 (d, *J* = 234.5 Hz), 132.9, 129.7 (d, J = 9.4 Hz), 126.7, 111.5 (d, *J* = 4.8 Hz), 110.2 (d, *J* = 26.4 Hz), 110.0 (d, *J* = 9.7 Hz), 104.3 (d, *J* = 23.2 Hz), 78.0, 73.5, 35.9, 9.7. IR (neat): 3263, 1429,

900, 1224, 927, 787 cm^{-1} HRMS (APPI+): calc'd for $C_{12}H_{10}FN$ $[M+H]^+$ 188.0870, found 188.0876.

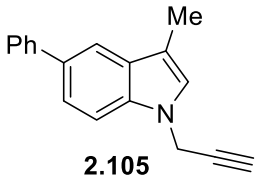

2.105

^1H NMR (500 MHz, $CDCl_3$): δ 7.76 (dd, *J* = 1.7, 0.6 Hz, 1H), 7.71 – 7.59 (m, 2H), 7.49 (dd, *J* = 8.5, 1.7 Hz, 1H), 7.47 – 7.38 (m, 3H), 7.39 – 7.22 (m, 1H), 6.98 (d, *J* = 1.0 Hz, 1H), 4.82 (d, *J* = 2.5 Hz, 2H), 2.37 (t, *J* = 2.5 Hz, 1H), 2.35 (d, *J* = 1.1 Hz, 3H). ^{13}C NMR (75 MHz, $CDCl_3$): δ 142.8, 135.8, 133.0, 129.8, 128.8, 127.6, 126.4, 125.7, 121.8, 118.0, 112.0, 109.5, 78.2, 73.4, 35.8, 9.8. IR (neat): 3282, 1473, 1181, 758, 695 cm^{-1} HRMS (APPI+): calc'd for $C_{18}H_{15}N$ $[M+H]^+$ 246.1277, found 246.1284.

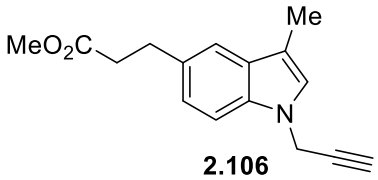

2.106

^1H NMR (300 MHz, $CDCl_3$): δ 7.37 (d, *J* = 0.9 Hz, 1H), 7.25 (d, *J* = 8.4 Hz, 1H), 7.07 (dd, *J* = 8.4, 1.6 Hz, 1H), 6.91 (d, *J* = 0.9 Hz, 1H), 4.74 (d, *J* = 2.5 Hz, 2H), 3.66 (s, 3H), 3.17 – 2.90 (m, 2H), 2.82 – 2.55 (m, 2H), 2.33 (t, *J* = 2.5 Hz, 1H), 2.29 (d, *J* = 1.0 Hz, 3H). ^{13}C NMR (75 MHz, $CDCl_3$): δ 173.8, 135.1, 131.5, 129.6, 125.3, 122.7, 118.5, 111.3, 109.3, 78.3, 73.2, 51.7, 36.9, 35.7, 31.4, 9.7. IR (neat): 3234, 1701, 1602, 1378, 1082, 744 cm^{-1} HRMS (APPI+): calc'd for $C_{16}H_{17}NO_2$ [M] 255.1259, found 255.1261.

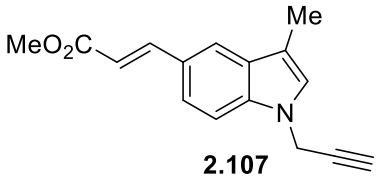

2.107

^1H NMR (300 MHz, $CDCl_3$): δ 7.85 (d, *J* = 15.9 Hz, 1H), 7.71 (d, *J* = 1.5 Hz, 1H), 7.44 (dd, *J* = 8.6, 1.6 Hz, 1H), 7.31 (d, *J* = 8.6 Hz, 1H), 6.96 (d, *J* = 1.0 Hz, 1H), 6.42 (d, *J* = 15.9 Hz, 1H), 4.78 (d, *J* = 2.5 Hz, 2H), 3.80 (s, 3H), 2.38 (t, *J* = 2.5 Hz, 1H), 2.31 (d, *J* = 1.1 Hz, 3H). ^{13}C NMR (75 MHz, $CDCl_3$): δ 168.1, 146.8, 137.4, 129.6, 126.1, 126.0, 121.6, 120.8, 114.6, 112.6, 109.8, 77.7, 73.7, 51.6, 35.6, 9.6. IR (neat): 3274, 1711, 1609, 1448, 1162, 806 cm^{-1} HRMS (APPI+): calc'd for $C_{16}H_{15}NO_2$ [M] 253.1103, found 253.1107.

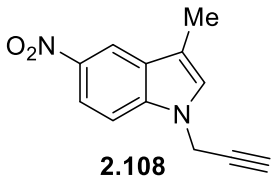

2.108

^{1}H NMR (300 MHz, $CDCl_3$): δ 8.54 (d, *J* = 2.3 Hz, 1H), 8.14 (dd, *J* = 9.0, 2.3 Hz, 1H), 7.38 (d, *J* = 9.0 Hz, 1H), 7.12 (d, *J* = 1.2 Hz, 1H), 4.87 (d, *J* = 2.6 Hz, 2H), 2.44 (t, *J* = 2.5 Hz, 1H) 2.36 (d, *J* = 1.2 Hz, 3H). ^{13}C NMR (75 MHz, $CDCl_3$): δ 141.5, 138.9, 128.7, 127.9, 117.6, 116.6, 114.3, 109.1, 76.9, 74.2, 36.0, 9.4. IR (neat): 3269, 1864, 1613, 1507, 1318, 1073, 787 cm^{-1} HRMS (APPI+): calc'd for $C_{12}H_{10}N_2O_2$ $[M+H]^+$ 215.0815, found 215.0810.

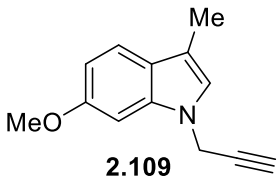

2.109

^{1}H NMR (300 MHz, $CDCl_3$): δ 7.43 (dd, *J* = 8.3, 0.7 Hz, 1H), 6.83 (d, *J* = 1.0 Hz, 1H), 6.82 – 6.77 (m, 2H), 4.74 (d, *J* = 2.5 Hz, 2H), 3.87 (s, 3H), 2.35 (t, *J* = 2.5 Hz, 1H), 2.28 (d, *J* = 1.0 Hz, 3H). ^{13}C NMR (75 MHz, $CDCl_3$): δ 156.7, 137.0, 123.8, 123.8, 119.9, 111.5, 109.0, 93.2, 78.2, 73.2, 55.9, 35.6, 9.8. IR (neat): 3257, 1625, 1443, 1333, 788 cm^{-1} HRMS (APPI+): calc'd for $C_{13}H_{13}NO$ $[M+H]^+$ 200.1070, found 200.1079.

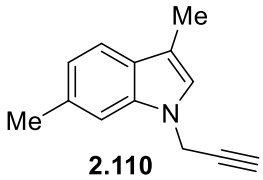

2.110

^{1}H NMR (300 MHz, $CDCl_3$): δ 7.44 (d, *J* = 8.0 Hz, 1H), 7.13 (d, *J* = 0.5 Hz, 1H), 6.96 (dd, *J* = 8.0, 0.8 Hz, 1H), 6.88 (d, *J* = 1.0 Hz, 1H), 4.76 (d, *J* = 2.5 Hz, 2H), 2.49 (s, 3H), 2.34 (t, *J* = 2.5 Hz, 1H), 2.29 (d, *J* = 1.0 Hz, 3H). ^{13}C NMR (75 MHz, $CDCl_3$): δ 136.7, 131.8, 127.2, 124.3, 121.1, 119.0, 111.4, 109.2, 78.4, 73.1, 35.5, 22.0, 9.8. IR (neat): 3286, 1620, 1465, 1328, 799 cm^{-1} HRMS (APPI+): calc'd for $C_{13}H_{13}N$ $[M+H]^+$ 183.1048, found 183.1125.

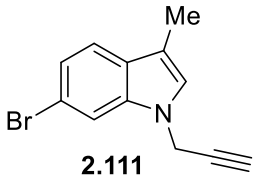

2.111

^{1}H NMR (300 MHz, $CDCl_3$): δ 7.51 (d, *J* = 1.5 Hz, 1H), 7.41 (d, *J* = 8.4 Hz, 1H), 7.22 (dd, *J* = 8.4, 1.7 Hz, 1H), 6.93 (d, *J* = 1.0 Hz, 1H), 4.76 (d, *J* = 2.5 Hz, 2H), 2.39 (t, *J* = 2.5 Hz, 1H), 2.29 (d, *J* = 1.0 Hz, 3H). ^{13}C NMR (75 MHz, $CDCl_3$): δ 137.0, 128.3, 125.6, 122.6, 120.6, 115.7, 112.4, 111.8, 77.7, 73.7, 35.8, 9.6. IR

(neat): 3290, 1462, 1332, 1181, 798, 633 cm^{-1} HRMS (APPI+): calc'd for $C_{12}H_{10}BrN$ $[M+H]^+$ 246.9997, found 247.0013.

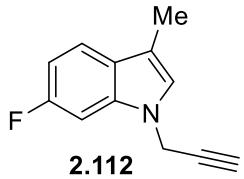

2.112

^1H NMR (300 MHz, $CDCl_3$): 7.45 (dd, *J* = 8.6, 5.3 Hz, 1H), 7.03 (dd, *J* = 9.9, 2.2 Hz, 1H), 6.92 – 6.85 (m, 2H), 4.73 (d, *J* = 2.5 Hz, 2H), 2.37 (t, *J* = 2.5 Hz, 1H), 2.29 (d, *J* = 1.1 Hz, 3H). ^{13}C NMR (75 MHz, $CDCl_3$): δ 160.2 (d, *J* = 237.8 Hz), 136.2 (d, *J* = 12.0 Hz), 125.9, 125.3 (d, *J* = 3.7 Hz) 120.1 (d, *J* = 10.2 Hz) 111.8, 108.0 (d, *J* = 24.5 Hz), 96.0 (d, *J* = 26.6 Hz), 77.8, 73.6, 35.8, 9.7. IR (neat): 3293, 1555, 1469, 1331, 1117, 830 cm^{-1} HRMS (APPI+): calc'd for $C_{12}H_{10}FN$ [M] 187.0797, found 187.0790.

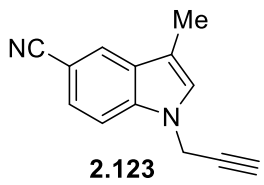

2.123

^1H NMR (300 MHz, $CDCl_3$): δ 7.89 (dd, *J* = 1.4, 0.7 Hz, 1H), 7.44 (dd, *J* = 8.5, 1.5 Hz, 1H), 7.38 (dd, *J* = 8.5, 0.6 Hz, 1H), 7.08 (d, *J* = 1.0 Hz, 1H), 4.83 (d, *J* = 2.6 Hz, 2H), 2.42 (t, *J* = 2.6 Hz, 1H), 2.31 (d, *J* = 1.1 Hz, 3H). ^{13}C NMR (75 MHz, $CDCl_3$): δ 137.7, 129.2, 127.2, 124.9, 124.89, 120.91, 112.6, 110.2, 102.4, 77.4, 74.1, 35.9, 9.4. IR (neat): 3289, 2213, 1574, 809, 639 cm^{-1} HRMS (APPI+): calc'd for $C_{13}H_{10}N_2$ $[M+H]^+$ 195.0922, found 194.0834.·

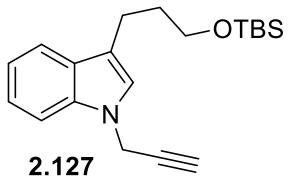

2.127

Note a change in the general procedure: propargyl bromide was added at –10 °C instead of 0 °C. ^1H NMR (300 MHz, $CDCl_3$): δ 7.64 – 7.57 (m, 1H), 7.36 (d, *J* = 8.2 Hz, 1H), 7.26 – 7.21 (m, 1H), 7.15 – 7.09 (m, 1H), 6.98 (s, 1H), 4.82 (d, *J* = 2.5 Hz, 2H), 3.69 (t, *J* = 6.3 Hz, 2H), 2.83 – 2.78 (m, 2H), 2.37 (t, *J* = 2.5 Hz, 1H), 1.97 – 1.88 (m, 2H), 0.92 (s, 9H), 0.06 (s, 6H). ^{13}C NMR (75 MHz, $CDCl_3$): δ 136.3, 128.7, 124.5, 122.0, 119.5, 119.3, 116.3, 109.3, 78.2, 73.3, 62.8, 35.7, 33.3, 26.1, 21.4, 18.5, 5.1. IR (neat): 3309, 2951, 2855, 1465, 1252, 1094, 833, 773 cm^{-1} HRMS (APPI+): calc'd for $C_{20}H_{29}NOSi$ $[M+H]^+$ 328.2097, found 328.2092.

Note a change in the general procedure: propargyl bromide was added at –10 °C instead of 0 °C.

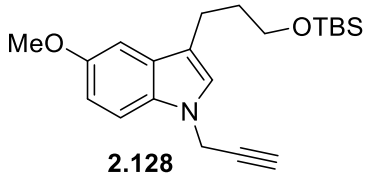

2.128

^{1}H NMR (300 MHz, $CDCl_3$): δ 7.25 (d, *J* = 8.8 Hz, 1H), 7.04 (d, *J* = 2.4 Hz, 1H), 6.95 (s, 1H), 6.89 (dd, *J* = 8.8, 2.4 Hz, 1H), 4.79 (d, *J* = 2.5 Hz, 2H), 3.86 (s, 3H), 3.70 (t, *J* = 6.3 Hz, 2H), 2.80 – 2.73 (m, 2H), 2.36 (t, *J* = 2.5 Hz, 1H), 1.96 – 1.86 (m, 2H), 0.92 (s, 9H), 0.07 (s, 6H). ^{13}C NMR (75 MHz, $CDCl_3$): δ 154.1, 131.7, 129.0, 125.3, 115.8, 112.0, 110.1, 101.5, 78.3, 73.3, 62.9, 56.1, 35.9, 33.3, 26.1, 21.4, 18.5, 5.1. IR (neat): 3287, 2928, 2855, 1485, 1253, 1228, 1094, 832, 773 cm^{-1} HRMS (APPI+): calc'd for $C_{21}H_{31}NO_2Si$ [M] 357.2124, found 357.2131.

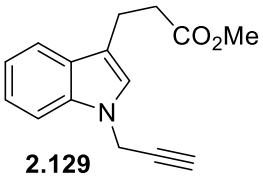

2.129

Note a change in the general procedure: propargyl bromide was added at –10 °C instead of 0 °C. ^{1}H NMR (300 MHz, $CDCl_3$): δ 7.61 – 7.57 (m, 1H), 7.36 (d, *J* = 8.2 Hz, 1H), 7.27 – 7.22 (m, 1H), 7.13 (ddd, *J* = 8.0, 7.1, 1.1 Hz, 1H), 7.01 (s, 1H), 4.82 (d, *J* = 2.5 Hz, 2H), 3.68 (s, 3H), 3.12 – 3.07 (m, 2H), 2.72 (dd, *J* = 8.4, 7.0 Hz, 2H), 2.37 (t, *J* = 2.5 Hz, 1H). ^{13}C NMR (75 MHz, $CDCl_3$): δ 173.9, 136.3, 128.3, 124.7, 122.2, 119.6, 119.2, 114.8, 109.5, 78.0, 73.5, 51.7, 35.7, 34.9, 20.7. IR (neat): 3281, 3053, 2950, 1728, 1465, 1435, 1331, 1161, 778, 425 cm^{-1} HRMS (APPI+) calc'd for $C_{15}H_{15}NO_2$ $[M+H]^+$ 242.1176, found 242.1165.

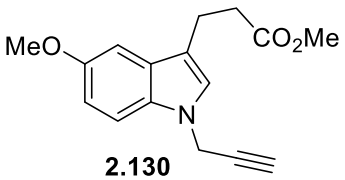

2.130

Note a change in the general procedure: propargyl bromide was added at –10 °C instead of 0 °C. ^{1}H NMR (300 MHz, $CDCl_3$): δ 7.26 (d, *J* = 8.8 Hz, 1H), 7.02 (d, *J* = 2.3 Hz, 1H), 6.98 (s, 1H), 6.90 (dd, *J* = 8.8, 2.4 Hz, 1H), 4.78 (d, *J* = 2.5 Hz, 2H), 3.87 (s, 3H), 3.69 (s, 3H), 3.05 (dd, *J* = 8.6, 6.8 Hz, 2H), 2.71 (dd, *J* = 8.5, 7.0 Hz, 2H), 2.37 (t, *J* = 2.5 Hz, 1H). ^{13}C NMR (75 MHz, $CDCl_3$): δ 173.9, 154.2, 131.6, 128.6, 125.4, 114.2, 112.3, 110.3, 101.1, 78.1, 73.4, 56.1, 51.7, 35.9, 34.8, 20.7. IR (neat):

3277, 2994, 2835, 1728, 1485, 1217, 1170, 1038, 791, 640 cm^{-1} HRMS (APPI+): calc'd for $C_{16}H_{17}NO_3$ $[M+H]^+$ 272.1208, found 272.1211.

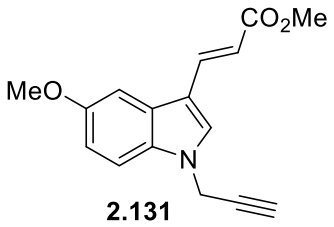

2.131

Note a change in the general procedure: propargyl bromide was added at –10 °C instead of 0 °C. ^1H NMR (300 MHz, $CDCl_3$): δ 7.89 (d, *J* = 16.0 Hz, 1H), 7.50 (s, 1H), 7.34 – 7.30 (m, 2H), 6.98 (dd, *J* = 9.0, 2.3 Hz, 1H), 6.35 (d, *J* = 16.0 Hz, 1H), 4.86 (d, *J* = 2.6 Hz, 2H), 3.90 (s, 3H), 3.81 (s, 3H), 2.48 (t, *J* = 2.6 Hz, 1H). ^{13}C NMR (75 MHz, $CDCl_3$): δ 168.8, 155.9, 138.2, 132.2, 131.6, 127.2, 113.3, 112.6, 112.4, 111.0, 102.9, 77.4, 74.8, 56.1, 51.6, 36.5. IR (neat): 3254, 3110, 2835, 1704, 1622, 1485, 1281, 1158, 1046, 797, 632 cm^{-1} HRMS (APPI+): calc'd for $C_{16}H_{15}NO_3$ $[M+H]^+$ 270.1130, found 270.1127.

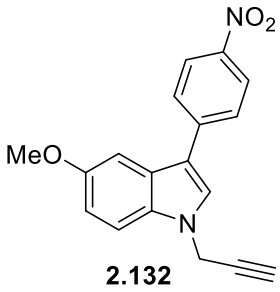

2.132

^1H NMR (300 MHz, $CDCl_3$): δ 8.32 – 8.28 (m, 2H), 7.80 – 7.76 (m, 2H), 7.53 (s, 1H), 7.38 – 7.37 (m, 2H), 7.01 (dd, *J* = 9.0, 2.3 Hz, 1H), 4.93 (d, *J* = 2.6 Hz, 2H), 3.90 (s, 3H), 2.49 (t, *J* = 2.6 Hz, 1H). ^{13}C NMR (75 MHz, $CDCl_3$): δ 155.7, 145.5, 142.8, 132.1, 127.3, 126.9, 126.7, 124.5, 115.4, 113.1, 111.0, 102.1, 77.4, 74.6, 56.2, 36.5. IR (neat): 3280, 3108, 2920, 1591, 1503, 1334, 1217, 1191, 845, 788, 657 cm^{-1}HRMS (APPI+): calc'd for $C_{18}H_{14}N_2O_3$ [M] 306.1004, found 306.1015.

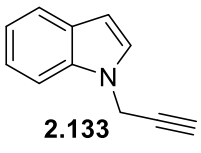

2.133

^1H NMR (300 MHz, $CDCl_3$): δ 7.63 (dt, *J* = 7.8, 1.0 Hz, 1H), 7.40 (dd, *J* = 8.2, 0.9 Hz, 1H), 7.28 – 7.21 (m, 1H), 7.20 (d, *J* = 3.2 Hz, 1H), 7.13 (ddd, *J* = 8.0, 7.1, 1.1 Hz, 1H), 6.53 (dd, *J* = 3.2, 0.8 Hz, 1H), 4.86 (d, *J* = 2.6 Hz, 2H), 2.37 (t, *J* = 2.6 Hz, 1H). ^{13}C NMR (75 MHz, $CDCl_3$): δ 135.9, 129.0, 127.4, 122.0, 121.3, 120.0, 109.4, 102.2, 77.9, 73.6, 35.9. IR (neat): 3285, 3052, 2919, 1469, 1311, 1123, 737 cm^{-1} HRMS (APPI+): calc'd for $C_{11}H_9N$ [M] 155.0735, found 155.0739.

Scheme 2.26: General Synthetic Scheme for the Synthesis of Substituted *N*-Butynylskatole Compounds

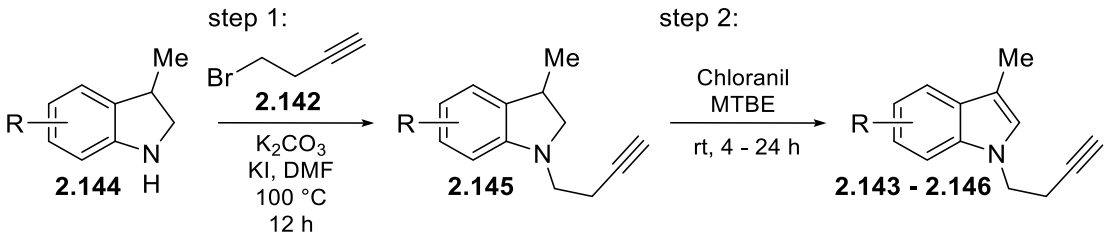

General Experimental Procedure B:

1) 4-Bromobutyne **2.142** (1.2 equiv) was added to a solution of KI (1.2 equiv) in DMF (1 mL/mmol of KI) in a round-bottom flask equipped with a stir bar and reflux condenser, under an N_2 atmosphere. The solution was heated to 100 °C for 30 min and then cooled to room temperature. K_2CO_3 (1.5 equiv) was then added to the reaction slurry, followed by the addition of a pre-dissolved solution of substituted indoline **2.144** (1.0 equiv) in DMF (0.4 mL/mmol of **2.144**). The reaction mixture was heated to 100 °C for ~12 h (overnight), then cooled to room temperature, and H_2O was added. The mixture was extracted three times with diethyl ether, washed twice with H_2O, washed once with brine, dried over anhydrous $MgSO_4$, and concentrated *in vacuo*. The resulting residue passed through a short silica gel plug using a 2% EtOAc in hexanes eluent. The corresponding alkylated indoline **2.145** was used without further purification.

2) Chloranil (1.1 equiv) was added to a solution of alkylated indolines **2.145** (1.0 equiv) in MTBE (0.2 M) in a round-bottom flask equipped with a stir bar at room temperature. The reaction mixture was stirred for 4-24 h. When the reaction was considered complete, as determined by TLC analysis, the mixture was filtered through a pad of Celite® and washed with diethyl ether. The resulting liquid was concentrated *in vacuo,* and the corresponding residue was purified by silica

gel flash column chromatography using a hexanes/EtOAc gradient to yield the substituted *N*-butynylskatoles **2.143 – 2.146**.

*Note: Substituted indoline starting materials (**2.143 – 2.146**) were synthesized following known literature procedures.*[32]

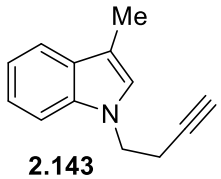

2.143

^{1}H NMR (300 MHz, $CDCl_3$): δ 7.57 – 7.54 (m, 1H), 7.30 – 7.27 (m, 1H), 7.20 (ddd, *J* = 8.2, 7.0, 1.2 Hz, 1H), 7.10 (ddd, *J* = 8.0, 7.0, 1.2 Hz, 1H), 6.89 (d, *J* = 0.9 Hz, 1H), 4.22 (t, *J* = 7.2 Hz, 2H), 2.62 (td, *J* = 7.2, 2.7 Hz, 2H), 2.31 (d, *J* = 1.1 Hz, 3H), 2.02 (t, *J* = 2.7 Hz, 1H). ^{13}C NMR (75 MHz, $CDCl_3$): δ 136.1, 129.1, 125.5, 121.7, 119.3, 119.0, 110.9, 109.0, 81.1, 70.8, 45.0, 20.6, 9.7. IR (neat): 3227, 1501, 1223, 1045, 923, 673 cm^{-1} HRMS (APPI+): calc'd for $C_{13}H_{13}N$ $[M]^+$ 183.1048, found 183.1057.

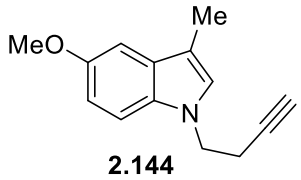

2.144

^{1}H NMR (300 MHz, $CDCl_3$): δ 7.19 (d, *J* = 8.8 Hz, 1H), 7.02 – 6.97 (m, 1H), 6.92 – 6.78 (m, 2H), 4.20 (t, *J* = 7.2 Hz, 2H), 3.87 (d, *J* = 1.8 Hz, 3H), 2.62 (td, *J* = 7.1, 2.6, 1.3 Hz, 2H), 2.36 – 2.20 (m, 3H), 2.06 – 2.02 (m, 1H). ^{13}C NMR (75 MHz, $CDCl_3$): δ 153.9, 131.4, 129.3, 126.2, 111.9, 110.3, 109.8, 101.2, 81.2, 70.8, 56.1, 45.2, 20.7, 9.8. IR (neat): 3257, 1490, 1227, 1045, 801, 671 cm^{-1} HRMS (APPI+): calc'd for $C_{14}H_{15}NO$ $[M+H]^+$ 214.1226, found 214.1222.

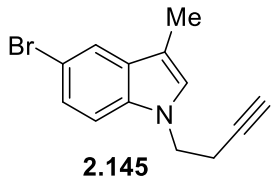

2.145

NMR (500 MHz, $CDCl_3$): δ 7.67 (d, *J* = 1.6 Hz, 1H), 7.28 – 7.26 (m, 1H), 7.16 (d, *J* = 8.6 Hz, 1H), 6.91 (s, 1H), 4.21 (t, *J* = 7.1 Hz, 2H), 2.63 (td, *J* = 7.1, 2.6 Hz, 2H), 2.26 (d, *J* = 0.9 Hz, 3H), 2.03 (t, *J* = 2.6 Hz, 1H). ^{13}C NMR (75 MHz, $CDCl_3$): δ 134.9, 130.8, 126.7, 124.5, 122.0, 112.4, 110.6, 110.5, 80.8, 71.0, 45.1, 20.6, 9.6. IR (neat): 3292, 2921, 1599, 1488, 1239, 798, 635 cm^{-1} HRMS (APPI+): calc'd for $C_{13}H_{12}BrN$ [M] 261.0153, found 261.0156.

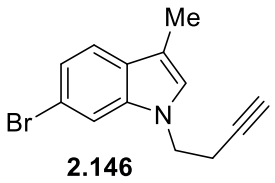

2.146

^{1}H NMR (300 MHz, $CDCl_3$): δ 7.44 (d, *J* = 1.6 Hz, 1H), 7.39 (d, *J* = 8.4 Hz, 1H), 7.19 (dd, *J* = 8.4, 1.7 Hz, 1H), 6.87 (d, *J* = 1.0 Hz, 1H), 4.18 (t, *J* = 7.1 Hz, 2H), 2.62 (td, *J* = 7.1, 2.7 Hz, 2H), 2.28 (d, *J* = 1.0 Hz, 3H), 2.04 (t, *J* = 2.7 Hz, 1H). ^{13}C NMR (75 MHz, $CDCl_3$): δ 137.0, 128.0, 126.1, 122.2, 120.6, 115.5, 112.1, 111.2, 80.8, 71.0, 45.1, 20.6, 9.6. IR (neat): 3292, 2918, 1678, 1469, 1358, 785 cm^{-1} HRMS (APPI+): calc'd for $C_{13}H_{12}BrN$ $[M+H]^+$ 262.0026, found 262.0164.

Scheme 2.27: General Synthetic Scheme for the Synthesis of **2.153** and **2.154** Compounds

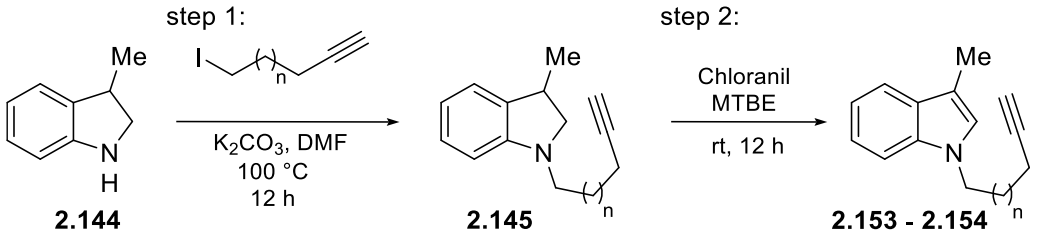

2.144 **2.145** **2.153 - 2.154**

General Experimental Procedure C:

1) Iodoalkyne (1.3 equiv) was added to a solution of K_2CO_3 (1.5 equiv) and 3-methylindoline **2.144** (1.0 equiv) in DMF (1 mL/mmol of methylindoline) in a round-bottom flask equipped with a stir bar and reflux condenser, under an N_2 atmosphere. The solution was heated to 100 °C for ~12 h (overnight), then cooled to room temperature, and H_2O was added. The mixture was extracted three times with diethyl ether, washed twice with H_2O, washed once with brine, dried over anhydrous $MgSO_4$, and concentrated *in vacuo*. The resulting residue was passed through a short silica gel plug using 2% hexanes in EtOAc eluent to yield alkylated indoline **2.145**. This material was used directly in the next reaction.

2) Chloranil (1.1 equiv) was added to a solution of alkylated indoline **2.145** (1.0 equiv) in MTBE (0.2 M) in a round-bottom flask equipped with a stir bar at room temperature. The reaction mixture was stirred for 12 h. When the reaction was considered complete, as determined by TLC

analysis, the mixture was filtered through a pad of Celite® and washed with diethyl ether. The resulting liquid was concentrated *in vacuo* and the corresponding residue was purified by silica gel flash column chromatography using a hexanes/EtOAc gradient (2 % EtOAc in hexanes – 3 % EtOAc in hexanes) to yield *N*-alkylskatoles **2.153 – 2.154.**

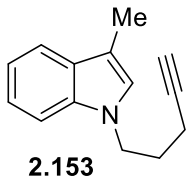

2.153

^{1}H NMR (300 MHz, $CDCl_3$): δ 7.57 – 7.54 (m, 1H), 7.32 (d, *J* = 8.2 Hz, 1H), 7.17 (dd, *J* = 8.2, 1.2 Hz, 1H), 7.08 (ddd, *J* = 7.9, 7.0, 1.1 Hz, 1H), 6.88 (d, *J* = 0.9 Hz, 1H), 4.20 (t, *J* = 6.6 Hz, 2H), 2.32 (d, *J* = 1.0 Hz, 3H), 2.18 – 2.10 (m, 2H), 2.05 – 2.02 (m, 1H), 2.01 – 1.95 (m, 2H). ^{13}C NMR (75 MHz, $CDCl_3$): δ 136.3, 128.9, 125.8, 121.6, 119.2, 118.8, 110.5, 109.2, 83.3, 69.6, 44.5, 29.0, 16.0, 9.7. IR (neat): 3287, 2885, 1466, 1205, 986, 736, 634 cm^{-1} HRMS (APPI+): calc'd for $C_{14}H_{15}N$ [M] 197.1204, found 197.1199.

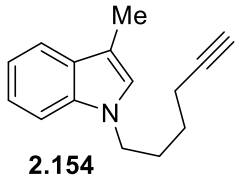

2.154

^{1}H NMR (300 MHz, $CDCl_3$): δ 7.58 – 7.52 (m, 1H), 7.29 – 7.25 (m, 1H), 7.23 – 7.15 (m, 1H), 7.08 (ddd, *J* = 7.9, 7.0, 1.1 Hz, 1H), 6.84 (d, *J* = 0.9 Hz, 1H), 4.05 (t, *J* = 7.0 Hz, 2H), 2.31 (d, *J* = 1.0 Hz, 3H), 2.18 (td, *J* = 7.0, 2.6 Hz, 2H), 1.98 – 1.80 (m, 3H), 1.58 – 1.43 (m, 1H). ^{13}C NMR (75 MHz, $CDCl_3$): δ 136.4, 128.9, 125.5, 121.5, 119.2, 118.6, 110.4, 109.2, 83.9, 69.0, 45.6, 29.5, 25.9, 18.2, 9.7. IR (neat): 3291, 2918, 1482, 1361, 1166, 1013, 736, 629 cm^{-1} HRMS (APPI+): calc'd for $C_{15}H_{17}N$ $[M+H]^+$ 212.1434, found 212.1438.

Synthesis and Characterization of Substituted Diazo Starting Materials

Diazodicarbonyl compounds **2.83, 2.90, 2.98 – 2.99** were synthesized following known literature procedures, and spectroscopic data for these compounds agreed with that previously reported in the literature.[33] The ^{1}H NMR data for each of these compounds is given below.

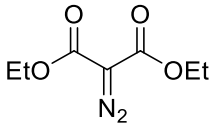

2.83

^{1}H NMR (300 MHz, $CDCl_3$): δ 4.31 (q, *J* = 7.1 Hz, 1H), 1.32 (t, *J* = 7.1 Hz, 6H)

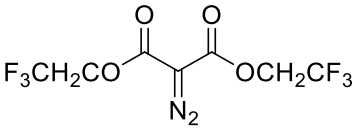

2.90

^{1}H NMR (500 MHz, $CDCl_3$): δ 4.63 (q, *J* = 8.2 Hz, 4H)

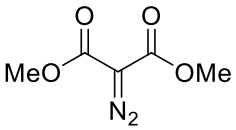

2.98

^{1}H NMR (300 MHz, $CDCl_3$): δ 3.85 (s, 6H)

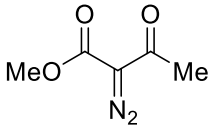

2.99

^{1}H NMR (300 MHz, $CDCl_3$): δ 3.85 (s, 3H), 2.48 (s, 3H).

Catalyst Control Experiments (characterization of products in this section can be found in the following section)

Scheme 2.28: Attempted $ZnBr_2$-catalyzed functionalization

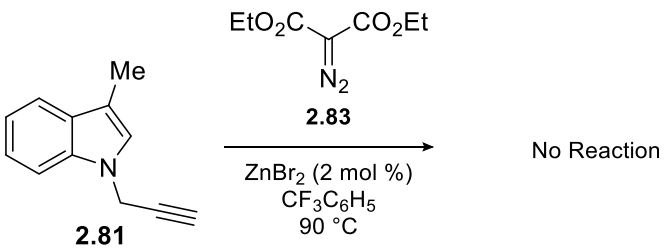

Procedure: **2.81** (22 mg, 0.13 mmol) and $ZnBr_2$ (2.5 mg, 0.011 mmol) were added to a reaction vessel equipped with a stir bar, and the vessel was then evacuated and backfilled with N_2. This cycle was repeated two additional times, followed by the addition of trifluorotoluene (0.65 mL) under a N_2 atmosphere. **2.83** (0.020 g, 0.11 mmol) was added to a separate reaction vessel and the vessel was then evacuated and backfilled with N_2. This cycle was repeated two additional times. The diazo reagent was then dissolved in trifluorotoluene (0.33 mL) under a N_2 atmosphere and transferred dropwise by syringe to the solution of indole starting material. Two sequential rinses and transfers using small quantities of trifluorotoluene were then conducted to ensure a complete transfer of the diazo reagent. The reaction mixture was then heated to 90 °C and stirred at this temperature for 48 h. TLC and crude ^{1}H NMR analysis indicated that no reaction had occurred under these conditions.

Scheme 2.29: Attempted $Rh_2(OAc)_4$-catalyzed Conia-ene cyclization

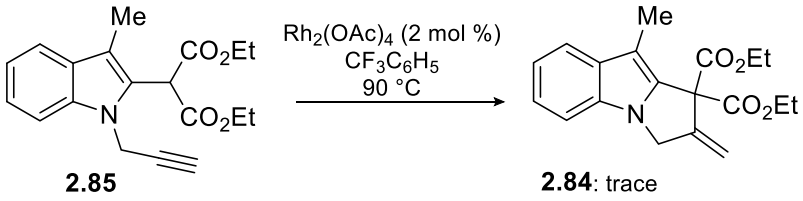

2.85 **2.84**: trace

Procedure: **2.85** (0.030 mg, 0.092 mmol) and $Rh_2(OAc)_4$ (1.0 mg, 0.0023 mmol) were added to a reaction vessel equipped with a stir bar, and the vessel was then evacuated and backfilled with N_2. This cycle was repeated two additional times followed by the addition of trifluorotoluene (0.50 mL) under a N_2 atmosphere. The reaction mixture was then heated to 90 °C and stirred at this temperature for 48 h. TLC and crude ^{1}H NMR analysis indicated trace product formation and with the major material being unconsumed starting material **2.85.**

Scheme 2.30: Attempted $ZnBr_2$ -catalyzed Conia-ene cyclization

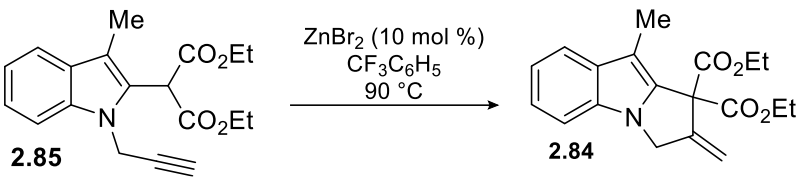

Procedure: **2.85** (0.030 mg, 0.092 mmol) and $ZnBr_2$ (2 mg, 0.009 mmol) were added to a reaction vessel equipped with a stir bar and the vessel was then evacuated and backfilled with N_2. This cycle was repeated two additional times followed by the addition of trifluorotoluene (0.50 mL) under a N_2 atmosphere. The reaction mixture was then heated to 90 °C and stirred at this temperature for 2 h. Upon completion (by TLC analysis), the reaction mixture was then directly loaded and purified by silica gel flash column chromatography (hexanes/EtOAc gradient) to obtain pyrroloindole **2.84** in 97% yield (29 mg, 0.089 mmol).

Scheme 2.31: Attempted one-pot, stepwise insertion then Conia-ene cyclization

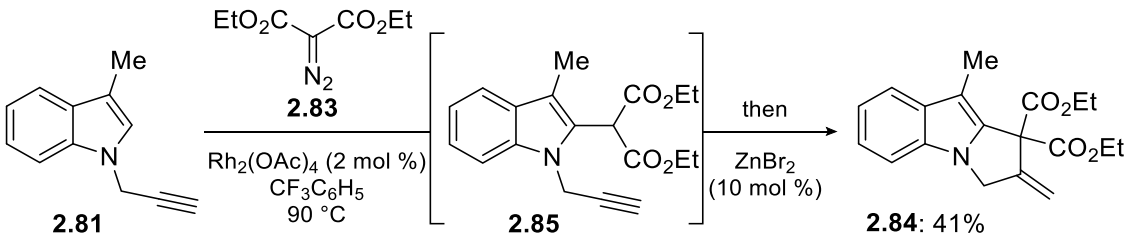

Procedure: **2.81** (43 mg, 0.25 mmol) and $Rh_2(OAc)_4$ (1.8 mg, 0.0041 mmol) were added to a reaction vessel equipped with a stir bar and the vessel was then evacuated and backfilled with N_2. This cycle was repeated two additional times followed by the addition of trifluorotoluene (1.0 mL) under a N_2 atmosphere. **2.83** (0.040 g, 0.21 mmol) was added to a separate reaction vessel and the vessel was then evacuated and backfilled with N_2. This cycle was repeated two additional

times. The diazo reagent was then dissolved in trifluorotoluene (0.60 mL) under a N_2 atmosphere and transferred dropwise by syringe to the solution of indole starting material. Two sequential rinses and transfers using small quantities of trifluorotoluene were then conducted to ensure a complete transfer of the diazo reagent. The reaction mixture was then heated to 90 °C and stirred at this temperature for 2 h. The reaction progress was monitored by TLC analysis and considered complete upon consumption of the diazo reagent. Upon completion, the reaction was cooled to room temperature, and $ZnBr_2$ (4.8 mg, 0.021 mmol) was added in one portion, and the reaction mixture was heated back to 90 °C for 2 h. The reaction mixture was cooled to room temperature, then directly loaded, and purified by silica gel flash column chromatography (hexanes/EtOAc gradient) to yield pyrroloindole **2.84** in 41% (28 mg, 0.086 mmol). This reaction is a direct comparison to the entry 10 (Table 2.3) in which the catalysts are both in the reaction at the beginning (not *via* stepwise addition), demonstrating the compatibility of this dual catalyst system.

Synthesis and Characterization of Substituted Dihydropyrrolo[1,2-a]indole (pyrroloindole) Products

Figure 2.32: General Synthetic Scheme for the Synthesis of Substituted Pyrroloindole Compounds *via* a Tandem C-H Insertion/Annulation Reaction

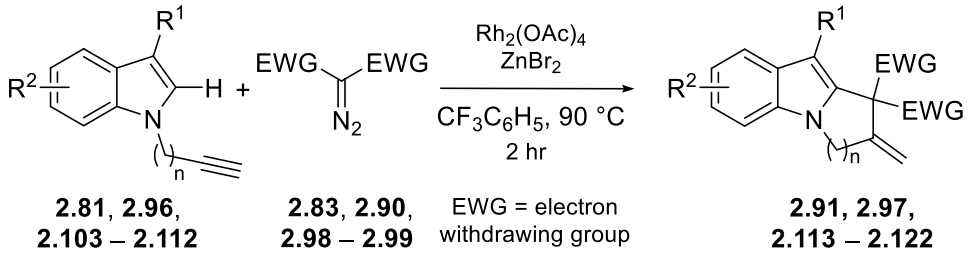

General Experimental Procedure D:

Substituted indole **2.81, 2.96, 2.103 – 2.112** (1.2 equiv) was added to a reaction vessel equipped with a stir bar and the vessel was then evacuated and backfilled with N_2. This cycle was repeated two additional times followed by the addition of trifluorotoluene (5 mL/mmol of indole) under a N_2 atmosphere. $Rh_2(OAc)_4$ (2 mol %) and $ZnBr_2$ (10 mol %) were then added to the reaction vessel and again the vessel was evacuated (quickly) and backfilled with N_2. Diazo reagent **2.83, 2.90, 2.98 – 2.99** (1.0 equiv) was added to a separate reaction vessel and the vessel was then evacuated and backfilled with N_2. This cycle was repeated two additional times. The diazo reagent was then dissolved in trifluorotoluene (3 mL/mmol of diazo) under a N_2 atmosphere and transferred dropwise by syringe to the solution of indole starting material. Two sequential rinses and transfers using small quantities of trifluorotoluene were then conducted to ensure complete transfer of the diazo reagent. The reaction mixture was then heated to 90 °C and stirred at this temperature for 2 h. The reaction progress was monitored by TLC analysis and considered complete upon consumption of diazo reagent. Upon completion, the reaction mixture was cooled to r.t and then directly loaded and purified by silica gel flash column chromatography (hexanes/EtOAc gradient) to yield the substituted pyrroloindole **2.91, 2.97, 2.113 – 2.122**. (for a 1 mmol scale representative example see **2.91**)

*Note: In the ^{1}H-NMR spectra of pyrroloindole products **2.84**, **2.91**,* **2.97, 2.100 – 2.102, 2.113 – 2.122**, **2.124 – 2.126** and **2.134 – 2.139**, *the anticipated splitting pattern for exomethylene protons is typically observed as a "triplet of doublets," as evident in compound **2.84**. However, in other compounds, particularly when bis(2,2,2-trifluoroethyl)-2-diazomalonate **2.90** is employed as a diazo reagent, the same exomethylene splitting pattern appears as either a "quartet" or a "doublet*

*of doublets." Consequently, to maintain consistency across all compounds except **2.84**, the exomethylene protons are designated as a "multiplet."*

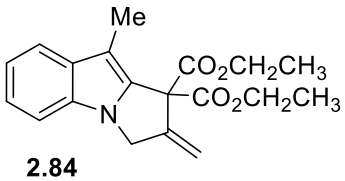

2.84

Pyrroloindole **2.84** was prepared using General Experimental Procedure D. Reagents employed: diethyl-2-diazomalonate **2.83** (0.100 g, 0.540 mmol), *N*-propargyl indole **2.81** (110 mg, 0.64 mmol), $Rh_2(OAc)_4$ (4.7 mg, 0.011 mmol), $ZnBr_2$ (12 mg, 0.054 mmol). **2.84** (0.0830 g, 0.254 mmol, 47%) was obtained as a thick greenish yellow oil. R_f = 0.30, 30% Et_2O in hexanes; ^1H NMR (300 MHz, $CDCl_3$) δ 7.62 – 7.54 (m, 1H), 7.24 – 7.21 (m, 1H), 7.21 – 7.14 (m, 1H), 7.14 – 7.08 (m, 1H), 5.74 (td, *J* = 2.3, 0.9 Hz, 1H), 5.57 (td, *J* = 2.0, 1.0 Hz, 1H), 4.80 (t, *J* = 2.2 Hz, 2H), 4.32 – 4.16 (m, 4H), 2.33 (s, 3H), 1.27 (t, *J* = 7.1 Hz, 6H). ^{13}C NMR (75 MHz, $CDCl_3$): δ 167.8, 144.9, 135.1, 132.6, 132.4, 121.8, 119.5, 119.2, 114.1, 109.7, 106.0, 63.2, 62.4, 48.3, 14.1, 9.1. IR (neat): 2918, 1732, 1456, 1227, 1250, 1095, 738, cm^{-1} HRMS (APPI+): calc'd for $C_{19}H_{21}NO_4$ $[M+H]^+$ 328.1543, found 328.1524.

1 mmol example:

Pyrroloindole **2.91** was prepared using General Experimental Procedure D. Reagents employed: bis(2,2,2-trifluoroethyl)-2-diazomalonate **2.90** (0.500 g, 1.70 mmol), *N*-propargyl indole **2.81** (0.345 g, 2.04 mmol), $Rh_2(OAc)_4$ (15.0 mg, 0.034 mmol), $ZnBr_2$ (38 mg, 0.17 mmol). **2.91** was obtained in 64% (468 mg, 1.08 mmol).

Smaller scale reaction:

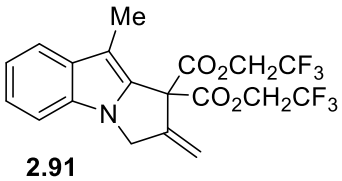

2.91

Pyrroloindole **2.91** was prepared using General Experimental Procedure D. Reagents employed: bis(2,2,2-trifluoroethyl)-2-diazomalonate **2.90** (0.100 g, 0.340 mmol), *N*-propargyl indole **2.81** (69 mg, 0.40 mmol), $Rh_2(OAc)_4$ (3.0 mg, 0.0068 mmol), $ZnBr_2$ (7.6 mg, 0.034 mmol). **2.91** (0.0950 g, 0.218 mmol, 64%) was obtained as a greenish yellow thick oil. Minor products 5 (0.0130 g, 0.030 mmol, 9%) and 6 (0.0090 g, 0.020 mmol, 6%) were obtained as thick yellowish green oils: R_f = 0.25, 20% acetone in hexanes; ^{1}H NMR (300 MHz, $CDCl_3$): δ 7.60 (dt, *J* = 7.9, 1.0 Hz, 1H), 7.24 – 7.21 (m, 2H), 7.17 – 7.11 (m, 1H), 5.76 – 5.73 (m, 1H), 5.68 – 5.66 (m, 1H), 4.83 (t, *J* = 2.2 Hz, 2H), 4.69 – 4.43 (m, 4H), 2.30 (s, 3H). ^{13}C NMR (75 MHz, $CDCl_3$): δ 165.8, 143.8, 132.7, 132.6, 132.5, 122.6 (q, *J* = 277.4 Hz), 122.5, 119.9, 119.6, 115.6, 109.8, 107.3, 62.1, 61.8 (q, *J* = 37.3 Hz) 48.1, 8.6. IR (neat): 2927, 1756, 1587, 1424, 1250, 1166, 1093, 646 cm^{-1} HRMS (APPI+): calc'd for $C_{19}H_{15}F_6NO_4$ $[M+H]^+$ 436.0978, found 436.0963.

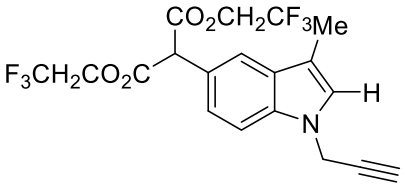

2.92

\+

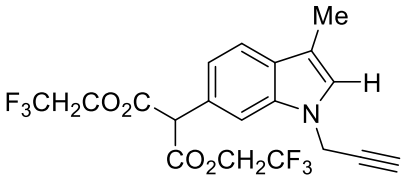

2.93

Compound **2.92**:

R_f = 0.20, 20% acetone in hexanes; ^{1}H NMR (300 MHz, $CDCl_3$): δ 7.58 (d, *J* = 1.6 Hz, 1H), 7.37 (d, *J* = 8.5 Hz, 1H), 7.25 (dd, *J* = 8.5, 1.8 Hz, 1H), 7.00 (d, *J* = 0.9 Hz, 1H), 4.93 (s, 1H), 4.81 (d, *J* = 2.5 Hz, 2H), 4.64 – 4.43 (m, 4H), 2.37 (t, *J* = 2.5 Hz, 1H), 2.31 (d, *J* = 1.0 Hz, 3H). ^{13}C NMR (75 MHz, $CDCl_3$): δ 166.7, 136.3, 129.6, 126.1, 122.8 (d, *J* = 277.3 Hz), 122.7, 121.6, 120.4,

112.0, 109.9, 77.9, 73.5, 61.4 (q, J = 277.3 Hz), 57.0, 35.8, 9.6. IR (neat): 3290, 2921, 1753, 1277, 1159, 1124, 800, 763, 647 cm^{-1} HRMS (APPI+): calc'd for $C_{19}H_{15}F_6NO_4$ [M] 435.0905, found 435.0908.

Compound **2.93**:

R_f = 0.20, 20% acetone in hexanes; ^1H NMR (300 MHz, $CDCl_3$): δ 7.57 (d, J = 8.2 Hz, 1H), 7.40 (d, J = 1.3 Hz, 1H), 7.12 (dd, J = 8.2, 1.6 Hz, 1H), 7.03 (d, J = 1.0 Hz, 1H), 4.94 (s, 1H), 4.82 (d, J = 2.5 Hz, 2H), 4.69 – 4.41 (m, 4H), 2.38 (t, J = 2.5 Hz, 1H), 2.33 – 2.29 (m, 3H). ^{13}C NMR (75 MHz, $CDCl_3$): δ 166.5, 136.2, 129.8, 126.3, 124.2, 122.7 (d, J = 277.3 Hz), 120.4, 119.9, 111.7, 110.1, 77.8, 73.7, 61.4 (q, J = 37.2 Hz), 66.0, 57.1, 9.6. IR (neat): 3290, 2923, 1753, 1275, 1158, 1125, 1056, 979, 647 cm^{-1} HRMS (APPI+): calc'd for $C_{19}H_{15}F_6NO_4$ [M] 435.0905, found 435.0903

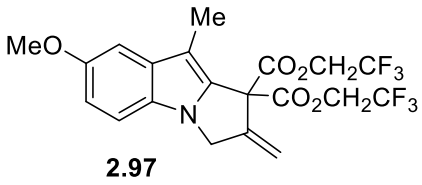

2.97

Pyrroloindole **2.97** was prepared using General Experimental Procedure D. Reagents employed: Bis(2,2,2-trifluoroethyl)-2-diazomalonate **2.90** (0.100 g, 0.340 mmol), *N*-propargyl indole **2.96** (81 mg, 0.40 mmol), $Rh_2(OAc)_4$ (3.0 mg, 0.0068 mmol), $ZnBr_2$ (7.6 mg, 0.034 mmol). **2.97** (120 mg, 0.26 mmol, 76%) was obtained as thick brown oil: R_f = 0.25, 25% EtOAc in hexanes; ^1H NMR (300 MHz, $CDCl_3$): δ 7.13 (d, J = 8.8 Hz, 1H), 7.02 (d, J = 2.3 Hz, 1H), 6.89 (dd, J = 8.8, 2.4 Hz, 1H), 5.75 – 5.73 (m, 1H), 5.67 – 5.65 (m, 1H), 4.81 (t, J = 2.2 Hz, 2H), 4.70 – 4.36 (m, 4H), 3.87 (s, 3H), 2.27 (s, 3H). ^{13}C NMR (75 MHz, $CDCl_3$) δ 165.8, 154.4, 143.8, 133.2, 132.8, 128.1, 122.6 (d, J = 277.4 Hz), 115.5, 113.1, 110.6, 106.8, 101.5, 62.3, 61.8 (q, J = 37.3 Hz), 56.1, 48.3, 8.7. IR (neat): 2924, 1755, 1440, 1281, 1156, 1053, 962, 648 cm^{-1} HRMS (APPI+): calc'd for $C_{20}H_{17}F_6NO_5$ $[M+H]^+$ 466.1084, found 466.1071.

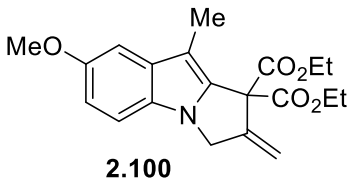

2.100

Pyrroloindole **2.100** was prepared using General Experimental Procedure D. Reagents employed: Diethyl-2-diazomalonate **2.83** (0.0800 g, 0.430 mmol), *N*-propargyl indole **2.96** (103 mg, 0.510 mmol), rhodium (II) acetate (2.7 mg, 0.0030 mmol), $ZnBr_2$ (9.0 mg, 0.040 mmol mmol). **2.100** (0.100 g, 0.280 mmol, 65%) was obtained as a thick oil: R_f = 0.30, 20% acetone in hexanes; ^{1}H NMR (300 MHz, $CDCl_3$): δ 7.14 – 7.08 (m, 1H), 7.02 (d, *J* = 2.2 Hz, 1H), 6.85 (dd, *J* = 8.8, 2.4 Hz, 1H), 5.74 – 5.72 (m, 1H), 5.56 – 5.55 (m, 1H), 4.76 (t, *J* = 2.2 Hz, 2H), 4.34 – 4.12 (m, 4H), 3.86 (s, 3H), 2.30 (s, 3H), 1.27 (t, *J* = 7.1 Hz, 6H). ^{13}C NMR (75 MHz, $CDCl_3$): δ 167.8, 154.1, 145.0, 135.8, 132.9, 127.9, 114.1, 112.1, 110.4, 105.6, 101.5, 63.4, 62.4, 56.1, 48.5, 14.1, 9.1. IR (neat): 2955, 1724, 1728, 1318, 1207, 729 cm^{-1} HRMS (APPI+): calc'd for $C_{20}H_{23}NO_5$ $[M+H]^+$ 358.1649, found 358.1676.

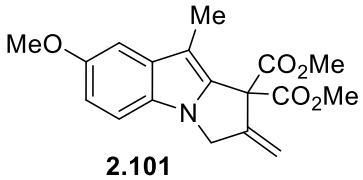

2.101

Pyrroloindole **2.101** was prepared using General Experimental Procedure D. Reagents employed: Dimethyl-2-diazomalonate **2.98** (0.050 g, 0.31 mmol), *N*-propargyl indole **2.96** (76 mg, 0.38 mmol), $Rh_2(OAc)_4$ (2.7 mg, 0.0030 mmol), $ZnBr_2$ (7 mg, 0.03 mmol). **2.101** (60 mg, 0.18 mmol, 58%) was obtained as a yellow thick oil: R_f = 0.35, 25% EtOAc in hexanes; ^{1}H NMR (300 MHz, $CDCl_3$): δ 7.11 (d, *J* = 8.8 Hz, 1H), 7.02 (d, *J* = 2.3 Hz, 1H), 6.86 (dd, *J* = 8.8, 2.4 Hz, 1H), 5.72 – 5.71 (m, 1H), 5.56 – 5.55 (m, 1H), 4.77 (t, *J* = 2.1 Hz, 2H), 3.86 (s, 3H), 3.78 (s, 6H), 2.27 (s, 3H). ^{13}C NMR (75 MHz, $CDCl_3$): δ 168.3, 154.2, 144.8, 135.5, 132.8, 127.8, 114.3, 112.3, 110.5, 105.6, 101.4, 63.0, 56.1, 53.4, 48.5, 8.8; IR (neat):2955, 1724, 1435, 1219, 1040, 1025, 907, 729 cm^{-1} HRMS (APPI+): calc'd for $C_{18}H_{19}NO_5$ $[M+H]^+$ 330.1336, found 330.1327.

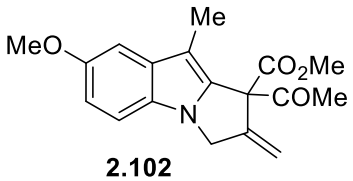

2.102

Pyrroloindole **2.102** was prepared using General Experimental Procedure D. Reagents employed: Methyl-2-diazo-3-oxobutanoate **2.99** (0.070 g, 0.50 mmol), *N*-propargyl indole **2.96** (117 mg, 0.590 mmol), $Rh_2(OAc)_4$ (4.2 mg, 0.010 mmol), $ZnBr_2$ (11 mg, 0.050 mmol). **2.102** (0.0330 g, 0.105 mmol, 21%) was obtained as a brown thick oil: R_f = 0.30, 20% acetone in hexanes; ^{1}H NMR (300 MHz, $CDCl_3$): δ 7.16 (dd, *J* = 8.8, 0.4 Hz, 1H), 7.03 (d, *J* = 2.3 Hz, 1H), 6.88 (dd, *J* = 8.8, 2.4 Hz, 1H), 5.68 - 5.55 (m, 2H), 4.81 (dt, *J* = 4.5, 2.2 Hz, 2H), 3.87 (s, 3H), 3.78 (s, 3H), 2.27 (s, 3H), 2.06 (s, 3H). ^{13}C NMR (75 MHz, $CDCl_3$): δ 200.3, 168.5, 154.2, 144.5, 136.0, 132.8, 128.0, 115.3, 112.5, 110.4, 105.7, 101.3, 69.8, 56.0, 53.0, 48.4, 26.2, 8.9. IR (neat): 2921, 2835, 1755, 1181, 1281, 1156, 1153 cm^{-1} HRMS (APPI+): calc'd for $C_{18}H_{19}NO_4$ $[M+H]^+$ 314.1387, found 314.1389.

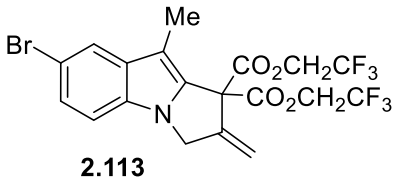

2.113

Pyrroloindole **2.113** was prepared using General Experimental Procedure D. Reagents employed: Bis(2,2,2-trifluoroethyl)-2-diazomalonate **2.90** (0.050 g, 0.17 mmol), *N*-propargyl indole **2.103** (51 mg, 0.20 mmol), $Rh_2(OAc)_4$ (1.5 mg, 0.0034 mmol), $ZnBr_2$ (3.8 mg, 0.017 mmol). **2.113** (0.0700 mg, 0.136 mmol, 80%) was obtained as a brown solid: R_f = 0.30, 20% acetone in hexanes; M.P. = 96.4-97.5 ^{o}C ^{1}H NMR (300 MHz, $CDCl_3$): δ 7.73 (d, *J* = 1.6 Hz, 1H), 7.30 (dd, *J* = 8.6, 1.8 Hz, 1H), 7.10 (d, *J* = 8.6 Hz, 1H), 5.78 – 5.75 (m, 1H), 5.70 – 5.68 (m, 1H), 4.82 (t, *J* = 2.2 Hz, 2H), 4.71 – 4.45 (m, 4H), 2.25 (s, 3H). ^{13}C NMR (75 MHz, $CDCl_3$): δ 165.5, 143.3, 134.1, 133.8, 131.3, 125.4, 122.6 (d, *J* = 277.5 Hz), 122.6, 116.0, 113.1, 111.3, 107.0, 62.7, 61.9 (q, *J* = 37.2 Hz), 48.3, 8.5. IR (neat): 2866, 1786, 1741, 1283, 1156, 1055, 780, 660 cm^{-1} HRMS (APPI+): calc'd for $C_{19}H_{14}BrF_6NO_4$ $[M]^+$ 513.0010, found 513.0019.

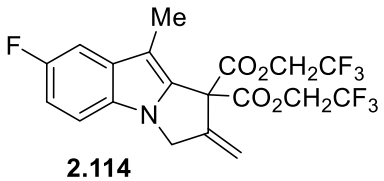

2.114

Pyrroloindole **2.114** was prepared using General Experimental Procedure D. Reagents employed: Bis(2,2,2-trifluoroethyl)-2-diazomalonate **2.90** (0.100 g, 0.340 mmol), *N*-propargyl indole **1.104** (75 mg, 0.40 mmol), $Rh_2(OAc)_4$ (3.0 mg, 0.0068 mmol), $ZnBr_2$ (7.6 mg, 0.034 mmol). **2.114** (127 mg, 0.280 mmol, 82%) was obtained as a brown solid: R_f = 0.35, 20% acetone in hexanes; M.P. = 107.0-108.0 ^oC ^1H NMR (300 MHz, $CDCl_3$): δ 7.27 – 7.20 (m, 1H), 7.14 (dd, *J* = 8.8, 4.3 Hz, 1H), 6.97 (td, *J* = 9.0, 2.4 Hz, 1H), 5.77 – 5.75 (m, 1H), 5.69 – 5.67 (m, 1H), 4.82 (t, *J* = 2.2 Hz, 2H), 4.71 – 4.45 (m, 4H), 2.25 (s, 3H). ^{13}C NMR (75 MHz, $CDCl_3$): δ 165.6, 158.0 (d, *J* = 235.5 Hz), 143.5, 134.3, 132.8 (d, *J* = 9.4 Hz), 129.4, 122.6 (q, *J* = 277.4 Hz), 115.8, 111.1 (d, *J* = 26.7 Hz), 110.5 (d, *J* = 9.7 Hz), 107.3 (d, *J* = 5.1 Hz), 104.9 (d, *J* = 23.4 Hz), 62.3, 61.9 (q, *J* = 37.4 Hz), 48.4, 8.6. IR (neat): 2922, 2853, 1785, 1484, 1282, 1145, 1009, 874, 839, 651 cm^{-1} HRMS (APPI+): calc'd for $C_{19}H_{14}F_7NO_4$ $[M+H]^+$ 454.0884, found 454.0875.

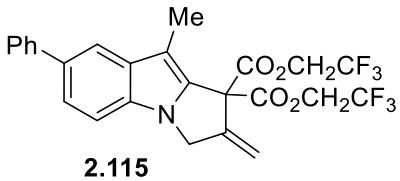

2.115

Pyrroloindole **2.115** was prepared using General Experimental Procedure D. Reagents employed: Bis (2, 2,2-trifluoroethyl)-2-diazomalonate **2.90** (0.080 g, 0.27 mmol), *N*-propargylindole **2.105** (0.80 g, 0.32 mmol), $Rh_2(OAc)_4$ (2.4 mg, 0.0054 mmol), $ZnBr_2$ (6.0 mg, 0.027 mmol). **2.115** (114 mg, 0.222 mmol, 82%) was obtained as a brown solid: R_f = 0.30, 20% acetone in hexanes; M.P. = 89.0-90.0 ^oC ^1H NMR (300 MHz, $CDCl_3$): δ 7.78 (d, *J* = 1.1 Hz, 1H), 7.69 – 7.60 (m, 2H), 7.51 – 7.41 (m, 3H), 7.34 – 7.25 (m, 2H), 5.76 – 5.74 (m, 1H), 5.68 – 5.66 (m, 1H), 4.87 (t, *J* = 2.1 Hz, 2H), 4.69 – 4.44 (m, 4H), 2.32 (s, 3H). ^{13}C NMR (75 MHz, $CDCl_3$): δ 165.7, 143.7, 142.6, 133.4, 133.3, 133.0, 132.2, 128.8, 127.6, 126.6, 122.6 (d, *J* = 277.4 Hz) 122.5, 118.5, 115.7, 110.1, 107.7, 62.2, 61.9 (q, *J* = 37.2 Hz), 48.2, 8.6. IR (neat): 2924, 1755, 1253, 1155, 1068, 977, 748, cm^{-1} HRMS (APPI+): calc'd for $C_{25}H_{19}F_6NO_4$ $[M+H]^+$ 512.1291, found 512.1288.

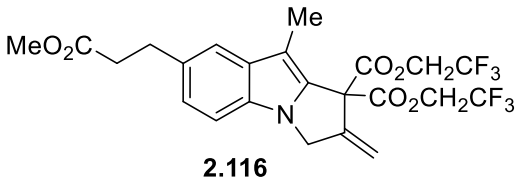

2.116

Pyrroloindole **2.116** was prepared using General Experimental Procedure D. Reagents employed: Bis(2,2,2-trifluoroethyl)-2-diazomalonate **2.90** (0.060 g, 0.20 mmol), *N*-propargyl indole **1.106** (63 mg, 0.24 mmol), $Rh_2(OAc)_4$ (1.8 mg, 0.0040 mmol), $ZnBr_2$ (4.5 mg, 0.020 mmol). **2.116** (85 mg, 0.16 mmol, 80%) was obtained as a yellow oil: R_f = 0.35, 20% acetone in hexanes; ^{1}H NMR (300 MHz, $CDCl_3$): δ 7.41 (d, *J* = 0.7 Hz, 1H), 7.16 (d, *J* = 8.3 Hz, 1H), 7.08 (dd, *J* = 8.4, 1.6 Hz, 1H), 5.75 – 5.73 (m, 1H), 5.67 – 5.65 (m, 1H), 4.80 (t, *J* = 2.1 Hz, 2H), 4.68 – 4.44 (m, 4H), 3.66 (s, 3H), 3.06 (t, *J* = 7.8 Hz, 2H), 2.67 (t, *J* = 7.8 Hz, 2H), 2.28 (s, 3H). ^{13}C NMR (75 MHz, $CDCl_3$): δ 173.7, 165.7, 143.8, 132.9, 132.7, 131.9, 131.5, 123.3, 122.6 (q, *J* = 277.4 Hz), 119.1, 115.5, 109.8, 106.9, 62.1, 61.8 (q, *J* = 37.3 Hz), 51.7, 48.2, 36.8, 31.4, 8.5. IR (neat): 2954, 1754, 1735, 1281, 1156, 1070, 965, 649 cm^{-1} HRMS (APPI+): calc'd for $C_{23}H_{21}F_6NO_6$ $[M+H]^+$ 522.1346, found 522.1336.

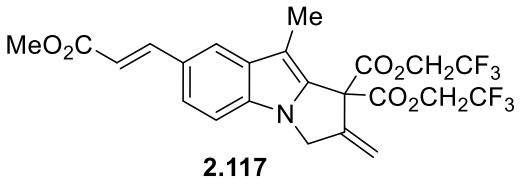

2.117

Pyrroloindole **2.117** was prepared using General Experimental Procedure D. Reagents employed: bis(2,2,2-trifluoroethyl)-2-diazomalonate **2.90** (0.058 g, 0.19 mmol), *N*-propargylindole **2.107** (61 mg, 0.24 mmol), $Rh_2(OAc)_4$ (1.8 mg, 0.0040 mmol), $ZnBr_2$ (4.5 mg, 0.020 mmol). **2.117** (80 mg, 0.15 mmol, 79%) was obtained as a green thick oil: R_f = 0.30, 20% acetone in hexanes; ^{1}H NMR (300 MHz, $CDCl_3$): δ 7.84 (d, *J* = 15.9 Hz, 1H), 7.75 (d, *J* = 1.4 Hz, 1H), 7.44 (dd, *J* = 8.6, 1.5 Hz, 1H), 7.21 (d, *J* = 8.5 Hz, 1H), 6.42 (d, *J* = 15.9 Hz, 1H), 5.78 – 5.76 (m, 1H), 5.70 – 5.68 (m, 1H), 4.84 (t, *J* = 2.1 Hz, 2H), 4.71 – 4.45 (m, 4H), 3.80 (s, 3H), 2.31 (s, 3H). ^{13}C NMR (75 MHz, $CDCl_3$): δ 168.1, 165.5, 146.6, 143.2, 133.8, 133.6, 132.7, 126.4, 122.6 (q, *J* = 277.3 Hz), 122.1, 121.4, 116.0, 115.0, 110.4, 108.4, 62.2, 62.0 (q, *J* =

37.3 Hz) 51.7, 48.2, 8.5. IR (neat): 2960, 1778, 1756, 1628, 1413, 1275, 1160, 958, 684 cm^{-1} HRMS (APPI+): calc'd $C_{23}H_{19}F_6NO_6$ [M] 519.1117, found 519.1127.

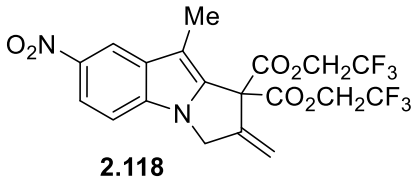

2.118

Pyrroloindole **2.118** was prepared using General Experimental Procedure D. Reagents employed: bis(2,2,2-trifluoroethyl)-2-diazomalonate **2.90** (0.100 g, 0.340 mmol), *N*-propargylindole **2.108** (87 mg, 0.40 mmol), $Rh_2(OAc)_4$ (3.0 mg, 0.0068 mmol), $ZnBr_2$ (7.6 mg, 0.034 mmol). **2.118** (35 mg, 0.073 mmol, 21%) was obtained as yellow thick oil R_f = 0.30, 20% acetone in hexanes; ^{1}H NMR (300 MHz, $CDCl_3$): δ 8.59 (d, *J* = 1.8 Hz, 1H), 8.14 (dd, *J* = 9.0, 2.2 Hz, 1H), 7.26 (d, *J* = 8.7 Hz, 2H), 5.84 – 5.81 (m, 1H), 5.76 – 5.74 (m, 1H), 4.91 (t, *J* = 2.2 Hz, 2H), 4.73 – 4.46 (m, 4H), 2.35 (s, 3H). ^{13}C NMR (75 MHz, $CDCl_3$): δ 165.1, 142.4, 141.8, 135.8, 135.2, 131.8, 122.5 (q, *J* = 37.4 Hz), 118.2, 117.4, 116.7, 110.5, 109.8, 62.1, 62.1 (q, *J* = 37.4 Hz), 48.4, 8.6. IR (neat): 2989, 1787, 1744, 1517, 1307, 1159, 1069 cm^{-1} HRMS (APPI+): calc'd for $C_{19}H_{14}F_6N_2O_6$ $[M+H]^+$ 481.0829, found 481.0823.

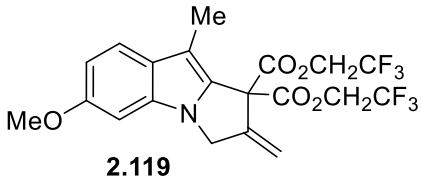

2.119

Pyrroloindole **2.119** was prepared using General Experimental Procedure D. Reagents employed: bis(2,2,2-trifluoroethyl)-2-diazomalonate **2.90** (0.100 g, 0.340 mmol), *N*-propargylindole **2.109** (0.80 g, 0.40 mmol), $Rh_2(OAc)_4$ (3.0 mg, 0.0068 mmol), $ZnBr_2$ (7.6 mg, 0.034 mmol). **2.119** (114 mg, 0.245 mmol, 72%) was obtained as a greenish white solid: R_f = 0.35, 25% acetone in hexanes; M.P. = 128.0-129.0 ^oC ^{1}H NMR (300 MHz, $CDCl_3$): δ 7.47 (d, *J* = 8.7 Hz, 1H), 6.81 (dd, *J* = 8.7, 2.2 Hz, 1H), 6.69 (d, *J* = 2.2 Hz, 1H), 5.75 – 5.73 (m, 1H), 5.68 – 5.66 (m, 1H), 4.79 (t, *J* = 2.0 Hz, 2H), 4.70 – 4.44 (m, 4H), 3.86 (s, 3H), 2.26 (s, 3H). ^{13}C NMR (75 MHz, $CDCl_3$): δ 165.9, 157.0, 143.9, 133.3, 131.1, 122.7 (q, *J* = 277.5 Hz), 126.9, 121.4, 119.5, 115.5, 109.7, 107.1, 61.8 (q, *J* = 37.3 Hz), 55.9, 48.0, 8.6. *(one carbon missing (sp^3-quat centre) presumably due to*

overlap at 62.0). IR (neat): 2928, 1755, 1624, 1339, 1248, 1084, 808, 662 cm^{-1} HRMS (APPI+): calc'd for $C_{20}H_{17}F_6NO_5$ $[M+H]^+$ 466.1084, found 466.1095.

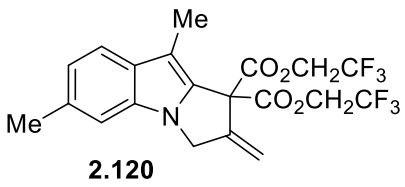

2.120

Pyrroloindole **2.120** was prepared using General Experimental Procedure D. Reagents employed: bis(2,2,2-trifluoroethyl)-2-diazomalonate **2.90** (0.100 g, 0.340 mmol), *N*-propargylindole **2.110** (75 mg, 0.40 mmol), $Rh_2(OAc)_4$ (3.0 mg, 0.0068 mmol), $ZnBr_2$ (7.6 mg, 0.034 mmol). **2.120** (122 mg, 0.272 mmol, 80%) was obtained as a brown solid: R_f = 0.35, 25% acetone in hexanes; M.P. = 106.3-107.9 ^oC ^1H NMR (300 MHz, $CDCl_3$): δ 7.48 (d, *J* = 8.2 Hz, 1H), 7.05 – 7.01 (m, 1H), 6.97 (dd, *J* = 8.2, 1.0 Hz, 1H), 5.74 – 5.72 (m, 1H), 5.67 – 5.65 (m, 1H), 4.80 (t, *J* = 2.2 Hz, 2H), 4.68 – 4.44 (m, 4H), 2.48 (s, 3H), 2.27 (s, 3H). ^{13}C NMR (75 MHz, $CDCl_3$): δ 165.8, 144.0, 133.1, 132.5, 131.9, 130.4, 122.6 (q, *J* = 277.4 Hz), 121.5, 119.6, 115.4, 109.7, 107.1, 61.8 (q, *J* = 37.3 Hz), 48.0, 21.9, 8.6. *(one carbon missing (sp^3-quat centre) presumably due to overlap at 62.0)* IR (neat): 2984, 1780, 1410, 1281, 1157, 1060, 815, 681 cm^{-1} HRMS (APPI+): calc'd for $C_{20}H_{17}F_6NO_4$ $[M+H]^+$ 450.1135, found 450.1124.

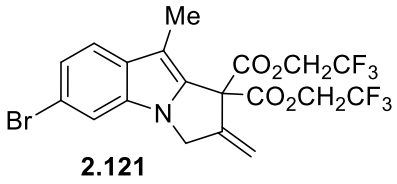

2.121

Pyrroloindole **2.121** was prepared using General Experimental Procedure D. Reagents employed bis(2,2,2-trifluoroethyl)-2-diazomalonate **2.90** (0.100 g, 0.340 mmol), *N*-propargylindole **2.11** (0.101 g, 0.408 mmol), $Rh_2(OAc)_4$ (3.0 mg, 0.0068 mmol), $ZnBr_2$ (7.6 mg, 0.034 mmol). **2.121** (143 mg, 0.278 mmol, 82%) was obtained as a brown solid: R_f = 0.35, 20% acetone in hexanes; M.P. = 101.0 -102.0 ^oC, ^1H NMR (500 MHz, $CDCl_3$): δ 7.48 (d, *J* = 8.5 Hz, 1H), 7.43 (d, *J* = 1.4 Hz, 1H), 7.27 (dd, *J* = 8.5, 1.7 Hz, 1H), 5.77 – 5.76 (m, 1H), 5.69 – 5.67 (m, 1H), 4.84 (t, *J* = 2.1 Hz, 2H), 4.71 – 4.52 (m, 4H), 2.31 (s, 3H). ^{13}C NMR (75 MHz, $CDCl_3$): δ 165.5, 143.2, 133.3, 133.2, 131.3, 122.6 (q, *J* = 277.4 Hz), 123.0, 121.2, 116.1, 116.0, 112.8, 107.6, 62.1, 61.9

(q, J = 37.4 Hz), 48.1, 8.5. IR (neat): 2985, 1757, 1411, 1280, 1248, 1158, 1059, 976, 645 cm^{-1} HRMS (APPI+): calc'd for $C_{19}H_{14}BrF_6NO_4$ $[M]^+$ 513.0010, found 513.0018.

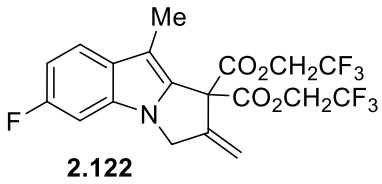

2.122

Pyrroloindole **2.122** was prepared using General Experimental Procedure D. Reagents employed: bis(2,2,2-trifluoroethyl)-2-diazomalonate **2.90** (0.100 g, 0.340 mmol), *N*-propargylindole **2.112** (75 mg, 0.40 mmol), $Rh_2(OAc)_4$ (3.0 mg, 0.0068 mmol), $ZnBr_2$ (7.6 mg, 0.034 mmol). **2.122** (114 mg, 0.251 mmol, 74%) was obtained as a brown solid: R_f = 0.30, 20% acetone in hexanes; M.P. = 93.0-94.0 ^oC. ^1H NMR (300 MHz, $CDCl_3$): δ 7.49 (dd, J = 9.4, 5.2 Hz, 1H), 6.94 – 6.84 (m, 2H), 5.77 – 5.75 (m, 1H), 5.68 – 5.66 (m, 1H), 4.78 (t, J = 2.2 Hz, 2H), 4.70 – 4.43 (m, 4H), 2.28 (s, 3H). ^{13}C NMR (75 MHz, $CDCl_3$): δ 165.7, 160.3 (d, J = 239.1 Hz), 143.4, 132.9 (d, J = 3.9 Hz), 132.5 (d, J = 12.5 Hz), 129.1, 122.6 (q, J = 277.5 Hz), 120.8 (d, J = 10.3 Hz), 115.8, 108.5 (d, J = 24.7 Hz), 107.6, 96.1 (d, J = 26.3 Hz), 62.1, 61.9 (q, J = 37.4 Hz), 48.1, 8.6. IR (neat): 2880, 1758, 1738, 1292, 1156, 1115, 1075, 963, 855, 652 cm^{-1} HRMS (APPI+): calc'd for $C_{19}H_{14}F_7NO_4$ $[M]^+$ 453.0811, found 453.0794.

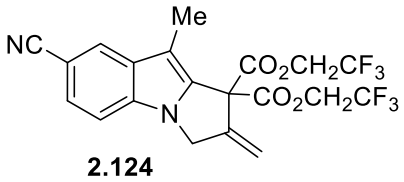

2.124

Pyrroloindole **2.124** was prepared using General Experimental Procedure D. Reagents employed: bis(2,2,2-trifluoroethyl)-2-diazomalonate **2.90** (0.075 g, 0.25 mmol), *N*-propargylindole **2.123** (60 mg, 0.3 mmol), $Rh_2(OAc)_4$ (2.2 mg, 0.0050 mmol), $ZnBr_2$ (5.6 mg, 0.025 mmol). **2.124** (15 mg, 0.032 mmol, 13%) was obtained as yellow oil, **2.125** (27 mg, 0.058 mmol, 23%) was obtained as greenish thick oil, and **2.126** (28 mg, 0.038 mmol, 15%) as a yellow thick oil: Compound **2.124**: R_f = 0.20, 25% acetone in hexanes; ^1H NMR (300 MHz, $CDCl_3$): δ 7.95 (d, J = 0.7 Hz, 1H), 7.45 (dd, J = 8.5, 1.5 Hz, 1H), 7.31 – 7.26 (m, 1H), 5.82 – 5.80 (m, 1H), 5.74 – 5.72 (m, 1H), 4.88 (t, J = 2.2 Hz, 2H), 4.72 – 4.48 (m, 4H), 2.31 (s, 3H). ^{13}C NMR (75 MHz, $CDCl_3$):

δ 165.2, 142.6, 135.0, 134.0, 132.2, 125.7, 125.4, 122.5 (q, *J* = 277.4 Hz), 120.7, 116.5, 110.7, 108.6, 102.9, 62.1, 62.0 (q, *J* = 37.4 Hz), 48.3, 8.5. IR (neat): 3551, 2924, 1753, 1640, 1156, 1097, 962, 804, 708, 645 cm^{-1} HRMS (APPI+): calc'd for $C_{20}H_{14}F_6N_2O_4$ $[M]^+$ 460.0858, found 460.0848.

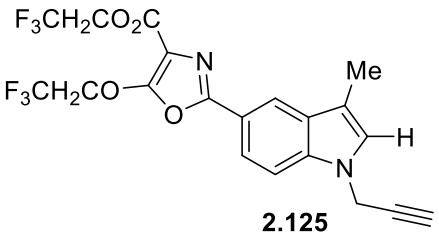

2.125

Compound **2.125**: R_f = 0.25, 20% acetone in hexanes; ^1H NMR (300 MHz, $CDCl_3$): δ 8.22 (d, *J* = 1.1 Hz, 1H), 7.85 (dd, *J* = 8.6, 1.6 Hz, 1H), 7.39 (d, *J* = 8.7 Hz, 1H), 7.04 (d, *J* = 0.9 Hz, 1H), 4.88 – 4.78 (m, 4H), 4.73 (q, *J* = 8.4 Hz, 2H), 2.41 (t, *J* = 2.5 Hz, 1H), 2.36 (d, *J* = 1.0 Hz, 3H). ^{13}C NMR (75 MHz, $CDCl_3$): δ 160.1, 159.6, 154.7, 137.6, 129.4, 126.6, 123.1 (d, *J* = 277.7 Hz), 122.3 (d, *J* = 278.3 Hz), 120.3, 118.6, 117.1, 112.9, 109.8, 109.0, 73.9, 60.6 (q, *J* = 37.3 Hz), 69.5 (q, *J* = 37.3 Hz), 35.9, 9.7. *(One carbon missing is presumably due to overlap)* IR (neat): 3289, 2924, 1735, 1623, 1586, 1428, 1158, 838, 645 cm^{-1} HRMS (APPI+): calc'd for $C_{20}H_{14}F_6N_2O_4$ $[M+H]^+$ 461.0931, found 461.0927.

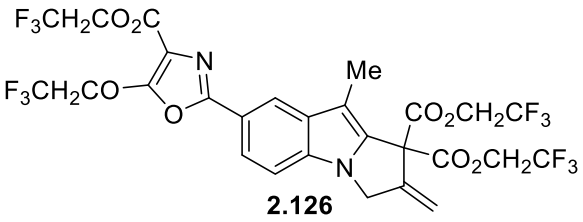

2.126

Compound **2.126**: R_f = 0.25, 20% acetone in hexanes; ^1H NMR (300 MHz, $CDCl_3$): δ 8.25 (d, *J* = 1.0 Hz, 1H), 7.87 (dd, *J* = 8.6, 1.6 Hz, 1H), 7.28 (d, *J* = 8.6 Hz, 1H), 5.80 – 5.78 (m, 1H), 5.72 – 5.71 (m, 1H), 4.87 (dd, *J* = 3.6, 1.5 Hz, 2H), 4.86 – 4.51 (m, 8H), 2.34 (s, 3H). ^{13}C NMR (75 MHz, $CDCl_3$): δ 165.4, 160.1, 159.6, 154.5, 143.0, 134.3, 133.9, 132.5, 123.1 (d, *J* = 277.5 Hz), 122.6 (q, *J* = 277.6 Hz), 122.3 (d, *J* = 278.1 Hz), 120.8, 119.1, 117.4, 116.2, 110.4, 109.1, 108.8, 69.6 (q, *J* = 37.4 Hz), 62.1, 62.0 (q, *J* = 37.3 Hz), 60.6 (q, *J* = 36.9 Hz), 48.2, 8.7. IR (neat): 2972, 1754, 1724, 1592, 1275, 1158, 964, 628 cm^{-1} HRMS (APPI+): calc'd for $C_{27}H_{18}F_{12}N_2O_8$ [M] 726.0872, found 726.0876.

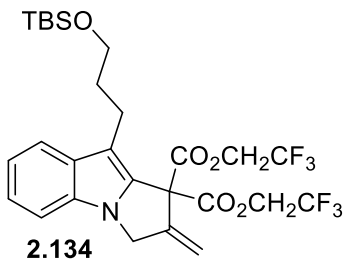

2.134

Pyrroloindole **2.134** was prepared using General Experimental Procedure D. Reagents employed: bis(2,2,2-trifluoroethyl)-2-diazomalonate **2.90** (0.100 g, 0.340 mmol), *N*-propargylindole **2.127** (98 mg, 0.32 mmol), $Rh_2(OAc)_4$ (3.0 mg, 0.0068 mmol), $ZnBr_2$ (7.6 mg, 0.034 mmol). **2.134** (77 mg, 0.13 mmol, 38%) was obtained as colorless oil: R_f = 0.35, 25% acetone in hexanes; ^{1}H NMR (300 MHz, $CDCl_3$): δ 7.71 – 7.63 (m, 1H), 7.27 – 7.21 (m, 2H), 7.17 – 7.09 (m, 1H), 5.74 – 5.72 (m, 1H), 5.67 – 5.65 (m, 1H), 4.85 (t, *J* = 2.1 Hz, 2H), 4.67 – 4.47 (m, 4H), 3.70 (t, *J* = 6.2 Hz, 2H), 2.86 – 2.74 (m, 2H), 1.94 – 1.74 (m, 2H), 0.93 (s, 9H), 0.08 (s, 6H). ^{13}C NMR (75 MHz, $CDCl_3$): δ 165.8, 144.0, 132.9, 132.5, 131.8, 122.5 (d, *J* = 277.5 Hz), 120.5, 119.6, 115.4, 111.9, 109.9, 63.3, 62.8 (q, *J* = 37.3 Hz), 62.3, 48.1, 33.4, 26.1, 21.0, 18.5, 5.2. IR (neat): 2956, 2857, 1754, 1280, 1158, 962, 810, 736, 661 cm^{-1} HRMS (APPI+): calc'd for $C_{27}H_{33}F_6NO_5Si$ $[M+H]^+$ 594.2105, found 594.2082.

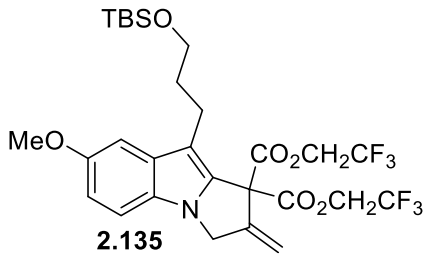

2.135

Pyrroloindole **2.135** was prepared using General Experimental Procedure D. Reagents employed: bis (2,2,2-trifluoroethyl)-2-diazomalonate **2.90** (0.0800 g, 0.272 mmol), *N*-propargylindole **2.128** (117 mg, 0.320 mmol), $Rh_2(OAc)_4$ (2.4 mg, 0.0054 mmol), $ZnBr_2$ (6.0 mg, 0.027 mmol). **2.135** (126 mg, 0.202 mmol, 74%) was obtained as brown oil: R_f = 0.40, 20% acetone in hexanes; ^{1}H NMR (300 MHz, $CDCl_3$): δ 7.14 (d, *J* = 8.8 Hz, 1H), 7.08 (d, *J* = 2.3 Hz, 1H), 6.89 (dd, *J* = 8.8, 2.4 Hz, 1H), 5.72 – 5.71 (m, 1H), 5.66 – 5.64 (m, 1H), 4.82 (t, *J* = 2.0 Hz, 2H), 4.64 – 4.48 (m, 4H), 3.86 (s, 3H), 3.76 – 3.62 (m, 2H), 2.82 – 2.73 (m, 2H), 1.87 – 1.77 (m, 2H), 0.93 (s, 9H), 0.08 (s, 6H). ^{13}C NMR (75 MHz, $CDCl_3$): δ 165.9, 154.3, 144.0, 133.1, 132.1, 128.3, 122.6 (d, *J* = 277.6 Hz), 115.4, 113.1, 111.4, 110.8, 102.0, 63.3, 62.5, 61.8 (q, *J* = 37.4 Hz), 56.1, 48.3, 33.3, 26.1, 21.0, 18.5, -5.2. IR (neat): 2954, 2858,

1758,1481, 1282, 1163, 1072, 834, 775, 660 cm^{-1} HRMS (APPI+): calc'd for $C_{28}H_{35}F_6NO_6Si$ $[M+H]^+$ 624.2211, found 624.2191.

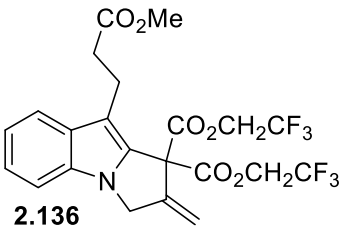

2.136

Pyrroloindole **2.136** was prepared using General Experimental Procedure D. Reagents employed: bis(2,2,2-trifluoroethyl)-2-diazomalonate **2.90** (92 mg, 0.31 mmol), *N*-propargylindole **2.129** (90 mg, 0.4 mmol), $Rh_2(OAc)_4$ (2.7 mg, 0.0062 mmol), $ZnBr_2$ (7 mg, 0.03 mmol). **2.136** (47 mg, 0.093 mmol, 30%) was obtained as yellow thick oil: R_f = 0.25, 20% acetone in hexanes; ^{1}H NMR (300 MHz, $CDCl_3$): δ 7.63 (dt, *J* = 7.9, 0.9 Hz, 1H), 7.26 – 7.23 (m, 2H), 7.19 – 7.09 (m, 1H), 5.78 – 5.76 (m, 1H), 5.69 – 5.67 (m, 1H), 4.85 (t, *J* = 2.2 Hz, 2H), 4.70 – 4.50 (m, 4H), 3.67 (s, 3H), 3.20 – 3.05 (m, 2H), 2.73 – 2.56 (m, 2H). ^{13}C NMR (75 MHz, $CDCl_3$): δ 173.7, 165.7, 143.6, 133.0, 132.9, 131.3, 122.7, 122.6 (q, *J* = 277.4 Hz), 120.1, 120.0, 115.8, 110.1, 110.0, 62.3, 61.9 (q, *J* = 37.3 Hz), 51.7, 48.2, 34.4, 20.1. IR (neat): 2955, 1754, 1281, 1280, 1157, 1072, 741 cm^{-1} HRMS (APPI+): calc'd for $C_{22}H_{19}F_6NO_6$ $[M+H]^+$ 508.1189, found 508.1168.

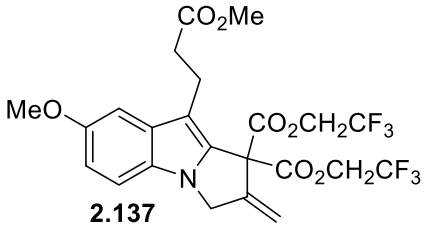

2.137

Pyrroloindole **2.137** was prepared using General Experimental Procedure D. Reagents employed: bis(2,2,2-trifluoroethyl)-2-diazomalonate **2.90** (0.100 g, 0.340 mmol), *N*-propargylindole **2.130** (109 mg, 0.40 mmol), $Rh_2(OAc)_4$ (3.0 mg, 0.0068 mmol), $ZnBr_2$ (7.6 mg, 0.034 mmol). **2.137** (105 mg, 0.195 mmol, 57%) was obtained as a greenish thick oil: R_f = 0.20, 25% Et_2O in hexanes; ^{1}H NMR (300 MHz, $CDCl_3$): δ 7.18 – 7.11 (m, 1H), 7.05 (d, *J* = 2.2 Hz, 1H), 6.90 (dd, *J* = 8.8, 2.4 Hz, 1H), 5.76 – 5.74 (m, 1H), 5.68 – 5.66 (m, 1H), 4.82 (t, *J* = 2.2 Hz, 2H), 4.72 – 4.45 (m, 4H), 3.87 (s, 3H), 3.68 (s, 3H), 3.14 – 3.01 (m, 2H), 2.69 – 2.55 (m, 2H). ^{13}C NMR (75 MHz, $CDCl_3$): δ 173.9, 165.8, 154.5, 143.6, 133.5, 131.7, 128.3, 122.5 (d, *J* = 277.5 Hz), 115.7, 113.2, 110.9, 109.5, 101.8, 62.7, 62.1 (q, *J* = 37.4 Hz), 56.2, 51.7,

48.4, 34.2, 20.1. IR (neat): 2955, 1754, 1735, 1411, 1281, 1158, 1072, 970, 741, 650 cm^{-1} HRMS (APPI+): calc'd for $C_{23}H_{21}F_6NO_7$ $[M+H]^+$ 538.1295, found 538.1301.

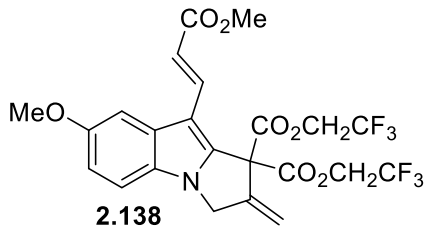

2.138

Pyrroloindole **2.138** was prepared using General Experimental Procedure D. Reagents employed: bis (2, 2,2-trifluoroethyl)-2-diazomalonate **2.90** (53 mg, 0.18 mmol), *N*-propargylindole **2.131** (58 mg, 0.21 mmol), $Rh_2(OAc)_4$ (1.6 mg, 0.0036 mmol), $ZnBr_2$ (4.0 mg, 0.018 mmol). **2.138** (39 mg, 0.073 mmol, 40%) was obtained as a yellow oil: R_f = 0.25, 25% EtOAc in hexanes; ^{1}H NMR (300 MHz, $CDCl_3$): δ 7.91 (d, *J* = 16.1 Hz, 1H), 7.36 (d, *J* = 2.3 Hz, 1H), 7.20 (d, *J* = 8.9 Hz, 1H), 6.97 (dd, *J* = 8.9, 2.3 Hz, 1H), 6.37 (d, *J* = 16.1 Hz, 1H), 5.83 – 5.81 (m, 1H), 5.74 – 5.72 (m, 1H), 4.89 (t, *J* = 2.3 Hz, 2H) 4.74 – 4.48 (m, 4H) 3.90 (s, 3H), 3.80 (s, 3H). ^{13}C NMR (75 MHz, $CDCl_3$): δ 168.3, 165.0, 156.2, 142.2, 138.8, 136.5, 130.2, 128.5, 122.5 (d, *J* = 277.7 Hz), 116.5, 114.5, 114.0, 111.4, 107.7, 103.8, 63.3, 62.1 (q, *J* = 37.6 Hz), 56.2, 51.5, 48.9. IR (neat): 2921, 2851, 1761, 1715, 1618, 1247, 1158, 1026, 788 cm^{-1} HRMS (APPI+): calc'd for $C_{23}H_{19}F_6NO_7$ $[M+H]^+$ 536.1138, found 536.1121.

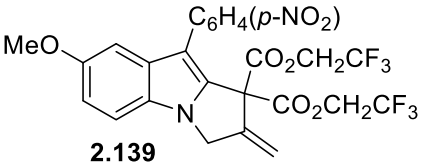

2.139

Pyrroloindole **2.139** was prepared using General Experimental Procedure D. Reagents employed: bis(2,2,2-trifluoroethyl)-2-diazomalonate **2.90** (0.050 g, 0.17 mmol), *N*-propargylindole **2.132** (62 mg, 0.20 mmol), $Rh_2(OAc)_4$ (1.5 mg, 0.0034 mmol), $ZnBr_2$ (3.8 mg, 0.017 mmol). **2.139** (27 mg, 0.047 mmol, 28%) was obtained as a yellow thick oil: R_f = 0.30, 20% acetone in hexanes; ^{1}H NMR (300 MHz, $CDCl_3$): δ 8.32 – 8.23 (m, 2H), 7.66 – 7.56 (m, 2H), 7.26 (d, *J* = 8.6 Hz, 1H), 7.11 – 6.94 (m, 2H), 5.76 – 5.70 (m, 2H), 4.94 (t, *J* = 2.2 Hz, 2H), 4.65 – 4.25 (m, 4H), 3.82 (s, 3H). ^{13}C NMR (75 MHz, $CDCl_3$): δ 165.5, 155.8, 146.3, 143.4, 141.6, 134.3, 131.1, 129.8, 128.3, 123.9, 122.3 (q, *J* = 277.7 Hz) 116.1, 114.3, 111.32, 111.25, 101.9, 63.1, 61.8 (q, *J* = 37.4 Hz),

56.1, 48.6. IR (neat): 2925, 1753, 1597, 1513, 1342, 1279, 1151, 1070, 847 cm^{-1} HRMS (APPI+): calc'd for $C_{25}H_{18}F_6N_2O_7$ $[M+H]^+$ 573.1096, found 573.1103.

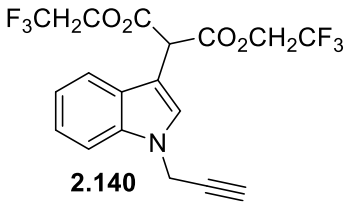

2.140

Functionalized indole **2.140** was prepared using General Experimental Procedure D. Reagents employed: bis(2,2,2-trifluoroethyl)-2-diazomalonate **2.90** (0.050 g, 0.17 mmol), *N*-propargylindole **2.133** (31 mg, 0.20 mmol), $Rh_2(OAc)_4$ (1.5 mg, 0.0034 mmol), $ZnBr_2$ (3.8 mg, 0.017 mmol). **2.140** (63 mg, 0.15 mmol, 88%) was obtained as a light-yellow oil: R_f = 0.25, 20% acetone in hexanes; ^{1}H NMR (300 MHz, $CDCl_3$): δ 7.61 (d, *J* = 7.9 Hz, 1H), 7.42 (s, 1H), 7.38 (d, *J* = 8.2 Hz, 1H), 7.31 – 7.23 (m, 1H), 7.22 – 7.15 (m, 1H), 5.12 (s, 1H), 4.80 (d, *J* = 2.5 Hz, 2H), 4.63 – 4.40 (m, 4H), 2.40 (t, *J* = 2.5 Hz, 1H). ^{13}C NMR (75 MHz, $CDCl_3$): δ 166.2, 136.0, 127.5, 127.2, 122.7 (q, *J* = 277.3 Hz), 122.9, 120.8, 119.3, 109.9, 104.8, 77.2, 74.3, 61.5 (q, *J* = 37.2 Hz), 48.8, 36.1. IR (neat): 3293, 2977, 1754, 1467, 1445, 1275, 1158, 1058, 978, 741, 647 cm^{-1} HRMS (APPI+): calc'd for $C_{18}H_{13}F_6NO_4$ $[M+H]^+$ 421.0749, found 422.0700.

Synthesis and Characterization of Substituted Tetrahydropyrido[1,2-a]indole (pyridoindole) Products

Pyridoindole **2.147** was prepared using General Experimental Procedure D. Reagents employed: bis(2,2,2-trifluoroethyl)-2-diazomalonate **2.90** (0.090 g, 0.31 mmol), *N*-butynylskatole **2.143** (67mg, 0.36 mmol), $Rh_2(OAc)_4$ (2.7 mg, 0.0060 mmol), $ZnBr_2$ (6.8 mg, 0.030 mmol). **2.147** (66 mg, 0.15 mmol, 48%) was obtained as a thick yellow oil: R_f = 0.35, 20% acetone in hexanes; ^{1}H NMR (300 MHz, $CDCl_3$): δ 7.58 (dt, *J* = 7.9, 1.0 Hz, 1H), 7.29 – 7.25 (m, 1H), 7.23 (dd, *J* = 8.2, 1.2 Hz, 1H), 7.14 (ddd, *J* = 8.0, 6.2, 1.8 Hz, 1H), 5.47 (bs, 1H), 5.19 (bs, 1H), 4.68 – 4.41 (m, 4H), 4.15 (t, *J* = 6.1 Hz, 2H), 2.87 (t, *J* = 6.1 Hz, 2H), 2.20 (s, 3H). ^{13}C NMR (75 MHz, $CDCl_3$): δ

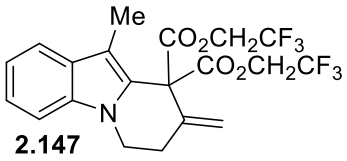

2.147

166.7, 138.9, 135.7, 128.8, 125.0, 122.5, 122.7 (q, *J* = 277.5 Hz), 119.8, 119.3, 116.7, 110.8, 109.0, 61.7 (q, *J* = 37.2 Hz), 61.1, 42.3, 31.8, 9.2. IR (neat): 2971, 1151, 1280, 1157, 10.92, 1073, 972, 739, 649 cm^{-1} HRMS (APPI+): calc'd for $C_{20}H_{17}F_6NO_4$ $[M+H]^+$ 451.1135 found 450.1141.

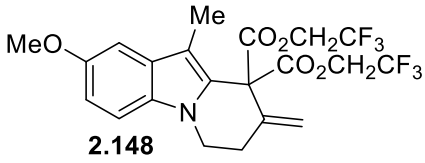

2.148

Pyridoindole **2.148** was prepared using General Experimental Procedure D. Reagents employed: bis(2,2,2-trifluoroethyl)-2-diazomalonate **2.90** (0.100 g, 0.340 mmol), *N*-butynylskatole **2.144** (87 mg, 0.40 mmol), $Rh_2(OAc)_4$ (3.0 mg, 0.0068 mmol), $ZnBr_2$ (7.6 mg, 0.034 mmol). **2.148** (0.0980 g, 0.204 mmol, 60%) was obtained as a light-yellow thick oil: R_f = 0.18, 20% acetone in hexanes; ^{1}H NMR (300 MHz, $CDCl_3$): δ 7.18 (d, *J* = 8.8 Hz, 1H), 7.00 (d, *J* = 2.3 Hz, 1H), 6.91 (dd, *J* = 8.8, 2.4 Hz, 1H), 5.46 (bs, 1H), 5.17 (bs, 1H), 4.68 – 4.36 (m, 4H), 4.12 (t, *J* = 6.1 Hz, 2H), 3.87 (s, 3H), 2.87 (t, *J* = 6.0 Hz, 2H), 2.17 (s, 3H). ^{13}C NMR (75 MHz, $CDCl_3$): δ 166.6, 154.3, 138.7, 130.9, 128.9, 125.4, 122.7 (d, *J* = 277.5 Hz), 116.5, 112.9, 110.1, 109.7, 100.7, 61.6 (q, *J* = 37.3 Hz), 60.7, 56.0, 42.2, 31.7, 9.2. IR (neat): 2972, 2889, 1151, 1280, 1157, 10.92, 785, 613 cm^{-1} HRMS (APPI+): calc'd for $C_{21}H_{19}F_6NO_5$ $[M+H]^+$ 480.1240, found 480.1230.

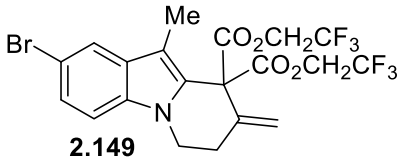

2.149

Pyridoindole **2.149** was prepared using General Experimental Procedure D. Reagents employed: bis(2,2,2-trifluoroethyl)-2-diazomalonate **2.90** (45 mg, 0.15 mmol), *N*-butynylskatole **2.145** (47 mg, 0.18 mmol), $Rh_2(OAc)_4$ (1.4 mg, 0.0030 mmol), $ZnBr_2$ (3.4 mg, 0.015 mmol). **2.149** (55 mg, 0.10 mmol, 67%) was obtained as a brown oil: R_f = 0.35, 20% EtOAc in hexanes; ^{1}H NMR (300 MHz, $CDCl_3$): δ 7.75 – 7.66 (m, 1H), 7.31 (dd, *J* = 8.7, 1.9 Hz, 1H), 7.19 – 7.09 (m, 1H), 5.48 (bs, 1H), 5.19 (bs, 1H), 4.67 – 4.42 (m, 4H), 4.13 (t, *J* = 6.2 Hz, 2H), 2.87 (t, *J* = 5.9 Hz, 2H), 2.15 (s, 3H). ^{13}C NMR (75 MHz, $CDCl_3$): δ 166.4, 138.4, 134.3, 130.4, 126.3, 125.4, 122.6 (d, *J*

= 277.5 Hz), 121.9, 117.0, 113.1, 110.6, 110.4, 61.7 (q, *J* = 37.2 Hz), 61.0, 42.4, 31.6, 9.2. IR (neat): 2927, 1756, 1734, 1286, 1158, 966, 780 cm^{-1} HRMS (APPI+): calc'd for $C_{20}H_{16}BrF_6NO_4$ $[M+H]^+$ 528.0240, found 528.0226.

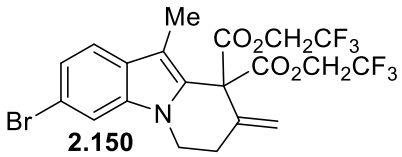

2.150

Pyridoindole **2.150** was prepared using General Experimental Procedure D. Reagents employed: bis(2,2,2-trifluoroethyl)-2-diazomalonate **2.90** (18 mg, 0.061 mmol), *N*-butynylskatole **2.146** (20 mg, 0.07 mmol), $Rh_2(OAc)_4$ (0.5 mg, 0.001 mmol), $ZnBr_2$ (1.4 mg, 0.0061 mmol). **2.150** (23 mg, 0.044 mmol, 72%) was obtained as a brown oil: R_f = 0.35, 20% EtOAc in hexanes; ^1H NMR (300 MHz, $CDCl_3$): δ 7.46 – 7.40 (m, 2H), 7.23 (dd, *J* = 8.5, 1.6 Hz, 1H), 5.49 (bs, 1H), 5.20 (bs, 1H), 4.70 – 4.42 (m, 4H), 4.11 (t, *J* = 6.2 Hz, 2H), 2.87 (t, *J* = 6.0 Hz, 2H), 2.17 (s, 3H). ^{13}C NMR (75 MHz, $CDCl_3$): δ 166.4, 138.4, 136.4, 127.6, 125.7, 123.1, 122.6 (d, *J* = 277.5 Hz), 120.6, 117.1, 116.3, 112.1, 111.1, 61.6 (q, *J* = 37.2 Hz), 61.0, 42.4, 31.6, 9.2. IR (neat): 2970, 1751, 1280, 1157, 1074, 973, 918, 689, 650 cm^{-1} HRMS (APPI+): calc'd for $C_{20}H_{16}BrF_6NO_4$ $[M+H]^+$ 528.0240, found 528.0234.

Synthesis and Characterization of Substituted Tetrahydroazepino[1,2-a]indole (azepinoindole) Products

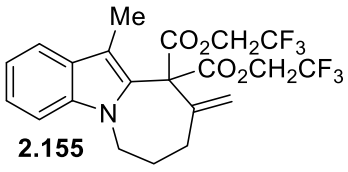

2.155

Azepinoindole **2.155** was prepared using General Experimental Procedure D. Reagents employed: bis(2,2,2-trifluoroethyl)-2-diazomalonate **2.90** (65 mg, 0.22 mmol), *N*-pentynylskatole **2.153** (52 mg, 0.26 mmol), $Rh_2(OAc)_4$ (2.0 mg, 0.0044 mmol), $ZnBr_2$ (5.0 mg, 0.022 mmol). **2.155** (29 mg, 0.062 mmol, 28%) was obtained as a thick yellow oil: R_f = 0.35, 10% EtOAc in hexanes; ^1H NMR (500 MHz, $CDCl_3$): δ 7.59 – 7.56 (m, 1H), 7.30 – 7.22 (m, 2H), 7.25 (dd, *J* = 6.6, 1.1 Hz,

1H), 7.11 (ddd, *J* = 7.9, 6.6, 1.4 Hz, 1H), 5.53 (bs, 1H), 5.51 (bs, 1H), 4.60 – 4.43 (m, 4H), 4.27 (t, *J* = 6.2 Hz, 2H), 2.42 (t, *J* = 6.9 Hz, 2H), 2.20 (s, 3H), 1.99 – 1.93 (m, 1H). ^{13}C NMR (75 MHz, $CDCl_3$): δ 166.6, 141.7, 135.7, 128.3, 127.2, 122.8, 122.6 (d, *J* = 277.5 Hz), 120.7, 119.3, 119.2, 112.0, 108.5, 64.2, 61.7 (q, *J* = 37.1 Hz), 40.2, 30.7, 28.2, 9.9. IR (neat): 3308, 2926, 1754, 1279, 1160, 978, 740, 643 cm^{-1} HRMS (APPI+): calc'd for $C_{21}H_{19}F_6NO_4$ $[M+H]^+$ 464.1291, found 464.1274.

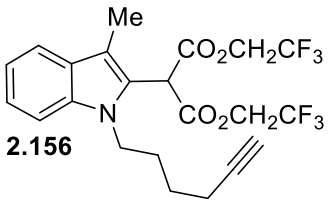

2.156

C2-Functionalized Indole **2.156** was prepared using General Experimental Procedure D. Reagents employed: bis(2,2,2-trifluoroethyl)-2-diazomalonate **2.90** (46 mg, 0.16 mmol), *N*-pentynylskatole **2.154** (54 mg, 0.31 mmol), $Rh_2(OAc)_4$ (1.4 mg, 0.0032 mmol), $ZnBr_2$ (3.6 mg, 0.016 mmol). **2.156** (38 mg, 0.080 mmol, 50%) was obtained as a yellow thick oil: R_f = 0.35, 10% EtOAc in hexanes; ^{1}H NMR (500 MHz, $CDCl_3$): δ 7.60 – 7.55 (m, 1H), 7.33 – 7.29 (m, 1H), 7.28 – 7.21 (m, 1H), 7.13 (ddd, *J* = 8.0, 6.8, 1.2 Hz, 1H), 5.19 (s, 1H), 4.73 – 4.42 (m, 4H), 4.18 – 4.12 (m, 2H), 2.29 (s, 3H), 2.23 (td, *J* = 6.9, 2.6 Hz, 2H), 1.96 (t, *J* = 2.6 Hz, 1H), 1.93 – 1.79 (m, 2H), 1.62 – 1.57 (m, 2H). ^{13}C NMR (75 MHz, $CDCl_3$): δ 165.0, 136.6, 128.3, 123.8, 122.9, 122.6 (q, *J* = 277.3 Hz), 119.6, 119.5, 112.6, 109.8, 83.8, 69.1, 61.7 (q, *J* = 37.2 Hz), 48.4, 43.6, 29.3, 25.7, 18.2, 9.1. IR (neat): 3332, 2899, 1639, 1370, 1158, 1050, 896, 763, 556 cm^{-1} HRMS (APPI+): calc'd for $C_{22}H_{21}F_6NO_4$ [M] 477.1375, found 477.1474.

Scheme 2.33: General Synthetic Scheme for the Synthesis of Bis-functionalized Pyrroloindole Compounds

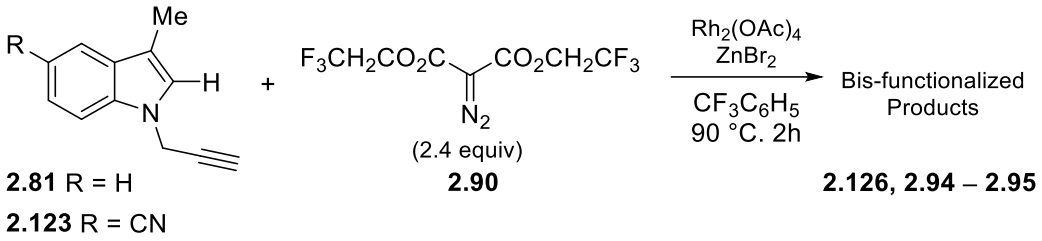

General Experimental Procedure E:

Substituted indole **2.81** or **2.123** (1.0 equiv) was added to a reaction vessel equipped with a stir bar, and the vessel was then evacuated and backfilled with N_2. This cycle was repeated two additional times, followed by the addition of trifluorotoluene (5 mL/mmol of indole) under a N_2 atmosphere. $Rh_2(OAc)_4$ (2mol %) and $ZnBr_2$ (10mol %) were then added to the reaction vessel and again the vessel was evacuated (quickly) and backfilled with N_2. bis(2,2,2-trifluoroethyl)-2-diazomalonate **2.90** (1.2 equiv) was added, and the reaction mixture was heated to 90 °C and stirred at this temperature for 2 h. Followed by the consumption of the first portion of the diazo reagent, which was monitored by TLC, an additional 1.2 equiv of **2.90** was added to the reaction mixture and the solution was heated to 90 °C for another 2 h. Upon completion, the reaction mixture was then directly loaded and purified by silica gel flash column chromatography (hexanes/EtOAc gradient) to yield the bis-functionalized pyrrolodindole (**2.94**/**2.95** or **2.126**).

Bis-functionalized pyrroloindole **2.94** and **2.95** were prepared using General Experimental Procedure E. Reagents employed: *N*-propargylindole **2.81** (150 mg, 0.89 mmol), bis(2,2,2-trifluoroethyl)-2-diazomalonate **2.90** (626 mg, 2.13 mmol), $Rh_2(OAc)_4$ (7.9 mg, 0.018 mmol), $ZnBr_2$ (20.0 mg, 0.089 mmol). **2.94** (232 mg, 0.331 mmol, 37%) was obtained as a yellow oil, and **2.95** (116 mg, 0.165 mmol, 19%) was obtained as a clear yellow oil: Note: Analytically pure pyrroloindole isomers **2.94** and **2.95** were separated by preparatory TLC purification in 20% acetone in hexanes.

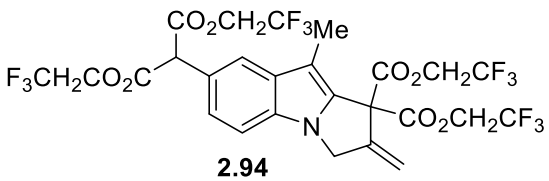

2.94

Compound **2.94**: R_f = 0.30, 20% acetone in hexanes; ^{1}H NMR (300 MHz, acetone-D_6) δ 7.71 (d, *J* = 1.3 Hz, 1H), 7.37 (dd, *J* = 8.5, 0.5 Hz, 1H), 7.30 (dd, *J* = 8.5, 1.7 Hz, 1H), 5.81 – 5.79 (m, 1H), 5.75 – 5.73 (m, 1H), 5.26 (s, 1H), 4.96 (t, *J* = 2.2 Hz, 2H), 4.93 – 4.72 (m, 8H), 2.30 (s, 3H). (Note: *acetone-D_6 was used as solvent signal overlap was observed in $CDCl_3$*) ^{13}C NMR (75 MHz, $CDCl_3$): δ 166.4, 165.6, 143.3, 134.0, 132.9, 132.6, 124.8, 122.7 (q, *J* = 277.4 Hz), 122.6 (q, *J* = 277.4 Hz), 120.8, 120.5, 115.9, 110.6, 107.5, 62.2, 61.9 (d, *J* = 37.2 Hz), 61.5 (d, *J* = 37.1 Hz), 57.0, 48.2, 8.5. IR (neat): 2927, 1754, 1410, 1280, 1156, 1067, 651 cm^{-1} HRMS (APPI+): calc'd for $C_{26}H_{19}F_{12}NO_8$ $[M+H]^+$ 702.0992, found 702.0977.

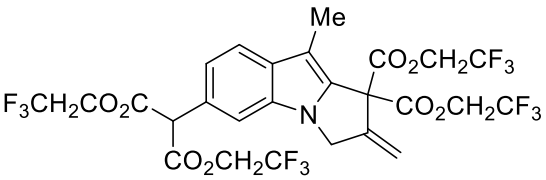

2.95

Compound **2.95**: R_f = 0.20, 20% acetone in hexanes; ^{1}H NMR (300 MHz, $CDCl_3$): δ 7.61 (d, *J* = 8.3 Hz, 1H), 7.32 (d, *J* = 1.3 Hz, 1H), 7.12 (dd, *J* = 8.3, 1.6 Hz, 1H), 5.78 – 5.75 (m, 1H), 5.71 – 5.69 (m, 1H), 4.93 (s, 1H), 4.85 (t, *J* = 2.1 Hz, 2H), 4.69 – 4.42 (m, 8H), 2.29 (s, 3H). ^{13}C NMR (75 MHz, $CDCl_3$): δ 164.4, 165.5, 143.3, 134.0, 132.9, 132.5, 124.7, 122.7 (d, *J* = 277.4 Hz), 122.6 (d, *J* = 276.9 Hz), 120.7, 120.5, 115.9, 110.6, 107.5, 62.1, 61.9 (q, *J* = 37.3 Hz), 61.5 (q, *J* = 37.2 Hz), 56.9, 48.2, 8.6. IR (neat): 2925, 1753, 1280, 1280, 1156, 1070, 969, 651 cm^{-1} HRMS (APPI+): calc'd for $C_{26}H_{19}F_{12}NO_8$ $[M+H]^+$ 702.0992, found 702.0994.

Bis-functionalized pyrroloindole **2.126** was prepared using General Experimental Procedure E. Reagents employed: *N*-propargylindole **2.123** (0.050 mg, 0.26 mmol), bis(2,2,2-trifluoroethyl)-2-diazomalonate **2.90** (183 mg, 0.624 mmol), $Rh_2(OAc)_4$ (2.3 mg, 0.0052 mmol), $ZnBr_2$ (5.8 mg,

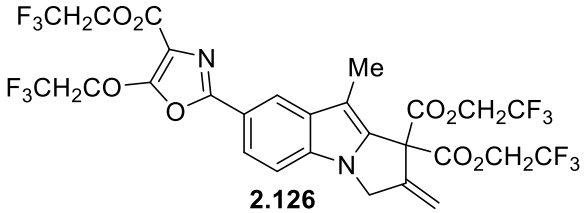

2.126

0.026 mmol). **2.126** (120 mg, 0.16 mmol, 61%) was obtained as a thick oil: The spectra match that previously reported.

Synthesis and Characterization of a Tetrahydropyrido[1,2-*a*] indole Products (2.86) *via* a 6-endo Cyclization

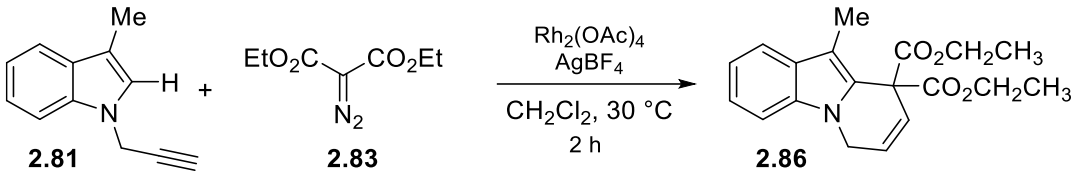

Tetrahydropyrido[1,2-a]indole **2.86** was prepared using General Experimental Procedure D. Reagents employed: diethyl-2-diazomalonate **2.83** (0.100 g, 0.537 mmol), *N*-propargylindole **2.81** (109 mg, 0.644 mmol), rhodium (II) acetate (4.7 mg, 0.010 mmol), $AgBF_4$ (10.5 mg, 0.0537 mmol). **2.86** (35 mg, 0.11 mmol, 20%) was obtained as light-yellow oil: R_f = 0.20, 20% acetone in hexanes; ^{1}H NMR (300 MHz, $CDCl_3$): δ 7.64 – 7.58 (m, 1H), 7.28 (ddd, *J* = 8.1, 1.5, 0.8 Hz, 1H), 7.24 (dt, *J* = 4.3, 1.3 Hz, 1H), 7.21 – 7.12 (m, 1H), 6.32 (dt, *J* = 10.3, 3.1 Hz, 1H), 6.21 (dt, *J* = 10.3, 2.3 Hz, 1H), 4.64 (apt t, *J* = 3.1 Hz, 2H), 4.29 – 4.16 (m, 4H), 2.32 (s, 3H), 1.25 (t, *J* = 7.1 Hz, 6H). ^{13}C NMR (75 MHz, $CDCl_3$): δ 168.5, 135.5, 128.8, 124.2, 123.6, 122.8, 122.0, 119.6, 119.0, 110.4, 109.0, 62.4, 61.7, 56.7, 41.8, 14.5, 9.9. IR (neat): 2981, 2139, 1727, 1457,1369, 1318, 1206, 1031, 858, 739, cm^{-1} HRMS (APPI+): calc'd for $C_{19}H_{21}NO_4$ $[M+H]^+$ 328.1543, found 328.1551.

Synthesis and Characterization of a Substituted Propargyl Indole Product 2.85 *via* a C-H Insertion Reaction

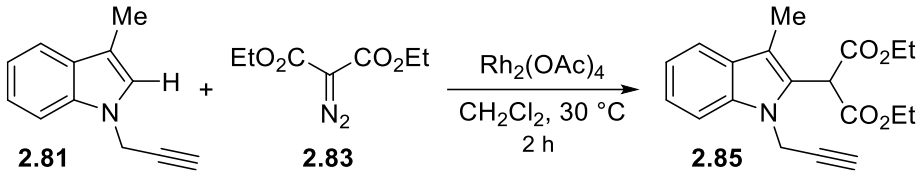

Substituted propargyl indole **2.85** was prepared using general experimental procedure D. Reagents employed: diethyl-2-diazomalonate **2.83** (0.100 g, 0.537 mmol), *N*-propargylindole **2.81** (109 mg, 0.640 mmol), $Rh_2(OAc)_4$ (4.8 mg, 0.010). **2.85** (0.060 g, 0.18 mmol, 34%) was obtained as light-yellow oil: R_f = 0.40, 25% EtOAc in hexanes; ^{1}H NMR (300 MHz, $CDCl_3$): δ 7.59 – 7.52 (m, 1H), 7.47 – 7.40 (m, 1H), 7.26 (ddd, *J* = 8.6, 4.9, 1.4 Hz, 1H), 7.14 (ddd, *J* = 8.0, 7.1, 1.0 Hz, 1H), 5.10 (s, 1H), 4.98 (d, *J* = 2.5 Hz, 2H), 4.36 – 4.13 (m, 4H), 2.31 (s, 3H), 2.24 (t, *J* = 2.5 Hz, 1H), 1.27 (t, *J* = 7.1 Hz, 6H). ^{13}C NMR (75 MHz, $CDCl_3$): δ 167.4, 136.7, 128.4, 126.3, 122.7, 119.8, 119.3, 112.2, 109.9, 78.6, 72.4, 62.4, 49.6, 34.2, 14.1, 9.2. IR (neat): 3277, 2981, 1728, 1464, 1143, 1028, 738, 654 cm^{-1} HRMS (APPI+): calc'd for $C_{19}H_{21}NO_4$ $[M+H]^+$ 328.1543, found 328.1527.

1.18 References

1. Roager, H.M.; Licht, T.R. *Nat. Commun*. **2018**, *9*, 3294.
2. Norwood, V. M.; Huigens, R. W. *ChemBioChem*. **2019**, *20*, 2273.
3. Davies, H. M. L.; Hedley. S. J. *Chem. Soc. Rev.* **2007**,*36*, 1109.
4. Kaushik, N. K.; Kaushik, N.; Attri, P.; Kumar, N.; Kim, C. H.; Verma, A. K.; Choi, E. H. *Molecules* **2013**, *18*, 6620.
5. Davies, H. M. L.; Hedley, S. J. *Chem. Soc. Rev.* **2007**, *36*, 1109.
6. Wenkert, E.; Alonso, M. E.; Gottlieb, H. E.; Sanchez, E. L. *J. Org. Chem.* **1977**, *42*, 3945
7. Gibe, R.; Kerr, M. A. *J. Org. Chem.* **2002**, *67*, 6247.
8. Johansen, M. B.; Kerr, M. A. *Org. Lett.* **2010**, 12, 4956.
9. Conia, J. M.; Le Perchec, P. *Synthesis* **1975**, *1*, 1.
10. Hack, D.; Blümel, M.; Chauhan, P.; Philipps, A. R.; Enders, D. *Chem. Soc. Rev.* **2015**, *44*, 6059.
11. Itoh, Y.; Tsuji, H.; Yamagata, K. I.; Endo, K.; Tanaka, I.; Nakamura, M.; Nakamura, E. *J. Am. Chem. Soc.* **2008**, *130*, 17161.
12. Nakamura, Y.; Suzuki, M.; Imai, Y.; Nishimura, J. *Org. Lett.* **2004**, *6*, 2797.
13. Lebold, T. P.; Leduc, A. B.; Kerr, M. A. *Org. Lett.* **2009**, *11*, 16, 3770.
14. Urabe, F.; Miyamoto, S.; Takahashi, K.; Ishihara, J.; Hatakeyama, S. *Org. Lett.* **2014**, *16*, 1004.
15. Liu, K.; Zhu, C.; Min, J.; Peng, S.; Xu, G.; Sun, J. *Angew. Chem. Int. Ed.* **2015**, *54*, 12962.
16. Hossain, M. L.; Wang, J. *Chem. Rec.* **2018**, *18*, 1548.
17. Hunter, A. C.; Schlitzer, S. C.; Sharma, I. *Chem. Eur. J.* **2016**, *22*, 16062.

18. Hunter, A.C.; Schlitzer, S.C.; Stevens, J.C.; Almutwalli, B.; Sharma, I. *J. Org. Chem.* **2018**, *83*, 2744.

19. Hunter, A. C.; Almutwalli, B.; Bain, A.; Sharma, I. *Tetrahedron* **2018**, *74*, 5451.

20. Davies, H. M. L.; Spangler, J. E. Reactions of Indoles with Metal-Bound Carbenoids. *In Advances in Heterocyclic Chemistry; Katritzky, A. R., Ed*.; Elsevier BV: **2013**,*110*, 43.

21. Kaushik, N. K.; Kaushik, N.; Attri, P.; Kumar, N.; Kim, C. H. Verma, A. K.; Choi, E. H. *Molecules* **2013**, *18*, 6620.

22. Regitz, M. *Angew. Chem. Int. Ed. Engl.* **1967**, *6*, 733.

23. (a) Zhao, X.; Zhang, Y.; Wang, J. *Chem. Commun.* **2012**, *48*, 10162.

24. For reviews, see: (a) Hack, D.; Blümel, M.; Chauhan, P.; Philipps, A. R.; Enders, D. *Chem. Soc. Rev.* **2015**, *44*, 6059. (b) Clarke, M. L.; France, M. B. *Tetrahedron* **2008**, *64*, 9003. For selected recent advancements in the Conia-ene reaction, see: Cu mediated: (d) Beltran, F.; Fabre, I.; Ciofini, I.; Miesch, L. *Org. Lett.* **2017**, *19*, 5042. (e) Tashima, S.; Sawada, T.; Saito, K.; Yamada, T. *Chem. Lett.* **2016**, *45*, 649. (f) Chen, Y.-J.; Chuang, C.-P. *Synthesis* **2016**, *48*, 3603. Ag-mediated: (g) Fang, G.; Zheng, C.; Cao, D.; Pan, Lu.; Hong, H.; Wang, H.; Zhao, G. *Tetrahedron* **2019**, *75*, 2706. (h) Blumel, M.; Hack, D.; Ronkartz, L.; Vermeeren, C.; Enders, D. *Chem. Commun.* **2017**, *53*, 3956. (i) Heinrich, C. F.; Fabre, I.; Miesch, L. *Angew. Chem. Int. Ed.* **2016**, *55*, 5170. (j) Hack, D.; Durr, A. B.; Deckers, K.; Chauhan, P.; Seling, N.; Rubenach, L.; Mertens, L.; Raabe, G.; Schoenebeck, F.; Enders, D. *Angew. Chem. Int. Ed.* **2016**, *55*, 1797. Zn-mediated: (k) Cao, M.; Yesilcimen, A.; Wasa, M. *J. Am. Chem. Soc.* **2019**, *141*, 4199.

25. Bain, A. I.; Chinthapally, K.; Hunter, A. C.; Sharma, I. *Eur. J. Org. Chem.* **2022**, *2022*, *e202101419.*

26.(a) Nozaki, H.; Moriuti, S.; Yamabe, M.; Noyori, R. *Tetrahedron Lett.* **1966**, *43*, 5239. (b) Boger, D. L.; Coleman, R. S.; Panek, J. S.; Huber, F. X.; Sauer, *J. J. Org. Chem.* **1985**, *50*, 5377.

27. Cotton, F. A.; Thompson, J. L. *Acta Cryst.* **1981**, *37*, 2235.

28. Connell, R.; Scavo, F.; Helquist, P.; Akermark, B. *Tetrahedron Lett.* **1986**, *27*, 5559.

29. Yang, X.-W.; Yang, C.-P.; Jiang, L.-P.; Qin, X.-J.; Liu, Y.-P.; Shen, Q.-S.; Chen, Y.-B.; Luo, X.-D. *Org. Lett.* **2014**, *16*, 5808.

30. Beesley, R. M.; Ingold, C. K.; Thorpe, J. F. *J. Chem. Soc., Trans.* **1915**, *107*, 1080.

31. Cheng, H.-G.; Lu, L.-Q.; Wang, T.; Yang, Q.-Q.; Liu, X.-P.; Li, Y.; Deng, Q.-H.; Chen, J.-R.; Xiao, W.-J. *Angew. Chem. Int. Ed.* **2013**, *52*, 3250

32. Xie, W.; Li, B.; Wang, B. *J. Org. Chem.* **2016**, *81*, 396.

33. Xie, S. B.; Yan, Z. Q.; Li, Y. H.; Song, Q.; Ma, M. M. *J. Org. Chem.* **2018**, *83*, 10916.

1.19 Appendix 1

^{1}H and ^{13}C NMR Spectra for Chapter 2

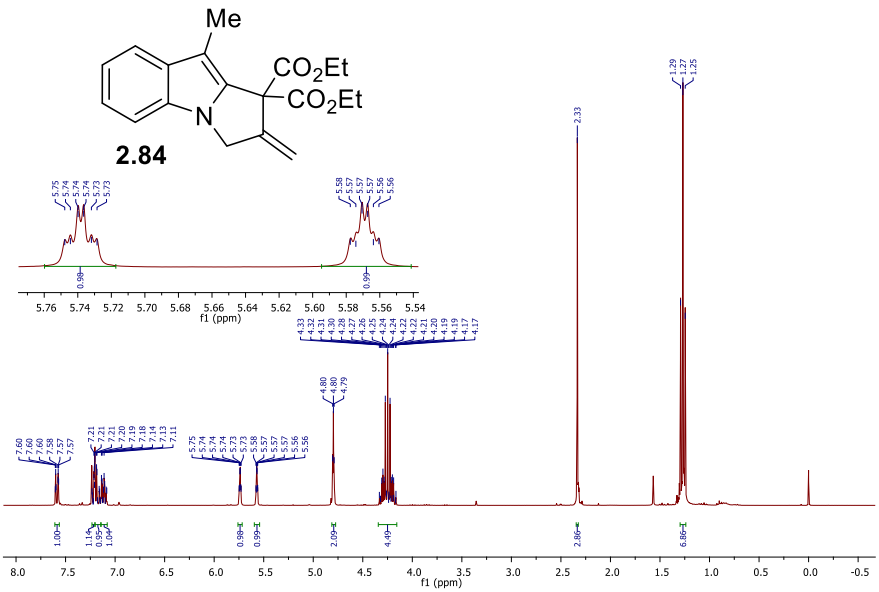

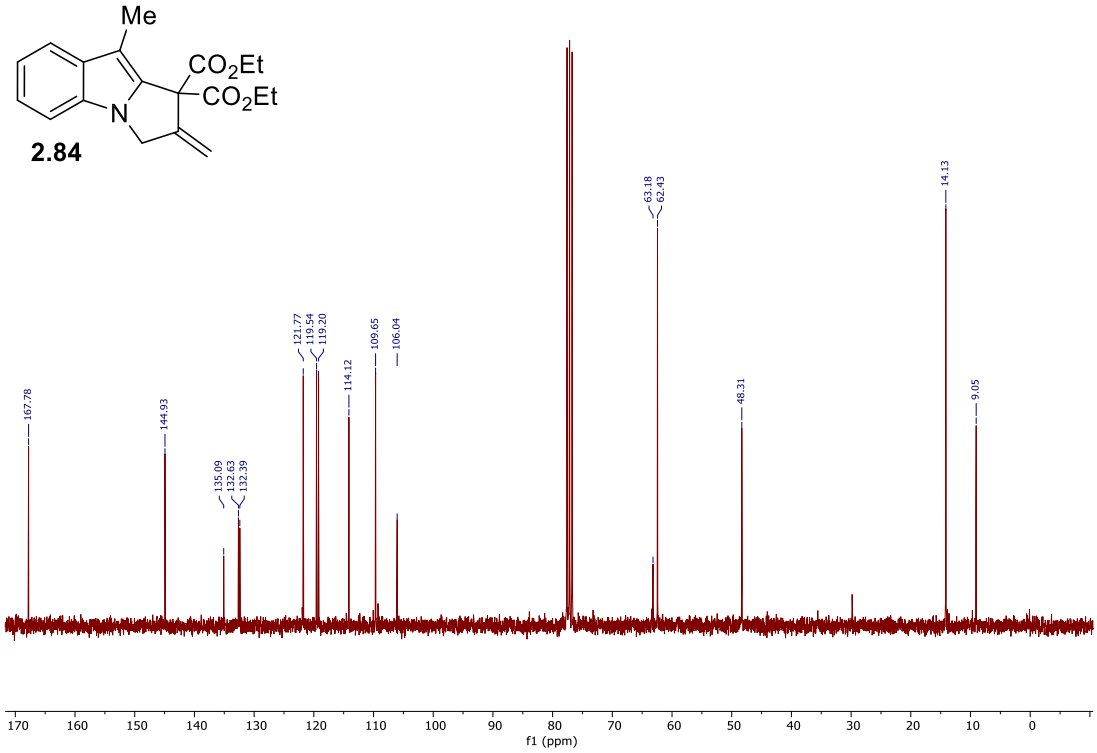

^{1}H NMR (300 MHz, $CDCl_3$) and ^{13}C NMR (75 MHz, $CDCl_3$) of compound **2.84**

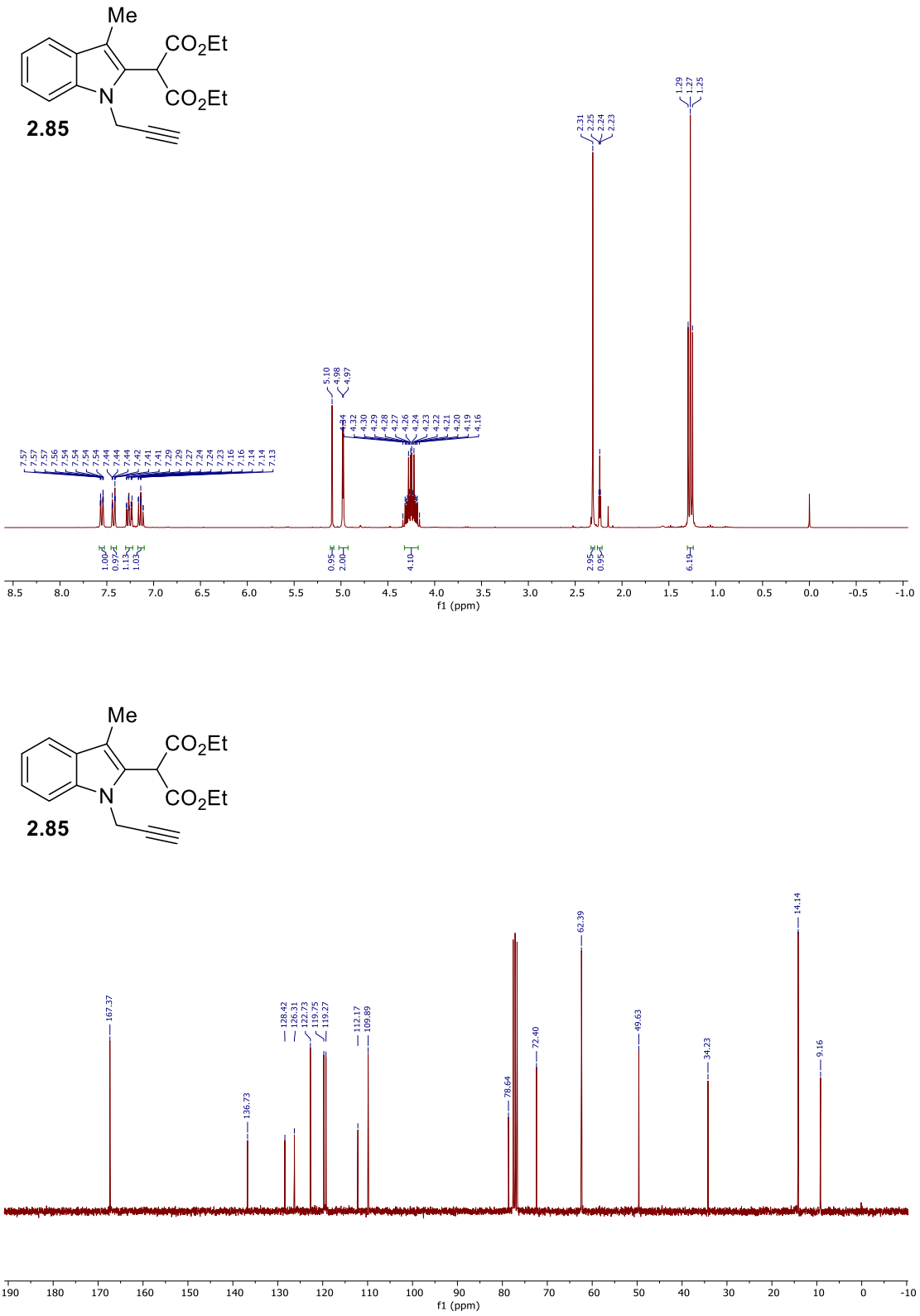

^{1}H NMR (300 MHz, $CDCl_3$) and ^{13}C NMR (75 MHz, $CDCl_3$) of compound **2.85**

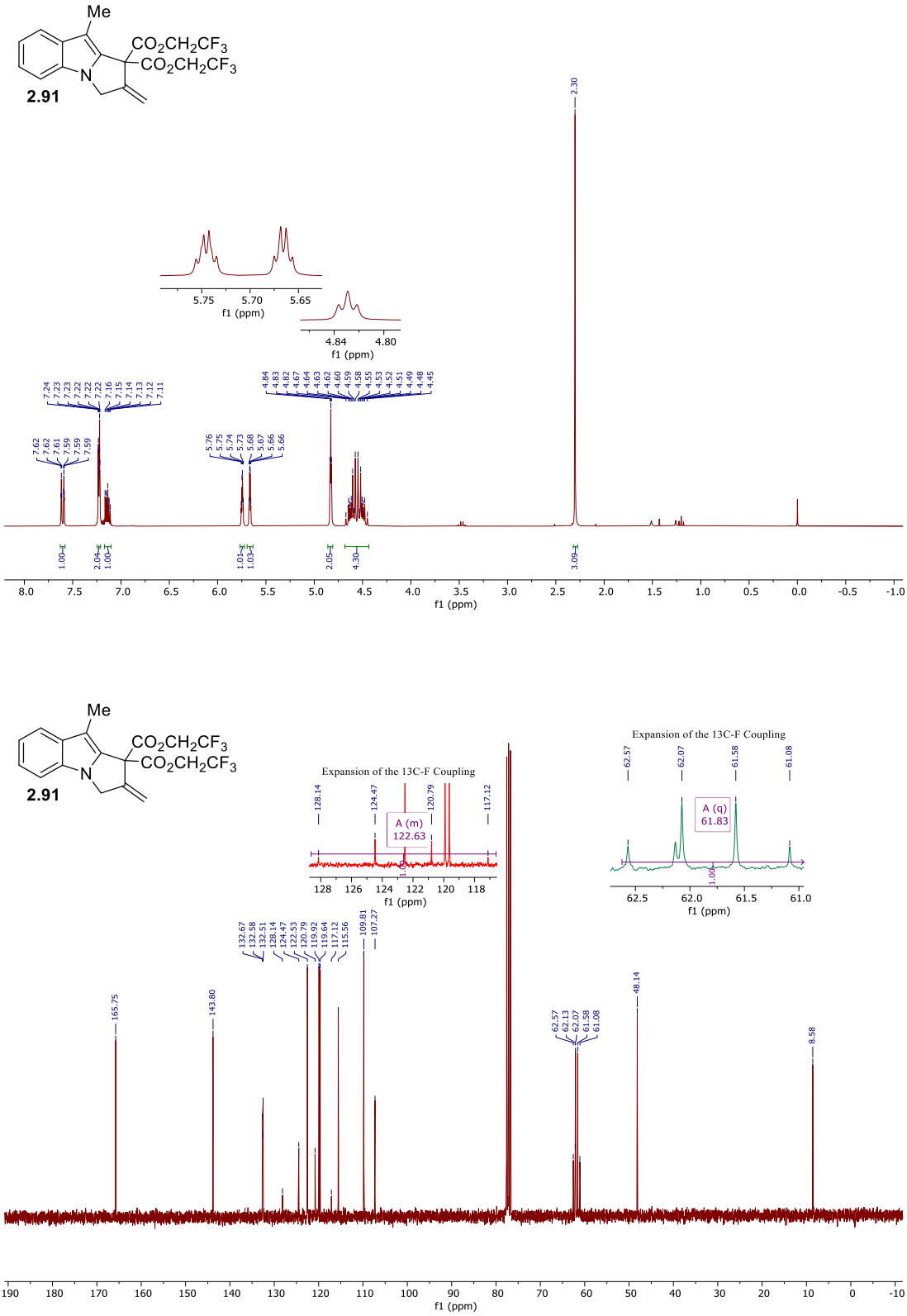

^{1}H NMR (300 MHz, $CDCl_3$) and ^{13}C NMR (75 MHz, $CDCl_3$) of compound **2.91**

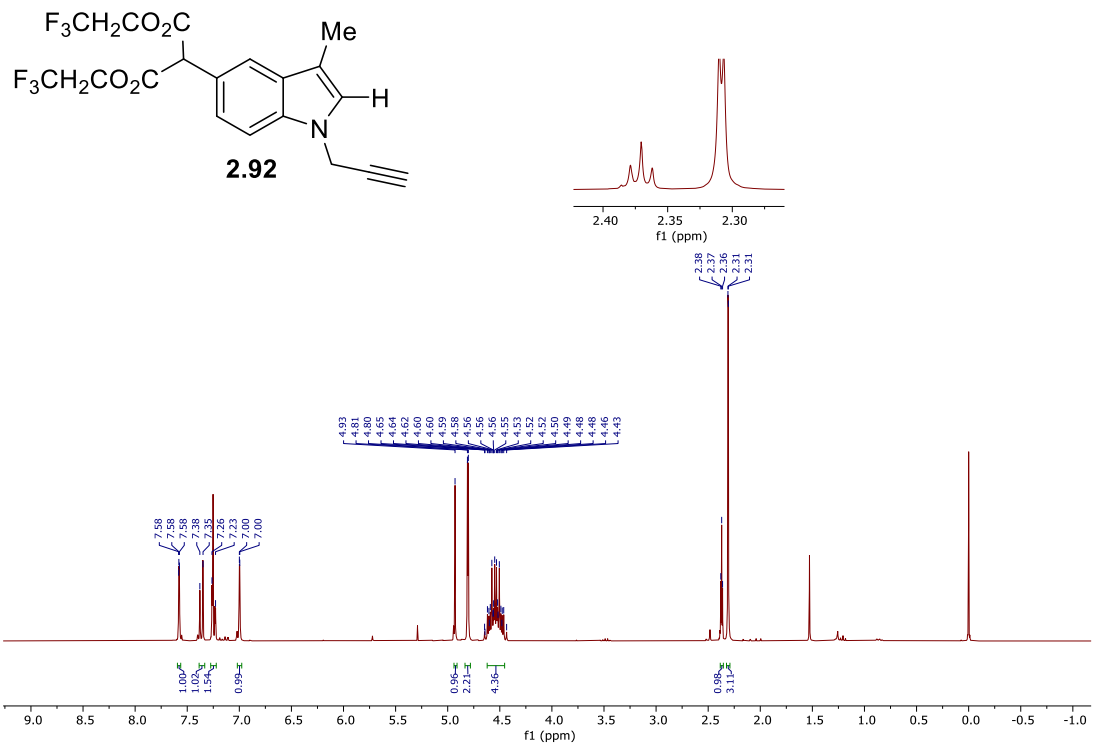

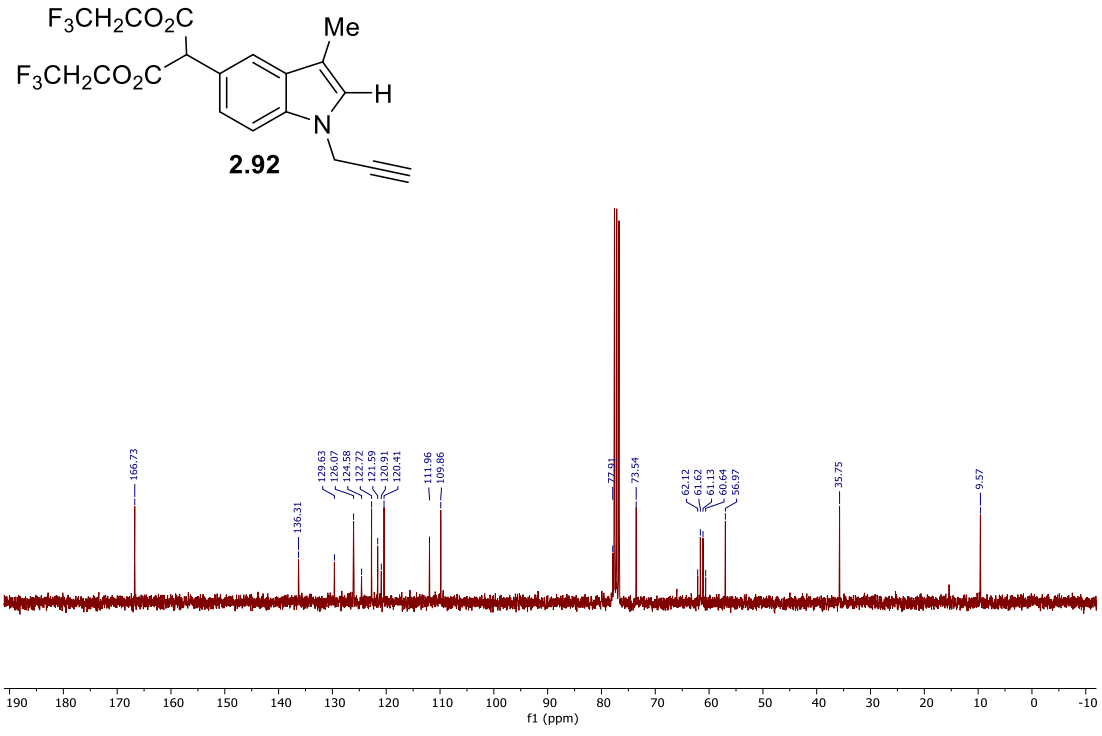

^{1}H NMR (300 MHz, $CDCl_3$) and ^{13}C NMR (75 MHz, $CDCl_3$) of compound **2.92**

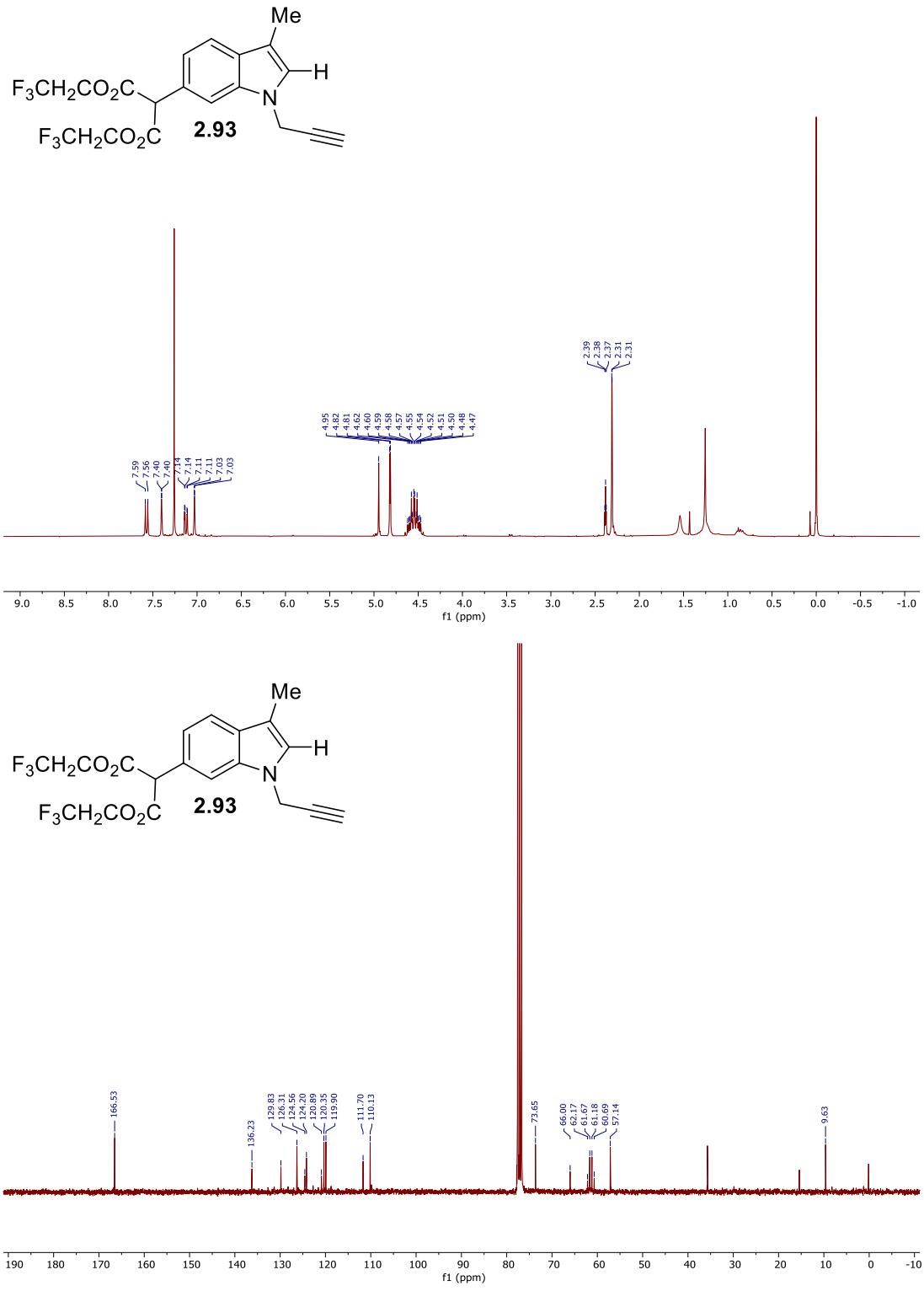

^{1}H NMR (300 MHz, $CDCl_3$) and ^{13}C NMR (75 MHz, $CDCl_3$) of compound **2.93**

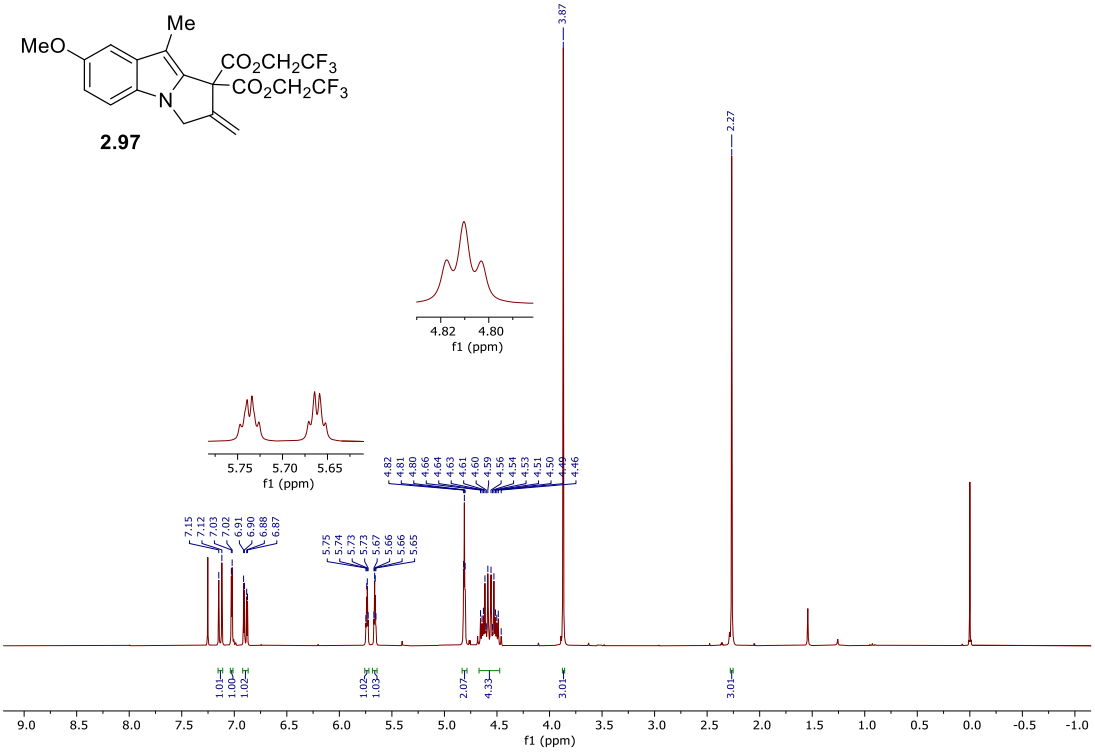

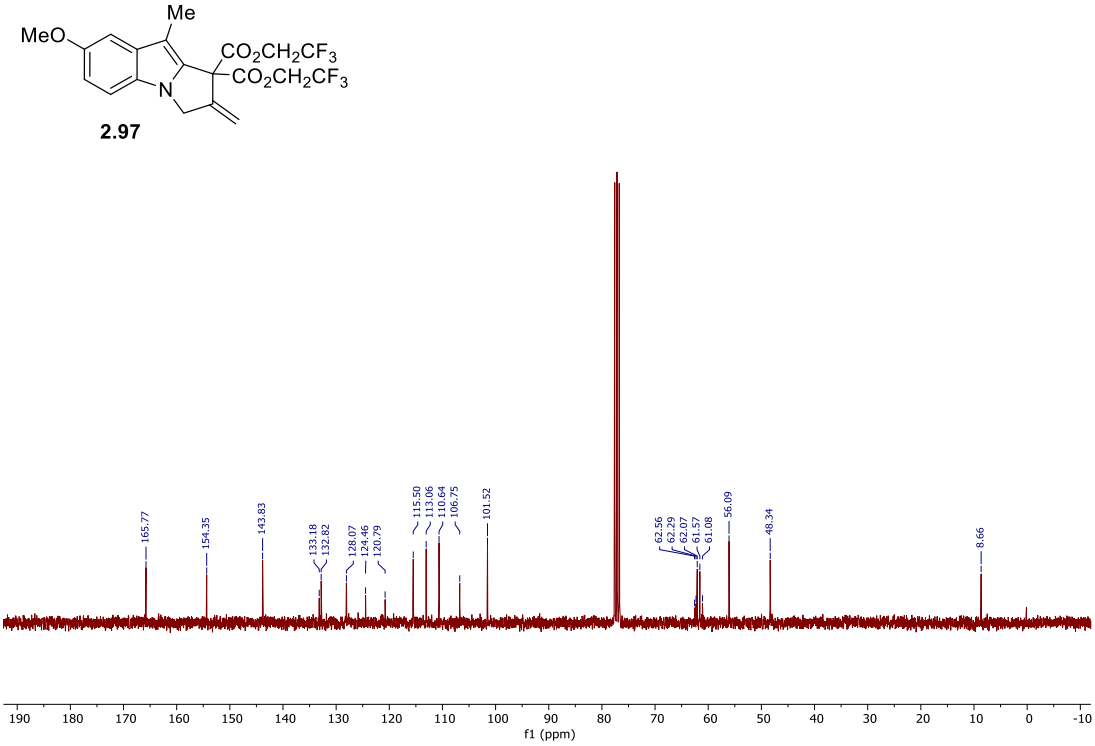

^{1}H NMR (300 MHz, $CDCl_3$) and ^{13}C NMR (75 MHz, $CDCl_3$) of compound **2.97**

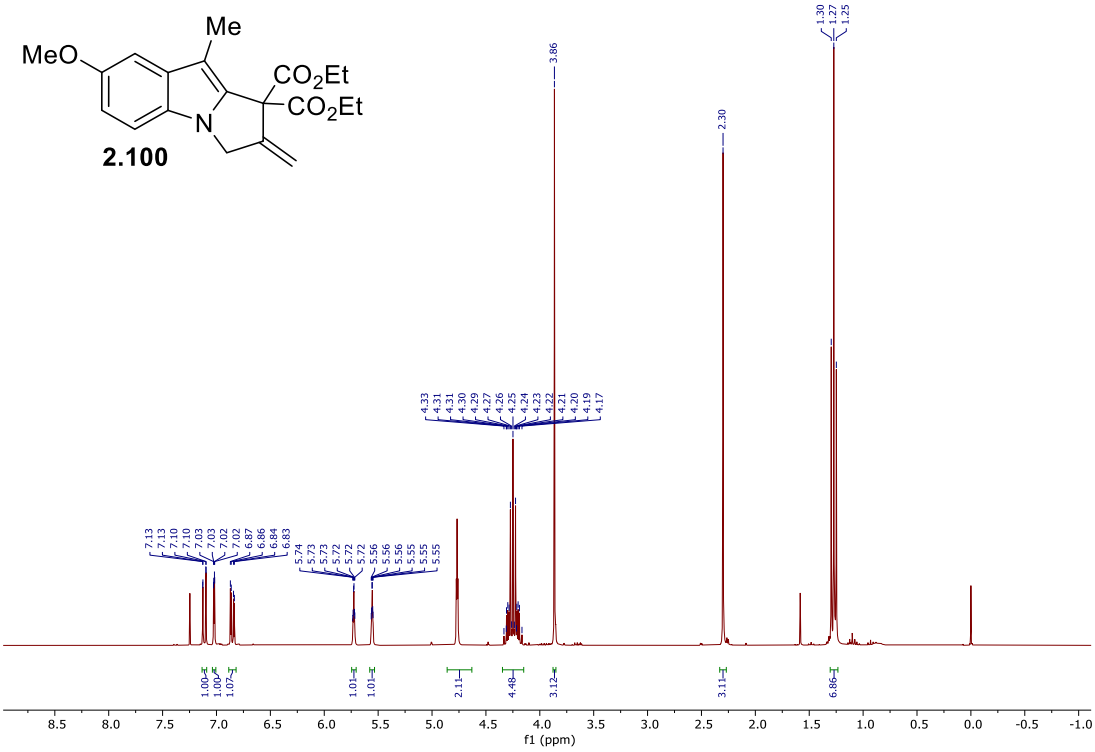

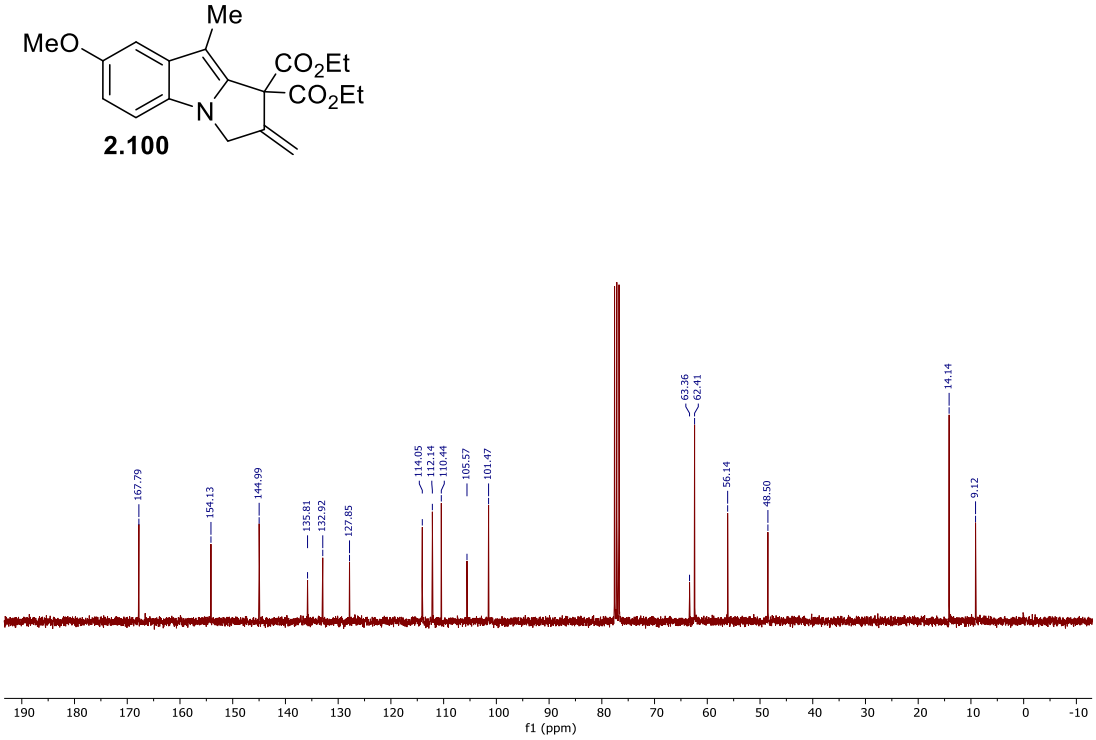

^{1}H NMR (300 MHz, $CDCl_3$) and ^{13}C NMR (75 MHz, $CDCl_3$) of compound **2.100**

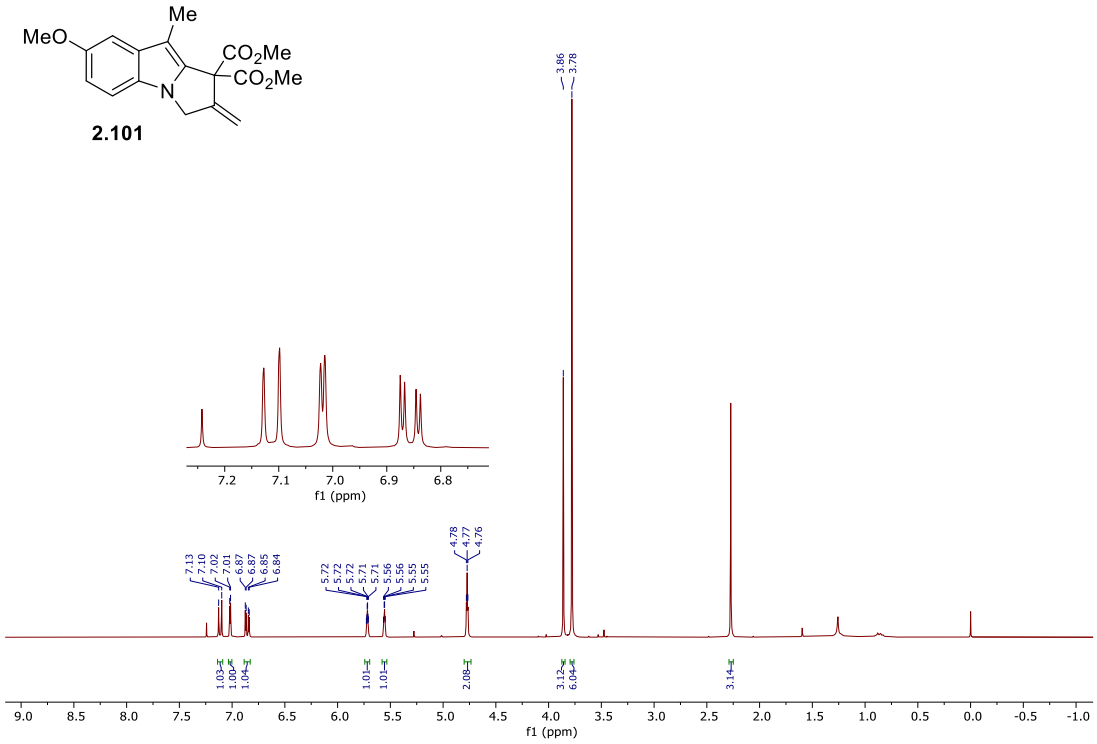

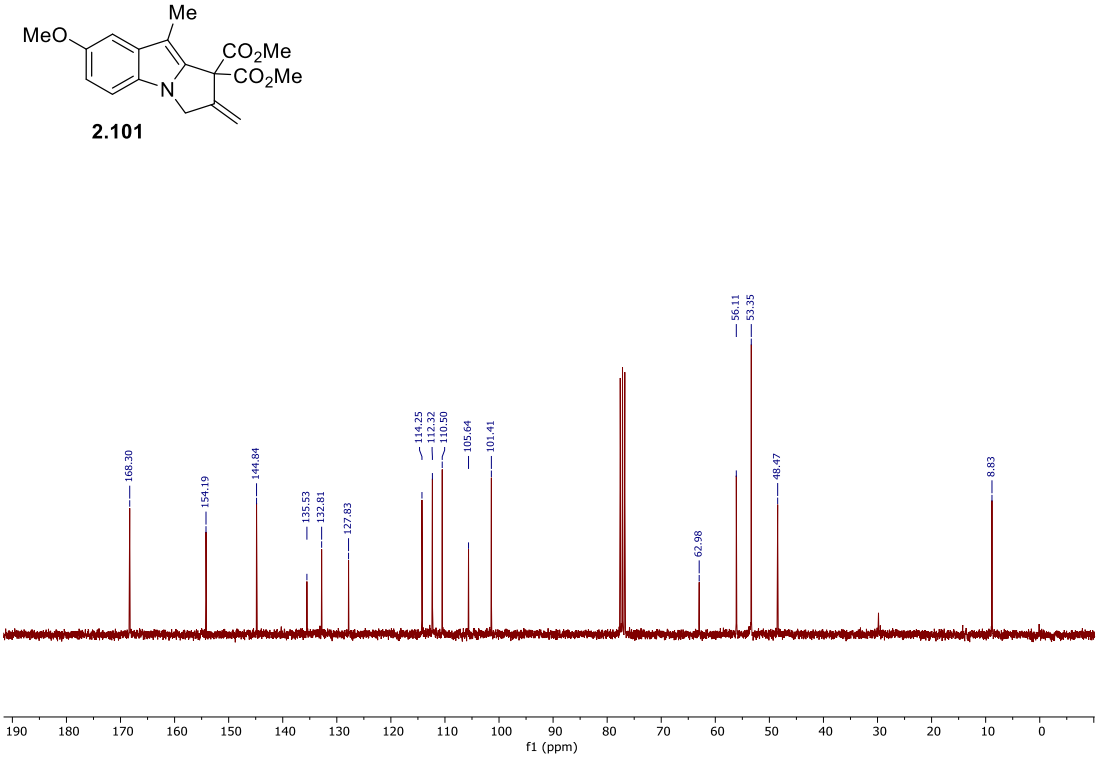

^{1}H NMR (300 MHz, $CDCl_3$) and ^{13}C NMR (75 MHz, $CDCl_3$) of compound **2.101**

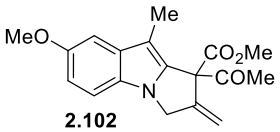

2.102

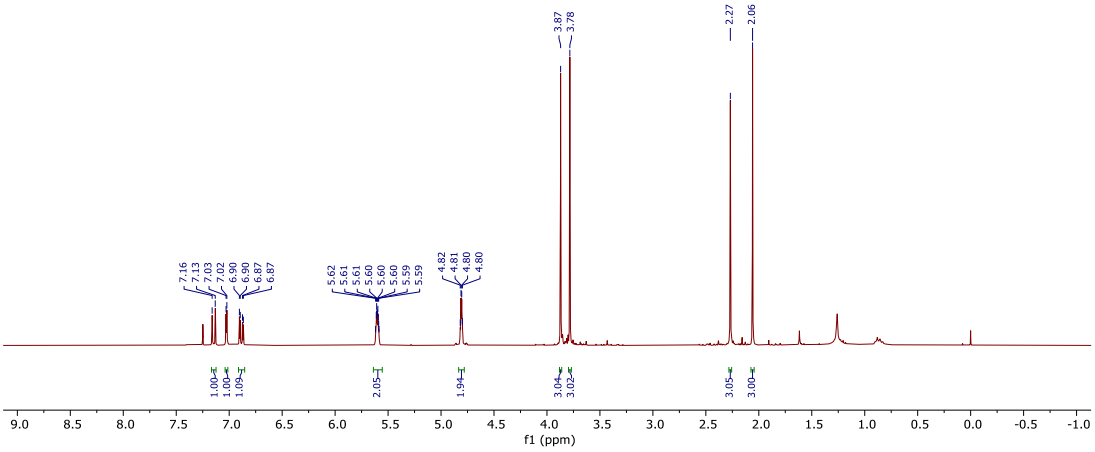

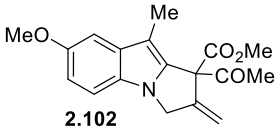

2.102

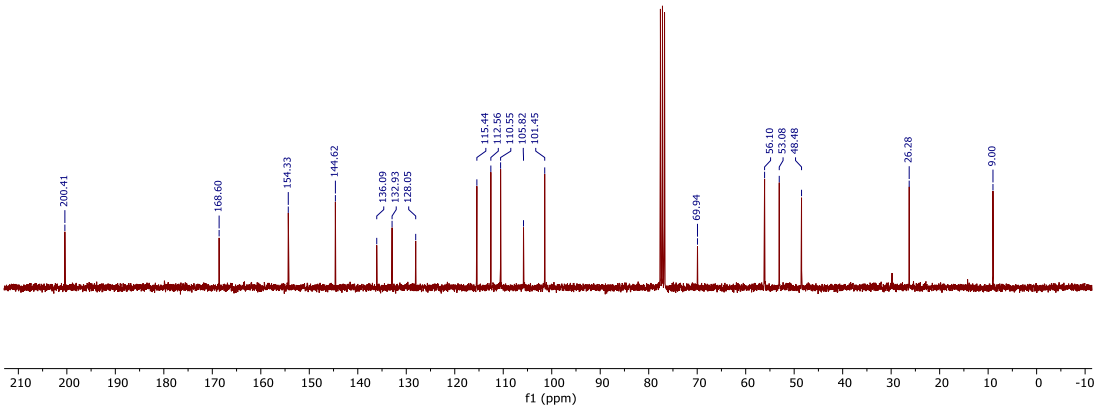

^{1}H NMR (300 MHz, $CDCl_3$) and ^{13}C NMR (75 MHz, $CDCl_3$) of compound **2.102**

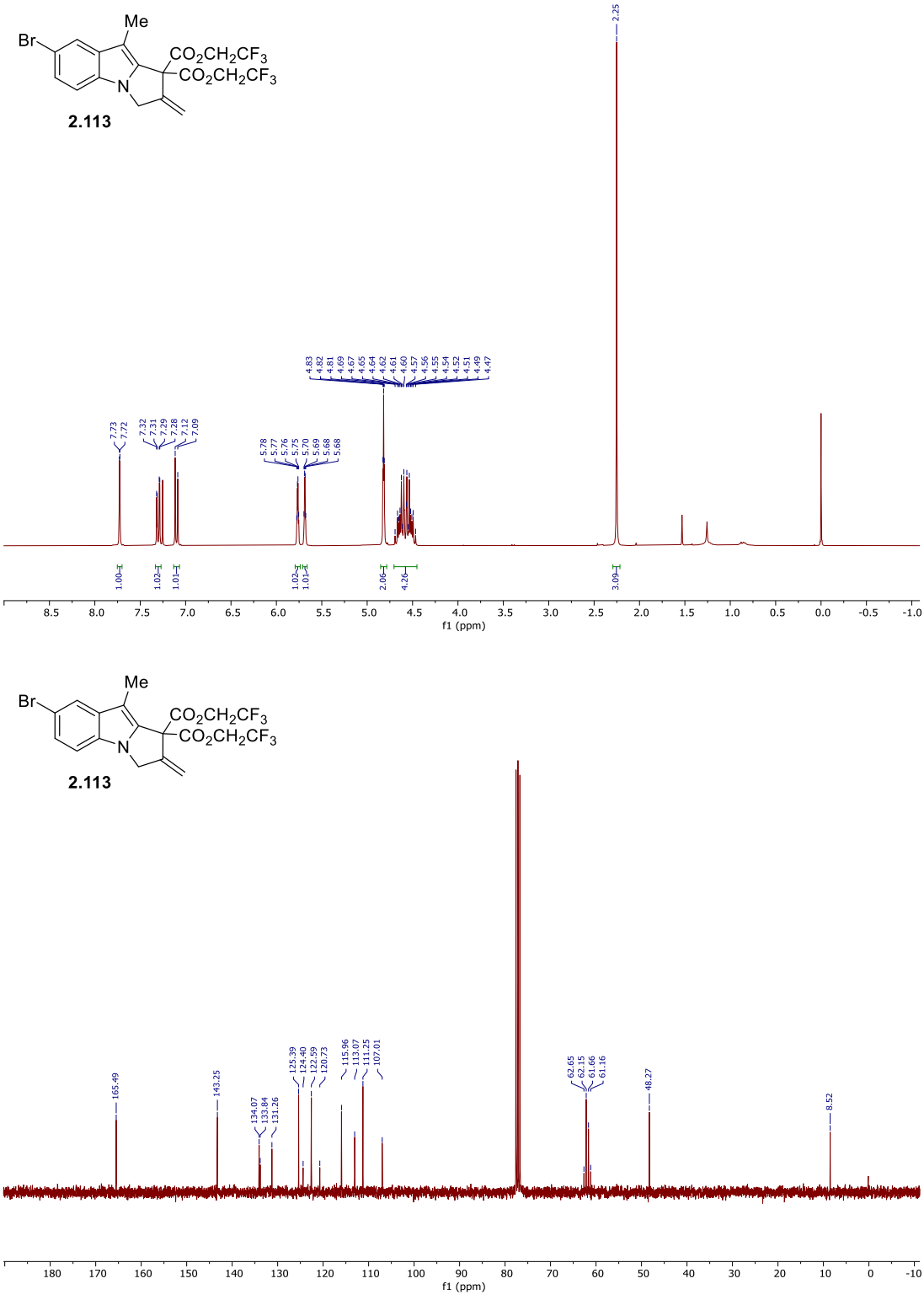

^{1}H NMR (300 MHz, $CDCl_3$) and ^{13}C NMR (75 MHz, $CDCl_3$) of compound **2.113**

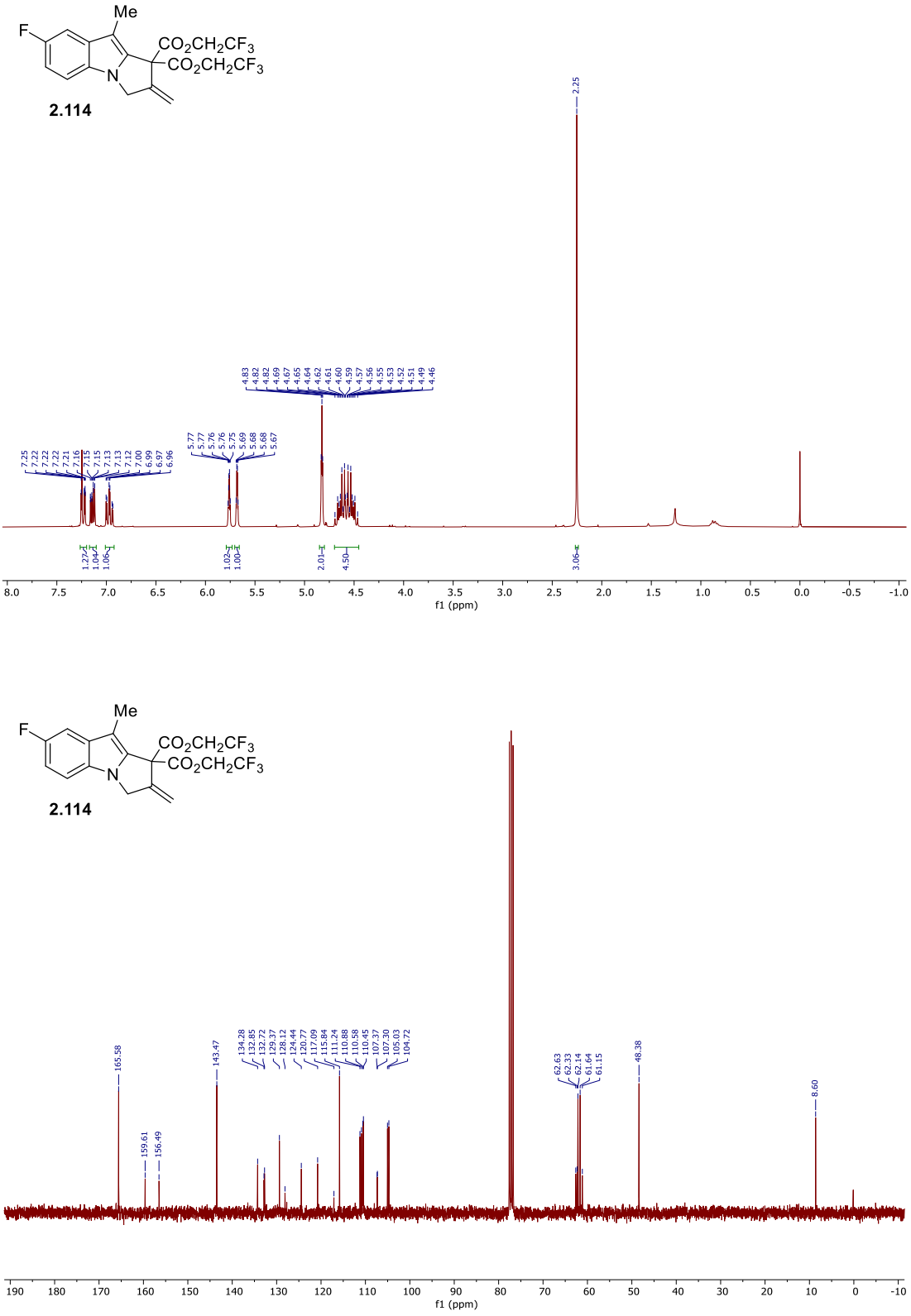

^{1}H NMR (300 MHz, $CDCl_3$) and ^{13}C NMR (75 MHz, $CDCl_3$) of compound **2.114**

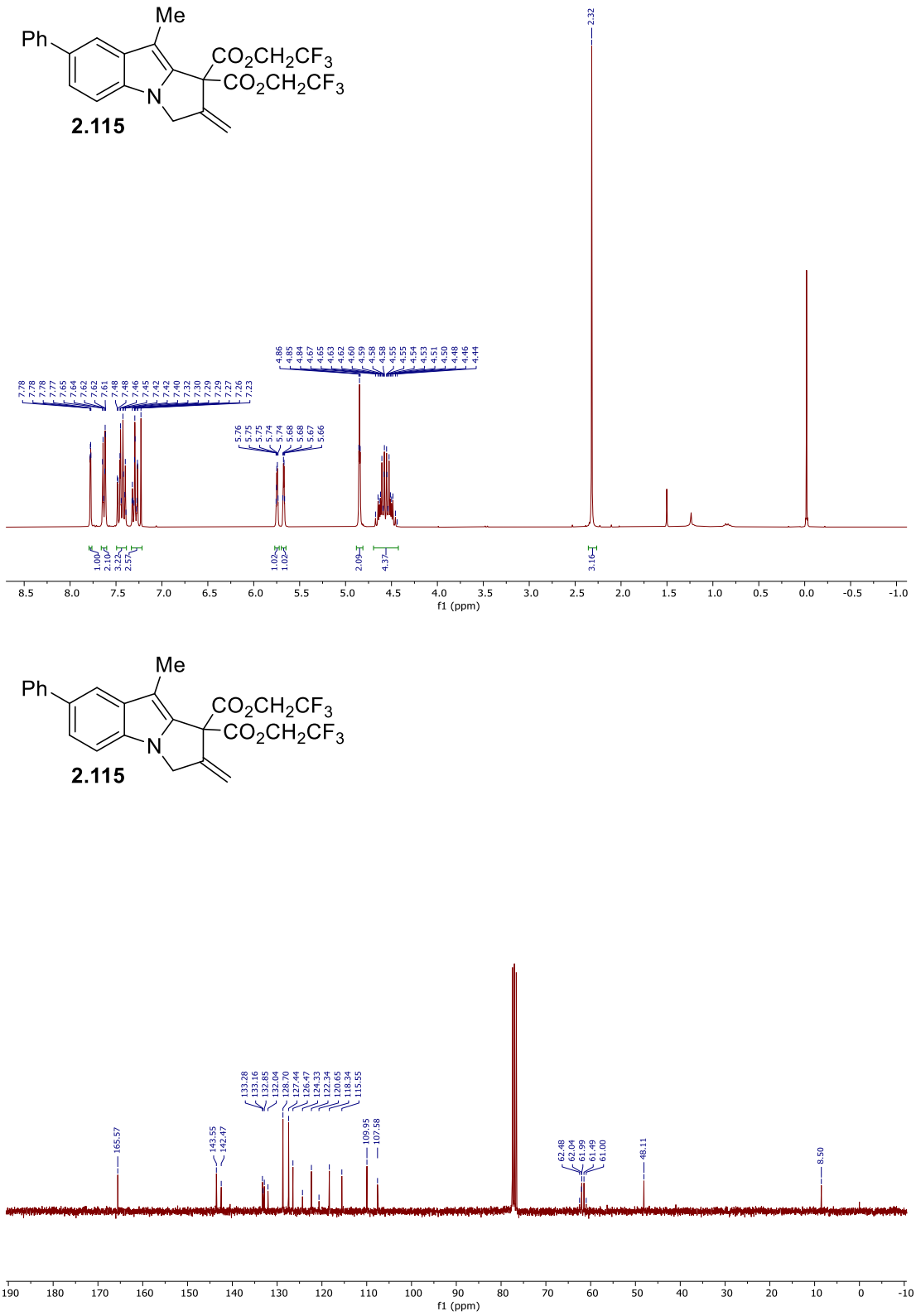

^{1}H NMR (300 MHz, $CDCl_3$) and ^{13}C NMR (75 MHz, $CDCl_3$) of compound **2.115**

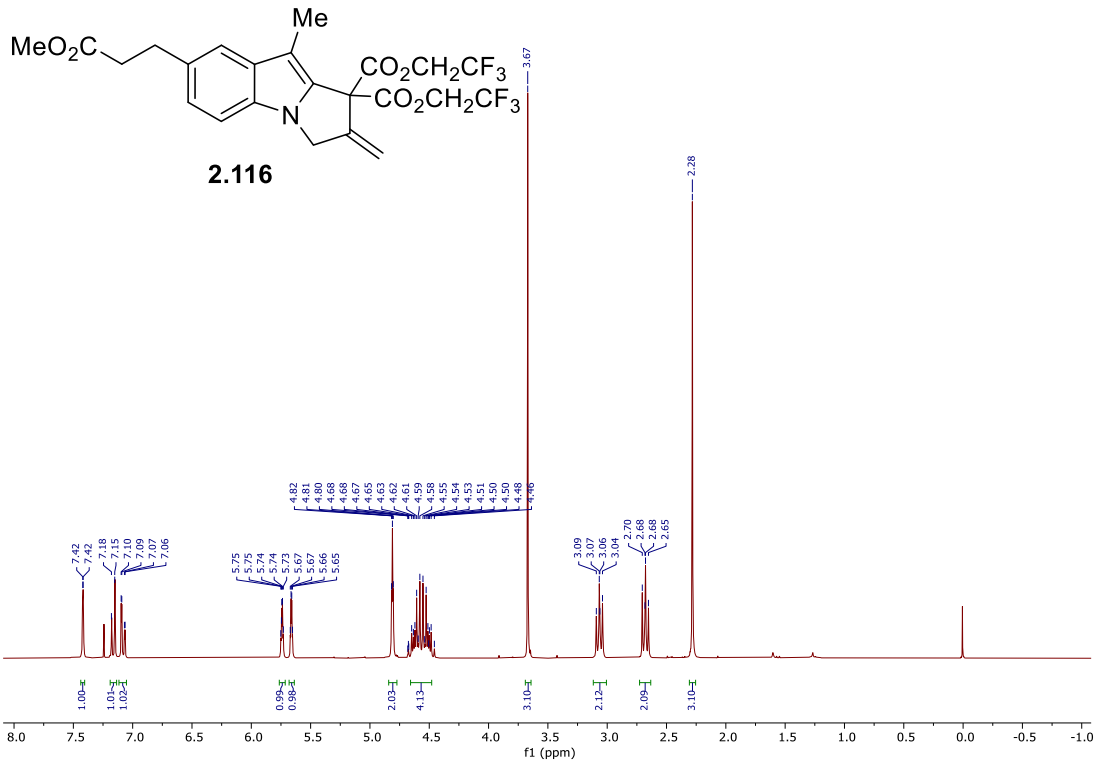

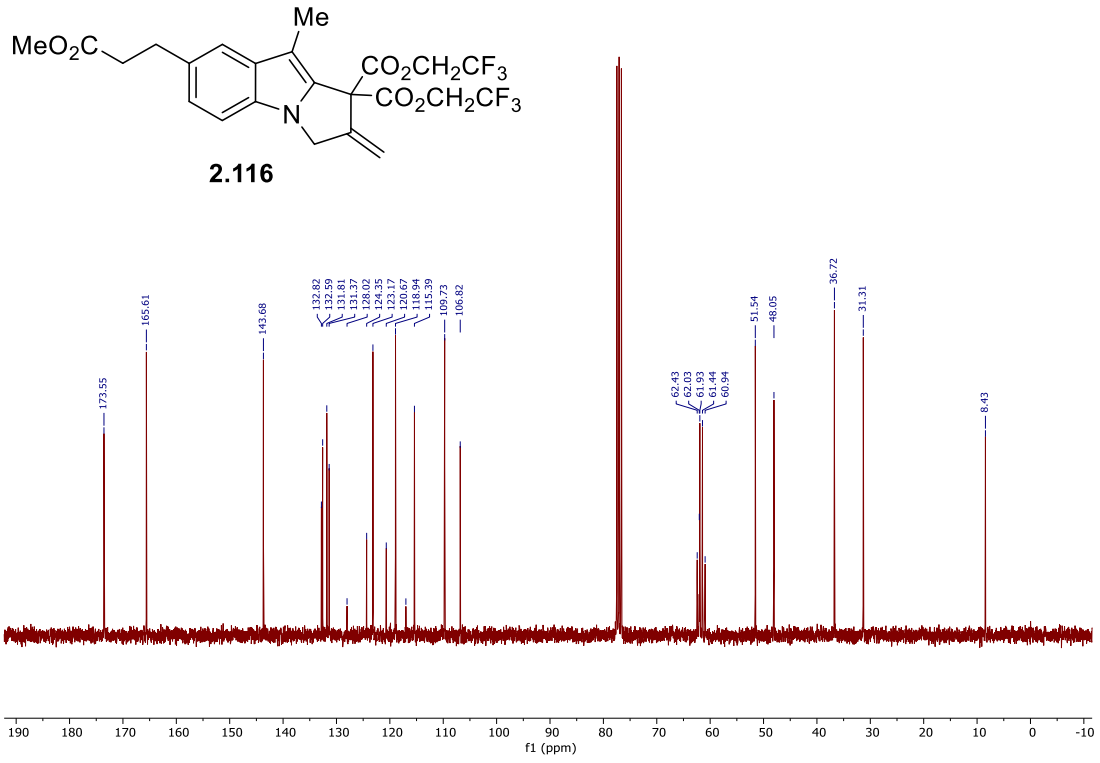

^{1}H NMR (300 MHz, $CDCl_3$) and ^{13}C NMR (75 MHz, $CDCl_3$) of compound **2.116**

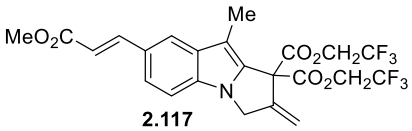

2.117

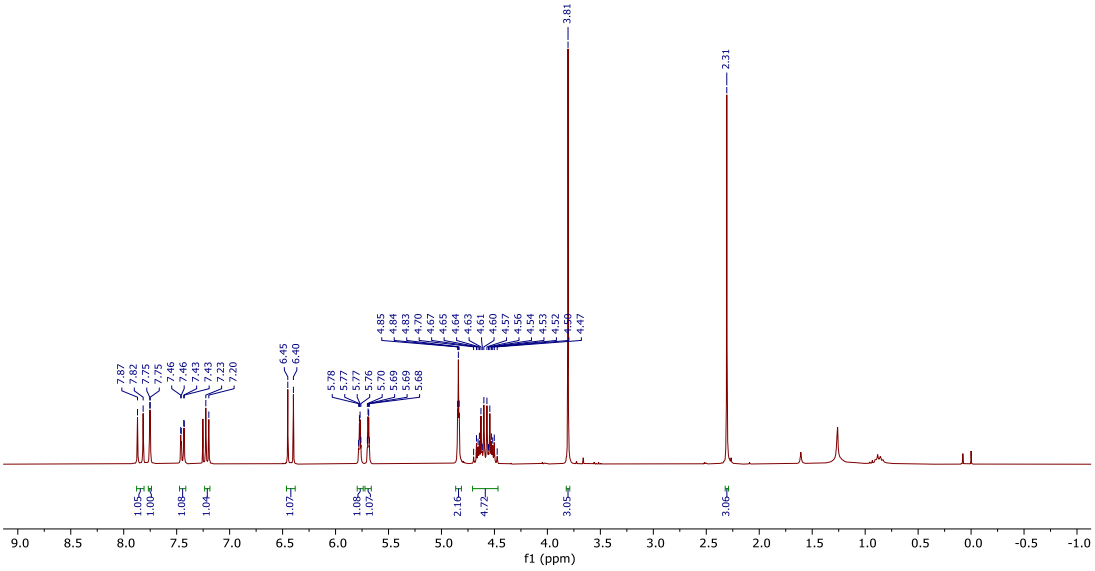

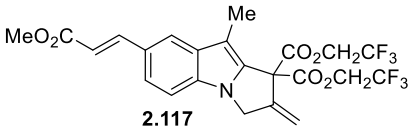

2.117

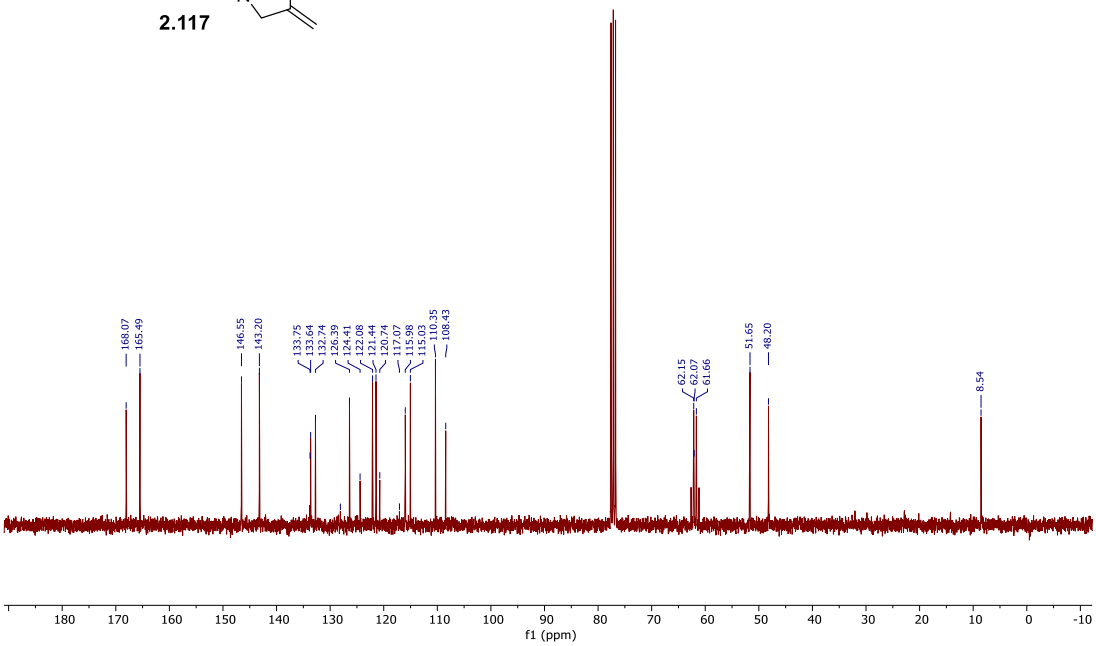

^{1}H NMR (300 MHz, $CDCl_3$) and ^{13}C NMR (75 MHz, $CDCl_3$) of compound **2.117**

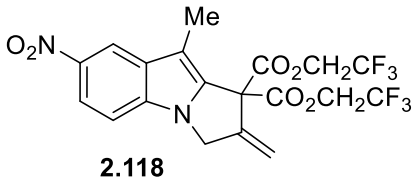

2.118

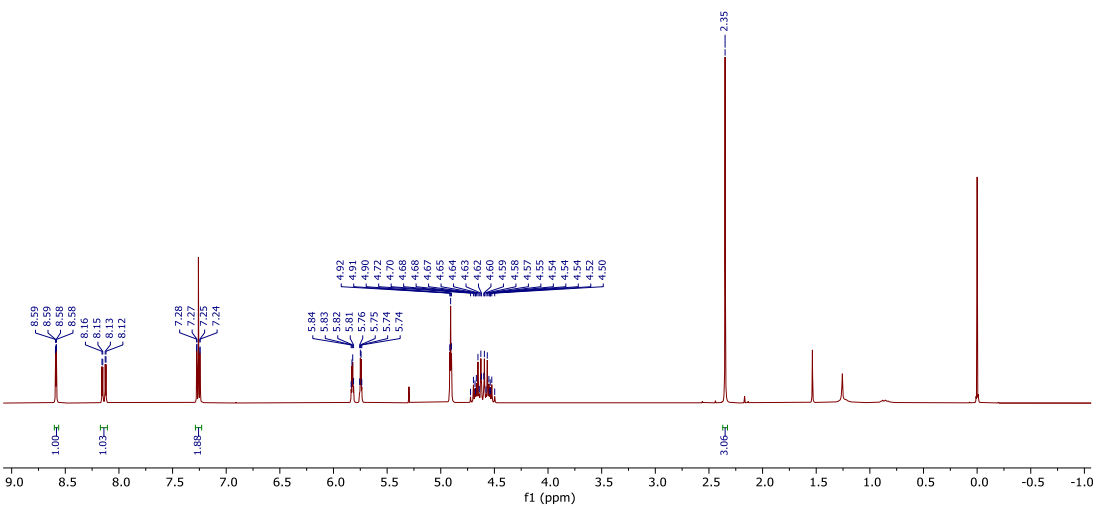

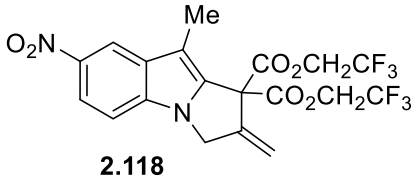

2.118

^{1}H NMR (300 MHz, $CDCl_3$) and ^{13}C NMR (75 MHz, $CDCl_3$) of compound **2.118**

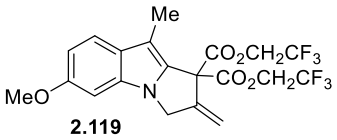

2.119

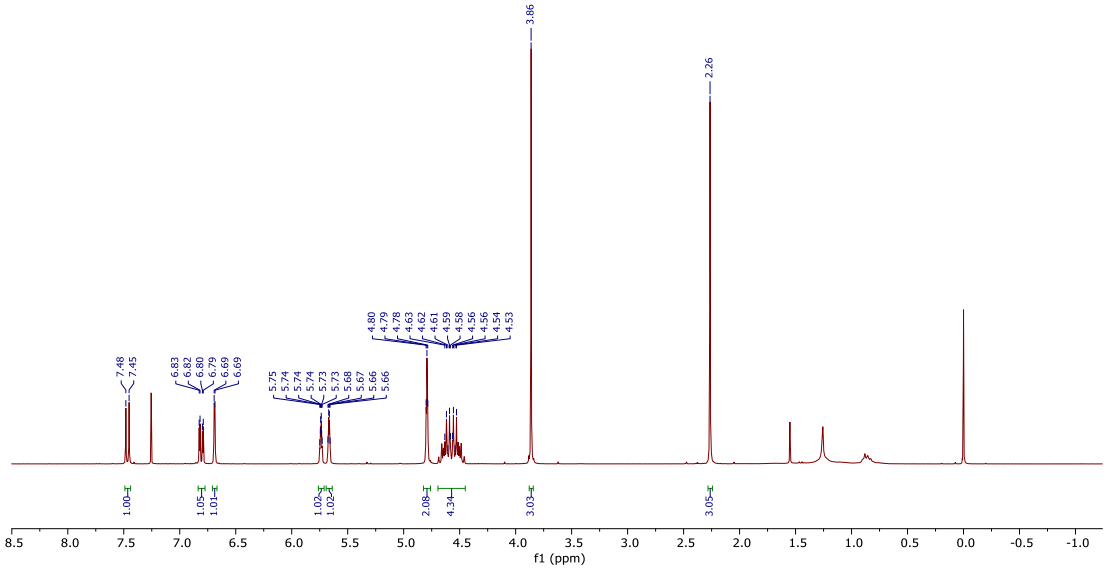

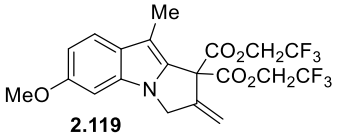

2.119

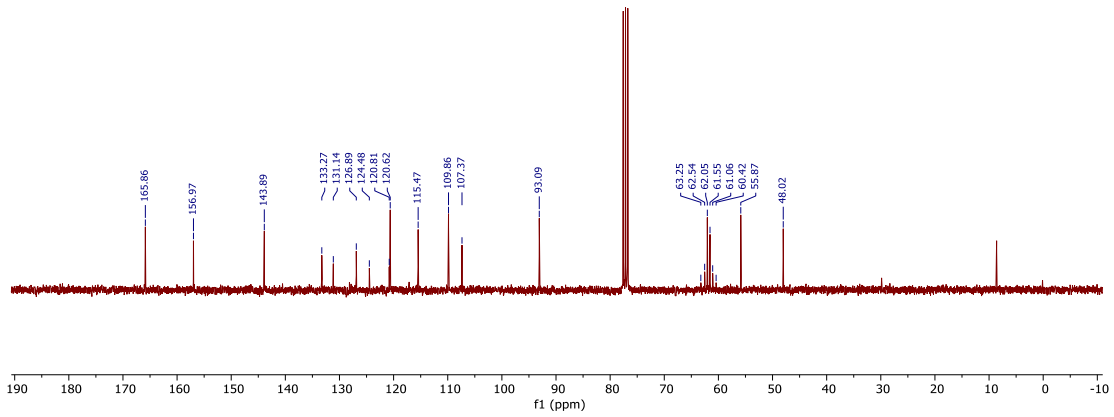

^{1}H NMR (300 MHz, $CDCl_3$) and ^{13}C NMR (75 MHz, $CDCl_3$) of compound **2.119**

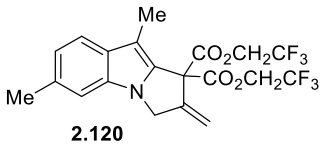

2.120

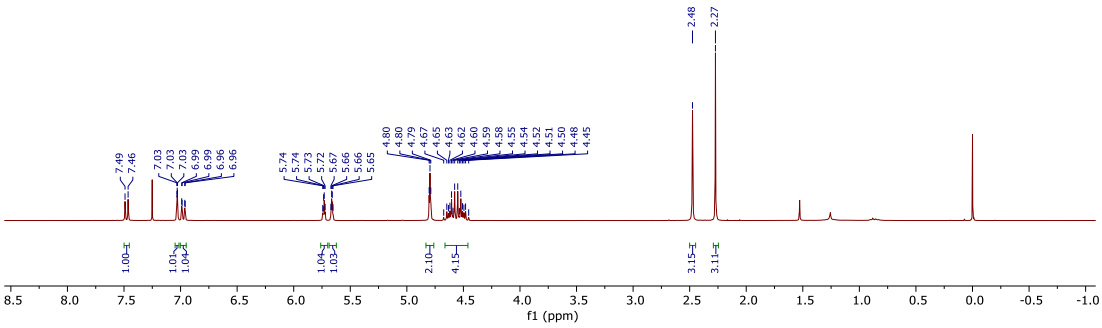

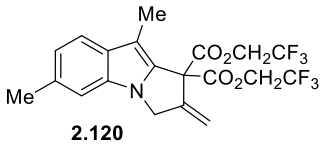

2.120

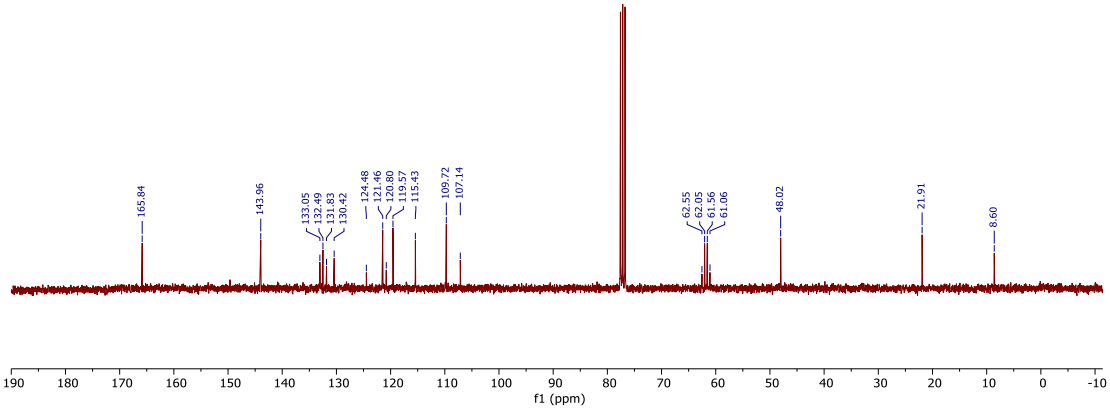

^{1}H NMR (300 MHz, $CDCl_3$) and ^{13}C NMR (75 MHz, $CDCl_3$) of compound **2.120**

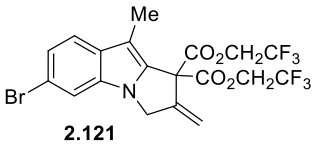

2.121

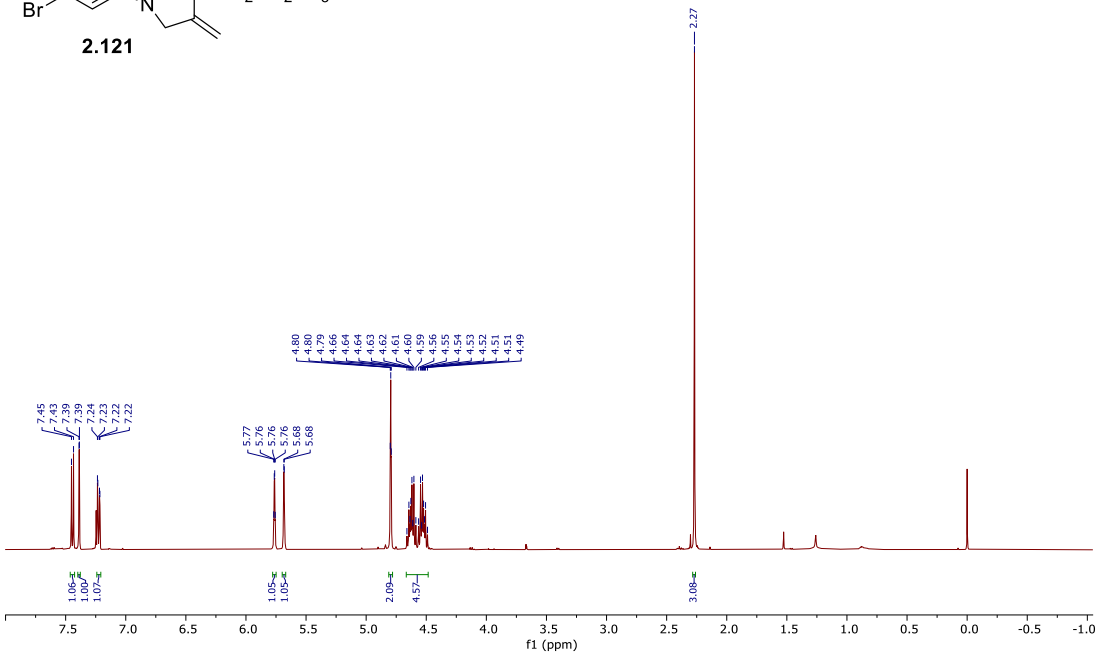

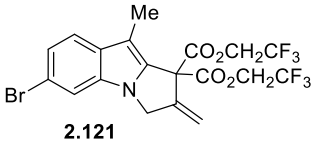

2.121

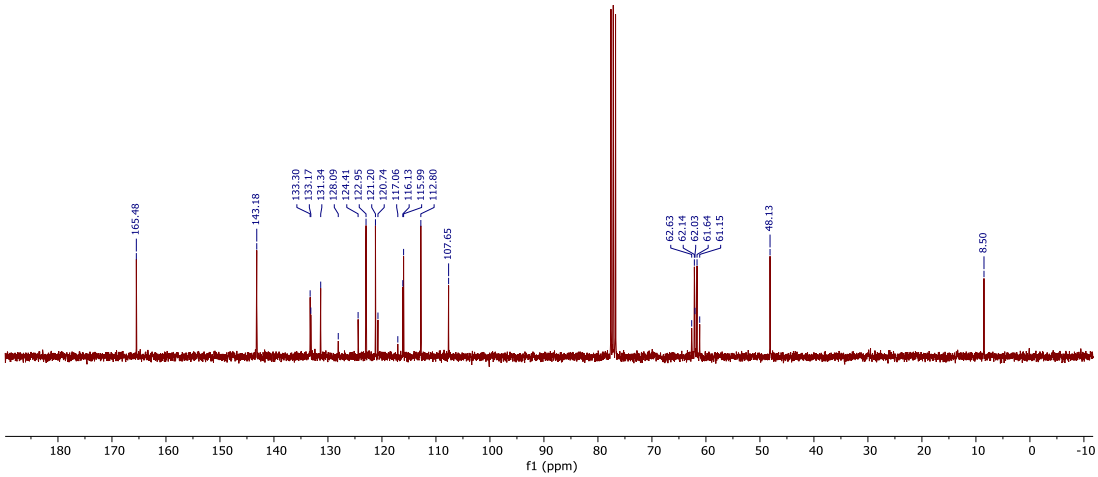

^{1}H NMR (300 MHz, $CDCl_3$) and ^{13}C NMR (75 MHz, $CDCl_3$) of compound **2.121**

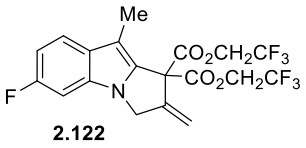

2.122

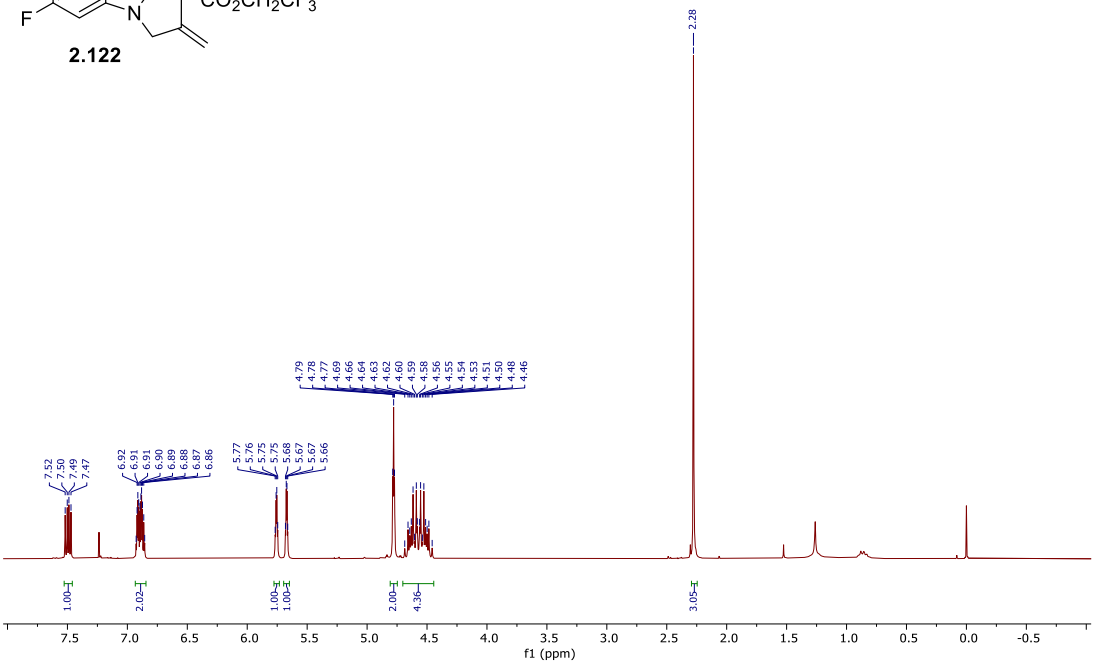

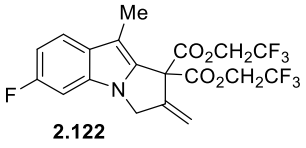

2.122

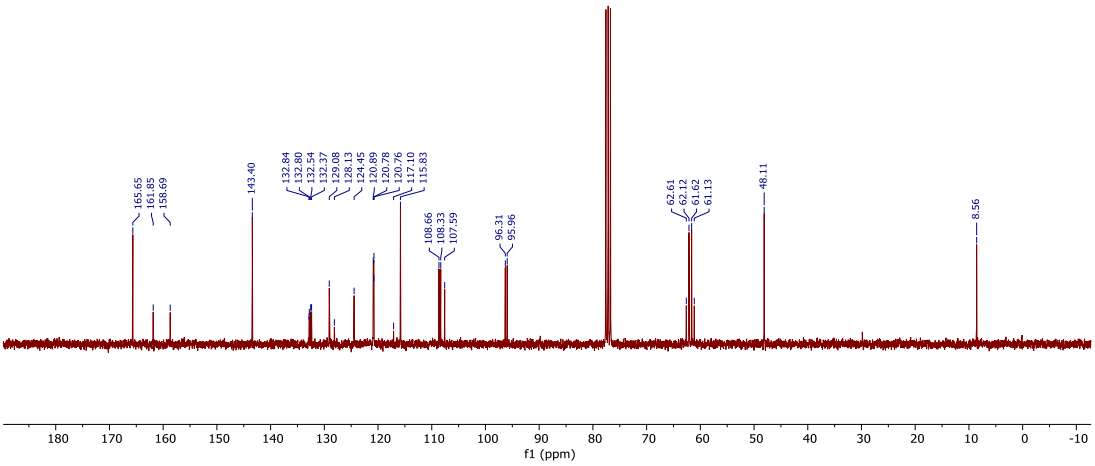

^{1}H NMR (300 MHz, $CDCl_3$) and ^{13}C NMR (75 MHz, $CDCl_3$) of compound **2.122**

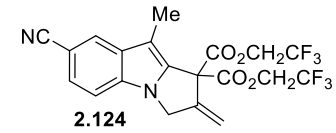

2.124

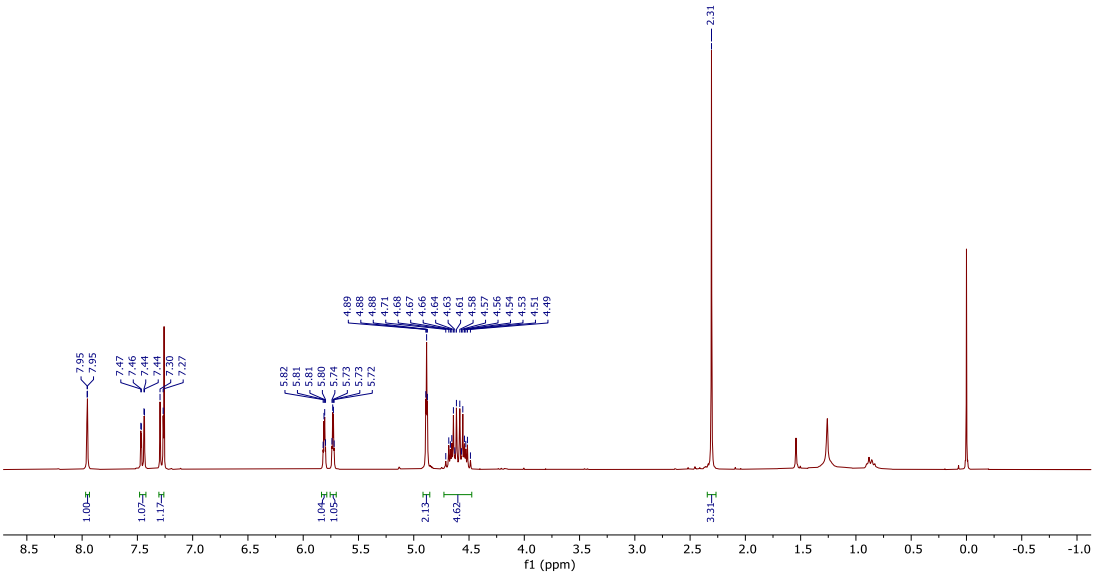

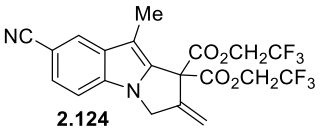

2.124

^{1}H NMR (300 MHz, $CDCl_3$) and ^{13}C NMR (75 MHz, $CDCl_3$) of compound **2.124**

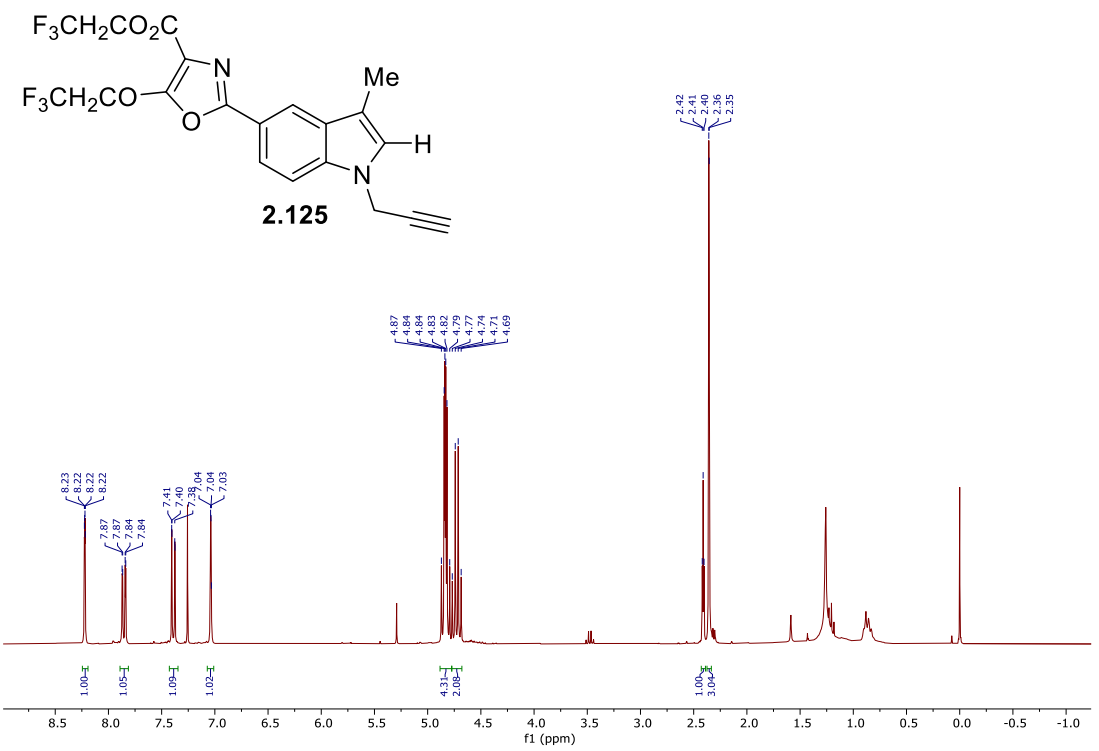

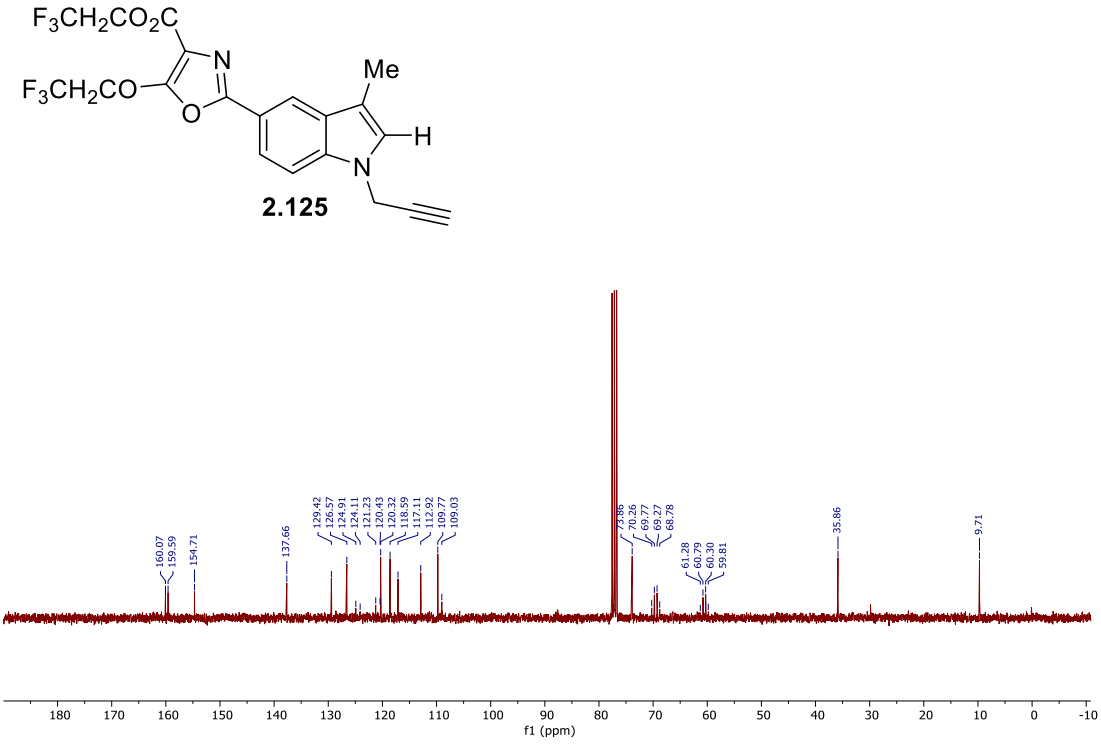

^{1}H NMR (300 MHz, $CDCl_3$) and ^{13}C NMR (75 MHz, $CDCl_3$) of compound **2.125**

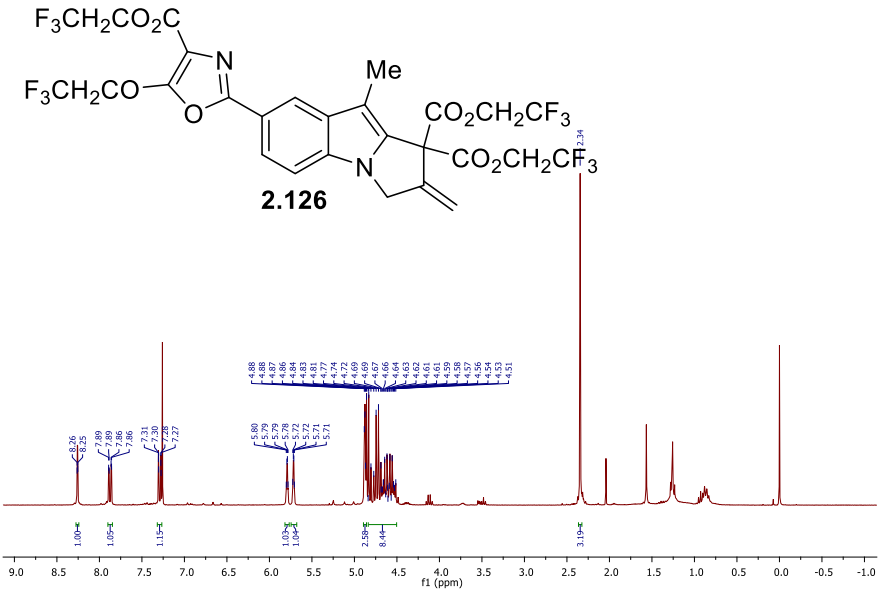

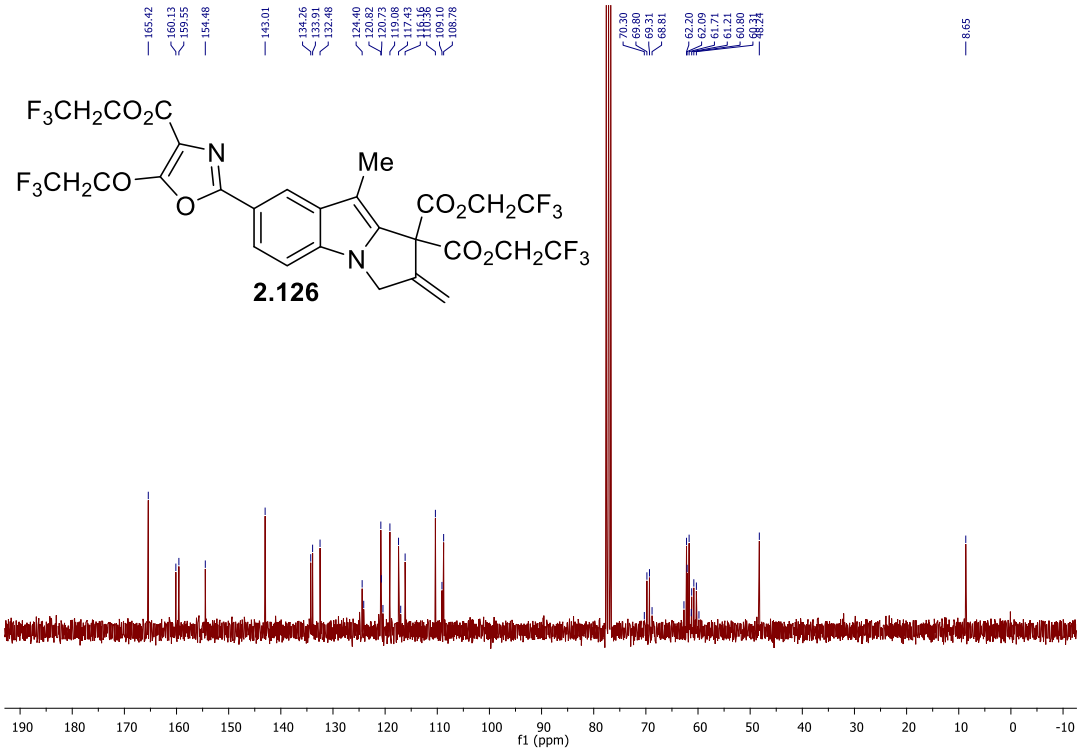

^{1}H NMR (300 MHz, $CDCl_3$) and ^{13}C NMR (75 MHz, $CDCl_3$) of compound **2.126**

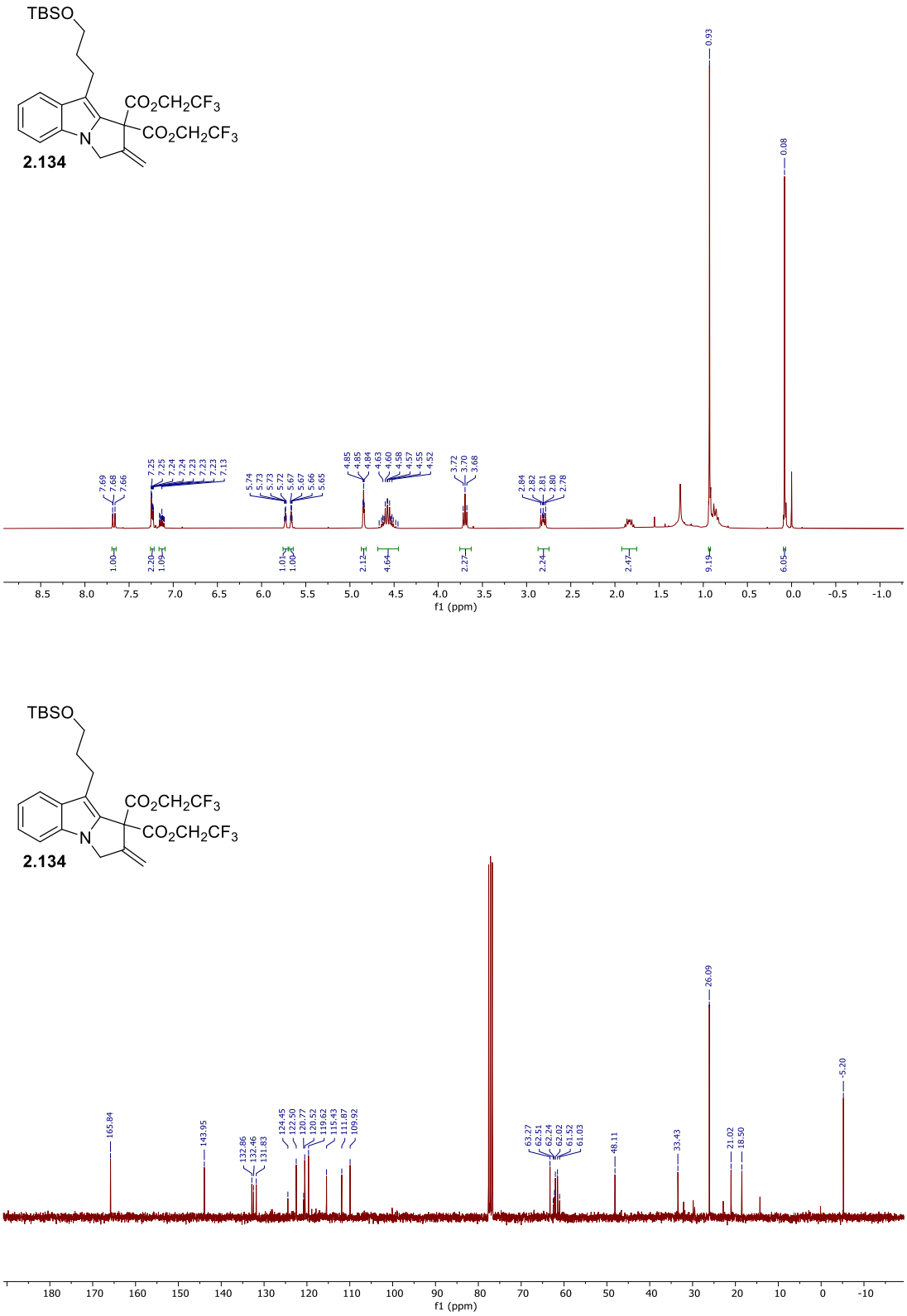

^{1}H NMR (300 MHz, $CDCl_3$) and ^{13}C NMR (75 MHz, $CDCl_3$) of compound **2.134**

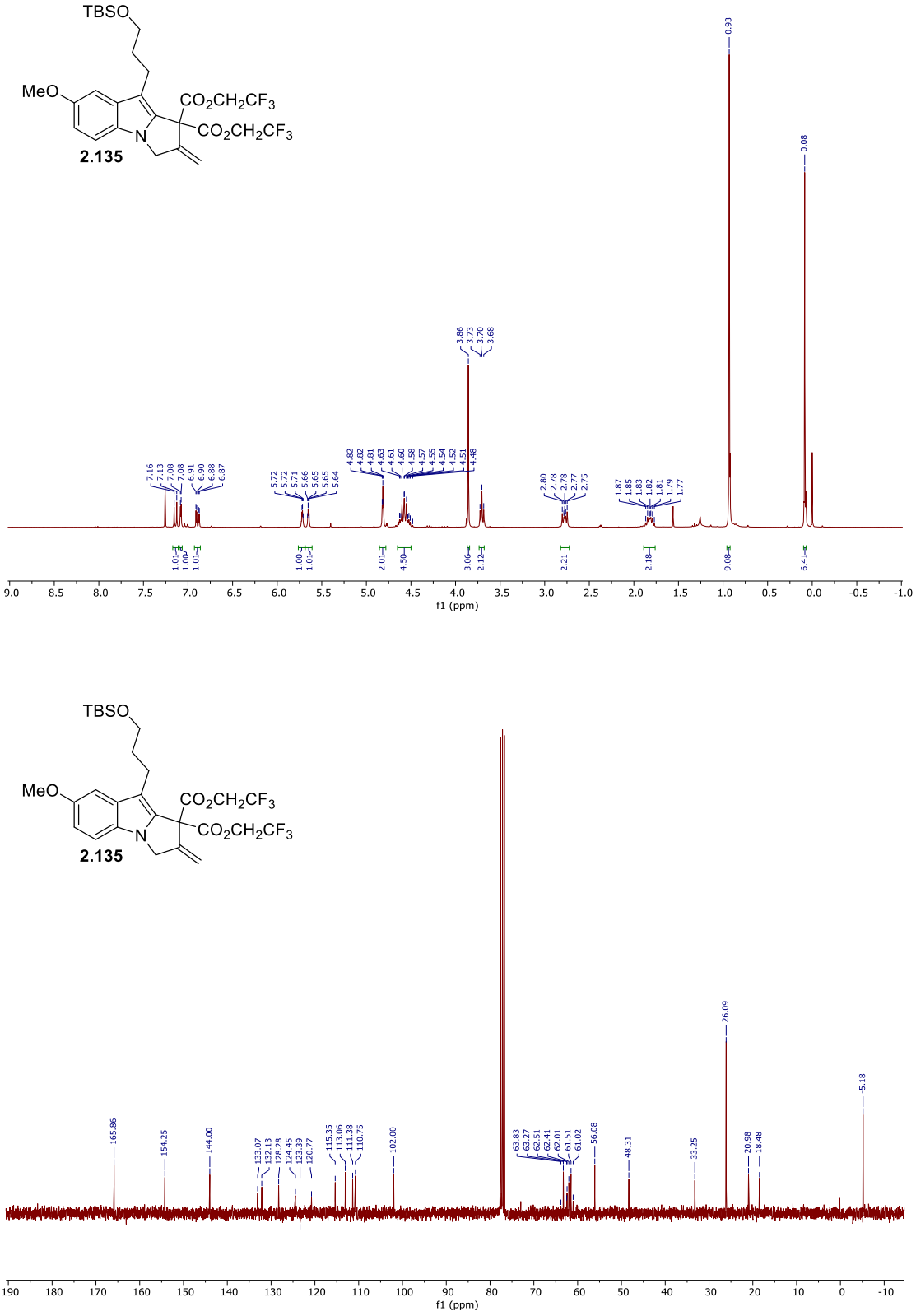

^{1}H NMR (300 MHz, $CDCl_3$) and ^{13}C NMR (75 MHz, $CDCl_3$) of compound **2.135**

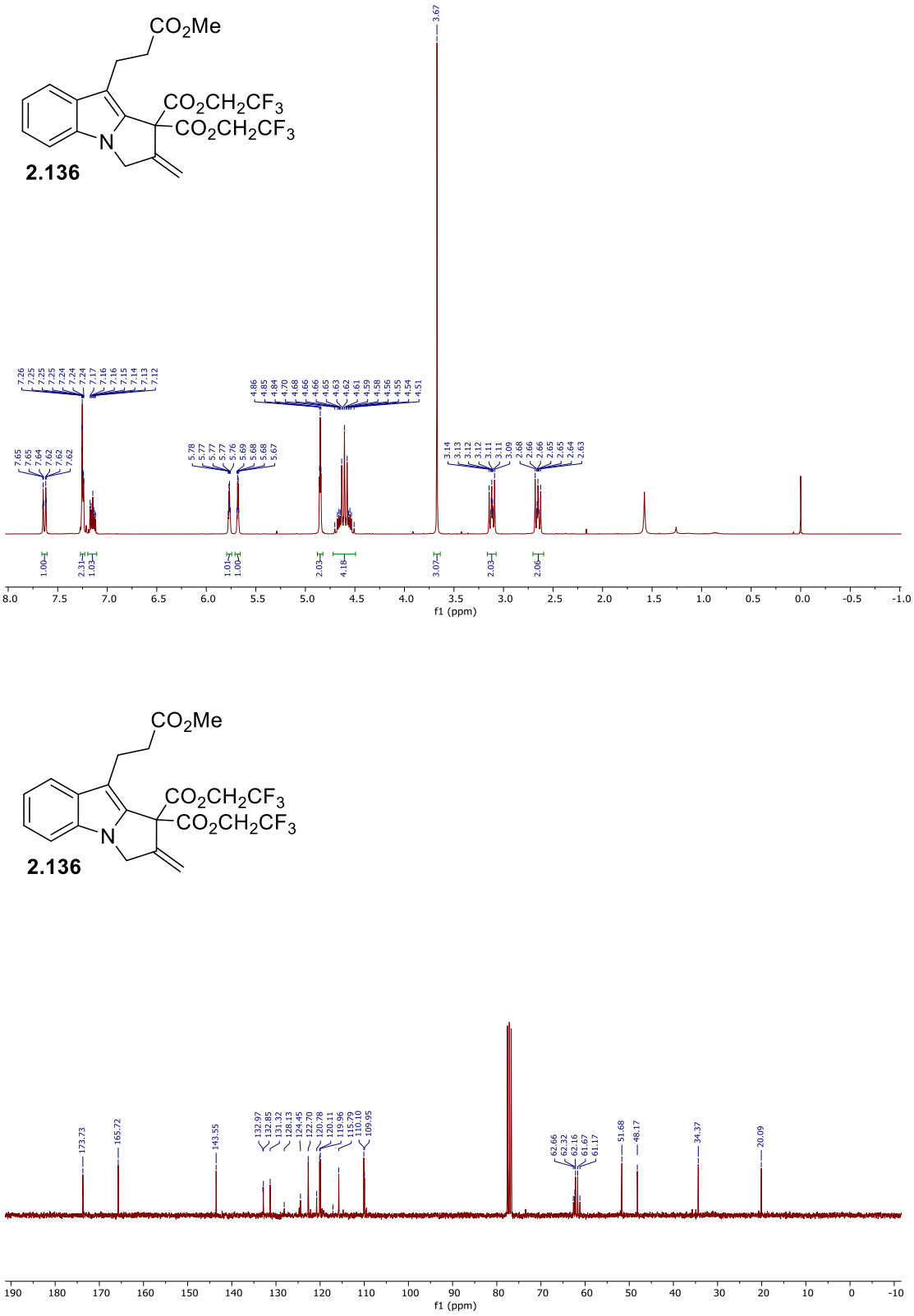

^{1}H NMR (300 MHz, $CDCl_3$) and ^{13}C NMR (75 MHz, $CDCl_3$) of compound **2.136**

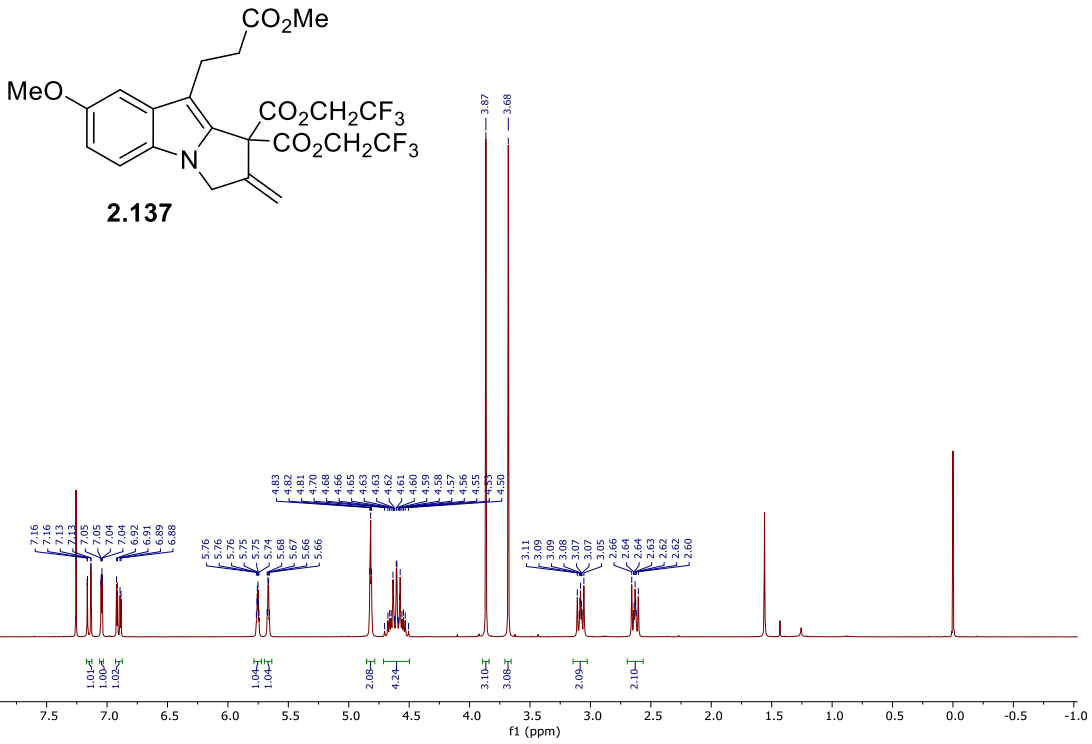

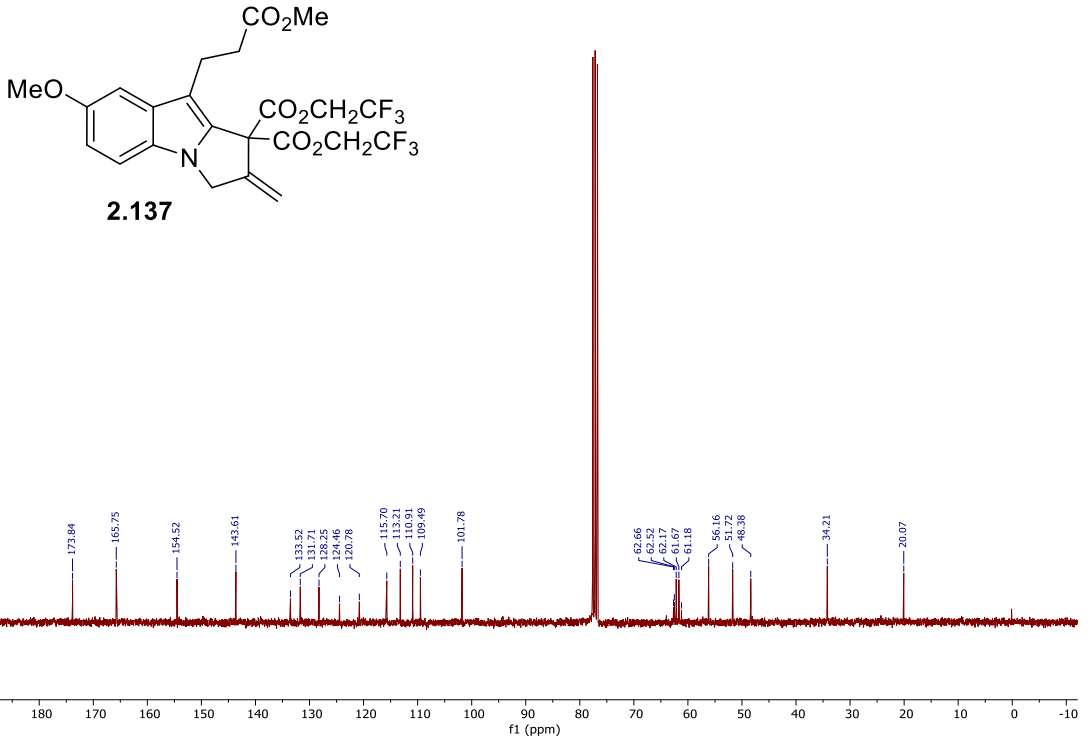

^{1}H NMR (300 MHz, $CDCl_3$) and ^{13}C NMR (75 MHz, $CDCl_3$) of compound **2.137**

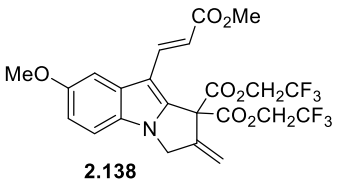

2.138

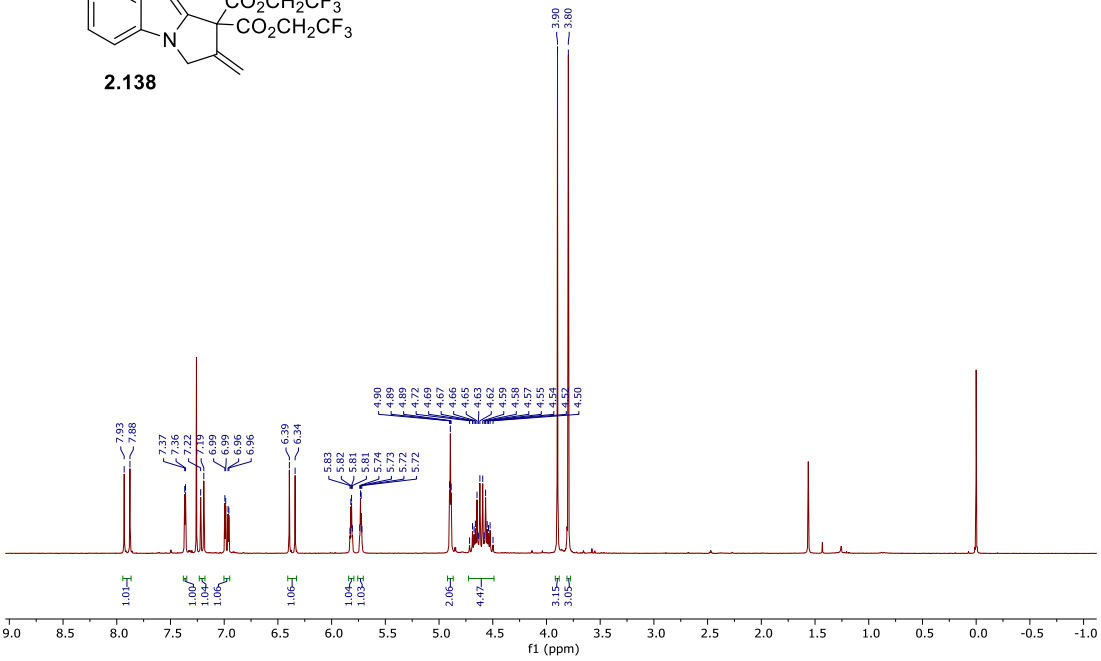

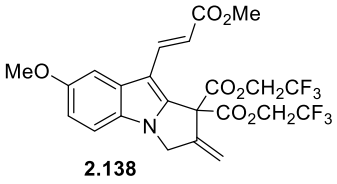

2.138

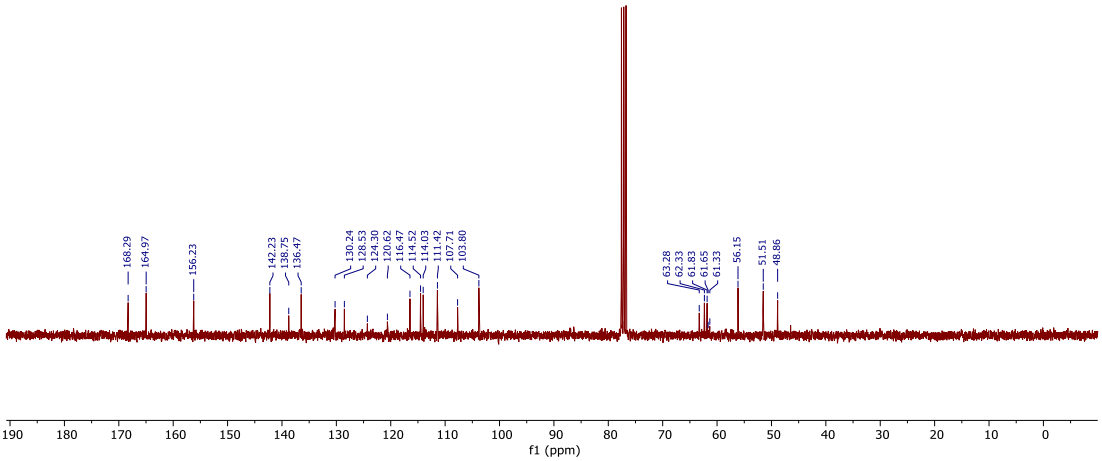

^{1}H NMR (300 MHz, $CDCl_3$) and ^{13}C NMR (75 MHz, $CDCl_3$) of compound **2.138**

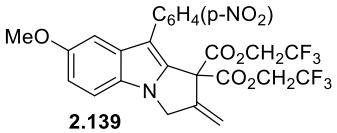

2.139

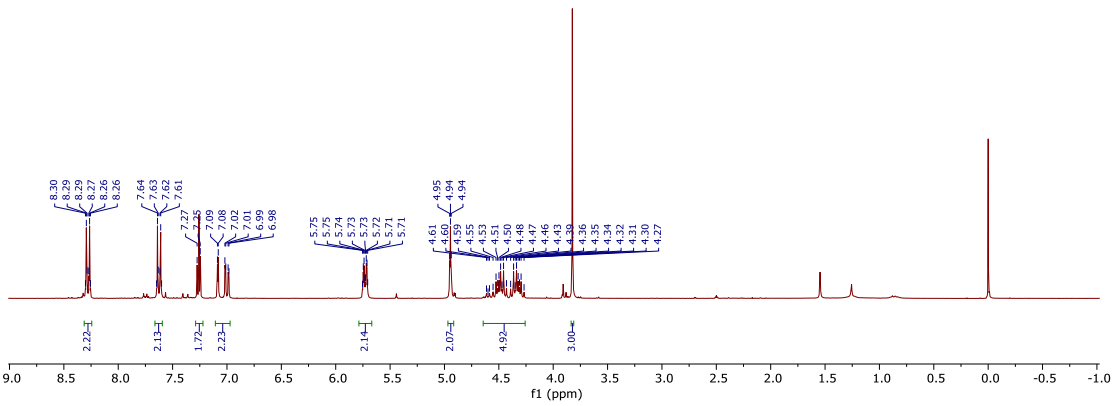

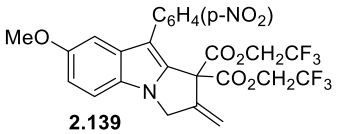

2.139

^{1}H NMR (300 MHz, $CDCl_3$) and ^{13}C NMR (75 MHz, $CDCl_3$) of compound **2.139**

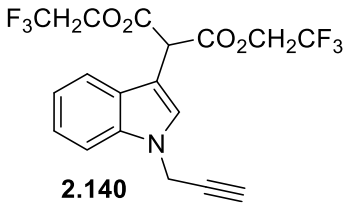

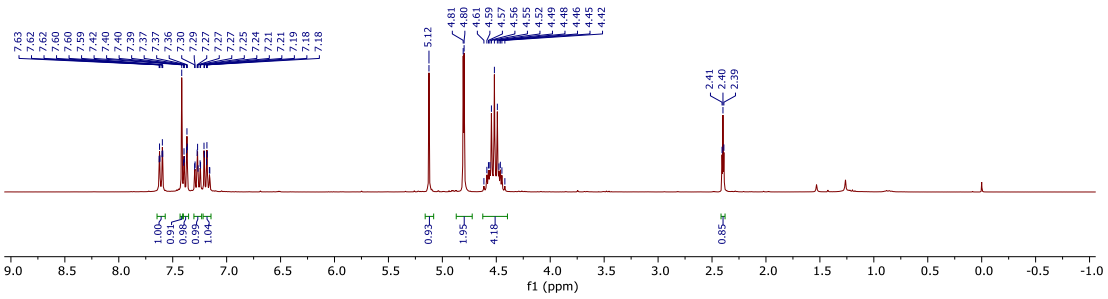

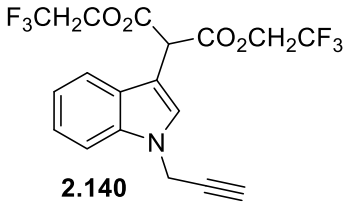

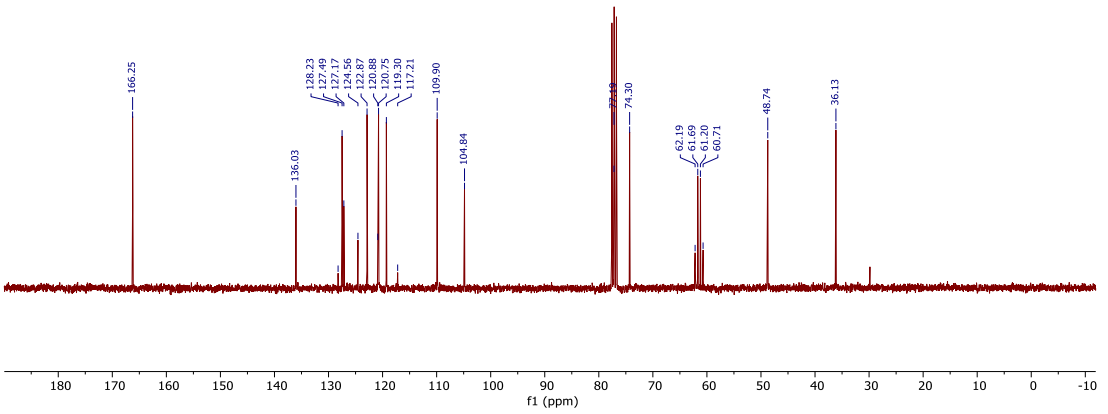

^{1}H NMR (300 MHz, $CDCl_3$) and ^{13}C NMR (75 MHz, $CDCl_3$) of compound **2.140**

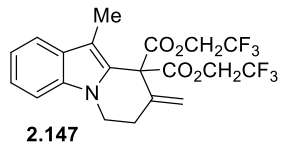

2.147

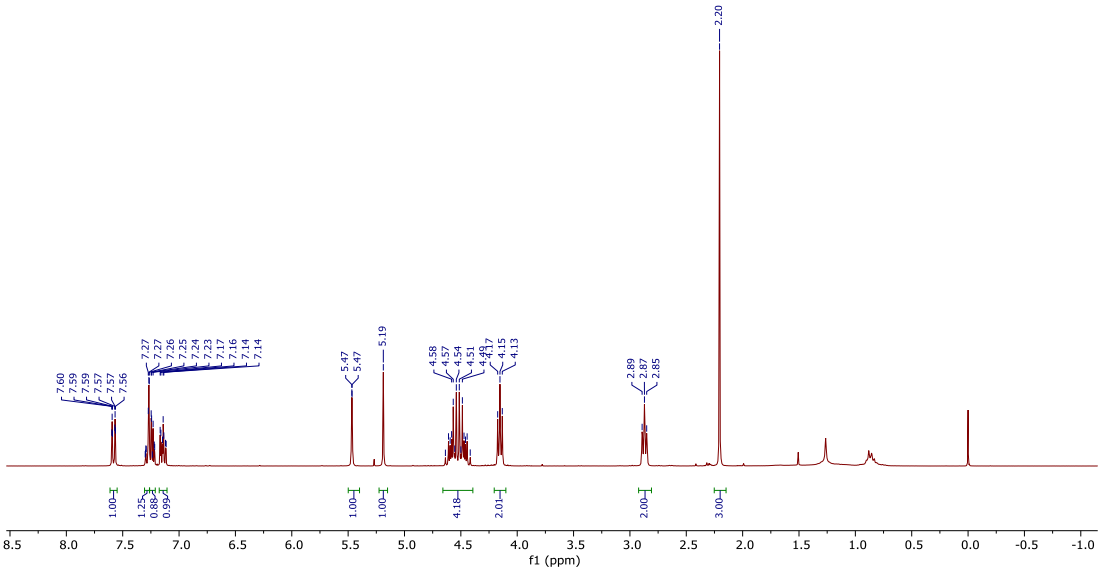

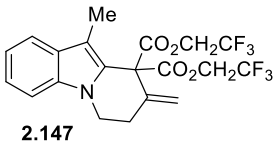

2.147

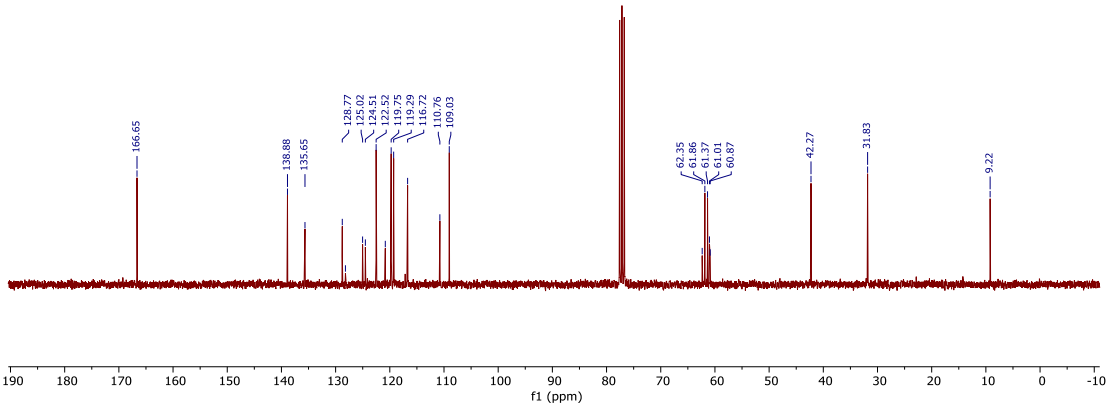

^{1}H NMR (300 MHz, $CDCl_3$) and ^{13}C NMR (75 MHz, $CDCl_3$) of compound **2.147**

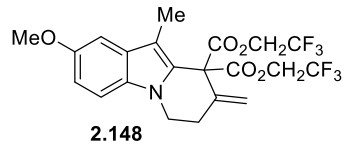

2.148

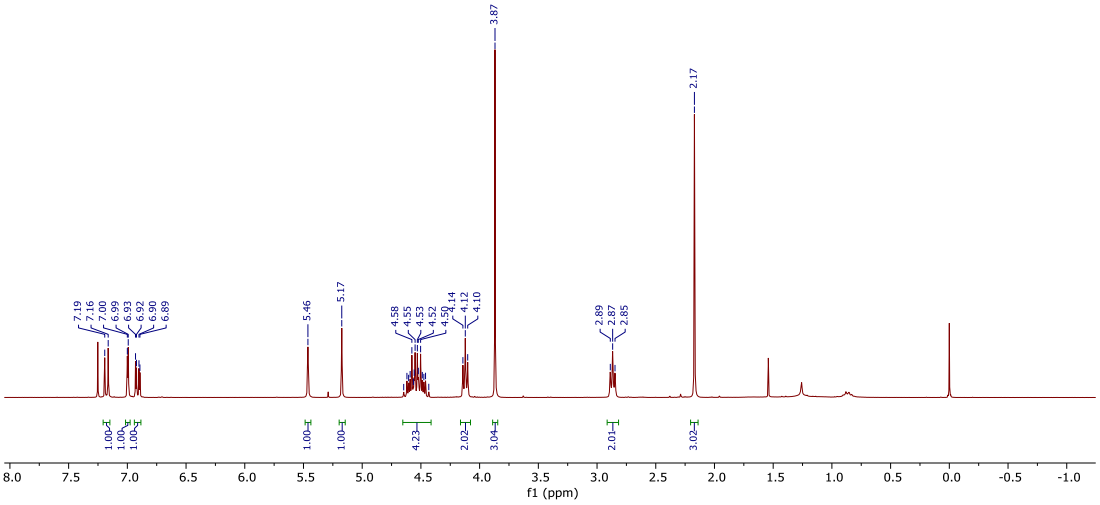

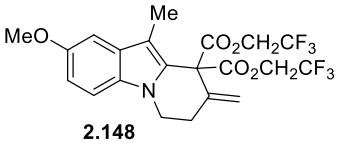

2.148

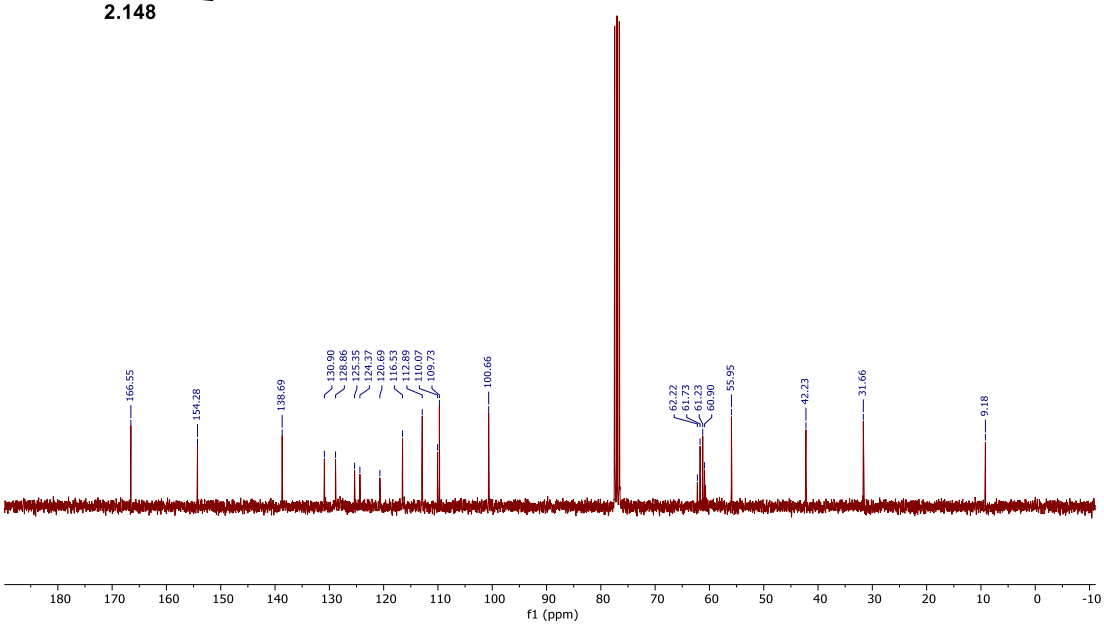

^{1}H NMR (300 MHz, $CDCl_3$) and ^{13}C NMR (75 MHz, $CDCl_3$) of compound **2.148**

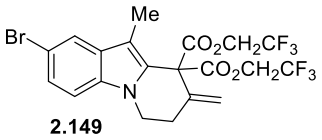

2.149

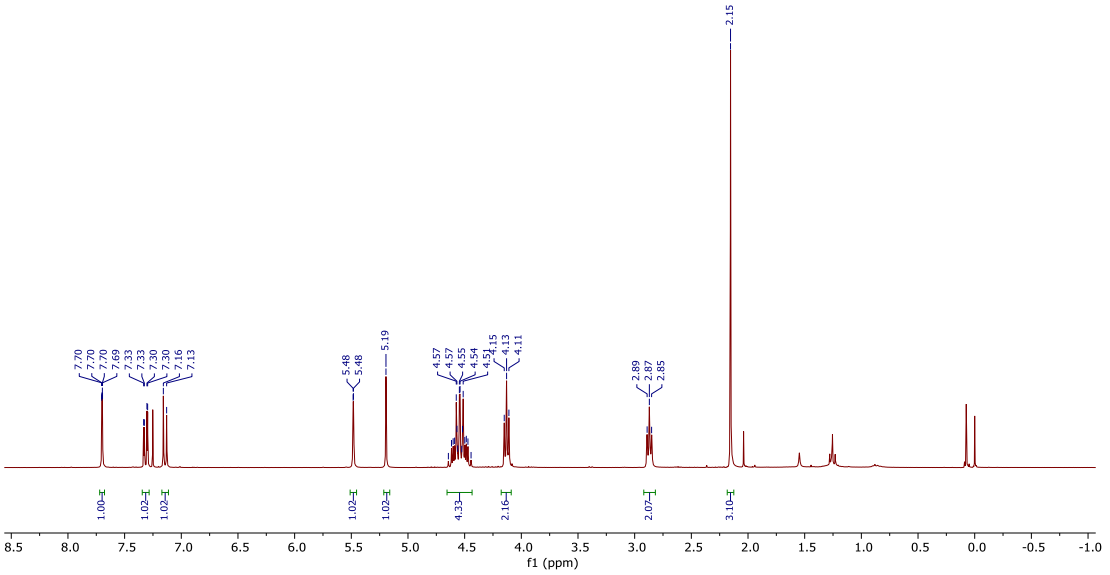

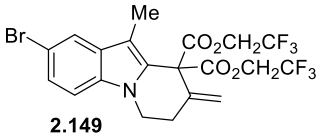

2.149

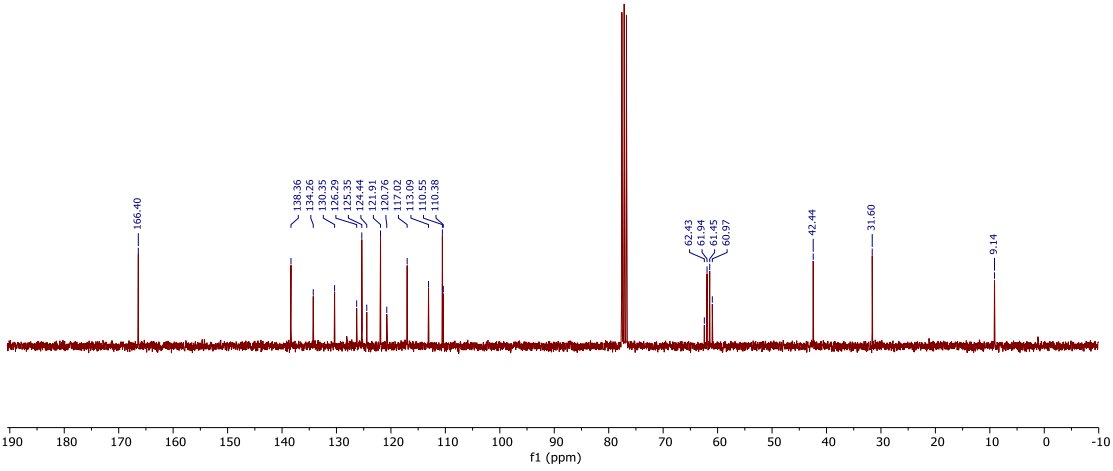

^{1}H NMR (300 MHz, $CDCl_3$) and ^{13}C NMR (75 MHz, $CDCl_3$) of compound **2.149**

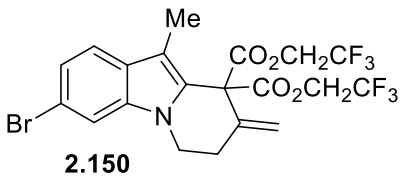

2.150

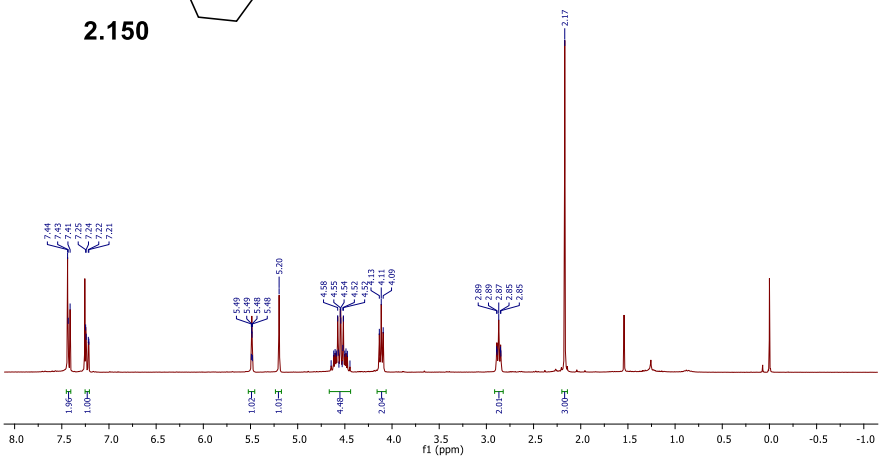

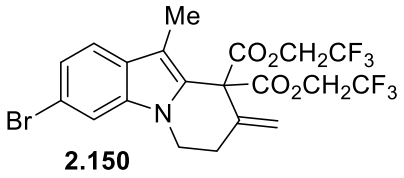

2.150

^{1}H NMR (300 MHz, $CDCl_3$) and ^{13}C NMR (75 MHz, $CDCl_3$) of compound **2.150**

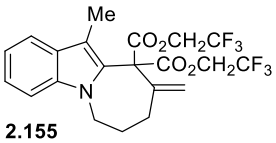

2.155

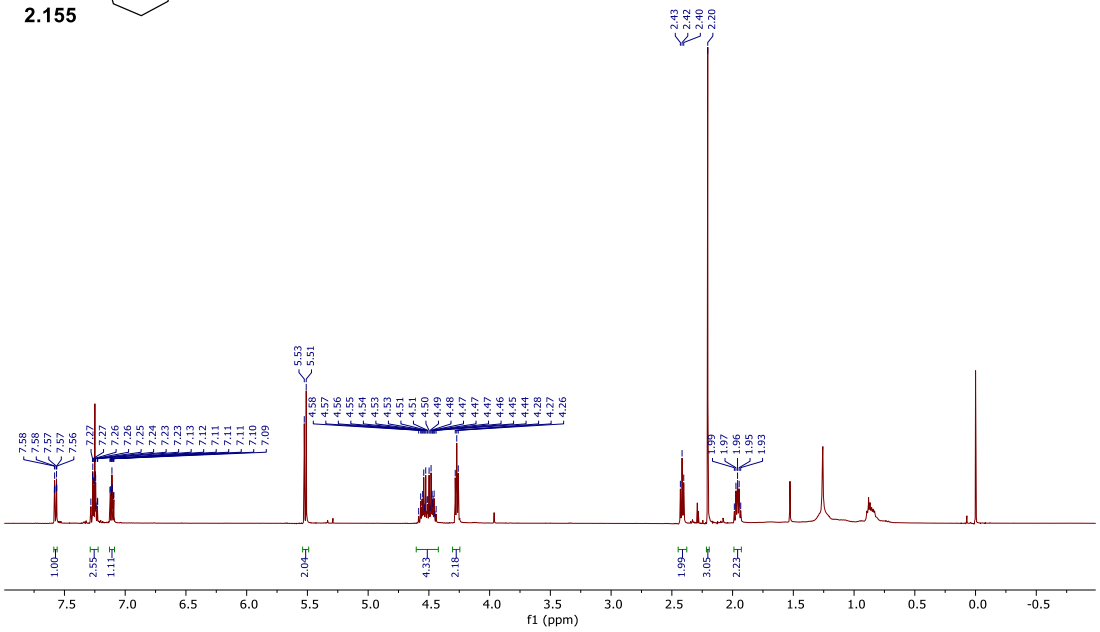

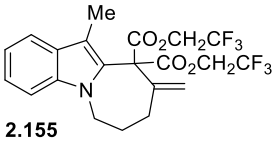

2.155

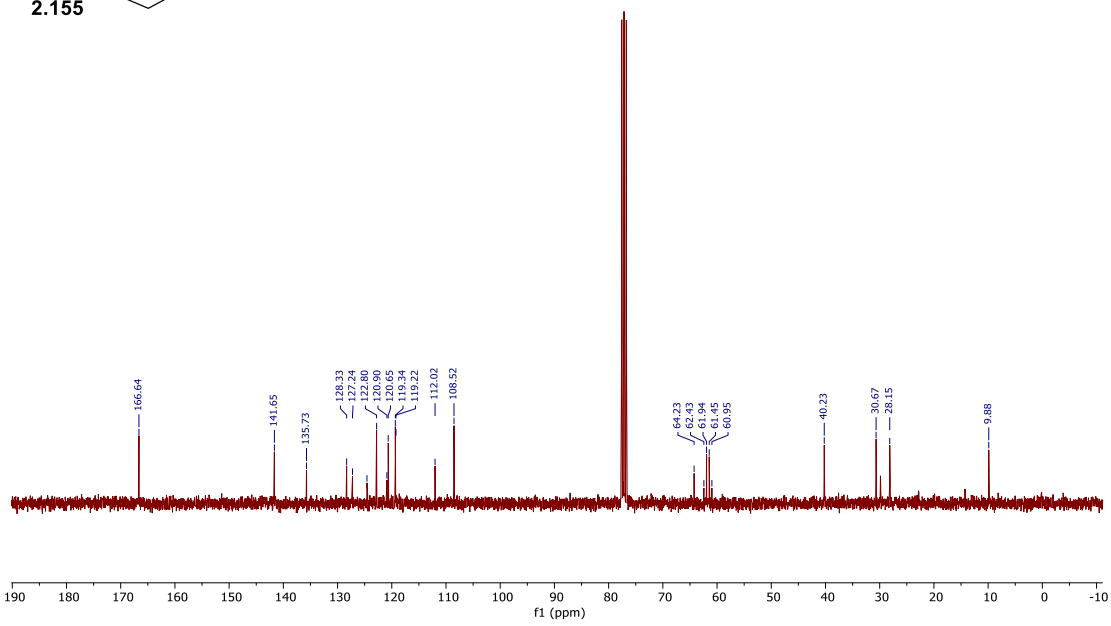

^{1}H NMR (300 MHz, $CDCl_3$) and ^{13}C NMR (75 MHz, $CDCl_3$) of compound **2.155**

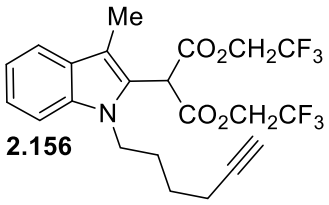

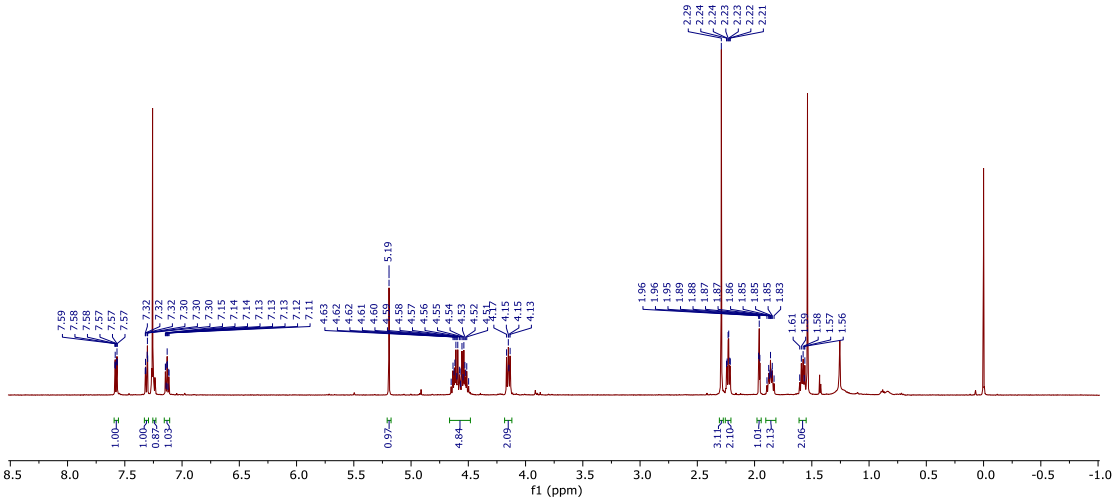

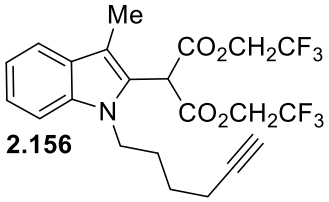

^{1}H NMR (300 MHz, $CDCl_3$) and ^{13}C NMR (75 MHz, $CDCl_3$) of compound **2.156**

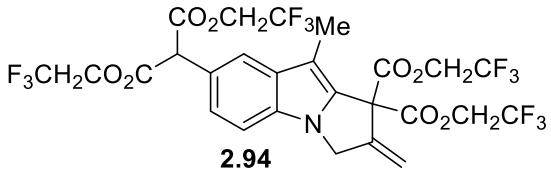

2.94

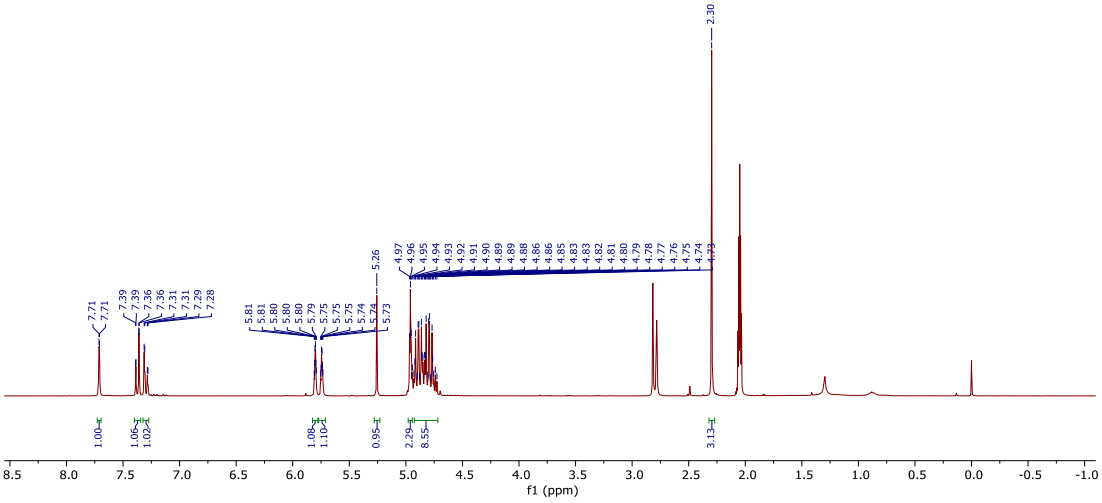

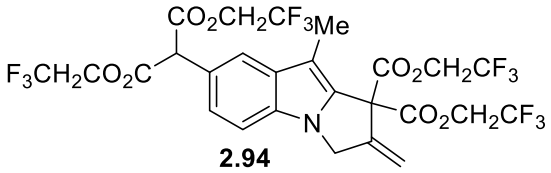

2.94

^{1}H NMR (300 MHz, $CDCl_3$) and ^{13}C NMR (75 MHz, $CDCl_3$) of compound **2.94**

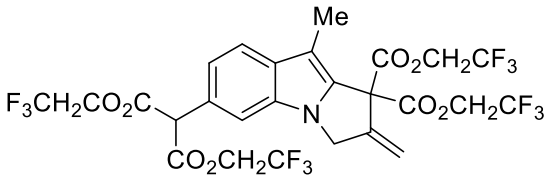

2.95

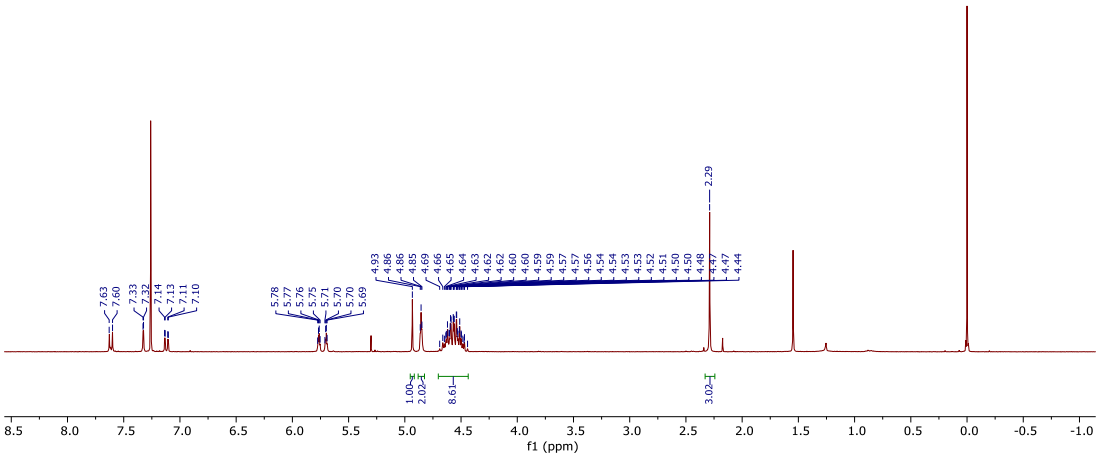

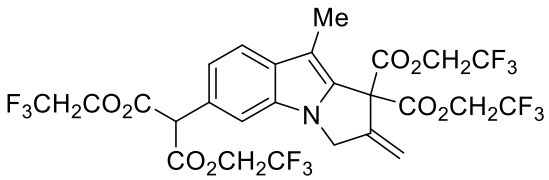

2.95

^{1}H NMR (300 MHz, $CDCl_3$) and ^{13}C NMR (75 MHz, $CDCl_3$) of compound **2.95**

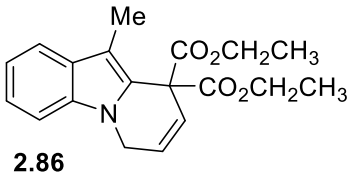

2.86

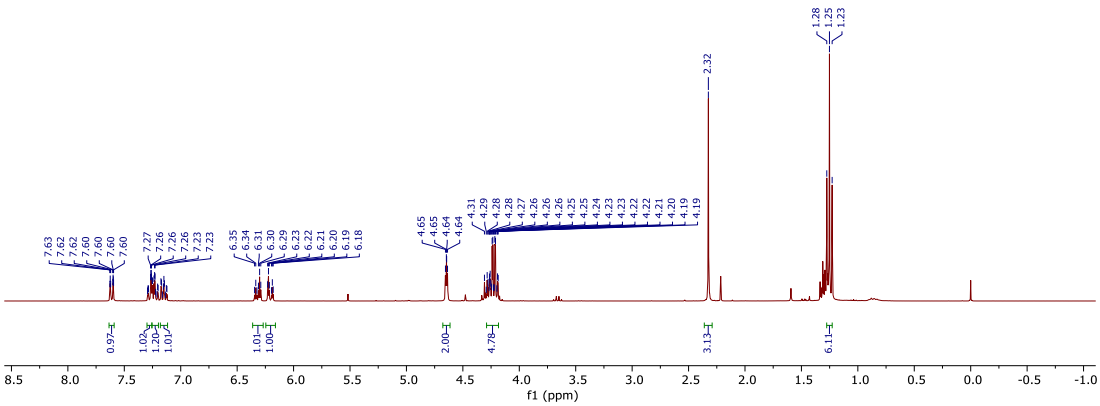

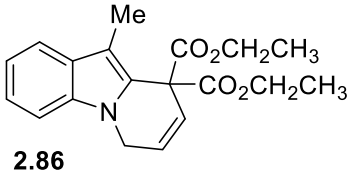

2.86

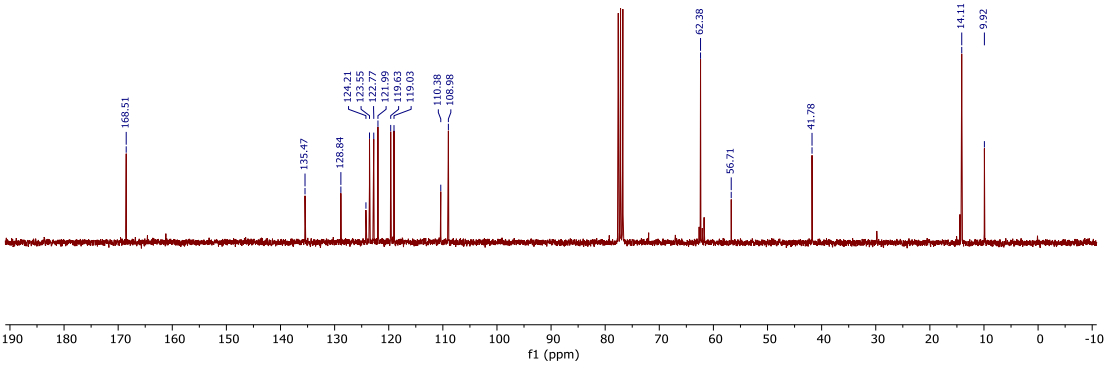

^{1}H NMR (300 MHz, $CDCl_3$) and ^{13}C NMR (75 MHz, $CDCl_3$) of compound **2.86**

CHAPTER 3: Stereoselective Copper-Catalyzed Heteroarene C–H Functionalization/Michael-Type annulation Cascade With *α*-Diazocarbonyls

With the publisher's permission, this chapter was adapted from the original manuscript: Aabid Bhat, Nathan Tucker, Jian-Bin Lin and Huck Grover. *Chem. Commun*., **2021**, *57,* 10556

Statement of Co-Authorship

Aabid Bhat (listed as the 1st author): contributed significantly to the synthetic work, physical data collection, and preparation of the manuscript and supporting information.

Nathan Tucker: contributed significantly to the synthetic work, physical data collection, and preparation of the manuscript and supporting information.

Dr. Jian-Bin Lin: Performed crystallographic structure determination to elucidate stereochemistry of several compounds.

Dr. Huck Grover: Principal investigator (PI) of this work, who led the project and contributed to the interpretation/analysis of data and the writing of the manuscript.

The article has been reproduced in this chapter in a modified form that includes the contributions of all the co-authors for the purpose of a complete discussion.

1.20 Introduction

1.20.1 Preliminary Results

In our first project, described in Chapter 2, we investigated the potential of using internal alkynes as electrophiles for C–H insertion/Conia-ene cyclization under Rh/Zn cooperative catalysis, which was an effort to expand the substrate scope (Scheme 3.1). However, when internal alkyne containing an alkyl substituent **3.1** at the terminal carbon was treated with trifluoro diazomalonate **3.2**, only noncyclized, C-2 functionalized product **3.3** was identified as determined by ^{1}H NMR analysis (Scheme 3.1A). In contrast, internal alkynes containing an electron-withdrawing substituent **3.4** successfully underwent tandem insertion/annulation, and cyclized product **3.5** was identified by NMR analysis (Scheme 3.1B). It is important to note that adding an electron-withdrawing group results in a more electrophilic alkyne, thus changing the annulation chemistry from Conia-ene to Michael-type addition.

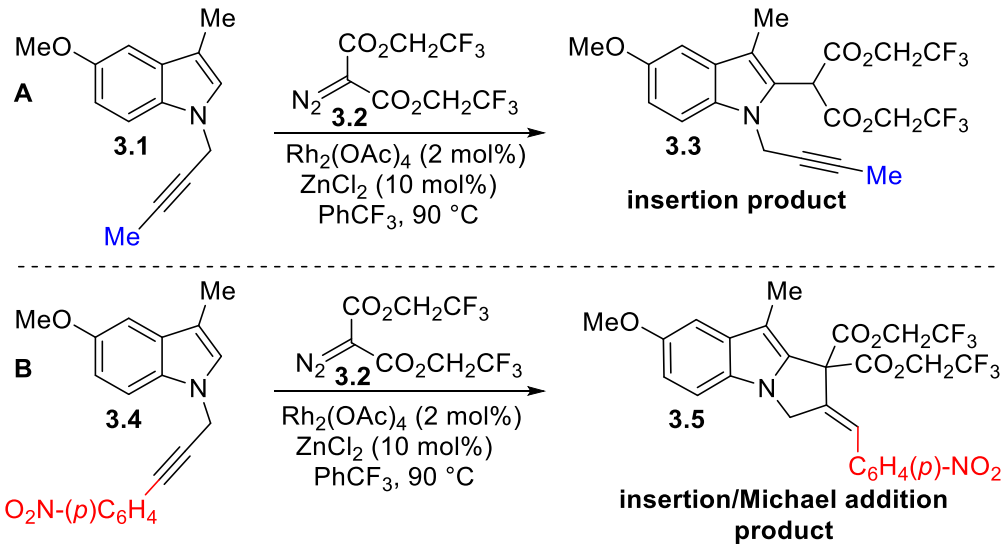

Scheme 0.1: (**A**) Attempted use of internal alkynes with electron donating group in cascade synthesis (**B**) Use of internal alkynes with electron withdrawing group in cascade synthesis.

1.20.2 Michael Addition Reaction

The 1,4-conjugate addition of enolates (donor reactant **3.6**), with *α,β*-unsaturated carbonyl compounds (acceptor reactant **3.7**), commonly referred to as the Michael addition reaction, has found a common place in synthetic chemistry for the construction of C–C bonds (Scheme 3.2A).[1] The importance of this reaction in the context of this thesis is the evolution of this reaction in tandem/cascade processes. One prominent method of utilizing this reaction in a tandem process is through trapping the enolate intermediate **3.11**, generated upon conjugate addition, with an appropriate electrophile (Scheme 3.2B). This approach would ultimately form two new bonds to the initial Michael acceptor reagent **3.10**.

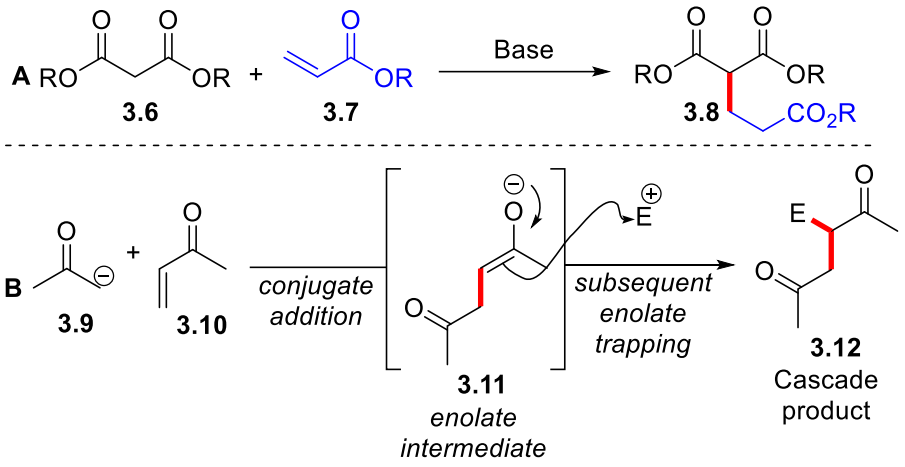

Scheme 0.2: (**A**) Michael addition reaction (**B**) Michael addition cascade reaction for constructing two C–C bonds.

In contrast, an alternative method of involving the Michael addition reaction in a tandem process can be achieved by using the Michael acceptor as an electrophilic trapping agent with an *in situ* generated enolate donor, which has been prepared by means other than deprotonation. In this respect, *α*-diazocarbonyl compounds **3.14** can serve as valuable precursors to the required enolate intermediate (**3.15**) *via* a formal carbon/heteroatom–H insertion process (Scheme 3.3). Following Michael addition of intermediate **3.15**, this approach would ultimately form two new

bonds to the initial diazo reagent while also generating potentially useful cyclic organic scaffolds (**3.16**).

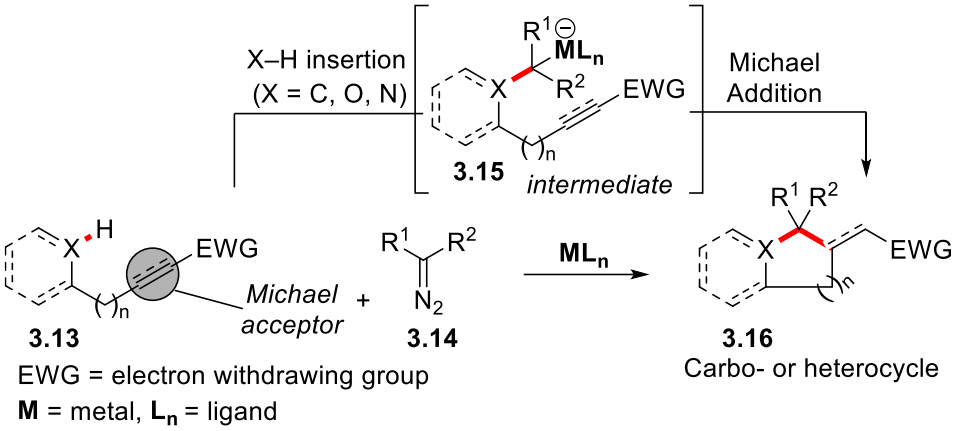

Scheme 0.3: X-H insertion/Michael addition cascade protocol.

1.20.3 Previous Tandem Reactions Involving Diazo Reagents and Michael Additions

Hu and coworkers in 2009 reported a tandem approach to synthesize tetrahydrofurans *via* rhodium-catalyzed O–H insertion of aryldiazoacetate **3.18** with a secondary allylic alcohol **3.17** followed by a highly stereoselective intramolecular Michael-type addition (Scheme 3.4).[2] This method highlights a one-flask approach to access highly functionalized tetrahydrofurans **3.20**. The authors proposed that the observed stereoselectivity was dictated by intermediate **3.19** from the O–H insertion event.

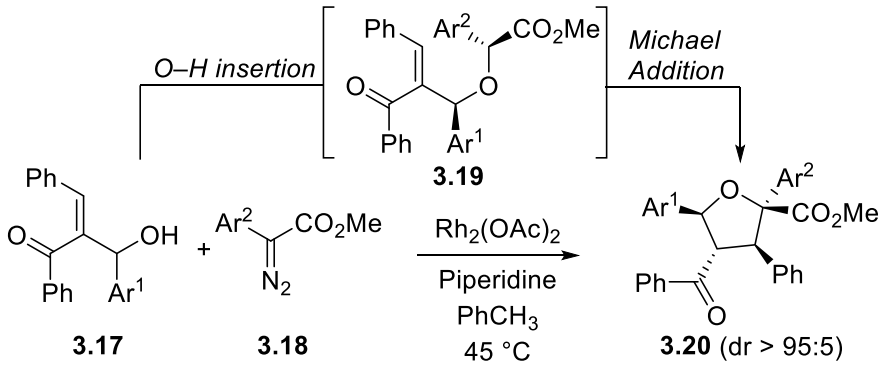

Scheme 0.4: Synthesis of substituted tetrahydrofurans **3.20** by the Hu group.

Recently, the Nemoto group from Chiba University explored the dual use of *α,β*-unsaturated enones as both a directing group and an electrophile for C–H insertion/Michael addition sequences involving *α*-diazocarbonyl compounds.[3] As reported in their publication in 2020, they developed a methodology for the synthesis of 3,4-fused tricyclic indoles. The reaction proceeds *via* an initial Rh(III)-catalyzed C–H activation and diazo coupling event between **3.21** and **3.22** to provide the C-4 functionalized indole intermediate **3.23** (Scheme 3.5). Without isolation, **3.23** could be treated with base to promote the Michael addition and furnish the desired cyclized product **3.24**. In addition, the authors conducted screens using chiral amines to show that the second C–C bond formation *via* Michael addition could proceed with high enantiocontrol (not shown in the scheme). Following their seminal report in this area, the Nemoto group has also explored other applications of the enone-directing group in selective C–H activation annulation cascades.[4]

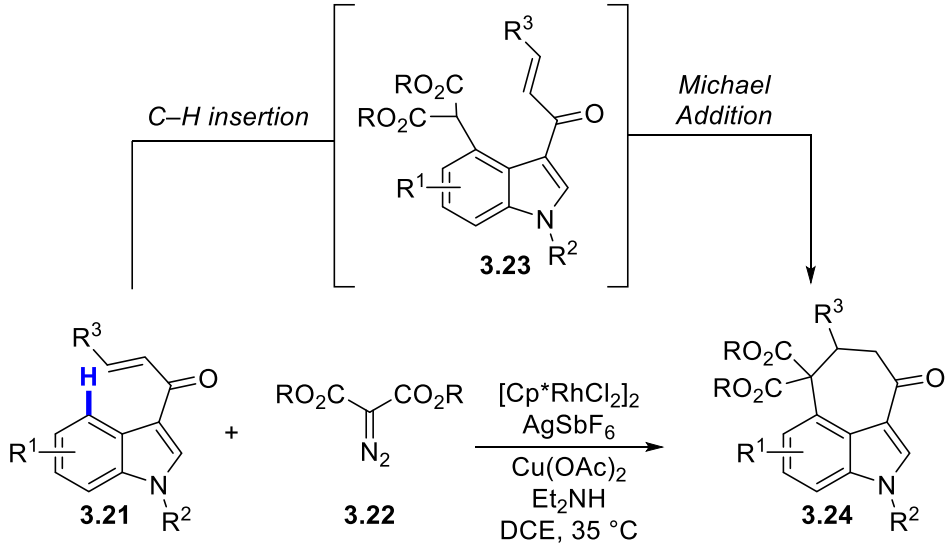

Scheme 0.5: Synthesis of chiral 3,4-fused tricyclic indoles **3.24** by the Nemoto group.

1.20.4 Hypothesis

Taking the preliminary findings (Scheme 3.1) and literature precedent into consideration, a tandem C–H insertion/Michael addition protocol involving *α*-diazocarbonyl compounds was envisioned (Scheme 3.6). It was hypothesized that the electron deficient internal alkyne (or alkene) moiety tethered to the indole nitrogen **3.25** could serve as a Michael-type acceptor to provide the [4+1] annulation product **3.28** *via* trapping of C–H insertion intermediate **3.27** in a single step. Additionally, we believed that the use of the Michael-type acceptor as an electrophile in this type of transformation could potentially allow for a single catalyst to be identified that would be capable of promoting both steps of the reaction.

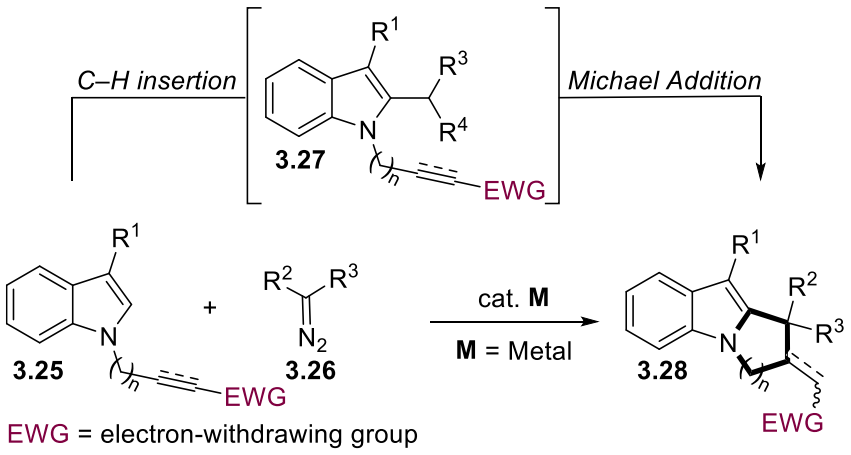

Scheme 0.6: Tandem C–H insertion/Michael-addition.

1.20.5 Results and Discussion — Synthesis of Starting Materials

We commenced our study with the synthesis of alkynoate ester starting material **3.30.** Freshly prepared *N*-propargyl substituted indole **3.29** was converted to **3.30** in a serviceable 63% yield in a single step *via* classical alkynylation conditions, which employ *n*-BuLi and methyl chloroformate (Scheme 3.7). Diethyl diazomalonate **3.31** was synthesized using same procedure as described in Chapter 2 (Scheme 2.12B).

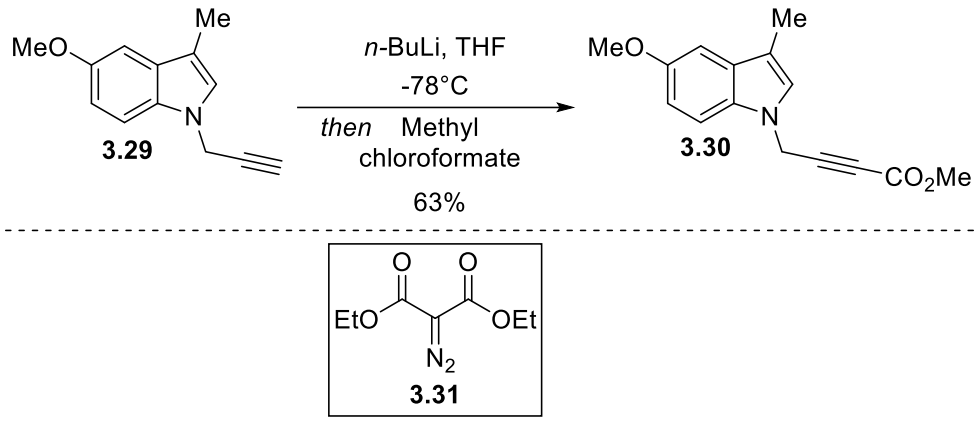

Scheme 0.7: Synthesis of alkynyl-ester substituted indole **3.30**.

1.20.6 Optimization and Scope

Having substitution at the C-3 and C-5 positions on indole substrate in place to control the regioselectivity of the initial carbene coupling, the primary objective of this study was to identify a cost-effective, single catalyst system capable of promoting the tandem reaction. To our delight, subjecting **3.30** and diethyl diazomalonate **3.31** in benzene under $Cu(acac)_2$ conditions provided the desired product **3.32** in 70% yield as a single stereoisomer (entry 1, Table 3.1). Other copper catalysts were also screened, and all resulted in the desired annulation product **3.32** as a single isomer in different isolated yields (entries 1-8). Further screening of solvents, temperatures, and catalyst loadings revealed that copper(II) trifluoroacetylacetonate ($Cu(tfacac)_2$) in benzene at 80 °C were the ideal reaction conditions for this transformation (entry 9). Even though copper loadings as low as 0.5 mol% proved effective (entry 10), reproducibly high yields (78%) were obtained on a large scale when 5 mol% copper was utilized (entry 11). Interestingly, when the Rh/Zn catalyst system, developed for related carbene annulation reactions with electron-rich π-electrophiles was used,[5] a significant decline in yield was observed despite the complete consumption of the limiting reagent **3.31** (entry 16). Potentially, the increased rate of decomposition of **3.31** under rhodium catalysis (*vs.* copper catalyst) leading to unfavorable

dimerization[6] and side reactions could be the reason for this low yield; however, further investigations are required to confirm this hypothesis.

Table 0.1: Screening of copper catalysts for the synthesis of **3.32.**

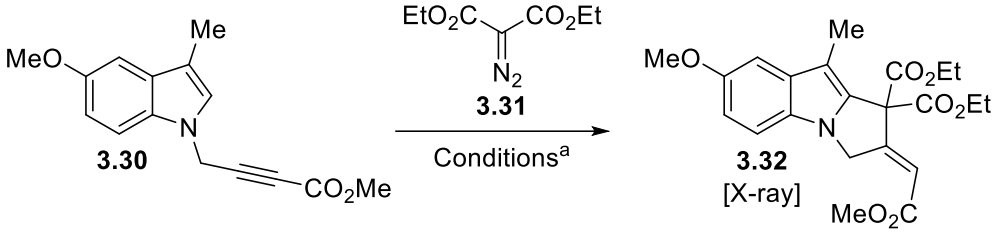

Entry	Catalyst	Loading	Solvent	Yield
1	$Cu(acac)_2$	10 mol%	C_6H_6	70%
2	$Cu(OAc)_2$	10 mol%	C_6H_6	58%
3	$Cu(OTf)_2$	10 mol%	C_6H_6	65%
4	$CuCl_2$	10 mol%	C_6H_6	42%
5	$CuBr{\cdot}S(CH_3)_2$	10 mol%	C_6H_6	41%
6	$Cu(OTf){\cdot}C_6H_6$	10 mol%	C_6H_6	61%
7	CuCl	10 mol%	C_6H_6	50%
8	$Cu(tfacac)_2$	1 mol%	C_6H_6	65%
9	$Cu(tfacac)_2$	5 mol%	C_6H_6	79%
10	$Cu(tfacac)_2$	0.5 mol%	C_6H_6	59%
11	$Cu(tfacac)_2$	5 mol%	C_6H_6	78%[b]
12	$Cu(tfacac)_2$	10 mol%	$PhCH_3$	59%
13	$Cu(tfacac)_2$	10 mol%	$PhCF_3$	48%
14	$Cu(tfacac)_2$	10 mol%	C_6F_6	63%
15	$Rh_2(OAc)_4$ / $ZnBr_2$	2 mol% / 10 mol%	C_6H_6	26%

[a] Reaction conditions: indole **3.32** (1.2 equiv), diazo **3.34** (1.0 equiv, 0.14 mmol), cat. (loading as indicated in the Table), in 1.0 M (solvent), Time (12 h) and Temp. 80 °C. [b]1.0 mmol scale of **3.34**.

Having observed the formation of a single cyclization isomer (^{1}H NMR analysis) in all copper-catalyzed reaction conditions tested, it became important to determine the configuration of the product in hopes to shed light on the mechanism. Therefore, X-ray quality crystals were prepared by vapor diffusion of pentane into a solution of **3.32** in ether. Single crystal X-ray diffraction (XRD) and structural elucidation of this crystal, performed by Dr. Jian-Bin Lin,[7]

indicated the *Z*-configuration of **3.32**. Based on this information, a plausible mechanism was proposed (Scheme 3.8). We envisioned that the copper serves two purposes in the mechanism of this reaction. First, copper can activate the *α*-diazocarbonyl **3.31** to form the copper carbenoid intermediate **A**, which can undergo a formal C–H insertion with substituted indole **3.30** to form copper complex **B**. The copper-bound enolate can then activate the alkyne electrophile **C**, to invoke a 5-*exo*-*dig* cyclization in a *syn*-addition fashion to give cyclized intermediate **D**. It is believed that this dual activation by the catalyst, where the copper activates both the nucleophile and the electrophile (enolate and Michael acceptor), is the root of the observed stereoselectivity.[8] Finally, protodemetalation of **D** generates the *Z*-alkene isomer **3.32** and regenerates the active catalytic species.

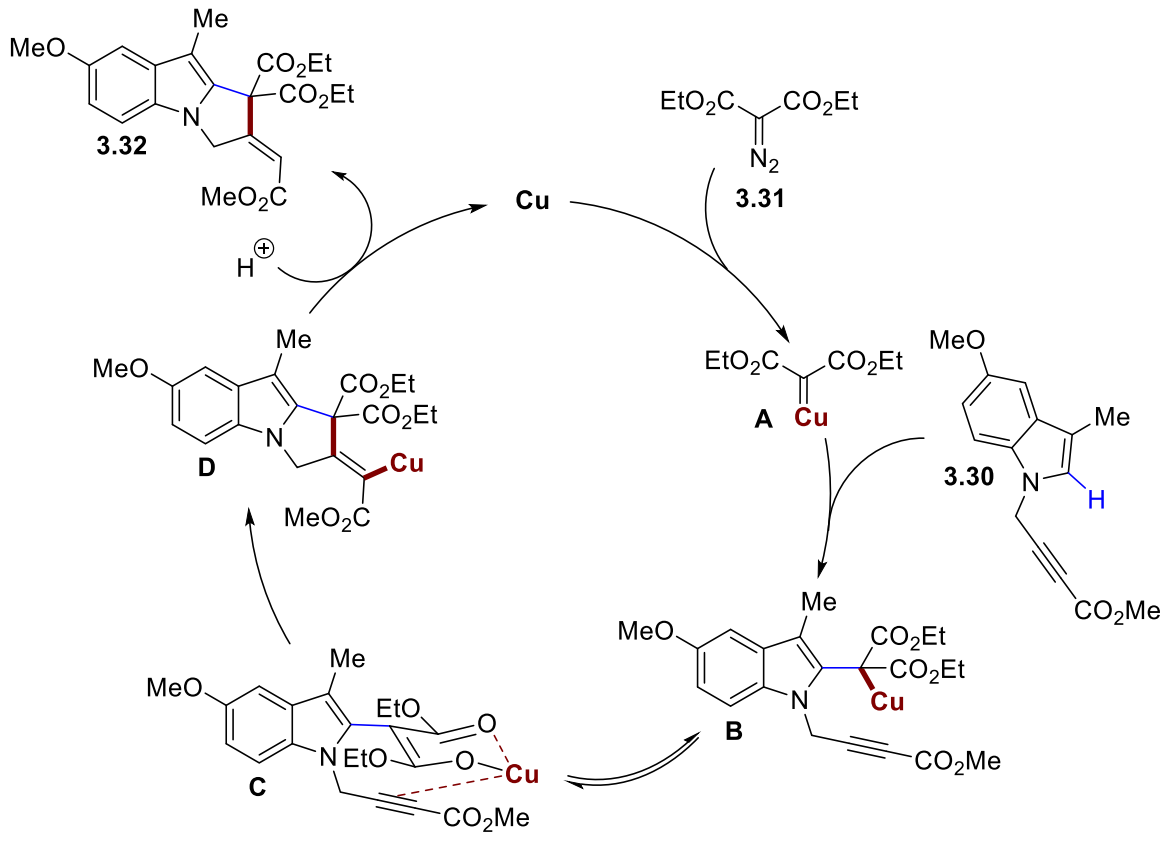

Scheme 0.8: Plausible reaction mechanism.

After establishing optimal conditions and a plausible mechanism, it was then decided to see what variations on the starting material structure could affect the yield and selectivity of this transformation. Thus, we next explored the scope of the reaction with regard to the indole coupling partner (Scheme 3.9). In accordance with our previous experience, when the indole starting material does not contain substitution on the benzenoid ring **3.33**, a noticeable decrease in the yield of the annulation product **3.38**, 69% was observed. The decrease in yield may be due to a lack of regio-control during the carbene coupling step of the reaction, leading to the formation of competitive benzenoid functionalization products. Changing the ester acceptor moiety on the indole starting material **3.30**, **3.33–3.37** did not impact the reaction under the current conditions, furnishing the desired cascade products **3.32, 3.39–3.42** in high yields as single stereoisomers.

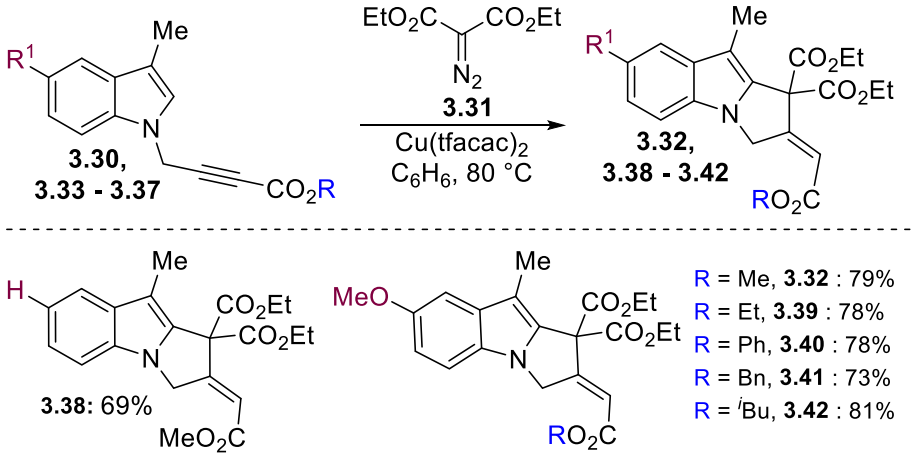

Scheme 0.9: Tandem C–H insertion/Michael-addition substrate scope of the alkynyl-ester electrophile.

Furthermore, we demonstrated that by extending the length of tethered alkyl electrophile on indole nitrogen **3.43**, pyridoindole **3.44** could be obtained in a 68% yield as a single stereoisomer as confirmed by X-ray crystallography (Scheme 3.10A).[7] However, when the chain length of the electrophile was extended further by one more carbon unit **3.45**, only the carbene coupling product **3.46** was isolated in 71% yield with no indication that an annulation event had occurred under the standard reaction conditions (Scheme 3.10B). Additionally, switching solvents

to toluene and elevating the temperature or prolonging the reaction time did not result in any desired cyclization product. This result indicates that the current method has a limited range for cyclization, restricting the formation of five-membered and six-membered rings as a result of the distance between the functionalized C–H bond and the electrophile. In a parallel result, switching the ester group at the terminal end of the alkyne acceptor for an alkyl group **3.1** resulted only in coupling product **3.47** in a 52% yield (Scheme 3.10C), indicating the importance of the alkynyl-ester in the current cascade reaction.

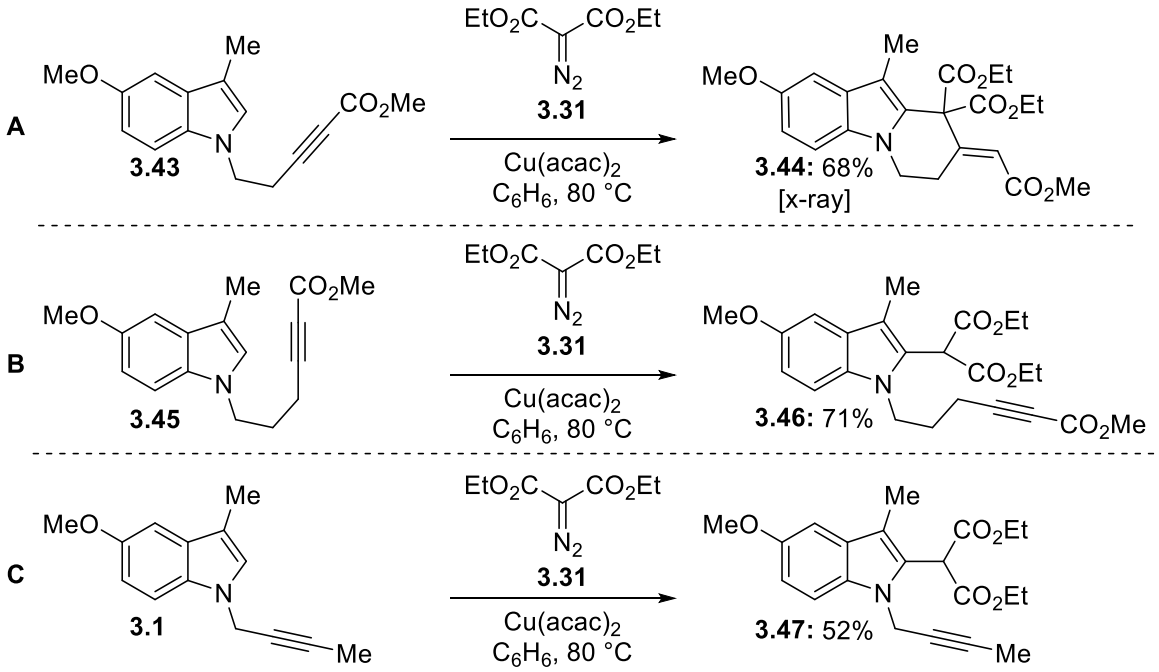

Scheme 0.10: (**A**) Synthesis of pyridoindole **3.44** (**B**) Synthesis coupling product **3.46** (**C**) Synthesis of insertion product **3.47**.

Next, we envisioned that varying the location of the Michael acceptor electrophile from the indole nitrogen to other positions on the indole starting material could provide access to a variety of fused indole products by employing our current tandem reaction manifold. Thus, the next objective became the synthesis of appropriately functionalized indole starting materials **3.49**

and **3.51** (Scheme 3.11). Synthetically, we envisioned that these targets could be accessible from the respective aldehyde starting materials **3.48** and **3.50**.

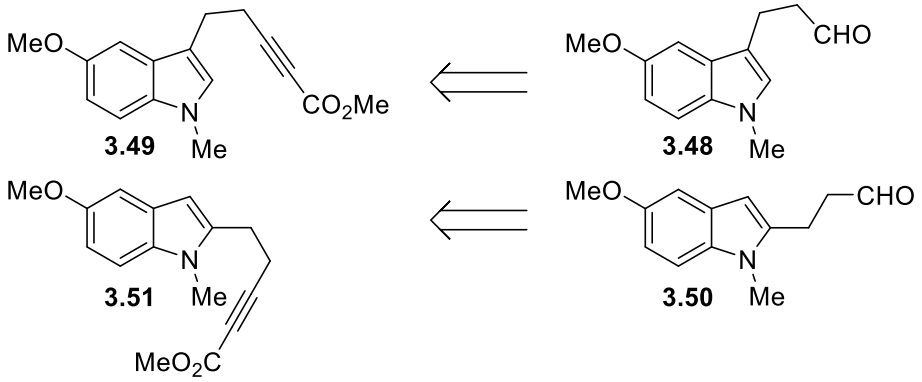

Scheme 0.11: Retrosynthesis of indoles **3.49** and **3.51**.

To this end, initial attempts to construct indole alkynylester **3.49** began from *N*-methyl substituted indole **3.55**. We first tried to construct aldehyde **3.48** *via* an aerobic oxidative coupling as described by Jiang and coworkers in 2013.[9] In the Jiang's report, when allyl alcohol **3.53** was treated with 1*H*-indole **3.52** under Pd-catalyzed oxidative reaction conditions, alkylation product **3.54** was obtained in 92% yield (Scheme 3.12A). Unfortunately, in our hands, when indole **3.55** and allyl alcohol **3.53** were subjected to the same oxidative coupling conditions in the presence of an atmospheric O_2, no desired aldehyde product **3.48** was obtained (Scheme 3.12B). Furthermore, using $Cu(OAc)_2$ as an oxidant and other solvents under elevated temperature conditions did not provide the desired alkylation product.

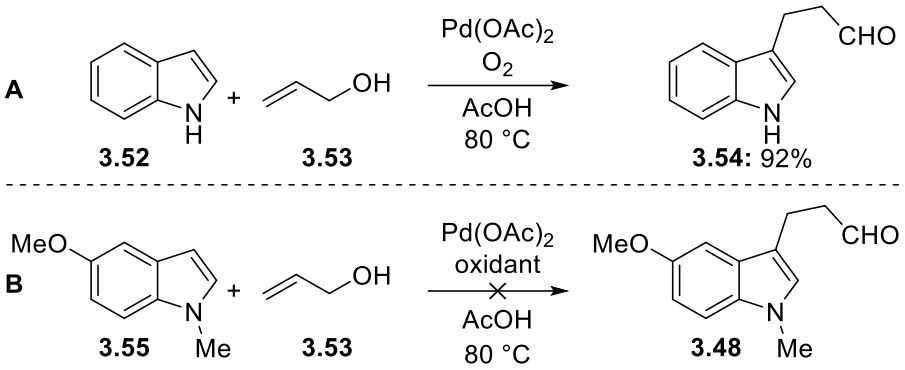

Scheme 0.12: (**A**) Synthesis of alkylated indole product **3.54** by Jiang group (**B**) Attempted synthesis of **3.48** using the reported conditions.

To overcome the problem in synthesizing **3.48**, indole **3.55** was subjected to oxidative Heck reaction with methyl acrylate to afford the C-3 alkenylation product **3.56** in 85% yield, which was subsequently hydrogenated to provide **3.57** in 98% yield (Scheme 3.13). Reduction of ester **3.57** to the corresponding aldehyde **3.48** with DIBAL in THF at −78 °C proved challenging, providing alcohol **3.58** as the primary product with only trace quantities of **3.48**. Additionally, the use of toluene and diethyl ether as solvents in this reduction reaction also failed to provide the aldehyde as the major product. Regrettably, attempts to oxidize alcohol product **3.58** using 2-iodoxybenzoic acid (IBX) in DMSO resulted primarily in forming an undesired double oxidation product **3.59**.

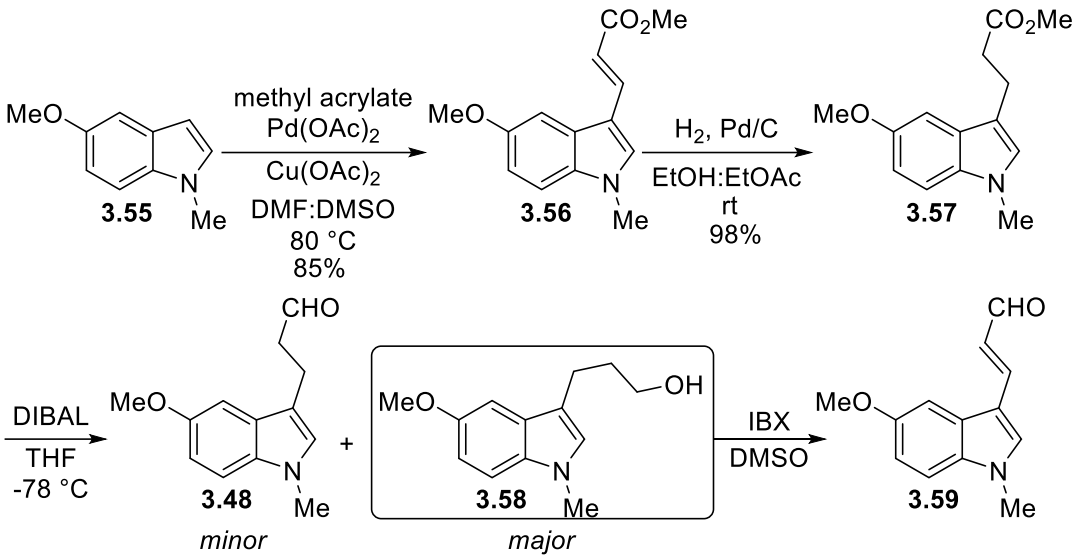

Scheme 0.13: An attempted route for the synthesis of aldehyde **3.48**.

Finally, through optimization of the DIBAL reduction, a simple change in solvent to dichloromethane allowed **3.48** to be isolated as the major product in a 57% yield (Scheme 3.14). With **3.48** in hand, a subsequent homologation reaction, with the Bestmann-Ohira reagent **3.60**,[10] provided alkyne product **3.61** in 76% yield. Using the same conditions described in Scheme 3.7, alkynoate ester **3.49** was synthesized in 86% yield.

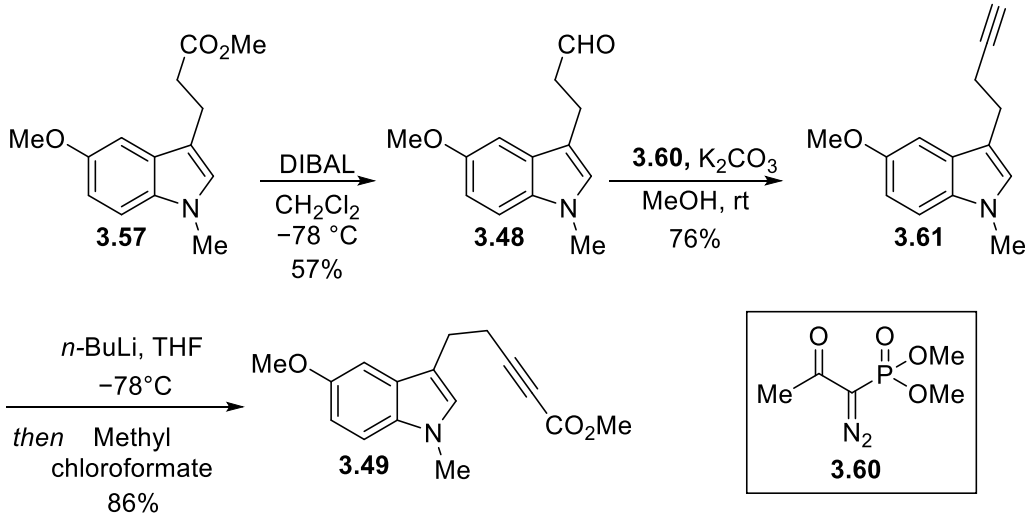

Scheme 0.14: Synthesis of C-3 substituted alknylester **3.49**.

Next, we turned to the synthesis of C-2 substituted alkynlester **3.51** (Scheme 3.15). *N*-Methyl substituted indole **3.55** was treated with *n*-BuLi at -78 °C, then quenched with DMF to obtain aldehyde product **3.62**, which was further subjected to a Horner–Wadsworth–Emmons (HWE) reaction to furnish *α,β*-unsaturated ester product **3.64** (67% over two-steps). **3.64** was hydrogenated using Pd/C catalysis to give ester **3.65** (90%), and further DIBAL reduction afforded aldehyde **3.50** (60%). Homologation of **3.50** with Ohira-Bestmann reagent **3.60** afforded alkyne **3.66** in a 75% yield. Finally, **3.66** was treated with *n*-BuLi at -78 °C and quenched with methyl chloroformate to obtain alkynoate ester product **3.51** in an 86% yield.

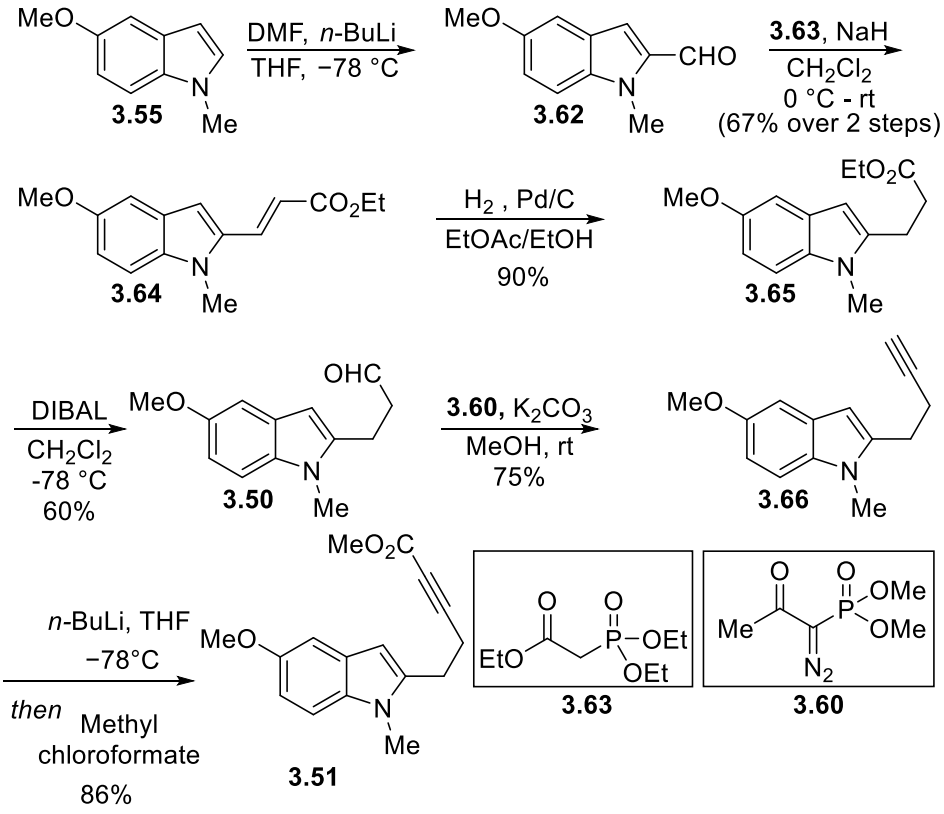

Scheme 0.15: Synthesis of C-2 substituted alknylester **3.51**.

The tandem insertion/annulation reaction of **3.31** with C-2 and C-3 appended alkynyl-ester starting materials **3.49** and **3.51** demonstrated compatibility with the reaction conditions, yielding **3.67** and **3.68** in excellent yields (Scheme 3.16). Interestingly, tetrahydrocarbazoles **3.67** and **3.68**

were isolated as single olefin isomers. This further demonstrated the generality of the reaction manifold in the construction of diverse structural scaffolds in a stereocontrolled manner.

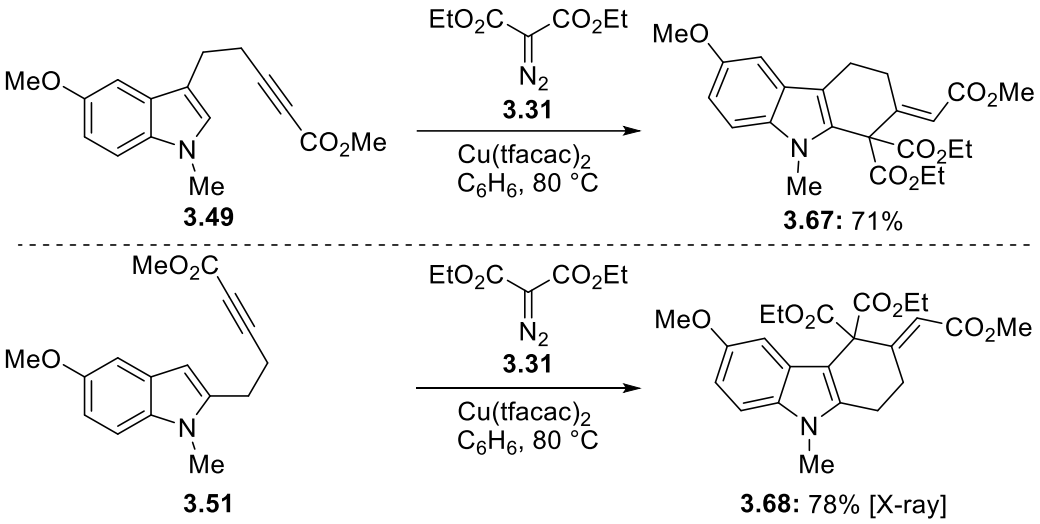

Scheme 0.16: Synthesis of tetrahydrocarbazoles **3.67** and **3.68**.

Next, we investigated the scope of the diazo coupling partner (Scheme 3.17). We explored other acceptor/acceptor α-diazocarbonyls such as **3.69** (R, R^1 = CO_2Me) and **3.70** (R = CO_2Me, R^1 = COMe), which underwent efficient stereoselective reactions with **3.31** leading to annulation products **3.71** and **3.72** in 74% and 38%, respectively. The low yield of the annulation product with **3.70** also provided a mixture of compounds that did not incorporate coupling partner **3.30**. This may suggest that the thermal instability of **3.70** is a possible cause of the low yield of the annulation product. Also, trifluoroethylester diazomalonate reagent **3.2**, which was used in the initial product, does not seem to react under these reaction conditions. Potentially, the loss of dinitrogen, from **3.72**, required to initiate the reaction is too slow under the current copper-catalyzed reaction conditions, a hypothesis that is supported by the complete recovery of both reactants **3.2** and **3.30**.

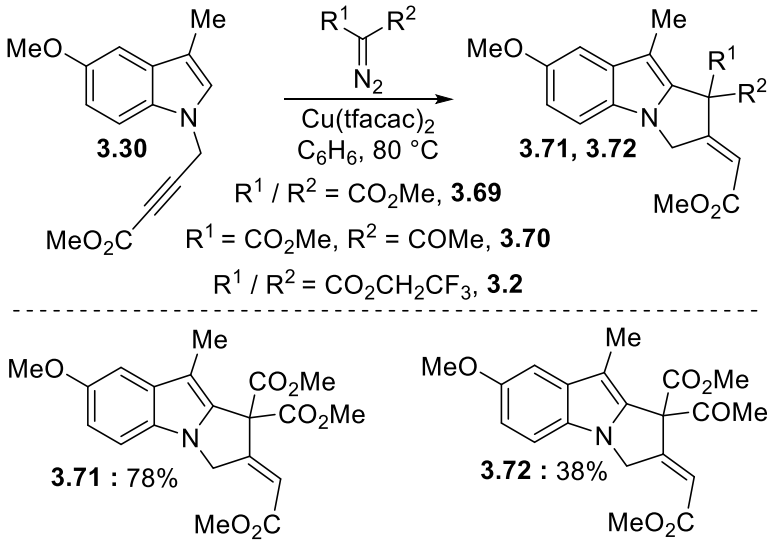

Scheme 0.17: Exploring the effect of substituents on α-diazocarbonyl compounds.

To extend the scope of the current cascade methodology, alkenyl-esters pendant to the indole nitrogen were considered viable Michael-acceptors to trap the intermediate generated from diazo insertion. To this end, synthesis of starting material **3.77** was commenced by subjecting indole **3.73** to reduction conditions using sodium cyanoborohydride in acetic acid to obtain indoline **3.74** (62%, Scheme 3.18). Next, methyl 4-iodocrotonoate, produced through the Finkelstein reaction,[11] was allowed to react with indoline **3.74** to obtain **3.76** in a 55% yield. Finally, oxidation of **3.76** with DDQ furnished *N*-alkenylester indole **3.77** in a serviceable 40% yield.

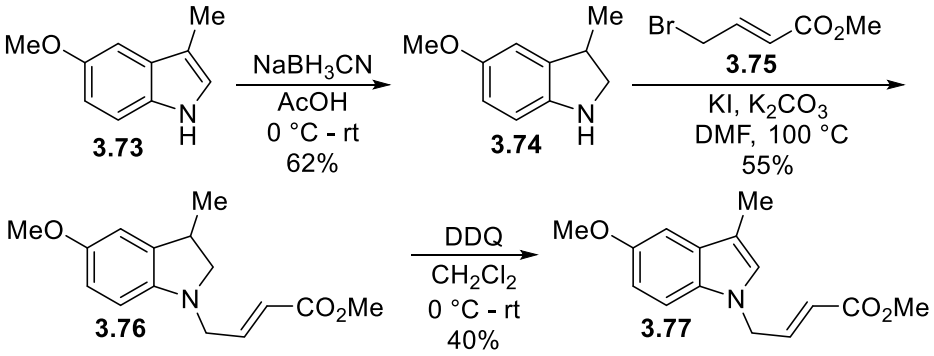

Scheme 0.18: Synthesis of alkenylester **3.82**.

Once the starting material was in hand, indole substrate **3.77** was treated with **3.31** under optimized conditions (Scheme 3.19A). However, under these reaction conditions, only trace amounts of annulation product **3.79** were observed and the carbene coupling intermediate **3.78** was identified as the major product. Inspired by the base-induced annulation work of Nemoto,[3] we envisioned that the addition of a base after the insertion event occurred, in a telescoped type process, could promote the annulation of **3.78** to provide **3.79** as the major product. Thus, we tested several bases to promote cyclization in a telescoping fashion, and cesium carbonate provided the best results. Subjecting indole substrate **3.77** and diethyl diazomalonate **3.31** to the copper catalyst conditions followed by the addition of cesium carbonate provided cyclized product **3.79** as the major product in a 41% yield (Scheme 3.19B).

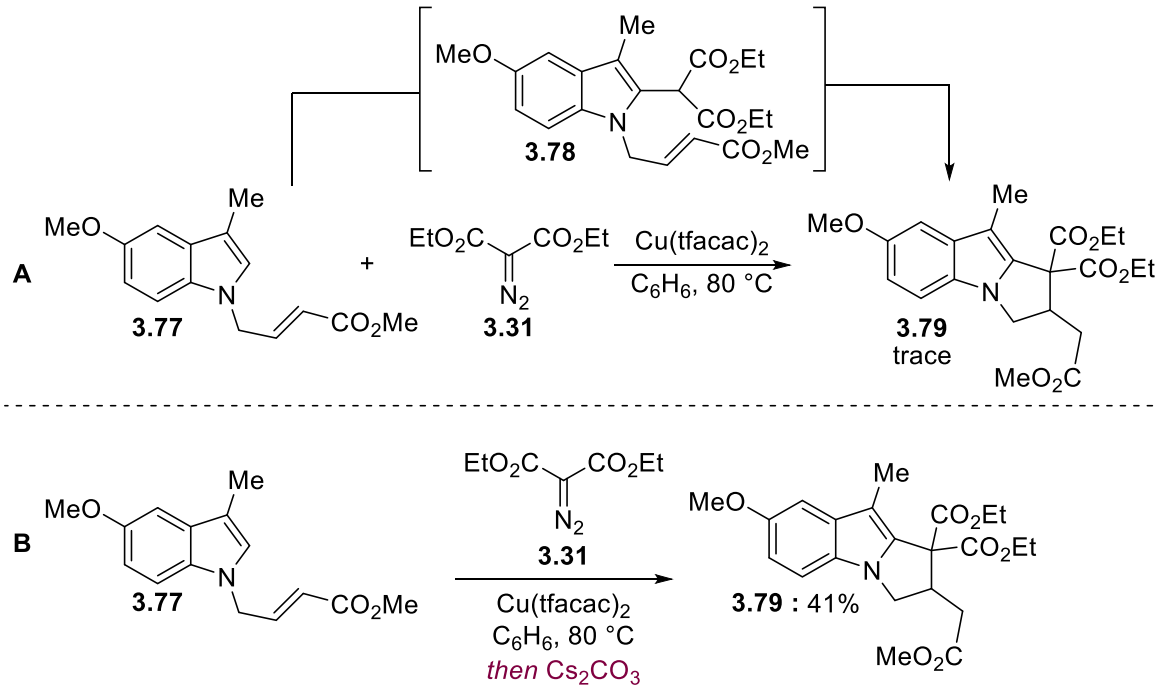

Scheme 0.19: (**A**) Attempted synthesis of **3.79** under optimized conditions (**B**) Synthesis of cyclized product **3.79** under telescoped conditions.

Finally, in a parallel approach to the alkynyl-ester examples **3.67** and **3.68** (Scheme 3.16), we decided to vary the location of the alkenyl-ester on C-2 and C-3 positions of indole (Scheme 3.20). Horner-Wadsworth-Emmons olefination of aldehydes **3.50** and **3.48** provided *α,β*-unsaturated alkenylester products **3.80** and **3.82** in 41% and 45% yields *via* path a and path b, respectively. Subjecting indoles **3.80** and **3.82** under the telescoping, copper then base, reaction conditions, tetrahydrocarbazoles **3.81** and **3.83** were produced in modest yields. It is important to note that while some cyclization can occur without a base, it proved necessary for a complete conversion to the desired carbazoles. It further demonstrates how telescoped conditions can be a valuable strategy to achieve structural complexity in a one-pot reaction.

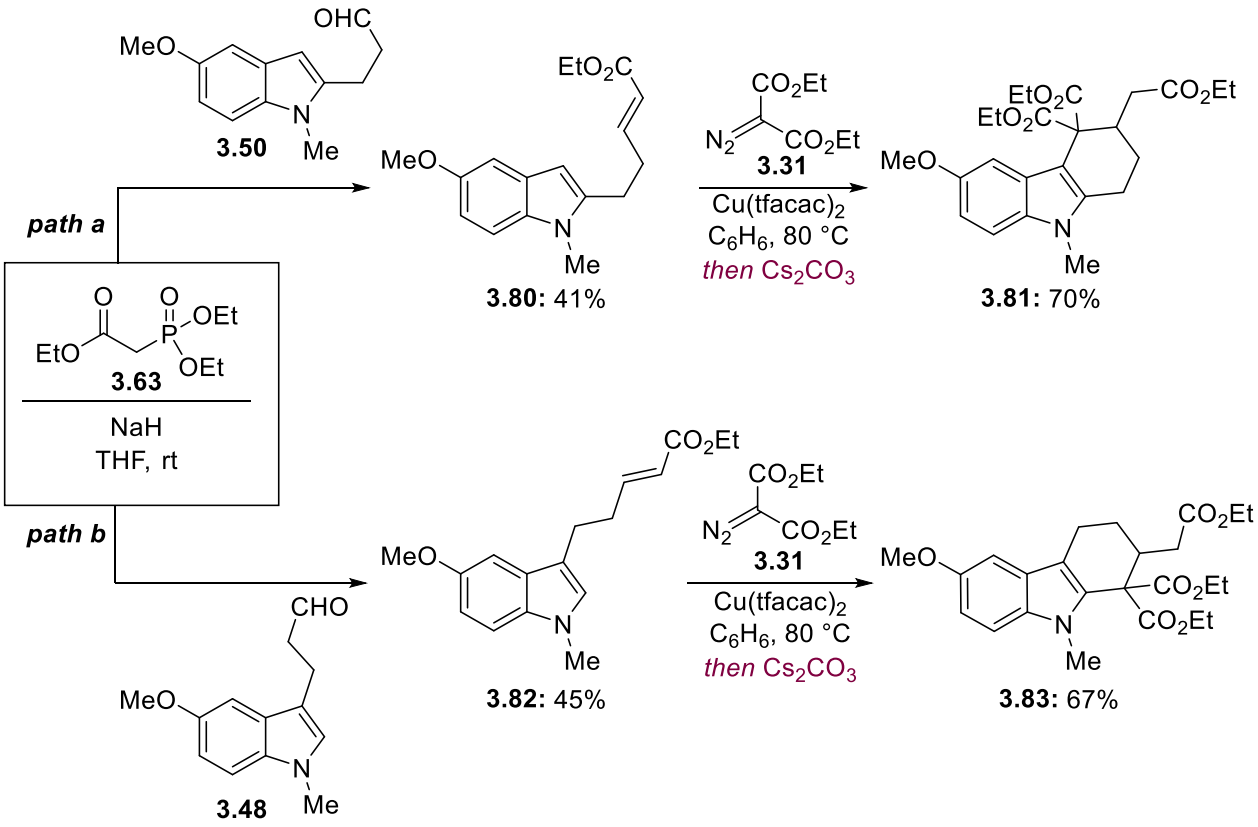

Scheme 0.20: Synthesis of tetrahydrocarbazoles **3.81** and **3.83**.

1.20.7 Summary and Future Work

In summary, using an inexpensive single catalyst system, we developed an efficient aromatic C–H functionalization/Michael annulation cascade between *α*-diazocarbonyls and appropriately functionalized indoles containing alkynyl-ester electrophiles. The method provides access to a variety of fused indole scaffolds in a stereoselective manner by varying the location of the electrophile on the indole starting in high yields. In addition, a one-pot copper carbene coupling/base-promoted annulation telescoping set of conditions was developed, which extended the electrophile scope past alkynyl-ester to furnish a series of interesting cyclized products. In the future, using a dual functional enone both as a directing group and an electrophile on indole substrate **3.84,** a C–H activation at C-2 position **3.86** will allow migratory carbene insertion of *α*-diazocarbonyl compounds **3.85**. After subsequent annulation on enone electrophile, this method has a potential for cascade synthesis of 8,9-dihydropyrido[1,2-*a*]indol-6(7*H*)-one **3.87** scaffolds. Interestingly, the dihydropyrido indole framework has a widespread presence in natural products.[12]

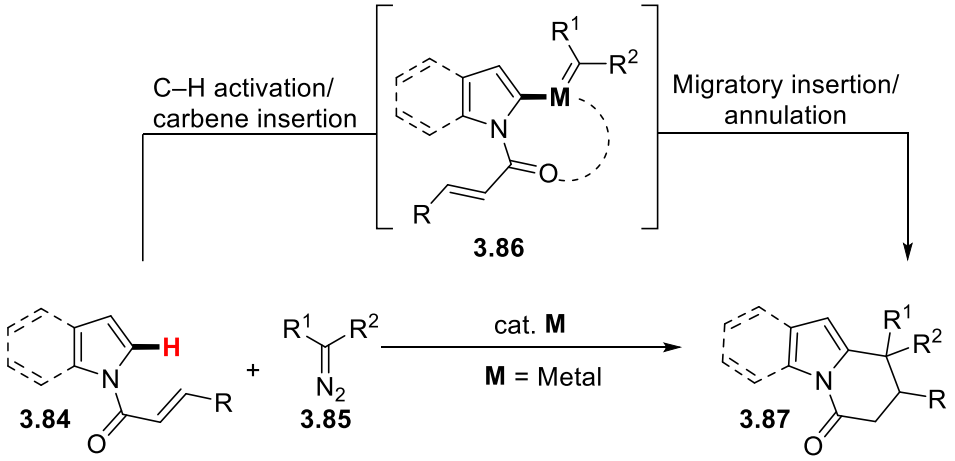

Scheme 0.21: Future outlook for the synthesis of **3.92** and using tandem C–H activation/migratory carbene insertion/Michael-addition approach.

1.21 Experimental

General Procedures

Unless stated otherwise, all reactions were performed in the oven- or flame-dried glassware under an atmosphere of dry nitrogen. Dry acetonitrile (CH_3CN), dichloromethane, and toluene were by passing these previously-degassed solvents through activated alumina columns. DMF was obtained from Sigma Aldrich SureSeal™ bottles. All other reagents were used as received from commercial sources, unless stated otherwise. A Silicon oil bath was used as the heat source for the reactions performed above room temperature. Reactions were monitored by thin layer chromatography (TLC) on Silicycle Siliaplate™ glass-backed TLC plates (250 μm thickness, 60 Å porosity, F254 indicator) and visualized by UV irradiation or development with anisaldehyde stain. Volatile solvents were removed under reduced pressure with a rotary evaporator. All flash column chromatography was performed using Silicycle SiliaFlash® F60, 230-400 mesh silica gel (40-63 μm). ^1H NMR and ^{13}C NMR spectra were recorded with Bruker AV spectrometers operating at 300 or 500 MHz for ^1H (75 or 125 MHz for ^{13}C) in chloroform-*d* ($CDCl_3$). Chemical shifts for ^1H NMR are reported relative to the signal of tetramethylsilane (TMS) at $\delta = 0$ ppm (internal standard). Chemical shifts for ^{13}C NMR are reported relative to the center line of residual solvent signal ($CDCl_3$) at $\delta = 77.16$ ppm. NMR data are reported as follows: chemical shift (multiplicity, coupling constants where applicable, number of hydrogens). Splitting is reported with the following symbols: s = singlet, bs = broad singlet, d = doublet, t = triplet, app t = apparent triplet, dd = doublet of doublets, ddd = doublet of doublet of doublets, dddd = doublet of doublet of doublet of doublets, m = multiplet. Note; unless otherwise stated, for simplicity AA'BB' systems are reported as pseudo doublets. Infrared (IR) spectra were recorded on Bruker Alpha and Bruker Tensor 27 FT-IR spectrometers. High resolution mass spectrometry (HRMS) data were

obtained using an Agilent 6200 series instrument, employing a TOF mass analyzer. Melting Points (M.P.) were obtained in open glass capillaries on an OptiMelt instrument (a digital apparatus) produced by Stanford Research Systems by scanning temperature ranges from 40 - 150 °C at a rate of 3 °C/s.

*Note: In the ^{1}H-NMR spectra of N- alkynyl-ester substituted indole starting material compounds, the methyl group at the C-3 position on the indole moiety exhibits coupling with the C-2 hydrogen, resulting in a characteristic "doublet" pattern. However, interestingly, in the reverse scenario, the C-2 hydrogen does not appear as expected "quartet", except in the case of compound **3.35**. Instead, it appears predominantly as a broad rounded "doublet" or, in some cases, as a broad rounded "singlet".*

Synthesis and Characterization of Indole Starting Materials:

Scheme 3.22: General Synthetic Scheme for the Synthesis of Alkynyl-Ester Substituted Indoles

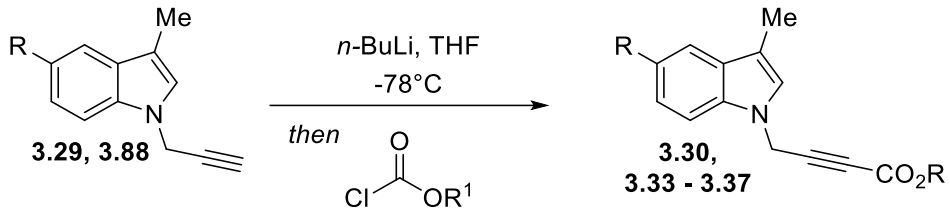

General Experimental Procedure A:

Substituted indole **3.29** (1.0 equiv) was added to a round-bottom flask equipped with a magnetic stir bar and dissolved in THF (0.2 M) under an N_2 atmosphere. The solution was cooled to −78 °C on acetone/dry ice cooling bath, and *n*-BuLi (2.5 M in hexanes, 1.5 equiv) was slowly added dropwise using a syringe on the side of round-bottom flask. The resulting reaction mixture was stirred for 30 min at the same temperature, before dropwise addition of the desired

chloroformate (1.5 equiv) at −78 °C. The reaction mixture was stirred for another 1.5 h, during which temperature reached –20 °C. The reaction was quenched with sat. aq. NH_4Cl and allowed to warm to room temperature. The mixture was extracted twice with Et_2O. The organic layers were then combined and washed with water, then brine, and then dried over $MgSO_4$. The solution was concentrated *in vacuo*, and the resulting crude material was purified by flash chromatography to yield **3.30, 3.33 - 3.37**.

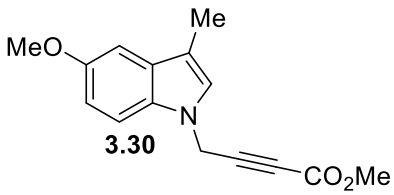

3.30 was prepared using General Experimental Procedure A. Reagents employed: 5-methoxy-*N*-propargylskatole **3.29** (1.60 g, 8.03 mmol), *n*-BuLi (4.81 mL, 12.1 mmol), Methyl chloroformate (0.930 mL, 12.1 mmol). **3.30** (1.30 g, 5.05 mmol, 63%) was obtained as a thick light brown color oil: R_f = 0.30, 20% EtOAc in hexanes; ^{1}H NMR (500 MHz, $CDCl_3$) δ = 7.20 (d, *J* = 8.8 Hz, 1H), 7.00 (d, *J* = 2.4 Hz, 1H), 6.91 (dd, *J* = 8.8, 2.4 Hz, 1H), 6.88 (s, 1H), 4.90 (s, 2H), 3.87 (s, 3H), 3.74 (s, 3H), 2.28 (s, 2H) ppm; ^{13}C NMR (75 MHz, $CDCl_3$) δ = 153.9, 153.8, 131.1, 129.4, 125.9, 111.9, 110.7, 109.6, 101.1, 85.8, 75.9 55.9, 52.7, 20.7, 9.6 ppm; IR (neat): ν_{max} = 2951, 2836, 2240, 1711, 1485, 1389, 1250, 1224, 1039, 748 cm^{-1}; HRMS (APPI+): calc'd for $C_{15}H_{16}NO_3$ $[M+H]^+$ 258.1125, found 258.1124.

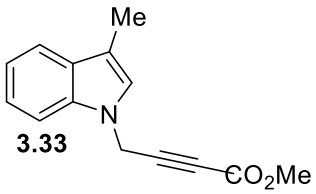

3.33 was prepared using General Experimental Procedure A. Reagents employed: *N*-propargylskatole **3.88** (0.800 g, 4.73 mmol), *n*-BuLi (2.80 mL, 7.10 mmol), Methyl chloroformate (0.550 mL, 7.10 mmol). **3.33** (579 mg, 2.55 mmol, 54%) was obtained as thick light brown color oil: R_f = 0.35, 20% EtOAc in hexanes; ^{1}H NMR (300 MHz, $CDCl_3$) δ = 7.57 (dt, *J* = 7.7, 1.0 Hz, 1H), 7.32 – 7.22 (m, 2H), 7.17 – 7.12 (m, 1H), 6.89 (d, *J* = 1.2 Hz, 1H), 4.91 (s, 2H), 3.73 (s, 3H), 2.31 (d, *J* = 1.1 Hz, 3H) ppm; ^{13}C NMR (75 MHz, $CDCl_3$) δ = 153.5, 136.3, 129.4, 124.8, 122.3, 119.6, 119.4, 112.2, 109.0,

81.8, 76.2, 53.0, 35.5, 9.7 ppm; IR (neat): ν_{max} = 2919, 2241, 1711, 1462, 1250, 1034, 879, 738 cm^{-1}; HRMS (APPI+): calc'd for $C_{14}H_{13}NO_2$ $[M]^+$ 227.0946, found 227.0948.

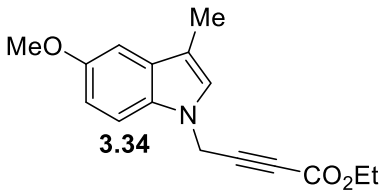

3.34

3.34 was prepared using General Experimental Procedure A. Reagents employed: 5-methoxy-*N*-propargylskatole **3.29** (0.500 g, 2.51 mmol), *n*-BuLi (1.50 mL, 3.76 mmol), ethyl chloroformate (0.360 mL, 3.76 mmol). **3.34** (339 mg, 1.25 mmol, 50%) was obtained as a thick light brown oil: R_f = 0.46, 25% EtOAc in hexanes; ^{1}H NMR (300 MHz, $CDCl_3$) δ = 7.22 (dd, *J* = 8.8, 0.6 Hz, 1H,), 7.00 (dd, *J* = 2.5, 0.6 Hz, 1H), 6.94 – 6.90 (m, 1H), 6.89 (s, 1H), 4.91 (s, 2H), 4.21 (q, *J* = 7.1 Hz, 2H), 3.87 (s, 3H), 2.29 (d, *J* = 1.1 Hz, 3H), 1.28 (t, *J* = 7.2 Hz, 3H) ppm; ^{13}C NMR (75 MHz, $CDCl_3$) δ = 154.3, 153.2, 131.6, 129.8, 125.7, 112.3, 111.7, 109.9, 101.4, 81.4, 76.5, 62.4, 56.1, 35.7, 14.1, 9.8 ppm; IR (neat): ν_{max} = 2926, 2239, 1707, 1486, 1248, 1179, 1040, 749 cm^{-1}; HRMS (APPI+): calc'd for $C_{16}H_{18}NO_3$ $[M+H]^+$ 272.1278, found 272.1273.

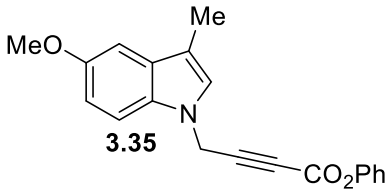

3.35

3.35 was prepared using General Experimental Procedure A. Reagents employed: 5-methoxy-*N*-propargylskatole **3.29** (0.500 g, 2.51 mmol), *n*-BuLi (1.50 mL, 3.77 mmol), Phenyl chloroformate (0.475 mL, 3.77 mmol). **3.35** (402 mg, 1.26 mmol, 50%) was obtained as a thick light brown oil: R_f = 0.40, 20% EtOAc in hexanes; ^{1}H NMR (300 MHz, $CDCl_3$) δ = 7.35 (td, *J* = 7.8, 1.8 Hz, 2H), 7.28 – 7.16 (m, 2H), 7.08 (dt, *J* = 8.1, 1.5 Hz, 2H), 7.01 (q, *J* = 1.7 Hz, 1H), 6.92 (dt, *J* = 8.8, 2.3 Hz, 1H), 6.87 (d, *J* = 1.4 Hz, 1H), 4.93 (d, *J* = 2.1 Hz, 2H), 3.86 (d, *J* = 1.6 Hz, 3H), 2.32 – 2.22 (m, 3H) ppm; ^{13}C NMR (75 MHz, $CDCl_3$) δ = 154.3, 151.4, 149.9, 131.5, 129.8, 129.7, 126.6, 125.6, 121.4, 112.4, 111.9, 109.9, 101.4, 84.1, 75.9, 56.0, 35.7, 9.7 ppm; IR (neat): ν_{max} = 2923, 2231, 1729, 1486, 1223, 1183, 999, 743, 687 cm^{-1}; HRMS (APPI+): calc'd for $C_{20}H_{17}NO_3$ $[M]^+$ 319.1208, found 319.1209.

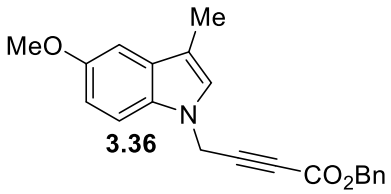

3.36 was prepared using General Experimental Procedure A. Reagents employed: 5-methoxy *N*-propargylskatole **3.29** (0.500 g, 2.51 mmol), *n*-BuLi (1.50 mL, 3.77 mmol), benzyl chloroformate (0.538 mL, 3.77 mmol). **3.36** (451 mg, 1.35 mmol, 54%) was obtained as a thick light brown oil: R_f = 0.40, 25% EtOAc in hexanes; ^{1}H NMR (300 MHz, $CDCl_3$) δ = 7.39 – 7.31 (m, 5H), 7.18 (d, *J* = 8.8 Hz, 1H), 6.99 (d, *J* = 2.4 Hz, 1H), 6.89 (dd, *J* = 8.8, 2.4 Hz, 1H), 6.85 (d, *J* = 1.2 Hz, 1H), 5.15 (s, 2H), 4.87 (s, 2H), 3.86 (s, 3H), 2.27 (d, *J* = 1.1 Hz, 3H) ppm; ^{13}C NMR (75 MHz, $CDCl_3$) δ = 154.3, 153.0, 134.7, 131.5, 129.7, 128.80, 128.77, 128.7, 125.6, 112.3, 111.7, 109.9, 101.4, 82.1, 76.2, 68.0, 56.1, 35.7, 9.7 ppm; IR (neat): ν_{max} = 2921, 2238, 1707, 1486, 1453, 1226, 1039, 835, 697 cm^{-1}; HRMS (APPI+): calc'd for $C_{21}H_{19}NO_3$ $[M]^+$ 333.1365, found 333.1368.

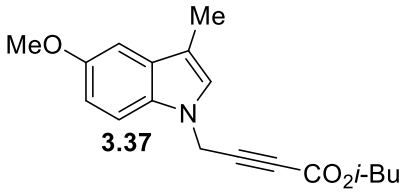

3.37 was prepared using General Experimental Procedure A. Reagents employed: 5-methoxy-*N*-propargylskatole **3.29** (0.500 g, 2.51 mmol), *n*-BuLi (1.50 mL, 3.77 mmol), benzyl chloroformate (0.492 mL, 3.76 mmol). **3.37** (421 mg, 1.41 mmol, 56%) was obtained as a thick brown oil: R_f = 0.40, 40% DCM in hexanes; ^{1}H NMR (300 MHz, $CDCl_3$) δ = 7.20 (d, *J* = 8.8 Hz, 1H), 7.00 (d, *J* = 2.4 Hz, 1H), 6.90 (dd, *J* = 8.8, 2.5 Hz, 1H), 6.86 (d, *J* = 1.2 Hz, 1H), 4.86 (s, 2H), 3.92 (d, *J* = 6.7 Hz, 2H), 3.86 (s, 3H), 2.27 (d, *J* = 1.1 Hz, 3H), 1.93 (dt, *J* = 13.4, 6.7 Hz, 1H), 0.91 (d, *J* = 6.7 Hz, 6H) ppm; ^{13}C NMR (75 MHz, $CDCl_3$) δ = 154.3, 153.3, 131.6, 129.7, 125.7, 112.3, 111.7, 109.9, 101.4, 81.5, 76.5, 72.3, 56.1, 35.7, 27.7, 19.1, 9.7 ppm; IR (neat): ν_{max} = 2962, 2240, 1707, 1487, 1248, 749 cm^{-1}; HRMS (APPI+): calc'd for $C_{18}H_{21}NO_3$ $[M]^+$ 299.1521, found 299.1520.

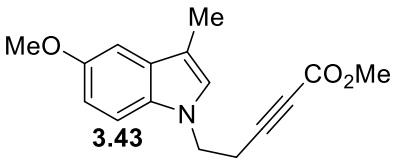

3.43

3.43 was prepared using General Experimental Procedure A. Reagents employed: Substituted indole **3.89** (0.730 g, 3.42 mmol), *n*-BuLi (2.05 mL, 5.13 mmol), Methyl chloroformate (0.396 mL, 5.13 mmol). **3.43** (586 mg, 2.16 mmol, 63%) was obtained as thick light brown color oil: R_f = 0.35, 20% EtOAc in hexanes; ^{1}H NMR (300 MHz, $CDCl_3$) δ = 7.14 (d, *J* = 8.8 Hz, 1H), 6.99 (d, *J* = 2.4 Hz, 1H), 6.86 (dd, *J* = 8.8, 2.4 Hz, 1H), 6.82 (d, *J* = 1.3 Hz, 1H), 4.20 (t, *J* = 7.1 Hz, 2H), 3.85 (s, 3H), 3.74 (s, 3H), 2.70 (t, *J* = 7.1 Hz, 2H), 2.26 (t, *J* = 1.4 Hz, 3H) ppm; ^{13}C NMR (75 MHz, $CDCl_3$) δ = 153.9, 153.8, 131.1, 129.4, 125.9, 111.9, 110.7, 109.6, 101.1, 85.8, 74.7, 55.9, 52.7, 44.1, 20.7, 9.6 ppm; IR (neat): ν_{max} = 3398, 2916, 2235, 1712, 1491, 1435, 1234, 1071, 1046, 896, 792 cm^{-1}; HRMS (APPI+) calc'd for $C_{16}H_{18}NO_3$ $[M+H]^+$ 272.1278, found 272.1283.

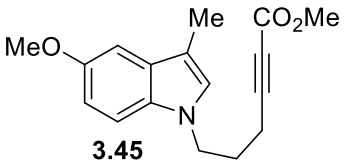

3.45

3.45 was prepared using General Experimental Procedure A. Reagents employed: substituted indole **3.90** (0.357 g, 1.57 mmol), *n*-BuLi (1.00 mL, 2.35 mmol), Methyl chloroformate (183 uL, 2.36 mmol). **3.45** (313 mg, 1.10 mmol, 70%) was obtained as thick light brown color oil: R_f = 0.25, 20% Et_2O in hexanes; ^{1}H NMR (300 MHz, $CDCl_3$) δ = 7.18 (d, *J* = 8.8 Hz, 1H), 6.99 (d, *J* = 2.4 Hz, 1H), 6.88 – 6.83 (m, 2H), 4.14 (t, *J* = 6.5 Hz, 2H), 3.86 (s, 3H), 3.77 (s, 3H), 2.28 (d, *J* = 1.1 Hz, 3H), 2.23 (t, *J* = 6.9 Hz, 2H), 2.04 (q, *J* = 6.6 Hz, 2H) ppm; ^{13}C NMR (75 MHz, $CDCl_3$) δ = 154.1, 153.8, 131.5, 129.2, 126.2, 111.9, 110.2, 109.9, 101.0, 88.1, 73.9, 56.0, 52.8, 44.5, 28.1, 16.1, 9.7 ppm; IR (neat): ν_{max} = 2923, 1730, 1449, 1217, 1033, 796 cm^{-1};

*Note: **3.89** and **3.90** were synthesized using the same procedure as described in chapter 2 (Scheme 2.20).*

Scheme 3.23: Synthesis of Indole Starting Material **3.1**

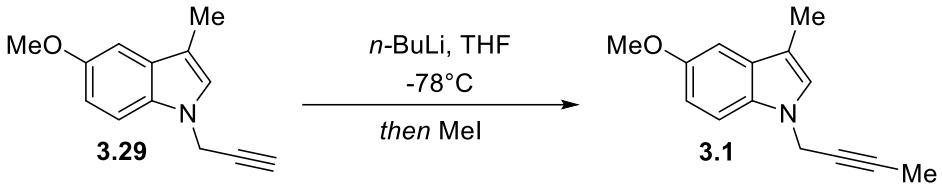

3.1 was prepared by the following procedure: Substituted indole **3.29** (0.400 g, 2.01 mmol) was added to a round-bottom flask equipped with a magnetic stir bar and dissolved in THF (0.2 M) under an N_2 atmosphere. The solution was cooled to −78 °C on acetone/dry ice cooling bath, and *n*-BuLi (2.5 M in hexanes, 1.20 mL, 3.01 mmol) was added dropwise using a syringe. The resulting reaction mixture was stirred for 30 min at the same temperature, before dropwise addition of the iodomethane (0.187 mL, 3.01 mmol) at −78 °C. The resulting reaction mixture was stirred for another 1.5 h, during which temperature reached to −20 °C. The reaction was quenched with sat. aq. NH_4Cl at and then allowed to warm to room temperature. The mixture was extracted twice with Et_2O. The organic layers were combined, washed with water, brine, and dried over $MgSO_4$. The solution was concentrated *in vacuo*, and the resulting crude material was purified by flash chromatography to yield **3.1** (279 mg, 1.31 mmol, 65%) as a light brown oil R_f = 0.35, 20% EtOAc in hexanes; ^{1}H NMR (500 MHz, $CDCl_3$) δ = 7.25 (s, 1H), 7.00 (d, *J* = 2.4 Hz, 1H), 6.95 (s, 1H), 6.88 (dd, *J* = 8.8, 2.4 Hz, 1H), 4.72 (d, *J* = 2.4 Hz, 2H), 3.87 (s, 3H), 2.29 (d, *J* = 0.8 Hz, 3H), 1.81 (t, *J* = 2.4 Hz, 3H) ppm; ^{13}C NMR (75 MHz, $CDCl_3$) δ = 154.0, 131.6, 129.5, 125.8, 111.9, 110.5, 110.2, 101.2, 81.0, 73.7, 56.1, 36.2, 9.8, 3.7 ppm; IR (neat): ν_{max} = 2918, 1489, 1443, 1220, 1035, 890, 779 cm^{-1}; HRMS (APPI+): calc'd for $C_{14}H_{16}NO$ $[M+H]^+$ 214.1224, found 214.1233.

Scheme 3.24: Synthesis of Indole Starting Material **3.51**

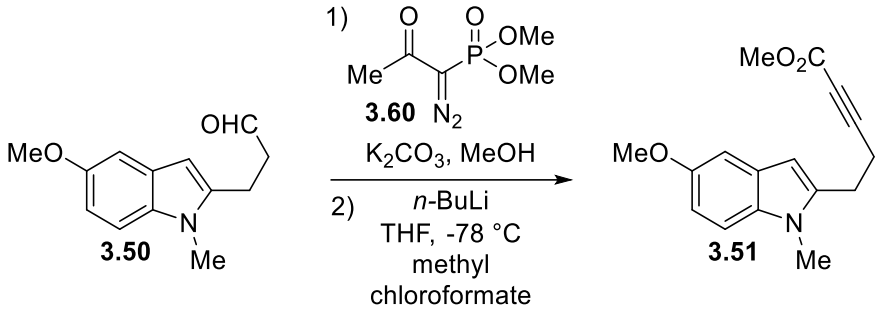

3.51 was prepared by the following two-step procedure:

Step 1:

To a suspension of aldehyde **3.50** (370 mg, 1.70 mmol, 1.0 equiv) and dimethyl (1-diazo-2-oxopropyl)phosphonate **3.60** (490 mg, 2.55 mmol, 1.5 equiv) in MeOH–THF (1:1, 9 mL) was added K_2CO_3 (352 mg, 2.55 mmol, 1.5 equiv) and the reaction mixture under N_2 atmosphere was stirred at r.t. for 12 h. Upon completion, the reaction mixture was concentrated *in vacuo* and the residue was purified by column chromatography (10-12 % EtOAc in hexanes) to give intermediate alkyne **3.66** (272 mg, 1.28 mmol) as a white fluffy solid in 75% yield, which was used directly in the next step.

Step 2: To a solution of the alkyne, **3.66** (192 mg, 0.900 mmol, 1.0 equiv) in THF (4.5 mL) was slowly added *n*-BuLi (0.800 mL, 1.35 mmol, 1.5 equiv) at −78 °C under the N_2 atmosphere. The resulting reaction mixture was stirred for 30 min at the same temperature before the dropwise addition of methyl chloroformate (104 uL, 1.35 mmol, 1.5 equiv) at −78 °C. The reaction mixture was then allowed to stir for another 1.5 h, during which temperature reached −20 °C. The reaction was quenched with sat. aq. NH_4Cl and allowed to warm to room temperature. The mixture was extracted with Et_2O, washed with brine, and then dried over $MgSO_4$ and

concentrated *in vacuo* to yield a crude reaction mixture. The resulting material was purified by column chromatography (12-18% EtOAc in hexanes) to obtain **3.51** (209 mg, 0.770 mmol) as light green foam in 86% yield. R_f = 0.35, 20% Et_2O in hexanes; ^1H NMR (300 MHz, $CDCl_3$) δ = 7.16 (d, *J* = 8.8 Hz, 1H), 7.02 (d, *J* = 2.4 Hz, 1H), 6.84 (dd, *J* = 8.8, 2.5 Hz, 1H), 6.26 – 6.20 (m, 1H), 3.84 (s, 3H), 3.76 (s, 3H), 3.65 (s, 3H), 3.08 – 2.97 (m, 2H), 2.88 – 2.63 (m, 2H) ppm; ^{13}C NMR (75 MHz, $CDCl_3$) δ = 154.2, 154.2, 138.8, 132.9, 128.0, 111.3, 109.7, 102.2, 99.0, 88.2, 73.7, 56.0, 52.8, 29.8, 25.4, 18.6 ppm; IR (neat): ν_{max} = 2924, 2235, 1742, 1488, 1253, 1215, 1069, 776 cm^{-1}; HRMS (APPI+): calc'd for $C_{16}H_{18}NO_3$ $[M+H]^+$ 272.1278, found 272.1300.

Scheme 3.25: Synthesis of Indole Starting Material **3.49**

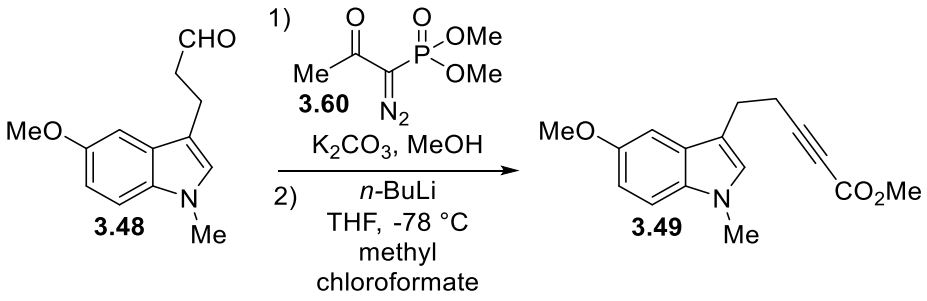

3.49 was prepared by the following two-step procedure:

Step 1:

To a suspension of aldehyde **3.48** (500 mg, 2.30 mmol, 1.0 equiv) and dimethyl (1-diazo-2-oxopropyl)phosphonate **3.60** (477 mg, 3.45 mmol, 1.5 equiv) in MeOH–THF (1:1, 12 mL) was added K_2CO_3 (633 mg, 3.45 mmol, 1.5 equiv) and the reaction mixture under N_2 atmosphere was stirred at r.t. for 12 h. Upon completion, the reaction mixture was concentrated *in vacuo* and purified by column chromatography (8-10 % EtOAc in hexanes) to give intermediate alkyne **3.61** (374 mg, 1.75 mmol) as a thick greenish oil in 76% yield and was used in the next step.

Step 2: To a solution of the alkyne **3.61** (374 mg, 1.75 mmol, 1.0 equiv) in THF (9 mL) was slowly added *n*-BuLi (1.00 mL, 2.63 mmol, 1.5 equiv) at −78 °C under the N_2 atmosphere. The resulting reaction mixture was stirred for 30 min at the same temperature before the dropwise addition of Methyl chloroformate (204 uL, 2.63 mmol, 1.5 equiv) at −78 °C. The reaction mixture was then allowed to stir for another 1.5 h, during which temperature reached -20 °C. The reaction was quenched with sat. aq. NH_4Cl and allowed to warm to room temperature. The mixture was extracted with Et_2O, washed with brine, and then dried over $MgSO_4$ and concentrated *in vacuo* to yield a crude reaction mixture. The resulting material was purified by column chromatography (10-15% EtOAc in hexanes) to obtain **3.49** (408 mg, 1.50 mmol) as a white solid in 86% yield. R_f = 0.35, 20% Et_2O in hexanes; M.P. = 125-128 °C ^{1}H NMR (300 MHz, $CDCl_3$) δ = 7.18 (d, *J* = 8.8 Hz, 1H), 6.99 (d, *J* = 2.4 Hz, 1H), 6.94 – 6.85 (m, 2H), 3.87 (s, 3H), 3.76 (s, 3H), 3.72 (s, 3H), 3.02 (t, *J* = 7.5 Hz, 2H), 2.68 (t, *J* = 7.5 Hz, 2H) ppm; ^{13}C NMR (75 MHz, $CDCl_3$) δ = 154.4, 153.9, 132.5, 127.7, 127.2, 112.2, 112.1, 110.2, 100.6, 89.9, 73.4, 56.1, 52.7, 32.9, 23.8, 20.4 ppm; IR (neat): ν_{max} = 2925, 2334, 1749, 1494, 1255, 1033, 787 cm^{-1}; HRMS (APPI+): calc'd for $C_{16}H_{18}NO_3$ $[M+H]^+$ 272.1278, found 272.1297.

Scheme 3.26: Synthesis of Indole Starting Material **3.77**

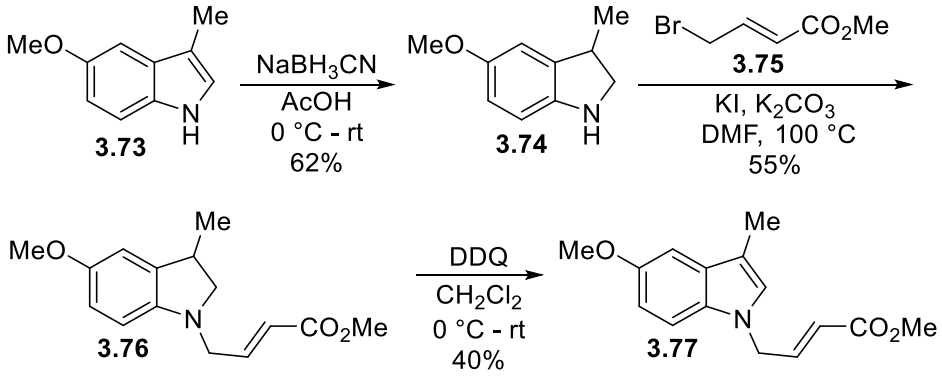

3.77 was prepared by the following three-step procedure:

Step 1: To a stirred solution of **3.73** (1.2 g, 7.4 mmol, 1.0 equiv) in acetic acid (30 mL) was added $NaBH_3CN$ (1.20 g, 18.5 mmol, 2.5 equiv) at 0 °C. The reaction was allowed to stir at room temperature for 4 h. The reaction mixture was diluted with H_2O, brought to pH ~9 with NaOH pellets and extracted with EtOAc (3 x 50 mL). The combined organic layers were washed with H_2O, brine, dried over $MgSO_4$, filtered, and concentrated under reduced pressure. The crude product was purified by flash column chromatography (18-20 % EtOAc in hexanes) to obtain **3.74** (745 mg, 4.56 mmol) as light-yellow color oil in 62% yield.

Step 2: Methyl 4-bromocrotonate **3.75** (643 uL, 5.47 mmol, 1.2 equiv) was added to a solution of KI (908 mg, 5.47 mmol, 1.2 equiv) in DMF (1 mL/mmol of KI) under an N_2 atmosphere. The solution was heated to 100 °C for 30 min then cooled to room temperature. K_2CO_3 (945 mg, 6.84 mmol, 1.5 equiv) was then added to the reaction mixture, followed by solution of **3.74** (745 mg, 4.56 mmol, 1.0 equiv) in DMF (0.4 mL/mmol). The reaction mixture was then heated to 100 °C for ~12 h (overnight), then cooled to room temperature, and H_2O was added. The mixture was extracted three times with diethyl ether, washed with brine, dried over anhydrous $MgSO_4$, and concentrated *in vacuo*. The resulting residue was passed through a short silica gel plug using 2% EtOAc in hexanes as eluent and **3.76** (661 mg, 2.53 mmol) was obtained as a brown oil in 55% yield.

Step 3: DDQ (651 mg, 2.87 mmol, 1.5 equiv) was added to a solution of **3.76** (0.500 g, 1.91 mmol, 1.0 equiv) in CH_2Cl_2 (10 mL) at 0 °C. The reaction mixture was stirred for 2 h at room temperature. When the reaction was considered complete as determined by TLC analysis, the mixture was filtered through a pad of Celite® and washed with CH_2Cl_2. The resulting liquid was concentrated *in vacuo,* and the corresponding residue was purified by silica gel flash column

chromatography (8-10 % EtOAc in hexanes) to give **3.77** (198 mg, 0.764 mmol) as thick brown color oil in 40% yield. R_f = 0.54, 25% EtOAc in hexanes; ^{1}H NMR (300 MHz, $CDCl_3$) δ = 7.08 – 6.98 (m, 3H), 6.85 (dd, *J* = 8.9, 2.4 Hz, 1H), 6.80 – 6.78 (m, 1H), 5.58 (dt, *J* = 15.6, 2.0 Hz, 1H), 4.76 (dd, *J* = 4.6, 2.0 Hz, 2H), 3.87 (s, 3H), 3.67 (s, 3H), 2.29 (d, *J* = 1.1 Hz, 3H) ppm; ^{13}C NMR (75 MHz, $CDCl_3$) δ = 166.4, 154.0, 143.8, 131.7, 129.3, 126.2, 122.0, 112.1, 111.0, 110.0, 101.1, 56.0, 51.7, 47.0, 9.8 ppm; IR (neat): ν_{max} = 2928, 2238, 1723, 1488, 1274, 1226, 1042, 784 cm^{-1}; HRMS (APPI+): calc'd for $C_{15}H_{18}NO_3$ $[M+H]^+$ 260.1278, found 260.1295.

Scheme 3.27: Synthesis of Indole Starting Material **3.80**

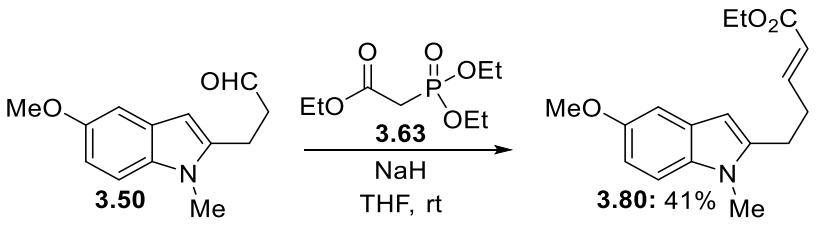

3.80 was prepared by the following procedure:

To a solution of triethyl phosphonoacetate reagent **3.63** (386 mg, 1.72 mmol, 1.2 equiv) in THF (9 mL) was added NaH (740 mg, 1.86 mmol, 1.3 equiv) in one portion at 0 ºC. The reaction was then stirred for 30 min at the same temperature before adding a solution of **3.50** (311 mg, 1.43 mmol, 1.0 equiv) in THF. The mixture was stirred at room temperature for another 2 h before quenching with water. The mixture was extracted with EtOAc (×2). The organic layers were combined, washed with brine, dried over $MgSO_4$, and concentrated *in vacuo*. The residue was purified by a flash column chromatography (8-10 % EtOAc in hexanes) to afford **3.80** (169 mg, 0.588 mmol, 41%) as light brown solid: R_f = 0.30, 20% EtOAc in hexanes; M.P. = 68-70 °C ^{1}H NMR (300 MHz, $CDCl_3$) δ = 7.11 (d, *J* = 8.8 Hz, 1H), 7.08 – 6.98 (m, 2H), 6.80 (dd, *J* = 8.8, 2.5 Hz, 1H), 6.16 (d, *J* = 1.0 Hz, 1H), 5.90 (dt, *J* = 15.6, 1.6 Hz, 1H), 4.17 (q, *J* = 7.1 Hz, 2H), 3.80 (s,

3H), 3.55 (s, 3H), 2.83 – 2.78 (m, 2H), 2.63 – 2.54 (m, 2H), 1.27 (t, *J* = 7.1 Hz, 3H) ppm; ^{13}C NMR (75 MHz, $CDCl_3$) δ = 166.4, 154.0, 147.5, 140.0, 132.7, 128.0, 122.2, 110.7, 109.4, 102.0, 98.6, 60.3, 55.9, 30.9, 29.5, 25.4, 14.3 ppm; IR (neat): ν_{max} = 2981, 1726, 1486, 1257, 1188, 1153, 1071, 746 cm^{-1}; HRMS (APPI+): calc'd for $C_{17}H_{22}NO_3$ $[M+H]^+$ 288.1591, found 288.1605.

Scheme 3.28: Synthesis of Indole Starting Material **3.82**

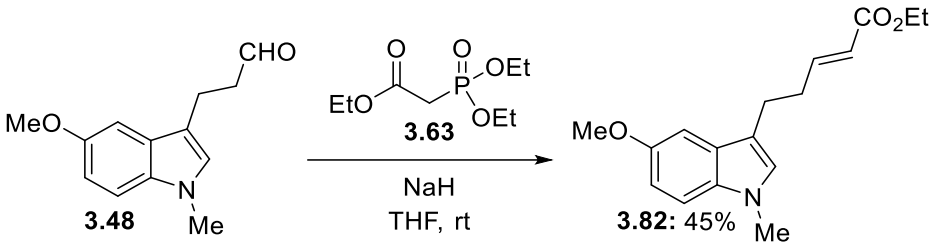

3.82 was prepared by the following procedure:

To a solution of triethyl phosphonoacetate reagent **3.63** (682 mg, 3.04 mmol, 1.2 equiv) in THF (15 mL) was added NaH (132 mg, 3.29 mmol, 1.3 equiv) in one portion at 0 ºC. The reaction was then stirred for 30 min at the same temperature before the adding a solution of **3.48** (550 mg, 2.53 mmol, 1.0 equiv) in THF. The mixture was stirred at room temperature for another 2 h before quenching with water. The mixture was extracted with EtOAc (×2). The organic layers were combined, washed with brine, dried over $MgSO_4$, and concentrated *in vacuo*. The residue was purified by a flash column chromatography (8-10 % EtOAc in hexanes) to afford **3.82** (327 mg, 1.14 mmol, 45%) as light brown solid: R_f = 0.30, 20% EtOAc in hexanes; M.P. = 47-49 °C ^{1}H NMR (300 MHz, $CDCl_3$) δ = 7.18 (d, *J* = 8.8 Hz, 1H), 7.08 (dt, *J* = 15.6, 6.8 Hz, 1H), 6.99 (d, *J* = 2.4 Hz, 1H), 6.89 (dd, *J* = 8.8, 2.4 Hz, 1H), 6.82 (s, 1H), 5.89 (dt, *J* = 15.7, 1.6 Hz, 1H), 4.19 (q, *J* = 7.1 Hz, 2H), 3.87 (s, 3H), 3.71 (s, 3H), 2.88 (dd, *J* = 8.6, 6.5 Hz, 2H), 2.64 – 2.56 (m, 2H), 1.28 (t, *J* = 7.1 Hz, 3H) ppm; ^{13}C NMR (75 MHz, $CDCl_3$) δ = 166.8, 153.8, 149.0, 132.6, 128.0, 126.9,

121.7, 113.2, 111.9, 110.1, 100.9, 60.3, 56.1, 32.9, 32.9, 23.9, 14.4 ppm; IR (neat): ν_{max} = 2920, 1708, 1649, 1492, 1175, 1032, 857, 799 cm^{-1}; HRMS (APPI+): calc'd for $C_{17}H_{22}NO_3$ $[M+H]^+$ 288.1591, found 288.1606.

Synthesis and Characterization of Annulation Products:

Scheme 3.29: Copper-Catalyzed Cascade Reaction with *α*-Diazo Carbonyl Compounds

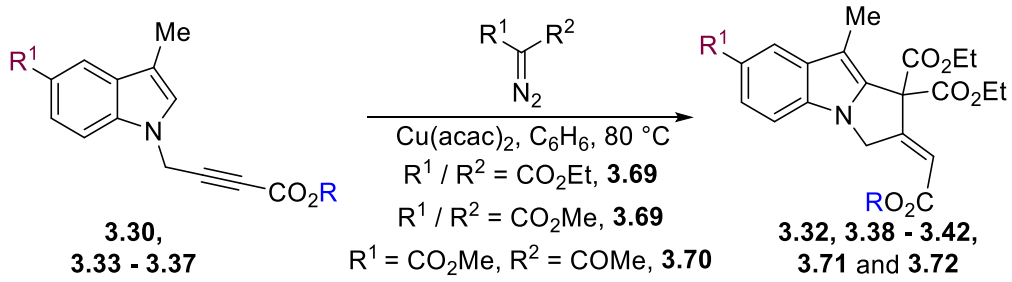

Scheme 3.30: Synthesis of Tetrahydrocarbazole **3.68** *via* a Copper-Catalyzed Cascade Reaction

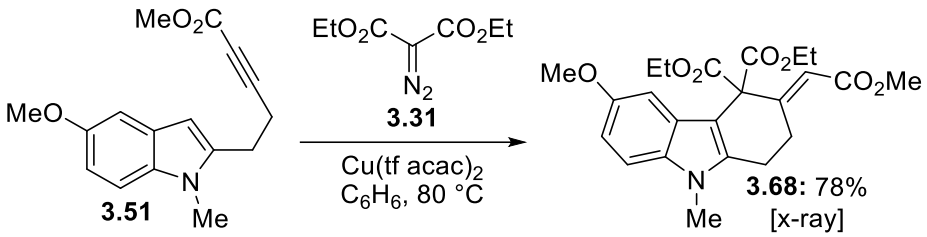

Scheme 3.31: Synthesis of Tetrahydrocarbazole **3.67** *via* a Copper-Catalyzed Cascade Reaction

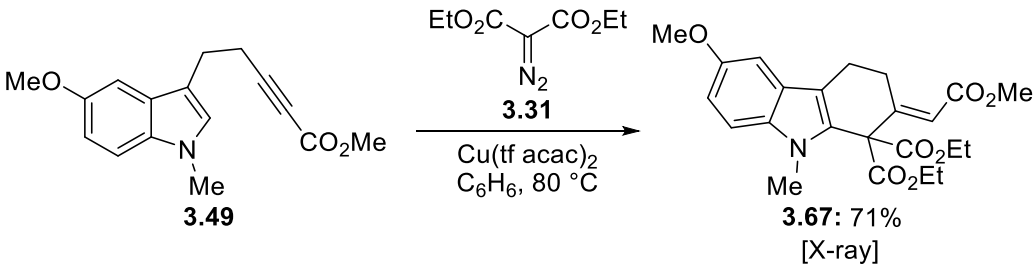

General Experimental Procedure B:

Indole starting material (**3.30**, **3.33 – 3.37**, **3.51**, **3.49**, 1.2 equiv) was added to a reaction vessel equipped with a stir bar, and the vessel was then evacuated and backfilled with N_2. This cycle was repeated two additional times, followed by the addition of benzene (5 mL/mmol of indole) under an N_2 atmosphere. $Cu(tfacac)_2$ (5 mol %) was then added to the reaction vessel, and again, the vessel was evacuated (quickly) and backfilled with N_2. Diazo reagent **3.31**, **3.69**, **3.70** (1.0 equiv) was added to a separate reaction vessel, and the vessel was then evacuated and backfilled with N_2. This cycle was repeated two additional times. The diazo reagent was then dissolved in Benzene (3 mL/mmol of diazo) under an N_2 atmosphere and transferred dropwise by syringe to the solution of indole starting material. Two sequential rinses and transfers using small quantities of benzene were then conducted to ensure a complete transfer of the diazo reagent. The reaction mixture was then heated to 80 °C and stirred at this temperature for 12 h. The reaction progress was monitored by TLC analysis and considered complete upon consumption of the diazo reagent. Upon completion, the reaction mixture was concentrated *in vacuo* and purified by silica gel flash column chromatography (hexanes/EtOAc gradient) to yield annulation products **3.32, 3.38 – 3.42**, **3.67, 3.68, 3.71,** and **3.72**.

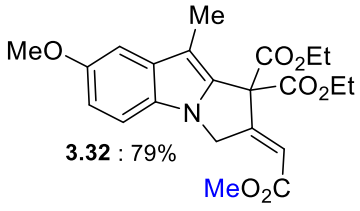

3.32 : 79%

3.32 was prepared using General Experimental Procedure B. Reagents employed: indole **3.30** (309 mg, 1.20 mmol), diethyl diazomalonate **3.31** (187 mg, 1.00 mmol), $Cu(tfacac)_2$ (18.5 mg, 0.0500 mmol). **3.32** (322 mg, 0.775 mmol, 78%) was obtained as a brown oil: X-ray quality crystal prepared by vapor diffusion in ether with pentane. R_f = 0.47, 25% EtOAc in hexanes; ^{1}H NMR (300 MHz, $CDCl_3$) δ = δ 7.19 (d, *J* = 8.8 Hz, 1H), 7.02 (d, *J* = 2.2 Hz, 1H), 6.88 (dd, *J* = 8.8, 2.4 Hz, 1H), 6.49 (t, *J* = 2.6 Hz, 1H), 5.22 (d, *J* = 2.6 Hz, 2H), 4.32 – 4.19 (m, 4H), 3.87 (s, 3H), 3.81 (s, 3H), 2.30 (s, 3H), 1.28 (t, *J* = 7.1 Hz, 6H) ppm; ^{13}C NMR (75

MHz, $CDCl_3$) δ = 166.9, 166.0, 156.3, 154.1, 133.6, 133.0, 127.6, 119.1, 112.3, 110.6, 105.6, 101.3, 64.3, 62.8, 56.0, 51.8, 48.9, 14.0, 9.1 ppm; IR (neat): ν_{max} = 2981, 2361, 1722, 1484, 1351, 1213, 1043, 795 cm^{-1}; HRMS (APPI+): calc'd for $C_{22}H_{25}NO_7$ $[M]^+$ 415.1631, found 415.1631.

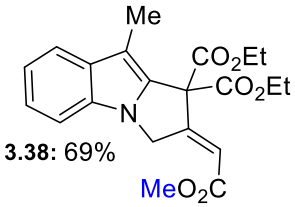

3.38: 69%

3.38 was prepared using General Experimental Procedure B. Reagents employed: substituted indole **3.33** (146 mg, 0.644 mmol), diethyl diazomalonate **3.31** (0.100 g, 0.537 mmol), $Cu(tfacac)_2$ (0.010 mg, 0.027 mmol). **3.38** (143 mg, 0.371 mmol, 69%) was obtained as a dark yellow oil: R_f = 0.50, 60% CH_2Cl_2 in hexanes; ^1H NMR (300 MHz, $CDCl_3$) δ = δ 7.60 (d, *J* = 7.9 Hz, 1H), 7.30 (d, *J* = 8.2 Hz, 1H), 7.25 – 7.19 (m, 1H), 7.16 – 7.11 (m, 1H), 6.51 (t, *J* = 2.6 Hz, 1H), 5.26 (d, *J* = 2.7 Hz, 2H), 4.35 – 4.18 (m, 4H), 3.82 (s, 3H), 2.34 (s, 3H), 1.28 (t, *J* = 7.1 Hz, 6H) ppm; ^{13}C NMR (75 MHz, $CDCl_3$) δ = 167.0, 166.1, 156.4, 133.0, 132.8, 132.3, 122.1, 119.6, 119.4, 119.3, 109.9, 106.2, 64.2, 63.0, 52.0, 48.8, 14.1, 9.1 ppm; IR (neat): ν_{max} = 2979, 2360, 1732, 1454, 1365, 1215, 743 cm^{-1}; HRMS (APPI+): calc'd for $C_{21}H_{24}NO_6$ $[M+H]^+$ 386.1595, found 386.1621.

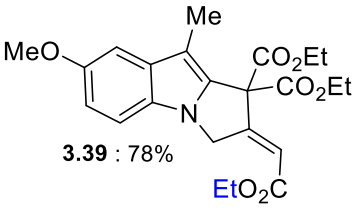

3.39 : 78%

3.39 was prepared using General Experimental Procedure B. Reagents employed: substituted *N*-propargylindole **3.34** (175 mg, 0.644 mmol), diethyl diazomalonate **3.31** (0.100 g, 0.537 mmol), $Cu(tfacac)_2$ (0.010 mg, 0.027 mmol). **3.39** (179 mg, 0.417 mmol, 78%) was obtained as a dark brown oil: R_f = 0.60, 50% CH_2Cl_2 in hexanes; ^1H NMR (300 MHz, $CDCl_3$) δ = δ 7.19 (d, *J* = 8.8 Hz, 1H), 7.02 (d, *J* = 2.3 Hz, 1H), 6.88 (dd, *J* = 8.8, 2.4 Hz, 1H), 6.48 (t, *J* = 2.6 Hz, 1H), 5.23 (d, *J* = 2.6 Hz, 2H), 4.36 – 4.18 (m, 6H), 3.87 (s, 3H), 2.31 (s, 3H), 1.34 (t, *J* = 7.1 Hz, 3H), 1.28 (t, *J* = 7.1 Hz, 6H) ppm; ^{13}C NMR (75 MHz, $CDCl_3$) δ = 167.0, 165.7, 156.1, 154.2, 133.7, 133.1, 127.7, 119.6, 112.4, 110.6, 105.6, 101.4, 64.4, 62.9, 60.9, 56.1,

49.0, 14.3, 14.1, 9.2 ppm; IR (neat): ν_{max} = 2978, 1731, 1473,1443, 1261, 1253, 1216, 1024, 855, 808 cm^{-1};HRMS (APPI+): calc'd for $C_{23}H_{28}NO_7$ $[M+H]^+$ 430.1858, found 430.1872.

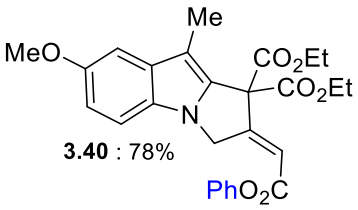

3.40 was prepared using General Experimental Procedure B. Reagents employed: substituted *N*-propargylindole **3.35** (206 mg, 0.644 mmol), diethyl diazomalonate **3.31** (0.100 g, 0.537 mmol), $Cu(tfacac)_2$ (0.010 mg, 0.027 mmol). **3.40** (201 mg, 0.421 mmol, 78%) was obtained as a dark brown oil : R_f = 0.60, 40% CH_2Cl_2 in hexanes; ^{1}H NMR (300 MHz, $CDCl_3$) δ = 7.45 – 7.39 (m, 2H), 7.30 – 7.24 (m, 1H), 7.19 – 7.14 (m, 3H), 7.03 (d, *J* = 2.1 Hz, 1H), 6.88 (dd, *J* = 8.7, 2.2 Hz, 1H), 6.73 (t, *J* = 2.6 Hz, 1H), 5.27 (d, *J* = 2.6 Hz, 2H), 4.40 – 4.22 (m, 4H), 3.87 (s, 3H), 2.33 (s, 3H), 1.31 (t, *J* = 7.1 Hz, 6H) ppm; ^{13}C NMR (75 MHz, $CDCl_3$) δ = 166.9, 164.1, 158.7, 154.3, 150.5, 133.5, 133.1, 129.6, 127.7, 126.2, 121.6, 118.8, 112.5, 110.6, 105.8, 101.5, 64.6, 63.1, 56.1, 49.2, 14.2, 9.2 ppm; IR (neat): ν_{max} = 2972, 2928, 1732, 1484, 1185, 1161, 1041, 688 cm^{-1}; HRMS (APPI+): calc'd for $C_{27}H_{28}NO_7$ $[M+H]^+$ 478.1858, found 478.1878.

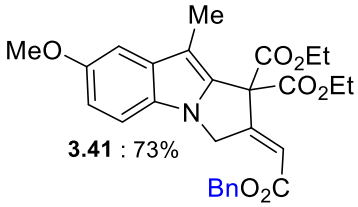

3.41 was prepared using General Experimental Procedure B. Reagents employed: substituted *N*-propargylindole **3.36** (215 mg, 0.644 mmol), diethyl diazomalonate **3.31** (0.100 g, 0.537 mmol), $Cu(tfacac)_2$ (0.010 mg, 0.027 mmol). **3.41** (192 mg, 0.391 mmol, 73%) was obtained as a pale-yellow solid: R_f = 0.50, 60% CH_2Cl_2 in hexanes; M.P. = 107-109 °C ^{1}H NMR (300 MHz, $CDCl_3$) δ = 7.43 – 7.33 (m, 5H), 7.17 (d, *J* = 8.8 Hz, 1H), 7.02 (d, *J* = 2.3 Hz, 1H), 6.88 (dd, *J* = 8.8, 2.4 Hz, 1H), 6.53 (t, *J* = 2.6 Hz, 1H), 5.23 (bs, 4H), 4.34 – 4.17 (m, 4H), 3.87 (s, 3H), 2.30 (s, 3H), 1.27 (t, *J* = 7.1 Hz, 6H) ppm; ^{13}C NMR (75 MHz, $CDCl_3$) δ = 166.9, 165.5, 156.8, 154.1, 135.7, 133.7, 133.1, 128.8, 128.6, 128.6, 127.8, 119.3, 112.5, 110.6, 105.7, 101.4, 66.8, 64.4, 63.0, 56.1, 49.1, 14.1, 9.2 ppm; IR (neat): ν_{max} = 2969, 2360, 1736, 1238, 1191,

1162, 1028, 846, 748 cm^{-1}; HRMS (APPI+): calc'd for $C_{28}H_{30}NO_7$ $[M+H]^+$ 492.2014, found 492.2011.

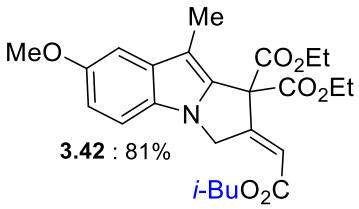

3.42 was prepared using General Experimental Procedure B. Reagents employed: substituted *N*-propargylindole **3.37** (193 mg, 0.644 mmol), diethyl diazomalonate **3.31** (0.100 g, 0.537 mmol), $Cu(tfacac)_2$ (0.010 mg, 0.027 mmol). **3.42** (198 mg, 0.433 mmol, 81%) was obtained as a yellow oil: R_f = 0.60, 40% CH_2Cl_2 in hexanes; ^1H NMR (300 MHz, $CDCl_3$) δ = 7.19 (d, *J* = 8.2 Hz, 1H), 7.02 (d, *J* = 2.4 Hz, 1H), 6.88 (dd, *J* = 8.8, 2.4 Hz, 1H), 6.50 (t, *J* = 2.6 Hz, 1H), 5.23 (d, *J* = 2.7 Hz, 2H), 4.37 – 4.16 (m, 4H), 3.98 (d, *J* = 6.6 Hz, 2H), 3.87 (s, 3H), 2.31 (s, 3H), 2.09 – 1.94 (m, 1H), 1.28 (t, *J* = 7.1 Hz, 6H), 0.99 (d, *J* = 6.7 Hz, 6H) ppm; ^{13}C NMR (75 MHz, $CDCl_3$) δ = 167.1, 165.8, 156.1, 154.2, 133.7, 133.1, 127.7, 119.6, 112.4, 110.6, 105.6, 101.4, 71.1, 64.4, 62.9, 56.1, 49.0, 27.9, 19.3, 14.1, 9.2 ppm; IR (neat): ν_{max} = 2964, 1726, 1477, 1214, 1040, 795 cm^{-1}; HRMS (APPI+): calc'd for $C_{25}H_{32}NO_7$ $[M+H]^+$ 458.2171, found 458.2195.

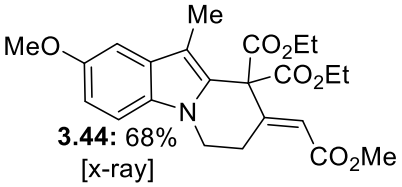

3.44 was prepared using General Experimental Procedure B. Reagents employed: substituted *N*-homopropargylindole **3.43** (175 mg, 0.644 mmol), diethyl diazomalonate **3.31** (0.100 g, 0.537 mmol), $Cu(tfacac)_2$ (0.010 mg, 0.027 mmol). **3.44** (158 mg, 0.368 mmol, 68%) was obtained as a pale-yellow crystal: X-ray quality crystal prepared by slow evaporation from ethanol. R_f = 0.45, 30% EtOAc in hexanes; M.P.=115-118 °C; ^1H NMR (300 MHz, $CDCl_3$) δ = 7.17 (d, *J* = 8.8 Hz, 1H), 7.00 (d, *J* = 2.3 Hz, 1H), 6.89 (dd, *J* = 8.8, 2.4 Hz, 1H), 5.97 (s, 1H), 4.30 – 4.20 (m, 4H), 4.13 (t, *J* = 6.2 Hz, 2H), 3.87 (s, 3H), 3.76 (s, 3H), 3.54 (t, *J* = 6.1 Hz, 2H), 2.21 (s, 3H), 1.25 (t, *J* = 7.1 Hz, 6H) ppm; ^{13}C NMR (75 MHz, $CDCl_3$) δ = 168.0, 166.2, 154.2, 151.7, 130.5, 129.0, 127.4, 119.5, 112.2, 109.7, 109.6, 100.6, 63.7, 62.7, 56.0, 51.6, 41.6, 26.1, 14.0, 9.6 ppm; IR (neat):

ν_{max} = 2926, 1728, 1255, 1162, 1068, 1023, 743 cm^{-1}; HRMS (APPI+): calc'd for $C_{23}H_{28}NO_7$ $[M+H]^+$ 430.1858, found 430.1875.

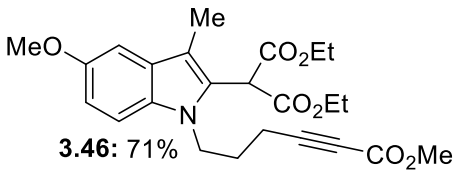

3.46: 71%

3.46 was prepared using General Experimental Procedure B. Reagents employed: Substituted indole **3.45** (184 mg, 0.644 mmol), diethyl diazomalonate **3.31** (0.100 g, 0.537 mmol), $Cu(tfacac)_2$ (0.010 mg, 0.027 mmol). **3.46** (0.170 g, 0.383 mmol, 71%) was obtained as a light green oil: **NOTE:** Additional attempts to promote the C–H functionalization/annulation cascade including (i) increased reaction times (48 h), (ii) elevated temperatures (reflux in toluene instead of benzene), and (iii) addition of base (Cs_2CO_3) provided **3.46** with no indication of the desired cyclized product. R_f = 0.50, 30% EtOAc in hexanes; ^{1}H NMR (300 MHz, $CDCl_3$) δ = 7.22 (d, *J* = 8.8 Hz, 1H), 6.99 (d, *J* = 2.2 Hz, 1H), 6.89 (dd, *J* = 8.8, 2.3 Hz, 1H), 4.96 (s, 1H), 4.32 – 4.16 (m, 6H), 3.86 (s, 3H), 3.78 (s, 3H), 2.35 (t, *J* = 6.9 Hz, 2H), 2.27 (s, 3H), 2.05 – 1.96 (m, 2H), 1.27 (t, *J* = 7.1 Hz, 6H) ppm; ^{13}C NMR (75 MHz, $CDCl_3$) δ = 167.2, 154.1, 154.1, 131.6, 128.7, 127.0, 112.7, 111.2, 110.4, 100.9, 88.1, 73.8, 62.2, 56.0, 52.8, 49.6, 42.8, 27.9, 16.2, 14.1, 9.3 ppm; IR (neat): ν_{max} = 2971, 2236, 1707, 1494, 1256, 1163, 1033, 751 cm^{-1}; HRMS (APPI+): calc'd for $C_{24}H_{30}NO_7$ $[M+H]^+$ 444.2017, found 444.2054.

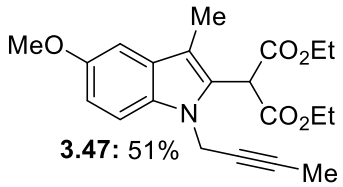

3.47: 51%

3.47 was prepared using General Experimental Procedure B. Reagents employed: substituted *N*-propargylindole **3.1** (137 mg, 0.644 mmol), diethyl diazomalonate **3.31** (0.100 g, 0.537 mmol), $Cu(tfacac)_2$ (0.010 mg, 0.027 mmol). **3.47** (104 mg, 0.280 mmol, 52%) was obtained as a yellow solid: **NOTE**: An attempt to promote the C–H functionalization/annulation cascade using $Rh_2(OAc)_4$ (2 mol%) and $ZnBr_2$ (10 mol%) in place of $Cu(tfacac)_2$ provided only insertion product **3.47** with no indication of the desired cyclized product. R_f = 0.50, 20% acetone in hexanes; ^{1}H

NMR (300 MHz, $CDCl_3$) δ = 7.32 (d, *J* = 8.8 Hz, 1H), 6.99 (d, *J* = 2.4 Hz, 1H), 6.91 (dd, *J* = 8.8, 2.5 Hz, 1H), 5.07 (s, 1H), 4.86 (q, *J* = 2.4 Hz, 2H), 4.36 – 4.16 (m, 4H), 3.87 (s, 3H), 2.28 (s, 3H), 1.73 (t, *J* = 2.4 Hz, 3H), 1.28 (t, *J* = 7.1 Hz, 6H) ppm; ^{13}C NMR (75 MHz, $CDCl_3$) δ = 167.4, 154.2, 131.9, 128.6, 126.9, 112.7, 111.3, 110.8, 101.1, 80.1, 74.1, 62.3, 56.1, 49.7, 34.5, 14.2, 9.3, 3.7 ppm; IR (neat): ν_{max} = 2933, 1729, 1306, 1207, 1163, 1030, 831 cm^{-1}; HRMS (APPI+): calc'd for $C_{21}H_{26}NO_5$ $[M+H]^+$ 372.1803, found 372.1786.

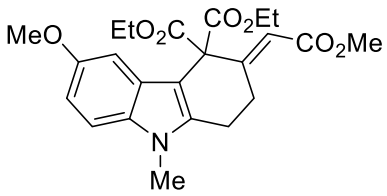

3.68: 78%
[x-ray]

3.68 was prepared using General Experimental Procedure B. Reagents employed: substituted indole **3.51** (175 mg, 0.644 mmol), diethyl diazomalonate **3.31** (0.100 g, 0.537 mmol), $Cu(tfacac)_2$ (0.010 mg, 0.027 mmol). **3.68** (180 mg, 0.42 mmol, 78%) was obtained as yellow crystals: X-ray quality crystal prepared by slow evaporation from ethanol. (see Appendix 2) R_f = 0.50, 40% acetone in hexanes; M.P.= 161-163 °C; ^1H NMR (300 MHz, $CDCl_3$) δ = 7.13 (d, *J* = 8.8 Hz, 1H), 6.96 (d, *J* = 2.4 Hz, 1H), 6.82 (dd, *J* = 8.8, 2.5 Hz, 1H), 5.87 (s, 1H), 4.34 – 4.15 (m, 4H), 3.81 (s, 3H), 3.73 (s, 3H), 3.57 (s, 3H), 3.44 (t, *J* = 6.4 Hz, 2H), 2.91 (t, *J* = 6.4 Hz, 2H), 1.25 (t, *J* = 7.1 Hz, 6H) ppm; ^{13}C NMR (75 MHz, $CDCl_3$) δ = 169.9, 166.6, 155.0, 154.0, 137.5, 132.9, 126.2, 118.1, 111.2, 109.6, 105.4, 102.7, 63.8, 62.1, 55.9, 51.4, 29.4, 24.9, 23.2, 14.2 ppm; IR (neat): ν_{max} = 2926, 1728, 1649, 1487, 1255, 1162, 1068, 802 cm^{-1}; HRMS (APPI+): calc'd for $C_{23}H_{28}NO_7$ $[M+H]^+$ 430.1858, found 430.1875.

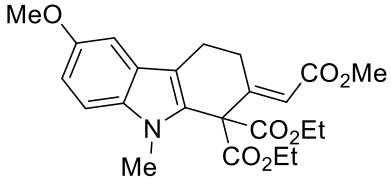

3.67: 71%
[X-ray]

3.67 was prepared using General Experimental Procedure B. Reagents employed: substituted indole **3.49** (175 mg, 0.644 mmol), diethyl diazomalonate **3.31** (0.100 g, 0.537 mmol), $Cu(tfacac)_2$ (0.010 mg, 0.027 mmol). **3.67** (164 mg, 0.382 mmol, 71%) was obtained as a yellow crystal: X-ray quality crystals prepared by slow evaporation from

ethanol (see Appendix 2): R_f = 0.40, 20% EtOAc in hexanes; ^{1}H NMR (300 MHz, $CDCl_3$) δ = 7.20 (d, *J* = 8.8 Hz, 1H), 6.96 (d, *J* = 2.3 Hz, 1H), 6.91 (dd, *J* = 8.8, 2.5 Hz, 1H), 5.78 (s, 1H), 4.28 (q, *J* = 7.1 Hz, 4H), 3.86 (s, 3H), 3.75 (s, 3H), 3.64 (s, 3H), 3.30 (t, *J* = 6.3 Hz, 2H), 2.91 (t, *J* = 6.3 Hz, 2H), 1.27 (t, *J* = 7.1 Hz, 6H) ppm; ^{13}C NMR (75 MHz, $CDCl_3$) δ = 168.6, 166.3, 155.5, 154.0, 133.7, 129.8, 125.6, 118.0, 112.7, 112.5, 110.1, 100.6, 64.6, 62.7, 56.0, 51.4, 31.3, 25.9, 21.7, 13.9 ppm; IR (neat): ν_{max} = 2932, 1728, 1663, 1487, 1250, 1162, 1068, 779 cm^{-1}; HRMS (APPI+): calc'd for $C_{23}H_{28}NO_7$ $[M+H]^+$ 430.1858, found 430.1875.

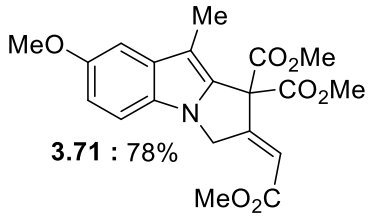

3.71 : 78%

3.71 was prepared using General Experimental Procedure B. Reagents employed: substituted *N*-propargylindole **3.30** (154 mg, 0.600 mmol), dimethyl diazomalonate **3.69** (79 mg, 0.50 mmol), $Cu(tfacac)_2$ (9.2 mg, 0.025 mmol). **3.71** (144 mg, 0.372 mmol, 74%) was obtained as a dark brown oil: R_f = 0.47, 25% EtOAc in hexanes; ^{1}H NMR (300 MHz, $CDCl_3$) δ = 7.19 (d, *J* = 8.7 Hz, 1H), 7.02 (d, *J* = 2.2 Hz, 1H), 6.88 (dd, *J* = 8.7, 2.3 Hz, 1H), 6.48 (t, 2.3 Hz, 1H), 5.23 (d, *J* = 2.5 Hz, 2H), 3.86 (s, 3H), 3.80 (s, 3H), 3.79 (s, 6H), 2.28 (s, 3H) ppm; ^{13}C NMR (75 MHz, $CDCl_3$) δ = 167.4, 165.9, 156.2, 154.3, 133.4, 132.9, 127.7, 119.3, 112.6, 110.7, 105.7, 101.4, 63.9, 56.1, 53.7, 51.9, 48.9, 8.8 ppm; IR (neat): ν_{max} = 2951, 2361, 1716, 1435, 1231, 1211, 1046, 904, 785 cm^{-1}; HRMS (APPI+): calc'd for $C_{20}H_{22}NO_7$ $[M+H]^+$ 388.1391, found 388.1406.

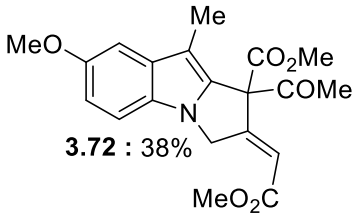

3.72 : 38%

3.72 was prepared using General Experimental Procedure B. Reagents employed: Substituted *N*-propargylindole **3.30 (**154 mg, 0.600 mmol), methyl 2-diazoacetoacetate **3.71** (71 mg, 0.50 mmol), $Cu(tfacac)_2$ (9.2 mg, 0.025 mmol). **3.72** (70 mg, 0.19 mmol, 38%) was obtained as a brown oil: R_f = 0.47, 25% EtOAc in hexanes; ^{1}H NMR (300 MHz, $CDCl_3$) δ =

7.23 (d, *J* = 8.8 Hz, 1H), 7.03 (d, *J* = 2.4 Hz, 1H), 6.92 (dd, *J* = 8.8, 2.4 Hz, 1H), 6.34 (t, *J* = 2.6 Hz, 1H), 5.35 – 5.19 (m, 2H), 3.88 (s, 3H), 3.82 (s, 3H), 3.81 (s, 3H), 2.28 (s, 3H), 2.05 (s, 3H) ppm; ^{13}C NMR (75 MHz, $CDCl_3$) δ = 199.1, 167.6, 165.9, 155.8, 154.4, 134.0, 133.1, 128.0, 120.1, 112.9, 110.8, 105.9, 101.4, 70.9, 56.1, 53.5, 52.0, 49.1, 26.7, 9.1 ppm; IR (neat): ν_{max} = 2952, 2360, 2191, 1715, 1485, 1349, 1218, 1162, 1041, 792 cm^{-1}; HRMS (APPI+): calc'd for $C_{20}H_{21}NO_6$ $[M]^+$ 371.1369, found 371.1373.

Scheme 3.32: One-Pot Copper/Cesium Annulation Reactions with Alkenyl-Ester Electrophiles

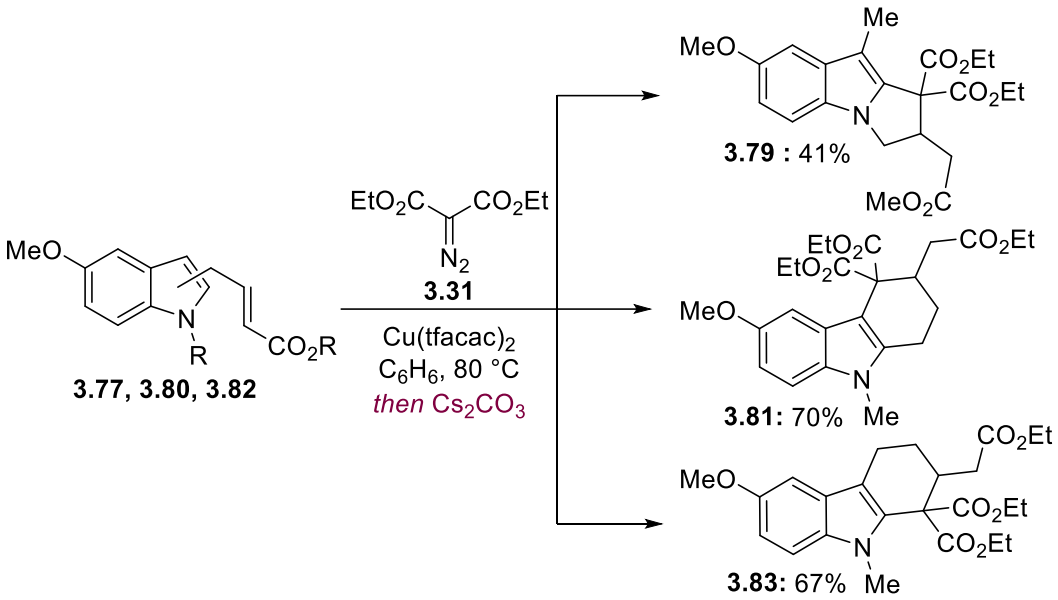

General Experimental Procedure C:

Indole starting material (**3.77, 3.80, 3.82** 1.2 equiv) was added to a reaction vessel equipped with a stir bar, and the vessel was then evacuated and backfilled with N_2. This cycle was repeated two additional times, followed by the addition of benzene (5 mL/mmol of indole) under an N_2 atmosphere. $Cu(tfacac)_2$ (5 mol%) was then added to the reaction vessel, and again, the vessel was evacuated (quickly) and backfilled with N_2. Diazo reagent **3.31** (1.0 equiv) was added to a separate

reaction vessel, and the vessel was then evacuated and backfilled with N_2. This cycle was repeated two additional times. The diazo reagent was then dissolved in benzene (3 mL/mmol of diazo) under an N_2 atmosphere and transferred dropwise by syringe to the solution of indole starting material. Two sequential rinses and transfers using small quantities of benzene were then conducted to ensure a complete transfer of the diazo reagent. The reaction mixture was then heated to 80 °C and stirred at this temperature for 12 h. The reaction progress was monitored by TLC analysis and considered complete upon consumption of the diazo reagent. Upon completion, Cs_2CO_3 (10 mol%) was added and allowed to stir for an additional 12 h. After 12 h had elapsed, the reaction mixture was filtered through Celite, concentrated *in vacuo*, and purified by silica gel flash column chromatography (hexanes/EtOAc gradient) to yield annulation products **3.79, 3.81, 3.83**.

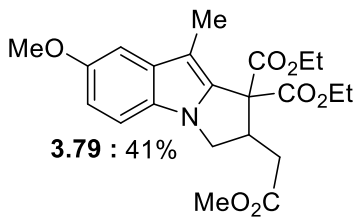

3.79 : 41%

3.79 was prepared using General Experimental Procedure C. Reagents employed: **3.77** (84 mg, 0.32 mmol), diethyl diazomalonate **3.31** (0.050 mg, 0.27 mmol), $Cu(tfacac)_2$ (5.0 mg, 0.014 mmol) and Cs_2CO_3 (9.0 mg, 0.027 mmol). **3.79** (45 mg, 0.11 mmol, 41%) was obtained as a brown oil: (Note: 10 mol% of Cs_2CO_3 was used) R_f = 0.50, 20% EtOAc in hexanes; ^{1}H NMR (300 MHz, $CDCl_3$) δ = 7.11 (d, *J* = 8.8 Hz, 1H), 7.00 (d, *J* = 2.4 Hz, 1H), 6.84 (dd, *J* = 8.8, 2.4 Hz, 1H), 4.49 – 4.42 (m, 1H), 4.36 – 4.13 (m, 4H), 3.89 – 3.80 (m, 5H), 3.73 (s, 3H), 2.93 – 2.74 (m, 2H), 2.30 (s, 3H), 1.31 (t, *J* = 7.1 Hz, 3H), 1.26 (t, *J* = 7.1 Hz, 3H) ppm; ^{13}C NMR (75 MHz, $CDCl_3$) δ = 172.5, 168.5, 167.8, 154.0, 135.0, 133.1, 128.2, 112.2, 110.5, 105.9, 101.4, 62.3, 62.1, 56.1, 52.1, 48.2, 45.9, 34.2, 14.24, 14.17, 9.3 ppm; *(Note: one carbon signal is missing presumably due to overlap with the signal at 62.09)* IR (neat): ν_{max} = 2933, 2361, 1732, 1444, 1370, 1256, 1160, 1038, 795 cm^{-1}; HRMS (APPI+): calc'd for $C_{22}H_{28}NO_7$ $[M+H]^+$ 418.1858, found 418.1873.

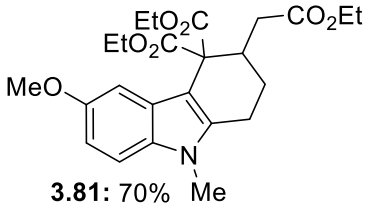

3.81: 70%

3.81 was prepared using General Experimental Procedure C. Reagents employed: **3.80** (92 mg, 0.32 mmol), diethyl diazomalonate (0.050 g, 0.27 mmol), $Cu(tfacac)_2$ (5.0 mg, 0.014 mmol) and Cs_2CO_3 (9.0 mg, 0.027 mmol). **3.81** (86 mg, 0.19 mmol, 70%) was obtained as yellow crystals: MP: 161-163 °C; R_f = 0.40, 25% acetone in hexanes; ^{1}H NMR (300 MHz, $CDCl_3$) δ = 7.14 (d, *J* = 8.8 Hz, 1H), 7.00 (d, *J* = 2.5 Hz, 1H), 6.82 (dd, *J* = 8.8, 2.5 Hz, 1H), 4.29 – 4.09 (m, 6H), 3.82 (s, 3H), 3.59 (s, 3H), 3.08 – 2.93 (m, 1H), 2.76 (t, *J* = 6.5 Hz, 2H), 2.69 – 2.52 (m, 2H), 2.30 – 2.08 (m, 2H), 1.30 – 1.22 (m, 9H) ppm; ^{13}C NMR (75 MHz, $CDCl_3$) δ = 172.9, 171.2, 170.1, 153.7, 137.5, 132.6, 126.7, 110.8, 109.3, 105.1, 103.7, 61.6, 61.3, 60.5, 58.1, 55.9, 37.0, 35.3, 29.3, 24.6, 20.3, 14.34, 14.28, 14.25 ppm; IR (neat): ν_{max} = 2981, 1726, 1621, 1486, 1371, 1251, 1188, 1071, 798 cm^{-1}; HRMS (APPI+): calc'd for $C_{24}H_{32}NO_7$ $[M+H]^+$ 445.2178, found 446.2207.

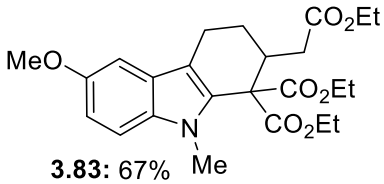

3.83: 67%

3.83 was prepared using General Experimental Procedure C. Reagents employed: **3.82** (92 mg, 0.32 mmol), diethyl diazomalonate (0.050 g, 0.27 mmol), $Cu(tfacac)_2$ (5.0 mg, 0.014 mmol) and Cs_2CO_3 (9.0 mg, 0.027 mmol). **3.83** (82 mg, 0.18 mmol, 67%) was obtained as light green oil: (Note: 10 mol% of Cs_2CO_3 was used) R_f = 0.40, 20% acetone in hexanes; ^{1}H NMR (300 MHz, $CDCl_3$) δ = 7.19 (d, *J* = 8.8 Hz, 1H), 6.95 (d, *J* = 2.4 Hz, 1H), 6.91 (dd, *J* = 8.8, 2.5 Hz, 1H), 4.28 – 4.10 (m, 6H), 3.86 (s, 3H), 3.63 (s, 3H), 3.20 – 3.12 (m, 1H), 2.80 (t, *J* = 6.4 Hz, 2H), 2.73 – 2.57 (m, 2H), 2.11 – 1.96 (m, 2H), 1.29 – 1.23 (m, 9H) ppm; ^{13}C NMR (75 MHz, $CDCl_3$) δ = 172.9, 170.2, 169.1, 154.0, 133.5, 130.6, 126.0, 112.6, 111.5, 110.1, 100.6, 62.3, 62.1, 60.6, 59.2, 56.2, 38.9, 35.6, 31.8, 25.8, 19.4, 14.4, 14.12, 14.08 ppm; IR (neat): ν_{max} = 2975, 2935, 2360, 1738, 1489, 1273, 1162, 1035, 798 cm^{-1}; HRMS (APPI+): calc'd for $C_{24}H_{32}NO_7$ $[M+H]^+$ 445.2178 found 446.2193.

1.22 References

1. (a) Mather, B. D.; Viswanathan, K.; Miller, K. M.; Long, T. E. *Prog. Polym. Sci.* **2006**, *31*, 487 (b) Michael, A. *Am. Chem. J.* **1887**, *9*, 115.
2. Xu, X.; Han, X.; Yang, L.; Hu, W. *Chem.Eur. J.* **2009**, *15*, 12604.
3. Harada, S.; Yanagawa, M.; Nemoto, T. *ACS Catal.* **2020**, *10*, 11971.
4. Yanagawa, M.; Harada, S.; Hirose, S.; Nemoto, T. *Adv. Synth. Catal.* **2021**, *363*, 2189.
5. For Rh/Zn-catalyzed reactions, see: (a) Bhat, A. H.; Alavi, S.; Grover, H. K. *Org. Lett.* **2020**, *22*, 224. (b) Liu, K.; Zhu, C.; Min, J.; Peng, S.; G. Xu, G.;Sun, J. *Angew. Chem. Int. Ed.*, **2015**, *54*, 12962. (c) F. Urabe, F.; S. Miyamoto, S.; K. Takahashi, K.; J. Ishihara, J.; Hatakeyama, S. *Org. Lett.* **2014**, *16*, 1004.
6. (a) Vovard-Le Bray, C.; Derien, S.; Dixneuf, P. H. *Angew. Chem. Int. Ed.* **2009**, *48*, 1439. (b) Hodgson, D. M.; Angrish, D. *Chem. Eur. J.* **2007**, *13*, 3470. (c) Del Zotto, A.; Baratta, W.; Verardo, G.; Rigo, P. *Eur. J. Org. Chem.* **2000**, 2795. (d) Scott, L. T.; DeCicco, G. J. *J. Am. Chem. Soc.* **1974**, *96*, 322.
7. For full details, see supporting information of Bhat, A.; Tucker, N.; Lin, J.-B.; Grover, H. *Chem. Commun.* **2021**, *57*, 10556.
8. Hack, D.; Blümel, M.; Chauhan, P.; Philipps, A. R.; Enders, D. *Chem. Soc. Rev.* **2015**, *44*, 6059.
9. Huang, L.; Qi, J.; Wu, X.; Wu, W.; Jiang, H. *Chem. Eur. J.* **2013**, *19*, 15462.
10. Müller, S.; Liepold, B.; Roth, G. J.; Bestmann, H. J. *Synlett* **1996**, 521.
11. Finkelstein, H. *Ber. Dtsch. Chem. Ges.* **1910**, *43*, 1528.
12. Yao, Y., Alami, M., Hamze, A., Provot, O. *Org. Biomol. Chem.* **2021**, *19*, 3509.

1.23 Appendix 2

^{1}H, ^{13}C NMR Spectra and X-ray Crystallographic Data for

Chapter 3

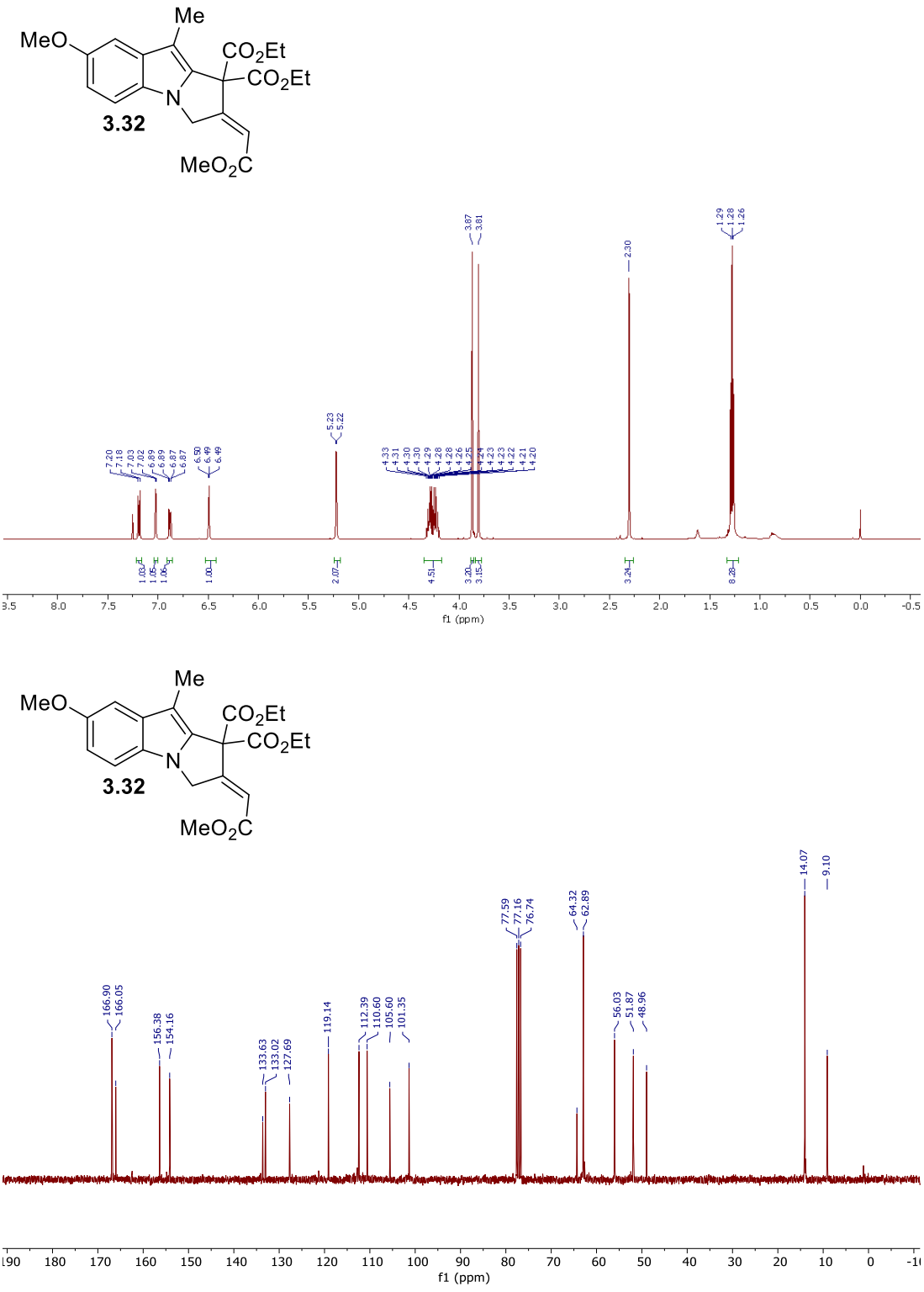

^{1}H NMR (300 MHz, $CDCl_3$) and ^{13}C NMR (75 MHz, $CDCl_3$) of compound **3.32**

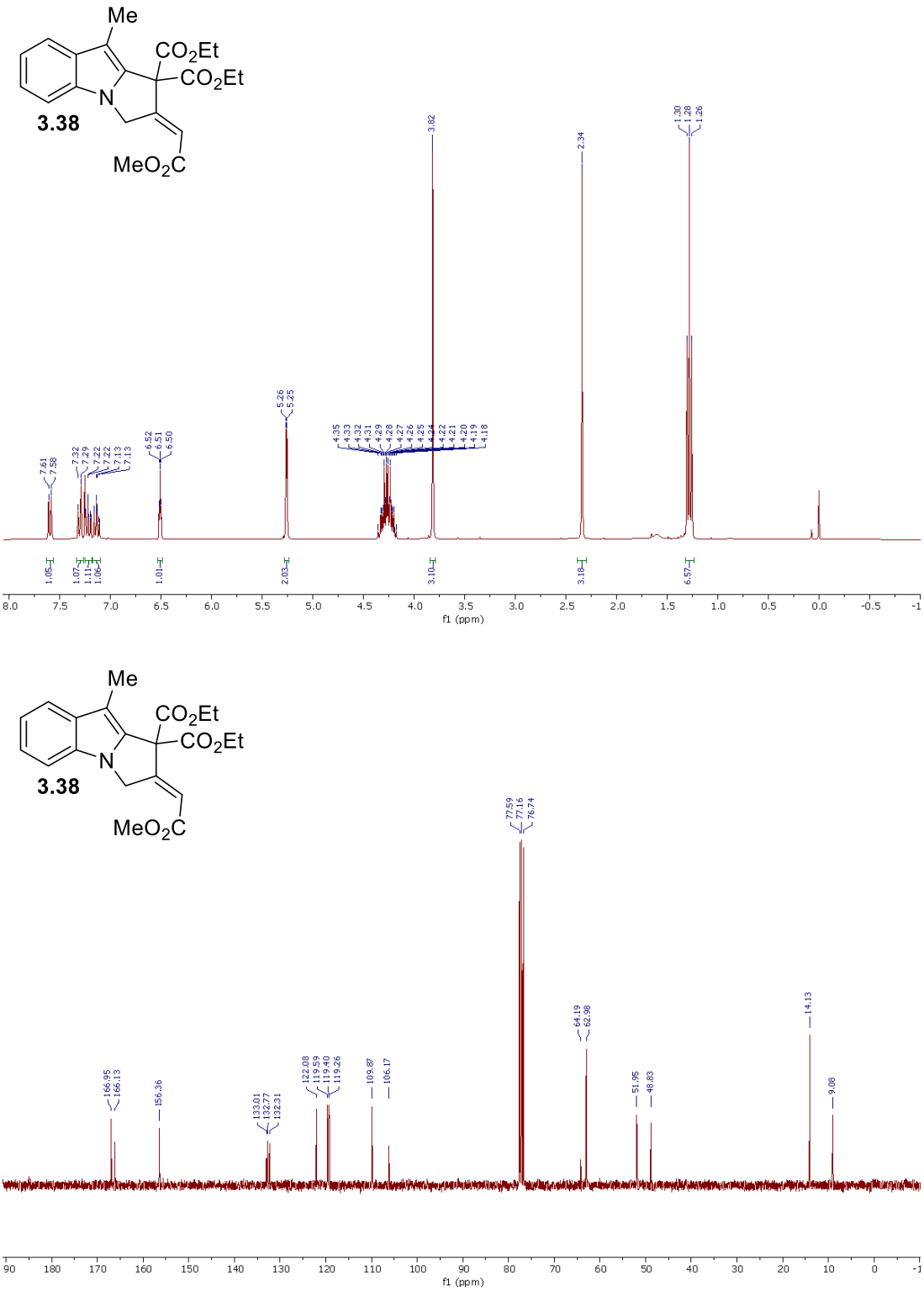

^{1}H NMR (300 MHz, $CDCl_3$) and ^{13}C NMR (75 MHz, $CDCl_3$) of compound **3.38**

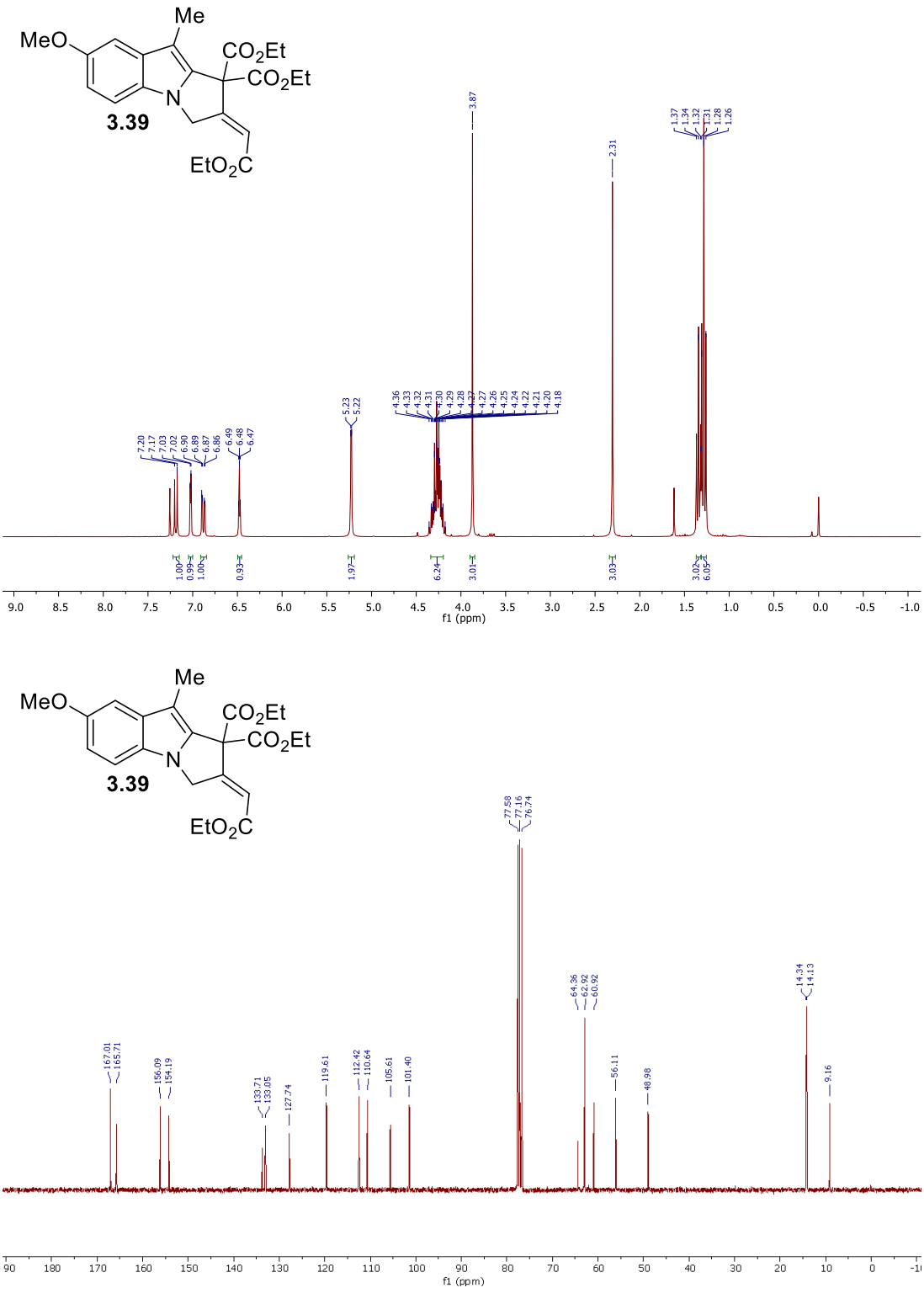

^{1}H NMR (300 MHz, $CDCl_3$) and ^{13}C NMR (75 MHz, $CDCl_3$) of compound **3.39**

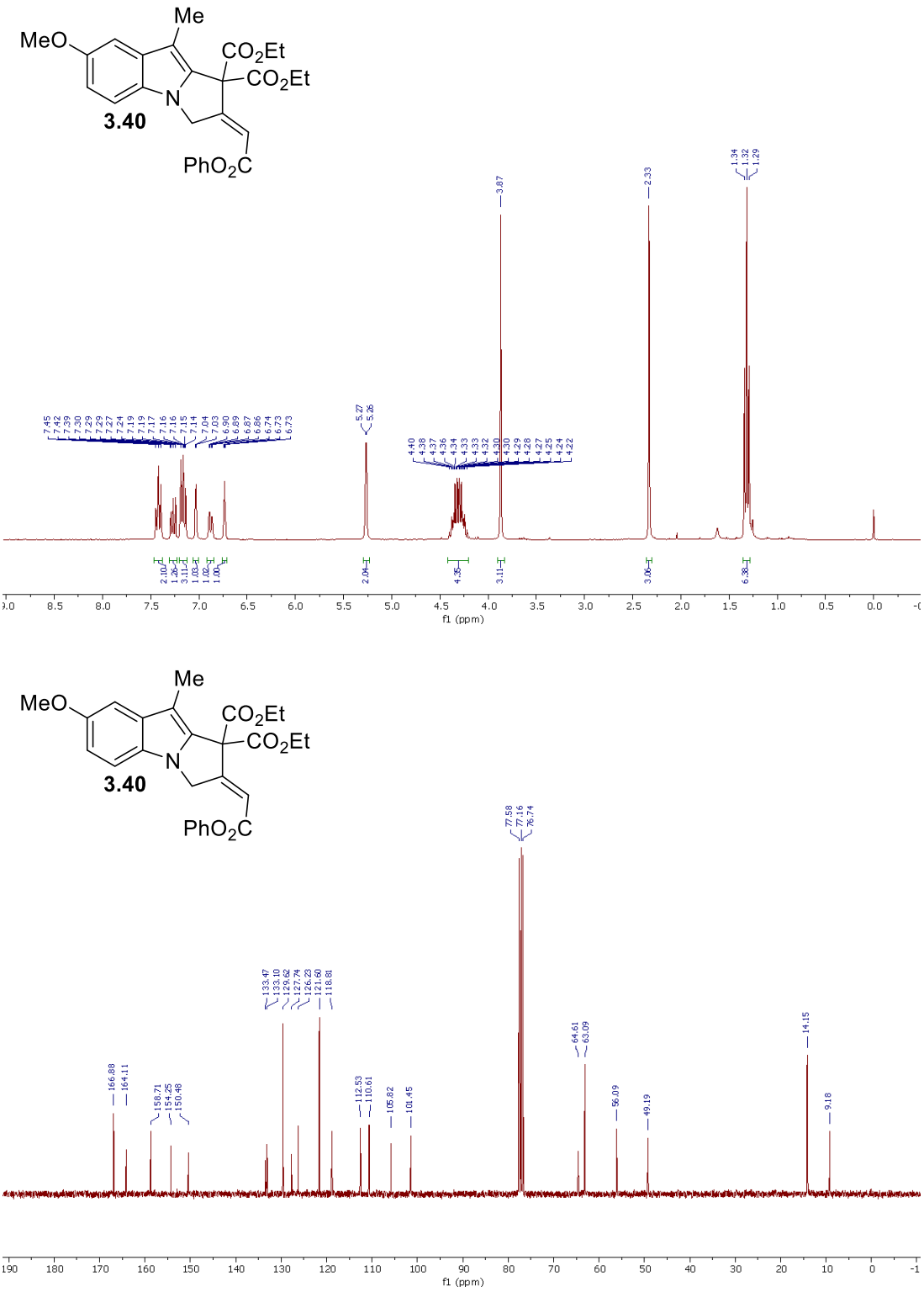

^{1}H NMR (300 MHz, $CDCl_3$) and ^{13}C NMR (75 MHz, $CDCl_3$) of compound **3.40**

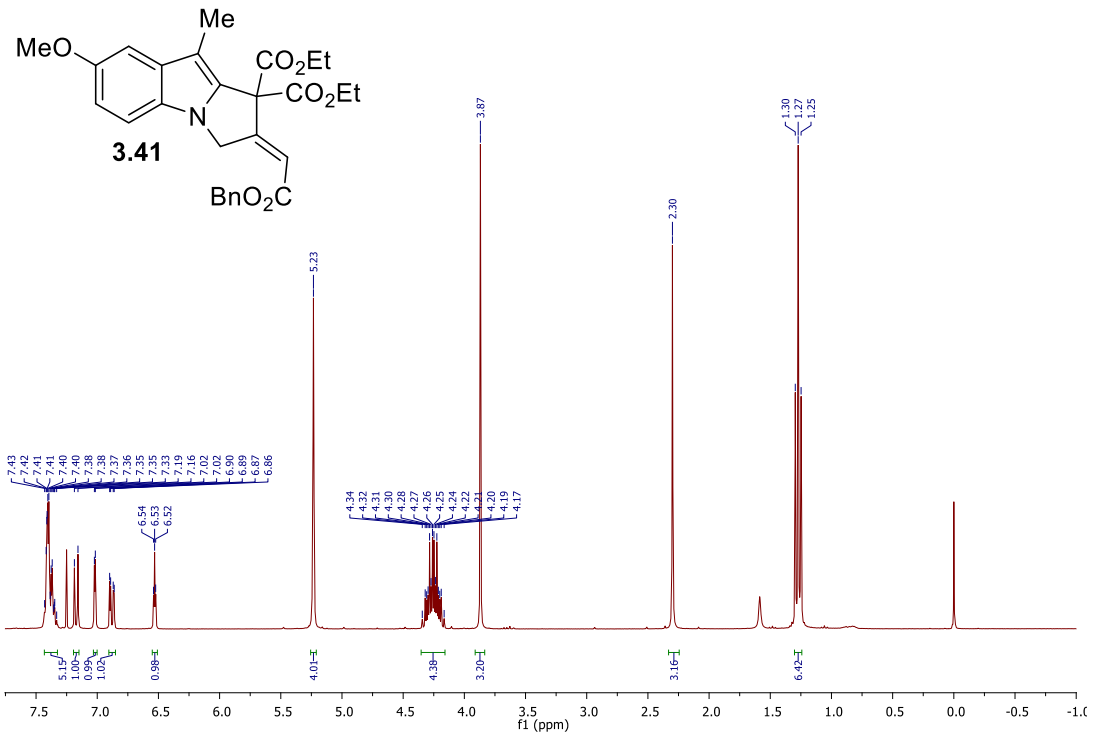

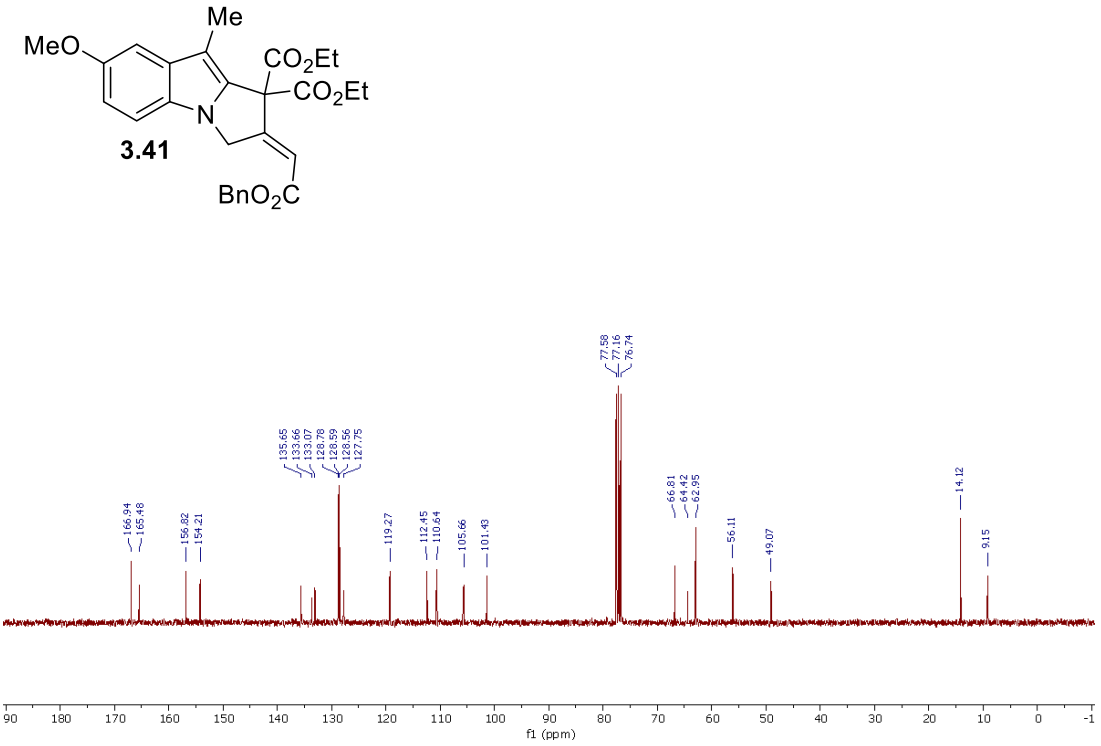

^{1}H NMR (300 MHz, $CDCl_3$) and ^{13}C NMR (75 MHz, $CDCl_3$) of compound **3.41**

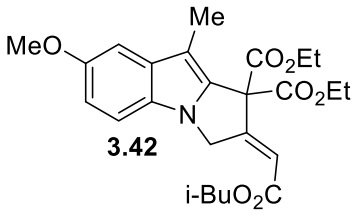

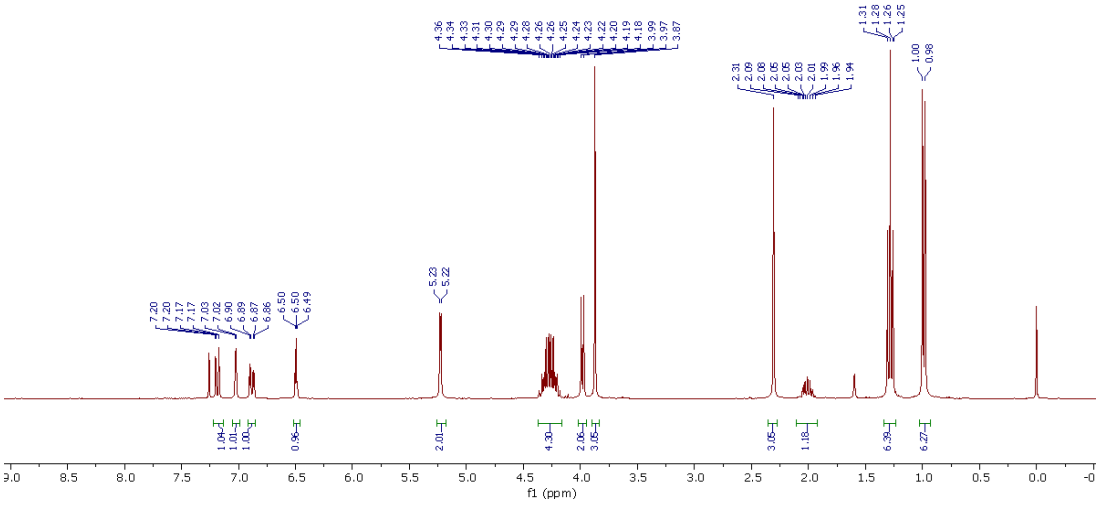

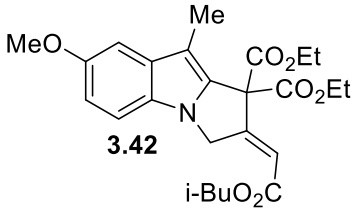

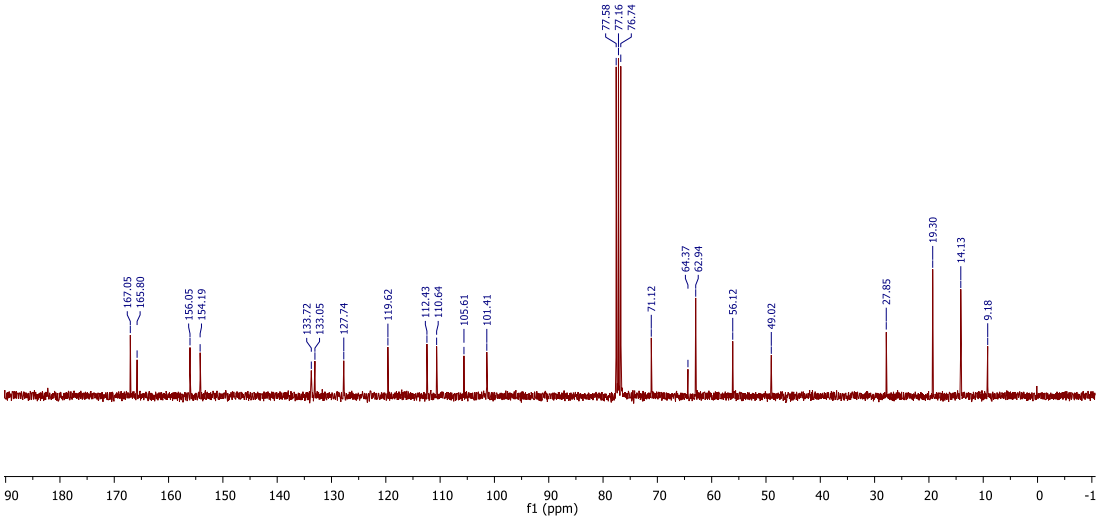

^{1}H NMR (300 MHz, $CDCl_3$) and ^{13}C NMR (75 MHz, $CDCl_3$) of compound **3.42**

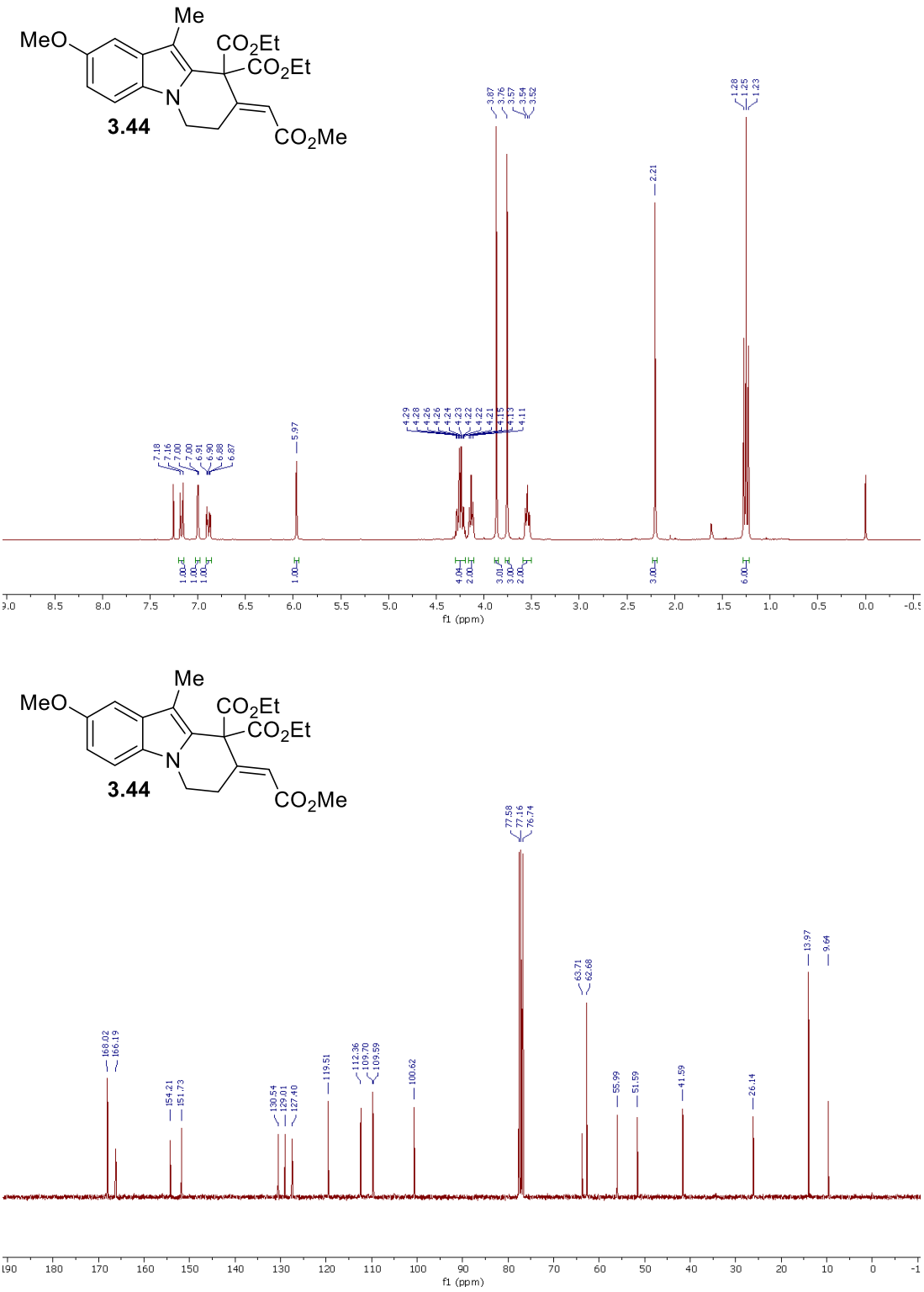

^{1}H NMR (300 MHz, $CDCl_3$) and ^{13}C NMR (75 MHz, $CDCl_3$) of compound **3.44**

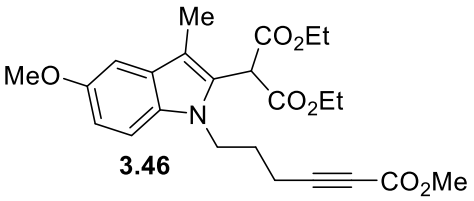

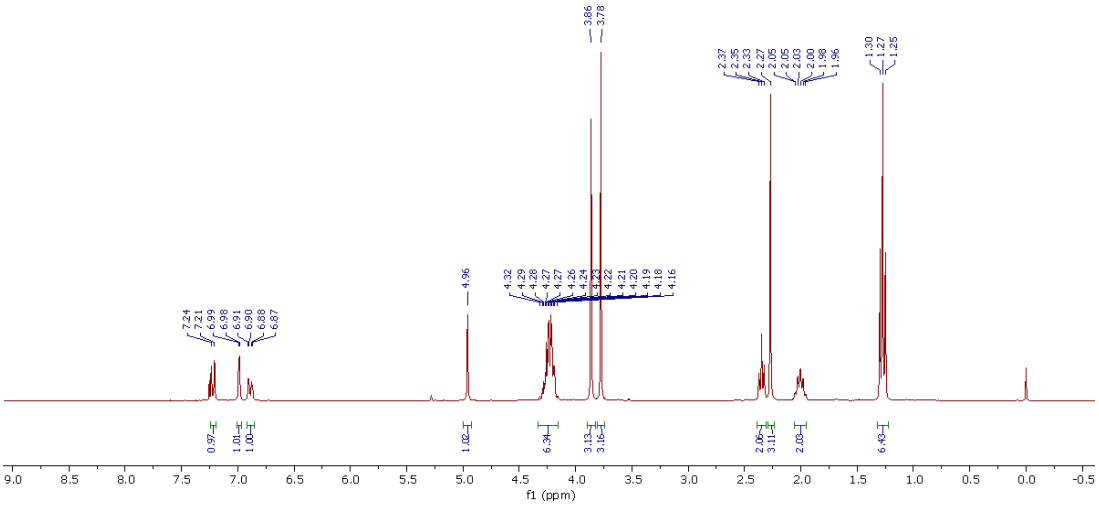

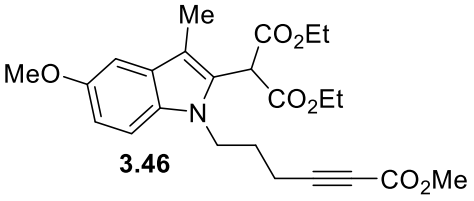

^{1}H NMR (300 MHz, $CDCl_3$) and ^{13}C NMR (75 MHz, $CDCl_3$) of compound **3.46**

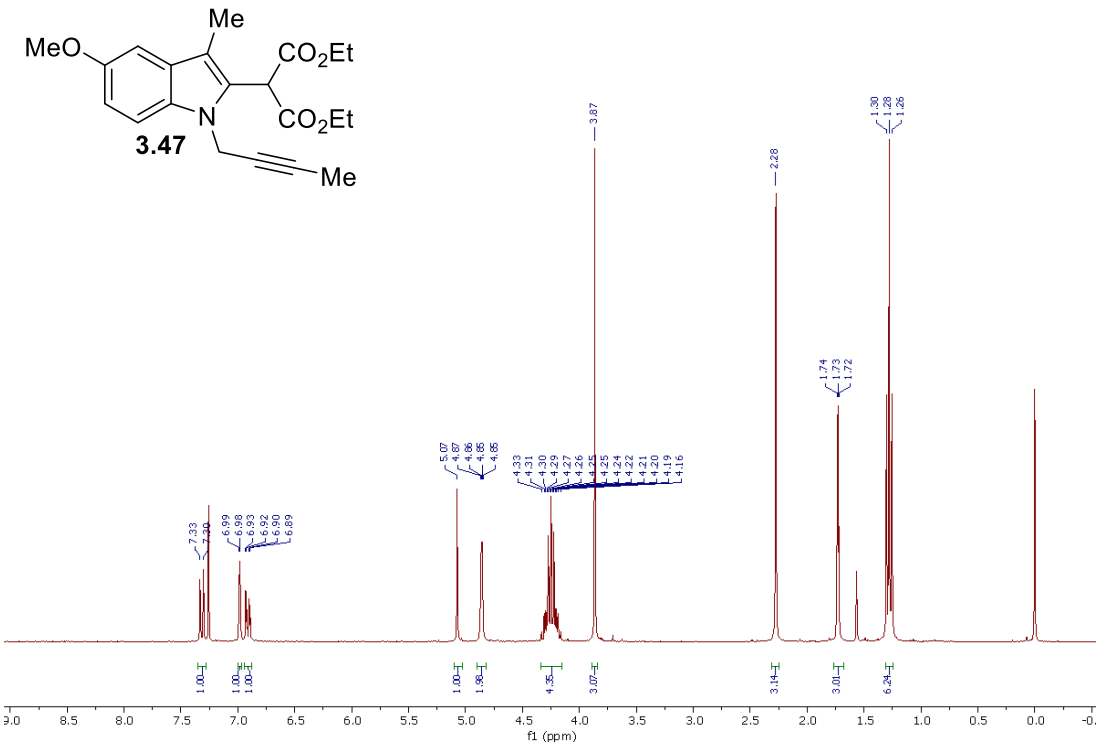

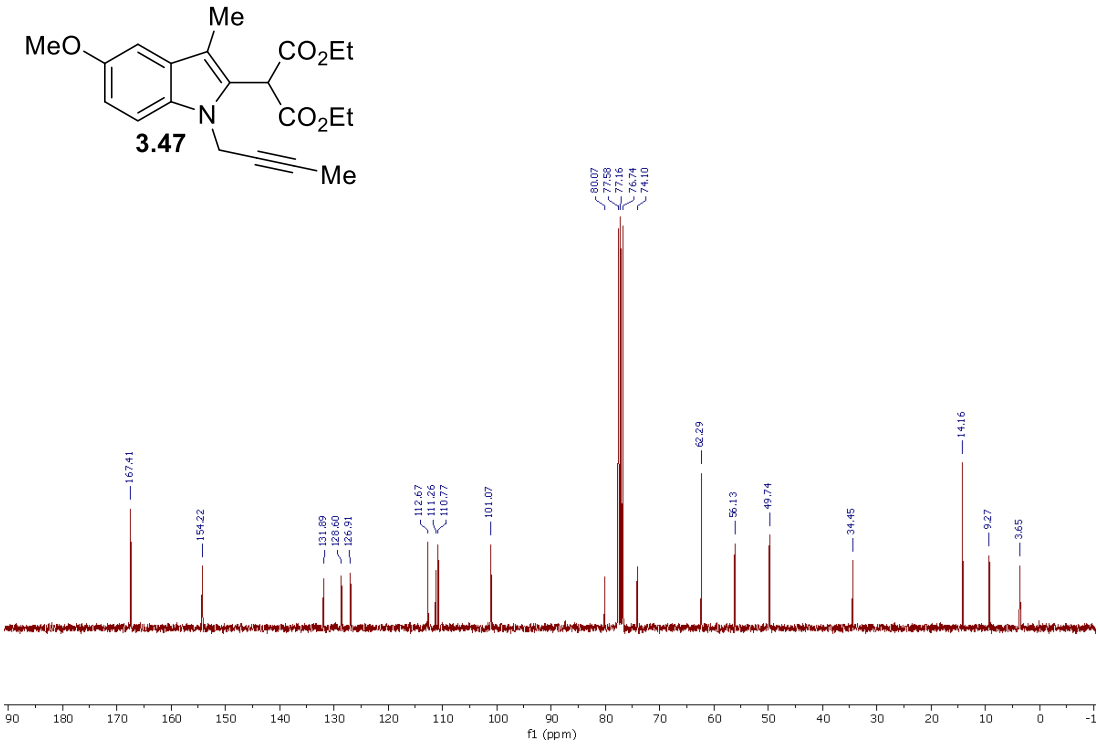

^{1}H NMR (300 MHz, $CDCl_3$) and ^{13}C NMR (75 MHz, $CDCl_3$) of compound **3.47**

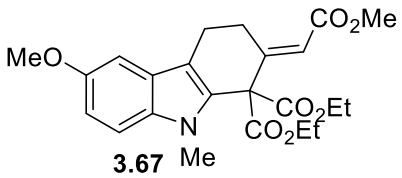

3.67

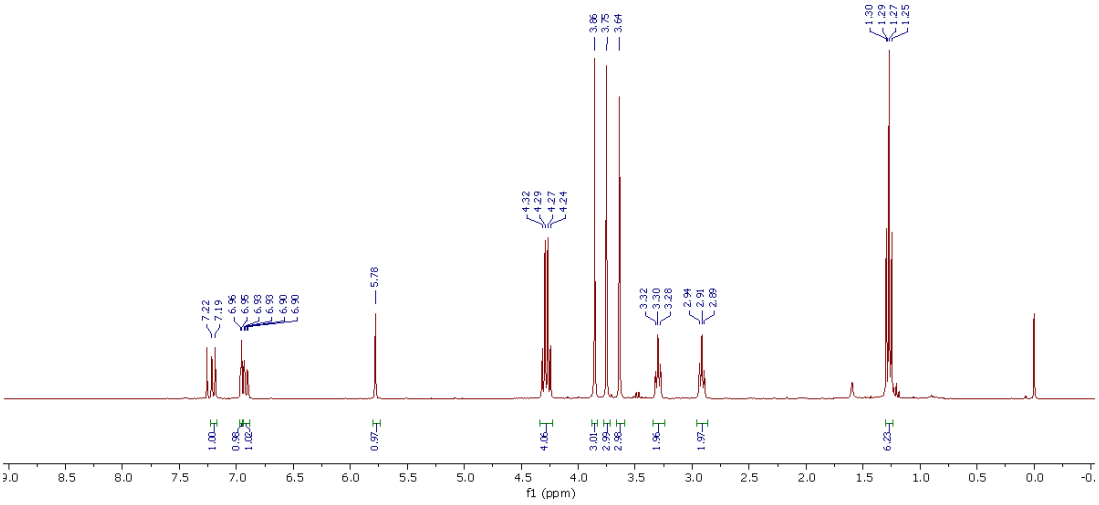

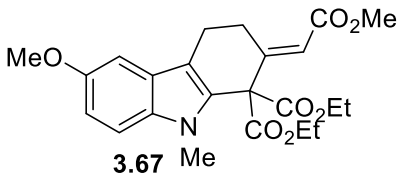

3.67

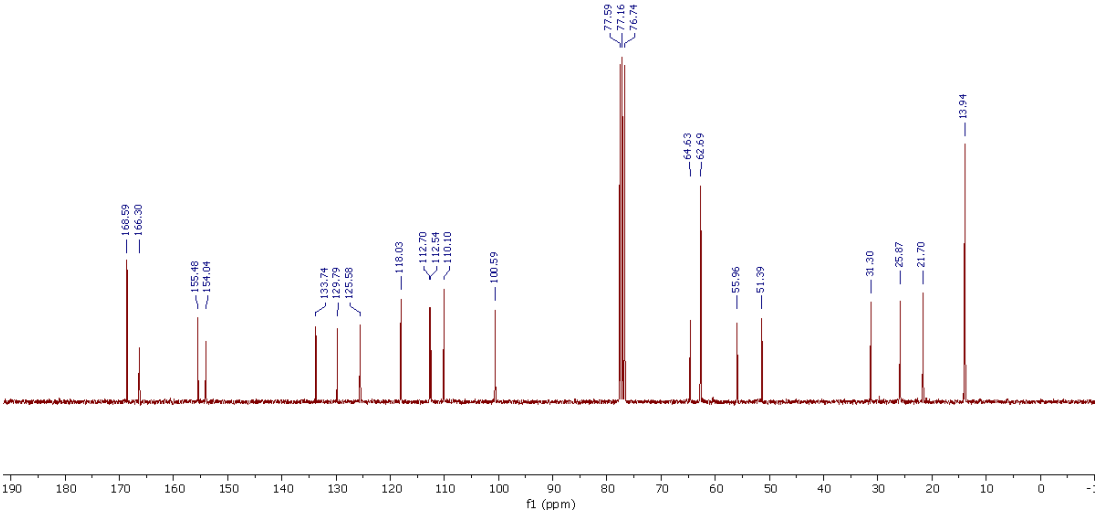

^{1}H NMR (300 MHz, $CDCl_3$) and ^{13}C NMR (75 MHz, $CDCl_3$) of compound **3.67**

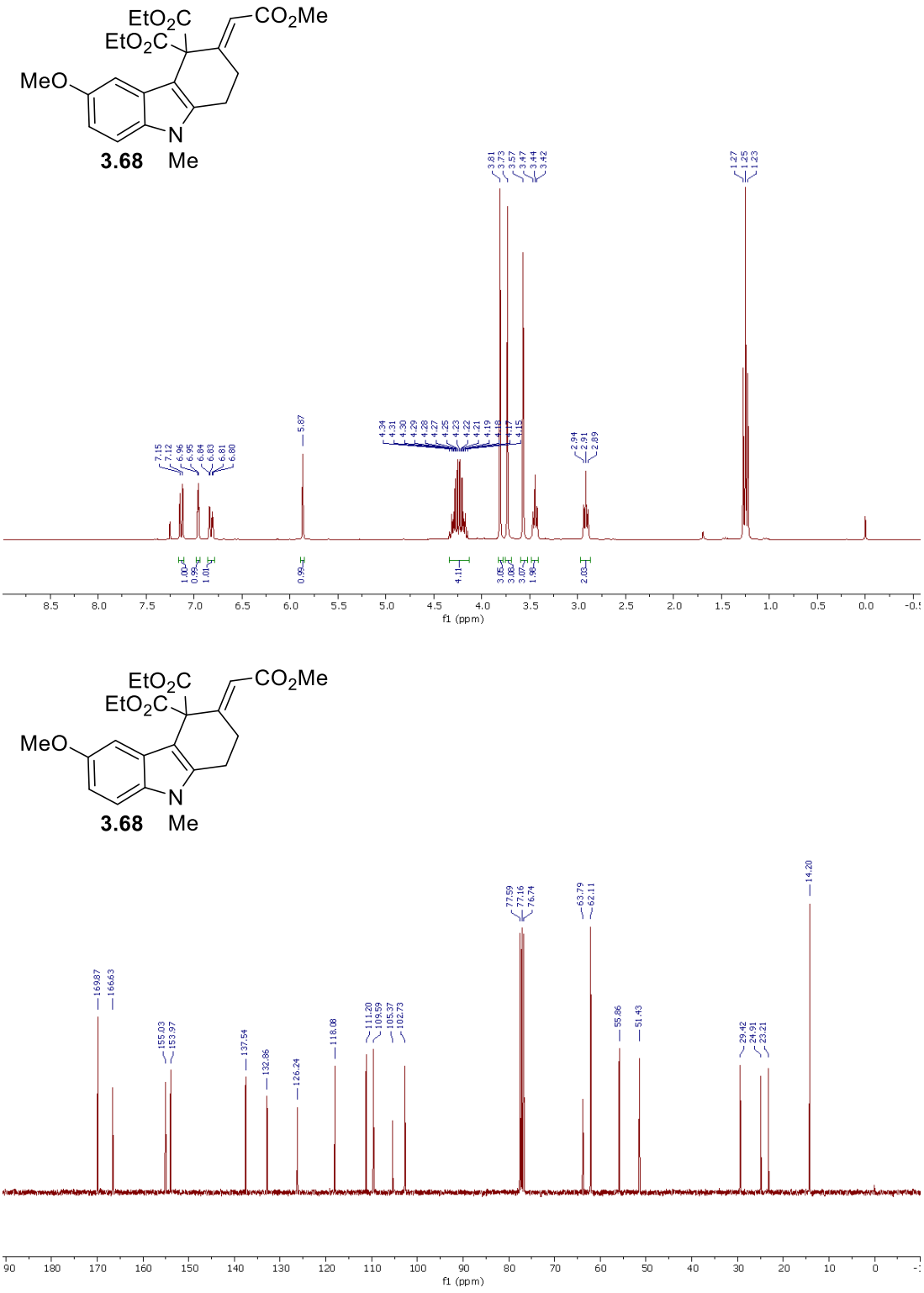

^{1}H NMR (300 MHz, $CDCl_3$) and ^{13}C NMR (75 MHz, $CDCl_3$) of compound **3.68**

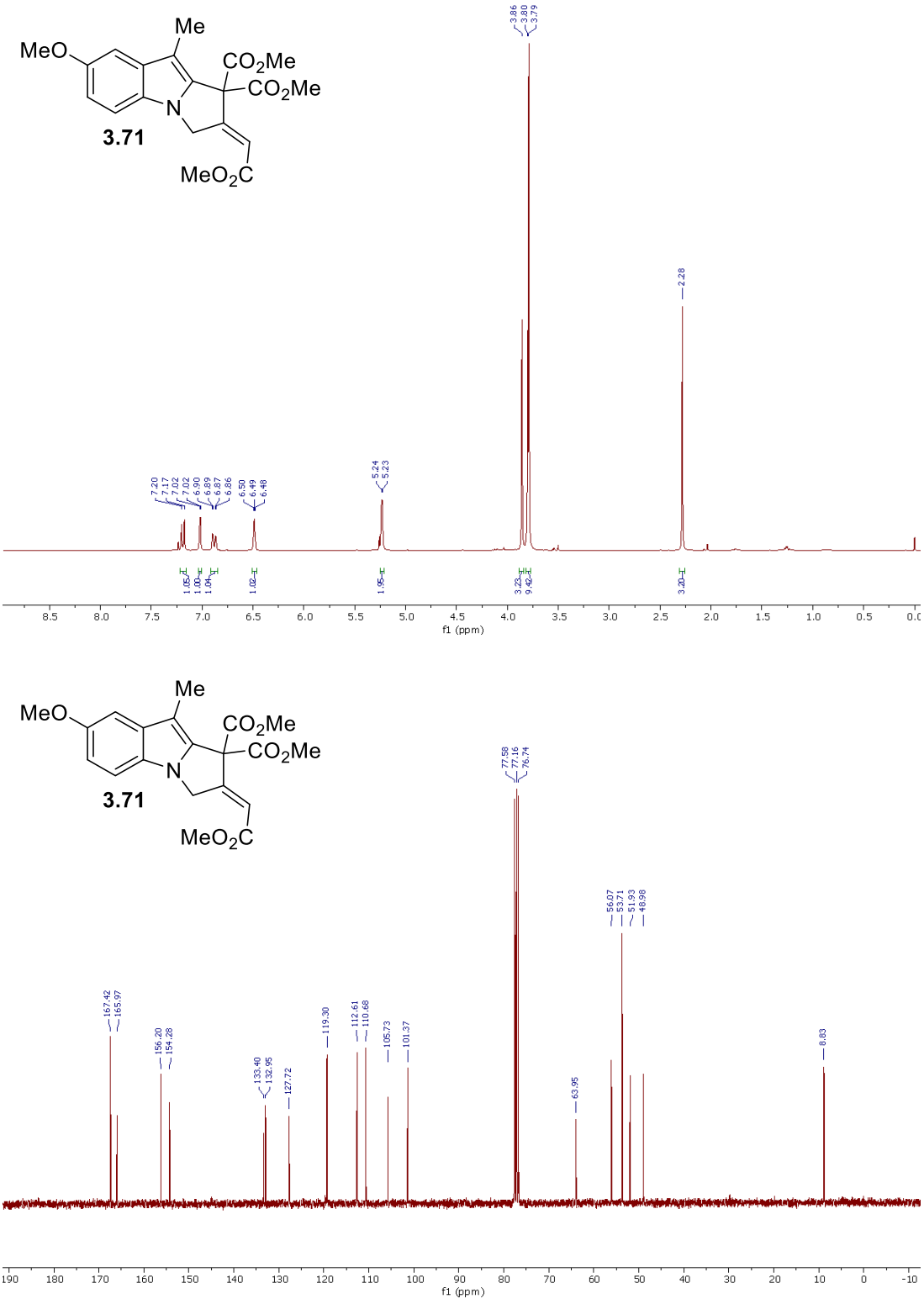

^{1}H NMR (300 MHz, $CDCl_3$) and ^{13}C NMR (75 MHz, $CDCl_3$) of compound **3.71**

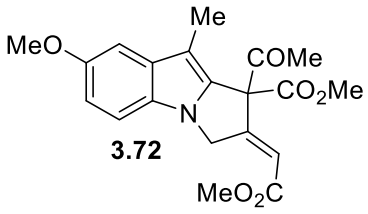

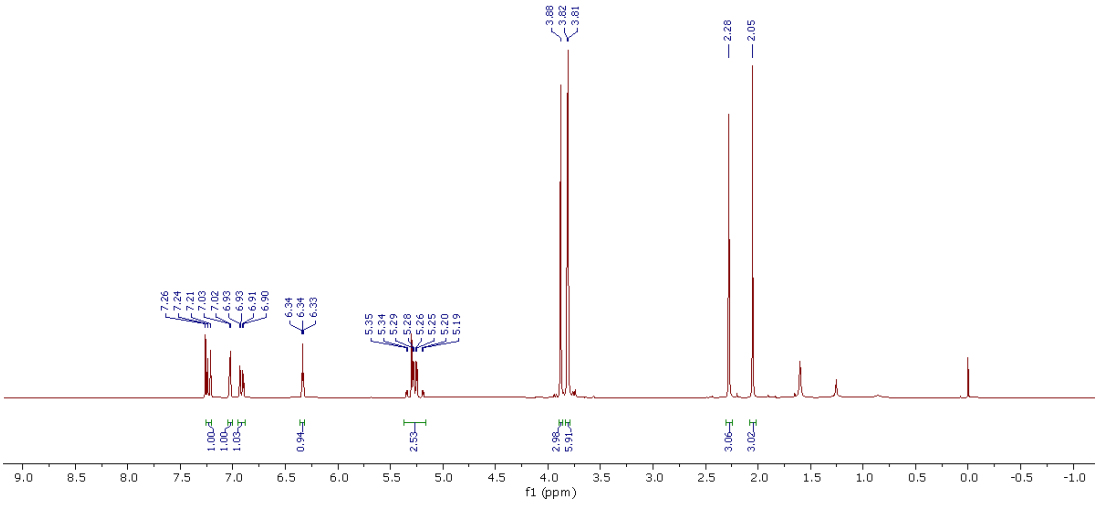

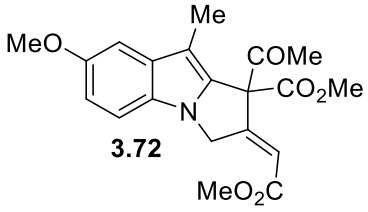

^{1}H NMR (300 MHz, $CDCl_3$) and ^{13}C NMR (75 MHz, $CDCl_3$) of compound **3.72**

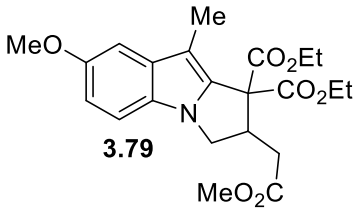

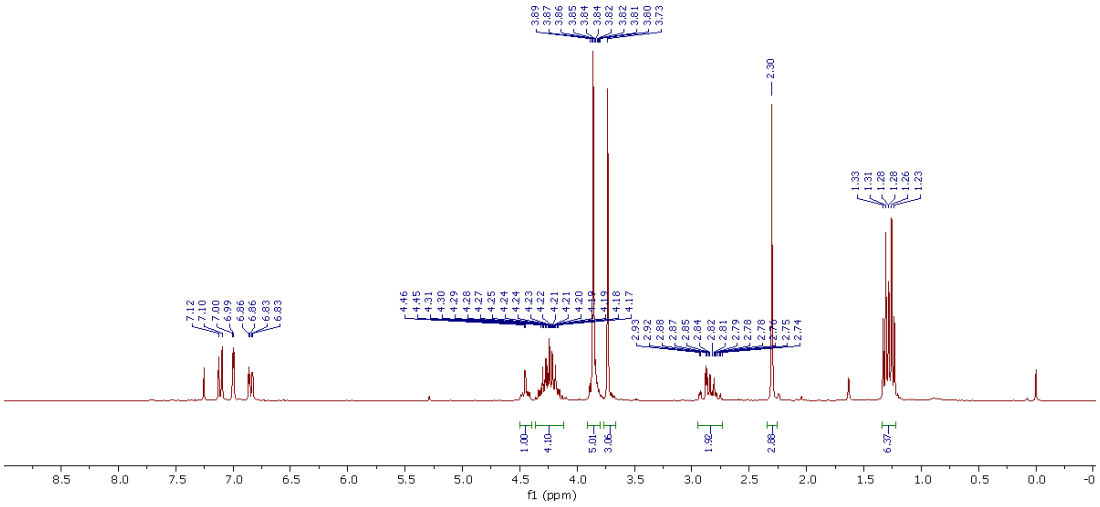

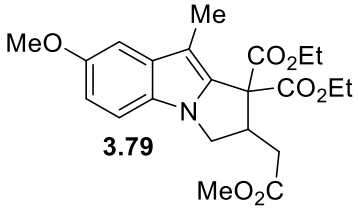

^{1}H NMR (300 MHz, $CDCl_3$) and ^{13}C NMR (75 MHz, $CDCl_3$) of compound **3.79**

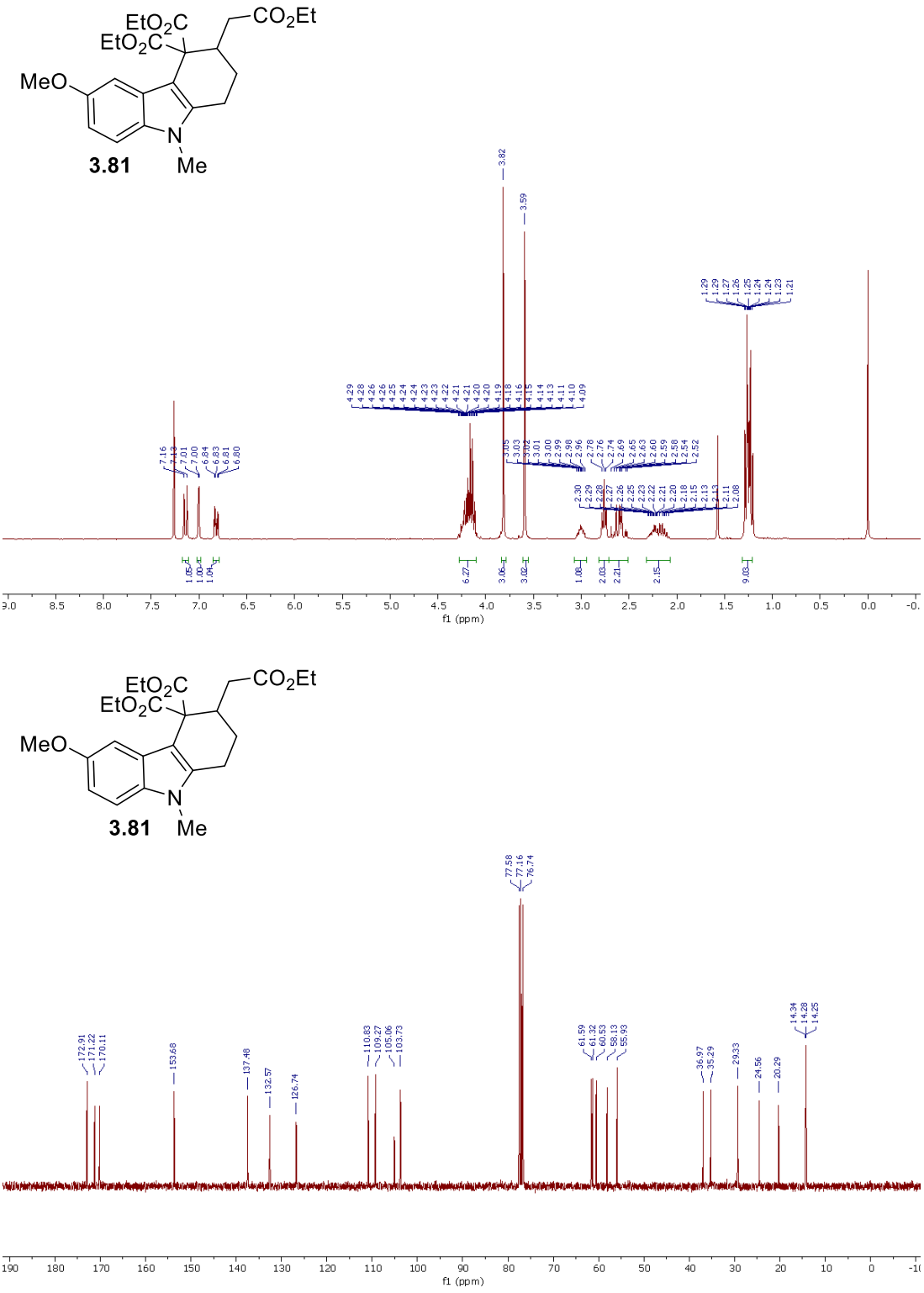

^{1}H NMR (300 MHz, $CDCl_3$) and ^{13}C NMR (75 MHz, $CDCl_3$) of compound **3.81**

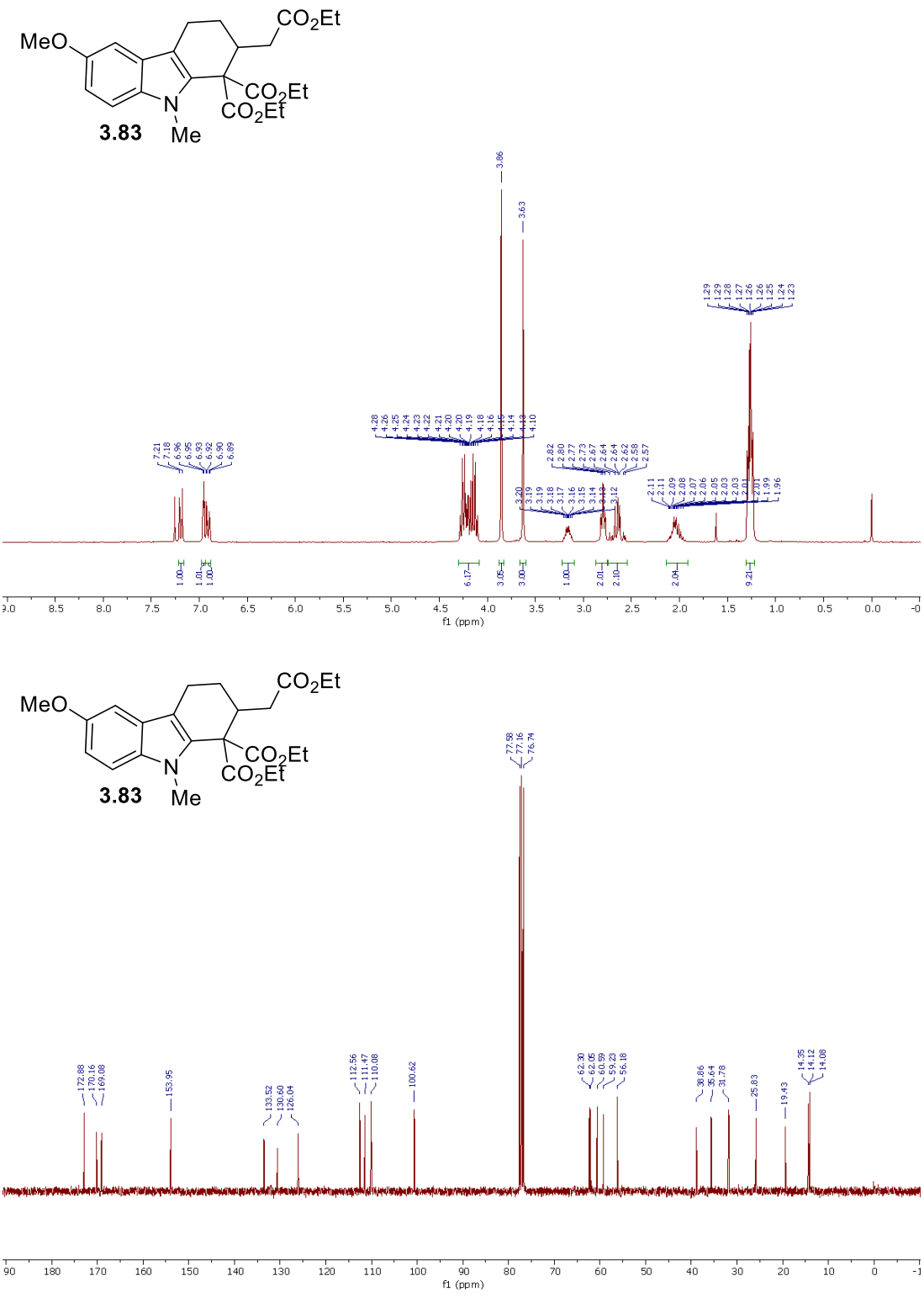

^{1}H NMR (300 MHz, $CDCl_3$) and ^{13}C NMR (75 MHz, $CDCl_3$) of compound **3.83.**

X-Ray Structure Details for Compounds 3.67 and 3.68.

Crystallization Procedure:

Tetrahydrocarbazole **3.67**

Crystals suitable for single crystal X-ray diffraction (XRD) were prepared by slow evaporation of the solvent from a saturated solution of **3.67** in ethanol at room temperature.

Tetrahydrocarbazole **3.68**

Crystals suitable for single crystal X-ray diffraction (XRD) were prepared by slow evaporation of the solvent from a saturated solution of **3.67** in ethanol at room temperature.

*Note: For X-ray structure details of Compounds **3.32** and **3.44**, see supporting information of Bhat, A.; Tucker, N.; Lin, J.-B.; Grover, H. Chem. Commun. **2021**, 57, 10556.*

Compound **3.67**

Sample: AHB-5-84

X-ray Structure Report

for

Dr. Huck Grover

Prepared by

Dr. Jian-Bin Lin

Centre for Chemical Analysis, Research and Training (C-CART),

Memorial University of Newfoundland

J.Lin@mun.ca

Feb 20, 2020

Experimental

Single-crystal X-ray diffraction data was collected at 100(2) K on a XtaLAB Synergy-S, Dualflex, HyPix-6000HE diffractometer using Cu *K*α radiation (λ = 1.5406 Å). Crystal was mounted on nylon CryoLoops with Paraton-N. The data collection and reduction were processed within *CrysAlisPro* (Rigaku OD, 2019). A multi-scan absorption correction was applied to the collected reflections. Using Olex^2 [1], the structure was solved with the ShelXT [2] structure solution program using Intrinsic Phasing and refined with the ShelXL [3] refinement package using Least Squares minimisation. All non-hydrogen atoms were refined anisotropically. The organic hydrogen atoms were generated geometrically.

1. Dolomanov, O.V., Bourhis, L.J., Gildea, R.J, Howard, J.A.K. & Puschmann, H. (2009), *J. Appl. Cryst*. 42, 339-341.

2. Sheldrick, G.M. (2015). *Acta Cryst*. A71, 3-8.

3. Sheldrick, G.M. (2015). *Acta Cryst*. C71, 3-8.

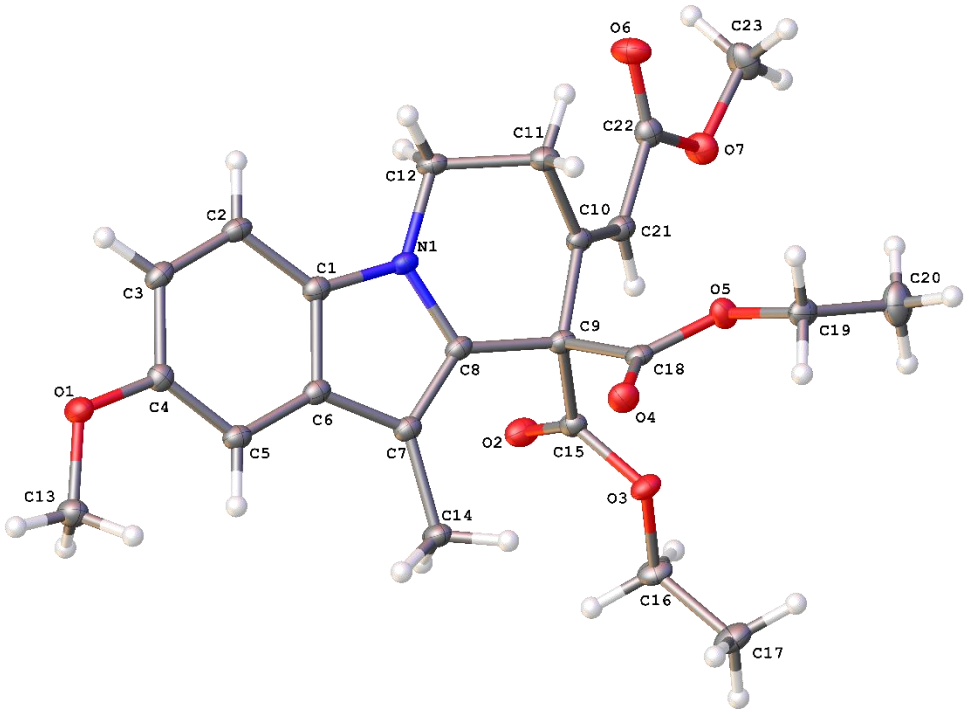

Figure 0-1: X-ray crystal structure of **3.67** (non-hydrogen atoms are represented by displacement ellipsoids at the 50% probability level).

Table 0.2: Crystal data and structure refinement for **3.67**.

Empirical formula	$C_{23}H_{27}NO_7$
Formula weight	429.45
Temperature/K	100(2)
Crystal system	triclinic
Space group	*P*-1
a/Å	8.24253(9)
b/Å	10.98466(11)
c/Å	12.92511(13)
α/°	111.4045(10)
β/°	93.4027(8)
γ/°	104.9018(9)
Volume/Å^3	1037.52(2)
Z	2
ρ_{calc}g/cm^3	1.375
μ/mm^{-1}	0.846
F(000)	456.0
Crystal size/mm^3	0.23 × 0.17 × 0.07
Radiation	Cu *K*α (λ = 1.54184)
2θ range for data collection/°	7.456 to 154.448
Index ranges	$-10 \leq h \leq 10$, $-13 \leq k \leq 13$, $-16 \leq l \leq 16$
Reflections collected	50608
Independent reflections	4341 [R_{int} = 0.0396, R_{sigma} = 0.0148]
Data/restraints/parameters	4341/0/285
Goodness-of-fit on F^2	1.037
Final *R* indexes [I>=2σ (I)]	R_1 = 0.0324, wR_2 = 0.0818
Final *R* indexes [all data]	R_1 = 0.0333, wR_2 = 0.0825
Largest diff. peak/hole / e Å^{-3}	0.32/-0.29

Table 0.3: Fractional Atomic Coordinates (×104) and Equivalent Isotropic Displacement Parameters ($Å^2$×103) for **3.67**. U_{eq} is defined as 1/3 of the trace of the orthogonalised U_{IJ} tensor.

Atom	*x*	*y*	*z*	U(eq)
O1	7298.4(9)	2147.8(8)	2002.9(6)	17.61(16)
O2	4980.1(9)	4356.3(7)	8264.9(6)	19.32(17)
O3	3746.8(9)	2303.7(7)	8305.9(6)	16.08(16)
O4	1672.3(9)	269.4(7)	5878.6(6)	17.68(16)
O5	135.2(9)	1328.8(7)	7088.5(6)	17.34(16)
O6	-850.1(10)	5499.5(8)	7510.6(7)	23.08(18)
O7	212.0(10)	6030.4(8)	9313.7(6)	20.54(17)
N1	3035.3(11)	3306.6(8)	5082.5(7)	13.90(17)
C1	4068.6(13)	3158.5(10)	4277.1(8)	14.1(2)
C2	4062.1(13)	3534.0(10)	3350.5(8)	15.5(2)
C3	5190.7(13)	3180.3(10)	2634.5(8)	15.9(2)
C4	6304.7(13)	2469.7(10)	2826.8(8)	14.7(2)
C5	6364.5(13)	2142.2(10)	3763.5(8)	14.6(2)
C6	5226.4(13)	2509.6(10)	4513.6(8)	14.0(2)
C7	4899.2(13)	2305.1(10)	5524.9(8)	14.1(2)
C8	3554.1(13)	2797.5(10)	5837.7(8)	13.36(19)
C9	2591.9(12)	2780.1(10)	6801.9(8)	13.3(2)
C10	1431.2(12)	3702.8(10)	6958.6(8)	13.8(2)
C11	444.6(13)	3465.3(10)	5847.0(8)	15.8(2)
C12	1703.8(13)	3973.9(10)	5167.2(8)	15.2(2)
C13	8518.6(14)	1504.5(11)	2178.5(9)	19.7(2)
C14	5885.0(13)	1694.8(11)	6109.5(9)	17.1(2)
C15	3914.9(13)	3255.6(10)	7873.9(8)	13.71(19)
C16	5055.4(14)	2648.9(11)	9271.1(9)	18.4(2)
C17	4759.4(15)	1412.6(12)	9565.3(9)	23.1(2)
C18	1427.1(12)	1290.5(10)	6519.2(8)	13.55(19)
C19	-1159.7(13)	30.6(10)	6870.4(9)	16.7(2)
C20	-1973.3(16)	231.2(12)	7903.5(10)	26.7(3)
C21	1334.9(13)	4584.4(10)	7970.0(9)	15.3(2)
C22	122.7(13)	5400.7(10)	8189.7(9)	16.6(2)
C23	-1057.0(15)	6722.3(12)	9644.3(10)	24.3(2)

Table 0.4: Selected Bond Distances (Å) for **3.67**.

Atom	Atom	Length/Å	Atom	Atom	Length/Å
O1	C4	1.3811(12)	C3	C4	1.4133(14)
O1	C13	1.4206(13)	C4	C5	1.3847(14)

O2	C15	1.2014(13)	C5	C6	1.4141(14)
O3	C15	1.3361(12)	C6	C7	1.4342(14)
O3	C16	1.4656(12)	C7	C8	1.3738(14)
O4	C18	1.2013(13)	C7	C14	1.5025(13)
O5	C18	1.3306(12)	C8	C9	1.5196(13)
O5	C19	1.4630(12)	C9	C10	1.5348(13)
O6	C22	1.2065(13)	C9	C15	1.5432(13)
O7	C22	1.3499(13)	C9	C18	1.5642(13)
O7	C23	1.4420(13)	C10	C11	1.5074(13)
N1	C1	1.3742(13)	C10	C21	1.3345(14)
N1	C8	1.3857(12)	C11	C12	1.5263(14)
N1	C12	1.4571(13)	C16	C17	1.5053(15)
C1	C2	1.4020(14)	C19	C20	1.4995(15)
C1	C6	1.4095(14)	C21	C22	1.4804(14)
C2	C3	1.3778(15)			

Table 0.5: Selected Bond Angles for **3.67**.

Atom	**Atom**	**Atom**	**Angle/°**	**Atom**	**Atom**	**Atom**	**Angle/°**
C4	O1	C13	116.63(8)	C7	C8	C9	129.76(9)
C15	O3	C16	114.99(8)	C8	C9	C10	110.44(8)
C18	O5	C19	117.75(8)	C8	C9	C15	107.90(8)
C22	O7	C23	114.87(9)	C8	C9	C18	109.53(8)
C1	N1	C8	108.30(8)	C10	C9	C15	111.67(8)
C1	N1	C12	125.50(8)	C10	C9	C18	107.44(8)
C8	N1	C12	126.07(9)	C15	C9	C18	109.87(8)
N1	C1	C2	129.69(9)	C11	C10	C9	111.53(8)
N1	C1	C6	107.97(9)	C21	C10	C9	122.53(9)
C2	C1	C6	122.34(9)	C21	C10	C11	125.93(9)
C3	C2	C1	117.08(9)	C10	C11	C12	108.09(8)
C2	C3	C4	121.39(9)	N1	C12	C11	108.76(8)
O1	C4	C3	113.74(9)	O2	C15	O3	124.23(9)
O1	C4	C5	124.41(9)	O2	C15	C9	123.36(9)
C5	C4	C3	121.85(9)	O3	C15	C9	112.40(8)
C4	C5	C6	117.50(9)	O3	C16	C17	107.30(8)
C1	C6	C5	119.72(9)	O4	C18	O5	125.50(9)
C1	C6	C7	107.39(9)	O4	C18	C9	124.53(9)
C5	C6	C7	132.82(9)	O5	C18	C9	109.97(8)
C6	C7	C14	125.47(9)	O5	C19	C20	106.71(8)
C8	C7	C6	106.11(9)	C10	C21	C22	125.13(9)
C8	C7	C14	128.41(9)	O6	C22	O7	122.77(10)
N1	C8	C9	119.96(9)	O6	C22	C21	127.99(10)
C7	C8	N1	110.20(9)	O7	C22	C21	109.21(9)

Table 0.6: Selected Torsion Angles for **3.67**.

A	B	C	D	Angle/°	A	B	C	D	Angle/°
O1	C4	C5	C6	-178.18(9)	C8	C9	C18	O5	-155.71(8)
N1	C1	C2	C3	-176.03(10)	C9	C10	C11	C12	-67.77(10)
N1	C1	C6	C5	175.48(9)	C9	C10	C21	C22	-173.65(9)
N1	C1	C6	C7	-1.92(11)	C10	C9	C15	O2	-61.97(13)
N1	C8	C9	C10	-15.03(12)	C10	C9	C15	O3	118.57(9)
N1	C8	C9	C15	-137.33(9)	C10	C9	C18	O4	144.09(10)
N1	C8	C9	C18	103.10(10)	C10	C9	C18	O5	-35.72(10)
C1	N1	C8	C7	-0.73(11)	C10	C11	C12	N1	54.46(10)
C1	N1	C8	C9	-177.75(8)	C10	C21	C22	O6	-6.84(18)
C1	N1	C12	C11	158.64(9)	C10	C21	C22	O7	171.37(10)
C1	C2	C3	C4	0.02(14)	C11	C10	C21	C22	5.76(16)
C1	C6	C7	C8	1.46(11)	C12	N1	C1	C2	-3.04(16)
C1	C6	C7	C14	-177.48(9)	C12	N1	C1	C6	177.69(9)
C2	C1	C6	C5	-3.87(15)	C12	N1	C8	C7	-176.74(9)
C2	C1	C6	C7	178.73(9)	C12	N1	C8	C9	6.23(14)
C2	C3	C4	O1	177.47(9)	C13	O1	C4	C3	176.40(8)
C2	C3	C4	C5	-2.56(15)	C13	O1	C4	C5	-3.57(14)
C3	C4	C5	C6	1.85(14)	C14	C7	C8	N1	178.43(9)
C4	C5	C6	C1	1.25(14)	C14	C7	C8	C9	-4.92(17)
C4	C5	C6	C7	177.87(10)	C15	O3	C16	C17	-174.54(9)
C5	C6	C7	C8	-175.46(10)	C15	C9	C10	C11	165.93(8)
C5	C6	C7	C14	5.60(17)	C15	C9	C10	C21	-14.59(13)
C6	C1	C2	C3	3.16(14)	C15	C9	C18	O4	-94.24(11)
C6	C7	C8	N1	-0.47(11)	C15	C9	C18	O5	85.94(9)
C6	C7	C8	C9	176.18(9)	C16	O3	C15	O2	-4.31(14)
C7	C8	C9	C10	168.60(10)	C16	O3	C15	C9	175.15(8)
C7	C8	C9	C15	46.30(13)	C18	O5	C19	C20	155.61(9)
C7	C8	C9	C18	-73.27(13)	C18	C9	C10	C11	-73.54(10)
C8	N1	C1	C2	-179.08(10)	C18	C9	C10	C21	105.95(10)
C8	N1	C1	C6	1.65(11)	C18	C9	C15	O2	178.93(9)
C8	N1	C12	C11	-26.01(13)	C18	C9	C15	O3	-0.53(11)
C8	C9	C10	C11	45.87(10)	C19	O5	C18	O4	-4.01(14)
C8	C9	C10	C21	-134.65(10)	C19	O5	C18	C9	175.80(8)
C8	C9	C15	O2	59.58(12)	C21	C10	C11	C12	112.76(11)
C8	C9	C15	O3	-119.88(9)	C23	O7	C22	O6	5.78(14)
C8	C9	C18	O4	24.11(13)	C23	O7	C22	C21	-172.54(8)

Compound **3.68**

Sample: AHB-A-106

X-ray Structure Report

for

Dr. Huck Grover

Prepared by

Dr. Jian-Bin Lin

Centre for Chemical Analysis, Research and Training (C-CART),

Memorial University of Newfoundland

J.Lin@mun.ca

Nov 2, 2020

Experimental

Single-crystal X-ray diffraction data was collected at 100(2) K on a XtaLAB Synergy-S, Dualflex, HyPix-6000HE diffractometer using Cu *K*α radiation (λ = 1.5406 Å). Crystal was mounted on nylon CryoLoops with Paraton-N. The data collection and reduction were processed within *CrysAlisPro* (Rigaku OD, 2019). A multi-scan absorption correction was applied to the collected reflections. Using Olex^2 [1], the structure was solved with the ShelXT [2] structure solution program using Intrinsic Phasing and refined with the ShelXL [3] refinement package using Least Squares minimisation. All non-hydrogen atoms were refined anisotropically. The organic hydrogen atoms were generated geometrically.

1. Dolomanov, O.V., Bourhis, L.J., Gildea, R.J, Howard, J.A.K. & Puschmann, H. (2009), *J. Appl. Cryst*. 42, 339-341.

2. Sheldrick, G.M. (2015). *Acta Cryst*. A71, 3-8.

3. Sheldrick, G.M. (2015). *Acta Cryst*. C71, 3-8.

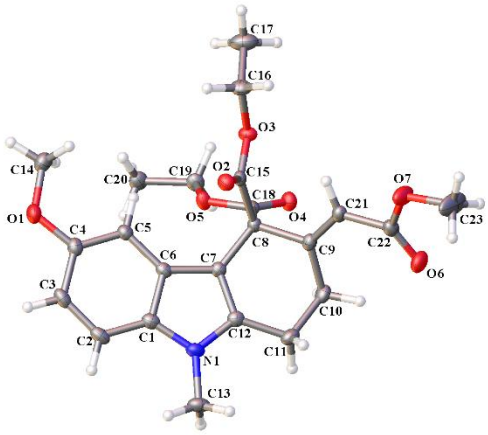

Figure 0-2: X-ray crystal structure of **3.68** (non-hydrogen atoms are represented by displacement ellipsoids at the 50% probability level).

Table 0.7: Crystal data and structure refinement for **3.68.**

Identification code	AHB-A-106
Empirical formula	$C_{23}H_{27}NO_7$
Formula weight	429.45
Temperature/K	100(2)
Crystal system	monoclinic
Space group	$P2_1/c$
a/Å	13.27378(13)
b/Å	17.12971(15)
c/Å	9.94500(9)
β/°	104.3152(10)
Volume/Å^3	2191.04(4)
Z	4
ρ_{calc}mg/mm^3	1.302
μ/mm^{-1}	0.801
F(000)	912.0
Crystal size/mm^3	0.199 × 0.136 × 0.074
2θ range for data collection	6.872 to 154.686°
Index ranges	$-15 \leq h \leq 16$, $-21 \leq k \leq 21$, $-10 \leq l \leq 12$
Reflections collected	19064
Independent reflections	4580 [R(int) = 0.0550]
Data/restraints/parameters	4580/0/286
Goodness-of-fit on F^2	1.060
Final R indexes [I>=2σ (I)]	R_1 = 0.0402, wR_2 = 0.1027
Final R indexes [all data]	R_1 = 0.0461, wR_2 = 0.1069
Largest diff. peak/hole / e Å^{-3}	0.25/-0.21

Table 0.8: Fractional Atomic Coordinates (×104) and Equivalent Isotropic Displacement Parameters ($Å^2$×103) for **3.68**. U_{eq} is defined as 1/3 of the trace of the orthogonalised U_{IJ} tensor.

Atom	***x***	***y***	***z***	**U(eq)**
O1	3799.3(8)	6228.6(6)	8214.9(9)	25.6(2)
O2	3940.5(7)	4509.9(5)	3899.1(9)	20.4(2)
O3	3788.9(7)	5496.4(5)	2363.7(9)	20.2(2)
O4	1436.0(7)	5882.2(6)	871.7(9)	21.8(2)
O5	2027.5(7)	6312.7(5)	3060.1(9)	19.2(2)
O6	1375.3(9)	3025.2(6)	-539.1(11)	31.3(2)
O7	3114.7(9)	2941.1(6)	-46.1(13)	37.0(3)
N1	902.8(9)	4168.5(7)	5272.1(11)	21.1(2)
C1	1579.5(10)	4667.5(8)	6152.1(13)	19.5(3)
C2	1725.4(11)	4796.9(8)	7573.3(14)	22.6(3)
C3	2472.2(11)	5327.4(8)	8207.2(13)	23.0(3)
C4	3068.6(10)	5730.9(8)	7437.4(13)	20.3(3)
C5	2918.6(10)	5615.7(7)	6022.7(13)	17.8(3)
C6	2169.6(10)	5068.4(7)	5368.2(13)	16.7(3)
C7	1818.5(10)	4785.9(7)	3972.9(12)	16.7(3)
C8	2221.7(10)	4964.7(7)	2706.1(12)	16.0(3)
C9	1822.4(10)	4320.2(7)	1627.0(12)	18.0(3)
C10	682.1(10)	4148.3(8)	1413.7(14)	22.3(3)
C11	454.6(10)	3801.1(8)	2735.3(14)	23.0(3)
C12	1049.0(10)	4249.7(7)	3958.6(13)	19.0(3)
C13	163.1(11)	3646.2(9)	5667.0(16)	27.4(3)
C14	4369.8(11)	6705.2(8)	7492.0(15)	26.4(3)
C15	3418.1(10)	4962.5(7)	3092.5(12)	16.1(2)
C16	4916.2(10)	5480.3(9)	2534.9(15)	25.4(3)
C17	5210.6(13)	6174.6(11)	1812(2)	38.8(4)
C18	1841.2(10)	5764.6(7)	2074.4(12)	16.4(2)
C19	1749.4(11)	7107.9(7)	2608.6(13)	20.8(3)
C20	1963.7(12)	7603.9(8)	3891.1(14)	25.3(3)
C21	2475.2(11)	3941.4(8)	1026.1(13)	19.3(3)
C22	2219.1(11)	3267.8(8)	66.6(13)	22.1(3)
C23	3008.3(17)	2265.0(12)	-941(3)	62.5(7)

Table 0.9: Selected Bond Distances (Å) for **3.68**.

Atom	Atom	Length/Å	Atom	Atom	Length/Å
O1	C4	1.3764(17)	C3	C4	1.4108(19)
O1	C14	1.4234(18)	C4	C5	1.3854(18)
O2	C15	1.2042(16)	C5	C6	1.4040(18)
O3	C15	1.3343(15)	C6	C7	1.4343(17)
O3	C16	1.4638(15)	C7	C8	1.5168(16)
O4	C18	1.2010(15)	C7	C12	1.3711(18)
O5	C18	1.3355(15)	C8	C9	1.5396(17)
O5	C19	1.4530(15)	C8	C15	1.5388(17)
O6	C22	1.2068(18)	C8	C18	1.5397(17)
O7	C22	1.3435(18)	C9	C10	1.5046(18)
O7	C23	1.4459(19)	C9	C21	1.3360(19)
N1	C1	1.3837(18)	C10	C11	1.5390(19)
N1	C12	1.3744(17)	C11	C12	1.4894(19)
N1	C13	1.4524(17)	C16	C17	1.491(2)
C1	C2	1.3960(19)	C19	C20	1.5001(19)
C1	C6	1.4123(18)	C21	C22	1.4823(18)
C2	C3	1.377(2)			

Table 0.10: Selected Bond Angles for **3.68**.

Atom	Atom	Atom	Angle/°	Atom	Atom	Atom	Angle/°
C4	O1	C14	117.42(10)	C7	C8	C18	111.78(10)
C15	O3	C16	115.32(10)	C9	C8	C18	109.39(10)
C18	O5	C19	116.45(9)	C15	C8	C9	109.18(10)
C22	O7	C23	115.54(13)	C15	C8	C18	108.56(10)
C1	N1	C13	125.88(11)	C10	C9	C8	113.55(11)
C12	N1	C1	108.45(11)	C21	C9	C8	120.69(12)
C12	N1	C13	125.67(12)	C21	C9	C10	125.66(12)
N1	C1	C2	130.11(12)	C9	C10	C11	110.99(11)
N1	C1	C6	108.25(11)	C12	C11	C10	108.79(11)
C2	C1	C6	121.64(12)	N1	C12	C11	123.60(12)
C3	C2	C1	118.17(12)	C7	C12	N1	109.74(11)
C2	C3	C4	120.79(12)	C7	C12	C11	126.65(12)
O1	C4	C3	114.24(11)	O2	C15	O3	125.04(12)
O1	C4	C5	124.27(12)	O2	C15	C8	123.82(11)

Atom	Atom	Atom	Angle/°	Atom	Atom	Atom	Angle/°
C5	C4	C3	121.48(13)	O3	C15	C8	111.05(10)
C4	C5	C6	118.26(12)	O3	C16	C17	108.13(12)
C1	C6	C7	106.15(11)	O4	C18	O5	124.69(12)
C5	C6	C1	119.64(11)	O4	C18	C8	125.21(11)
C5	C6	C7	134.21(11)	O5	C18	C8	110.09(10)
C6	C7	C8	129.68(11)	O5	C19	C20	106.74(10)
C12	C7	C6	107.40(11)	C9	C21	C22	126.52(12)
C12	C7	C8	122.79(11)	O6	C22	O7	123.11(12)
C7	C8	C9	107.63(10)	O6	C22	C21	128.76(13)
C7	C8	C15	110.27(10)	O7	C22	C21	108.13(11)

Table 0.11: Selected Torsion Angles for **3.68.**

A	B	C	D	Angle/°	A	B	C	D	Angle/°
O1	C4	C5	C6	177.71(11)	C9	C8	C18	O4	-10.53(17)
N1	C1	C2	C3	179.17(13)	C9	C8	C18	O5	169.51(10)
N1	C1	C6	C5	179.88(11)	C9	C10	C11	C12	43.36(14)
N1	C1	C6	C7	-0.15(14)	C9	C21	C22	O6	14.5(2)
C1	N1	C12	C7	0.76(15)	C9	C21	C22	O7	-165.55(13)
C1	N1	C12	C11	179.86(12)	C10	C9	C21	C22	-1.8(2)
C1	C2	C3	C4	0.3(2)	C10	C11	C12	N1	169.88(12)
C1	C6	C7	C8	-175.26(12)	C10	C11	C12	C7	-11.18(18)
C1	C6	C7	C12	0.60(14)	C12	N1	C1	C2	180.00(13)
C2	C1	C6	C5	-0.45(19)	C12	N1	C1	C6	-0.36(14)
C2	C1	C6	C7	179.53(12)	C12	C7	C8	C9	-13.57(16)
C2	C3	C4	O1	-178.63(12)	C12	C7	C8	C15	-132.57(12)
C2	C3	C4	C5	0.7(2)	C12	C7	C8	C18	106.57(13)
C3	C4	C5	C6	-1.57(19)	C13	N1	C1	C2	-0.1(2)
C4	C5	C6	C1	1.42(18)	C13	N1	C1	C6	179.59(12)
C4	C5	C6	C7	-178.55(13)	C13	N1	C12	C7	-179.19(12)
C5	C6	C7	C8	4.7(2)	C13	N1	C12	C11	-0.1(2)
C5	C6	C7	C12	-179.43(14)	C14	O1	C4	C3	-174.77(12)
C6	C1	C2	C3	-0.43(19)	C14	O1	C4	C5	5.90(19)
C6	C7	C8	C9	161.73(12)	C15	O3	C16	C17	-172.38(12)
C6	C7	C8	C15	42.73(17)	C15	C8	C9	C10	166.98(10)
C6	C7	C8	C18	-78.13(16)	C15	C8	C9	C21	-9.68(16)
C6	C7	C12	N1	-0.84(14)	C15	C8	C18	O4	108.52(14)

A	B	C	D	Angle/°	A	B	C	D	Angle/°
C6	C7	C12	C11	-179.91(12)	C15	C8	C18	O5	-71.44(12)
C7	C8	C9	C10	47.28(13)	C16	O3	C15	O2	3.47(18)
C7	C8	C9	C21	-129.38(12)	C16	O3	C15	C8	-173.17(10)
C7	C8	C15	O2	38.17(16)	C18	O5	C19	C20	176.46(11)
C7	C8	C15	O3	-145.14(10)	C18	C8	C9	C10	-74.36(13)
C7	C8	C18	O4	-129.63(13)	C18	C8	C9	C21	108.98(13)
C7	C8	C18	O5	50.41(13)	C18	C8	C15	O2	160.93(11)
C8	C7	C12	N1	175.37(11)	C18	C8	C15	O3	-22.38(13)
C8	C7	C12	C11	-3.7(2)	C19	O5	C18	O4	-2.48(18)
C8	C9	C10	C11	-65.50(14)	C19	O5	C18	C8	177.48(10)
C8	C9	C21	C22	174.46(12)	C21	C9	C10	C11	110.96(14)
C9	C8	C15	O2	-79.88(14)	C23	O7	C22	O6	-0.6(2)
C9	C8	C15	O3	96.81(12)	C23	O7	C22	C21	179.43(16)

Chapter 4: Rh(III)-Catalyzed C–H Activation/Migratory Carbene Insertion and Decarboxylation Cascade — A key Strategy Toward Synthesis of Pyranocarbazoles From *Murraya Koenigii.*

Statement of Co-Authorship

Aabid H. Bhat: Performed the synthetic work, data collection and data analysis.

Huck K. Grover: Principal investigator (PI) of the work, who led the project and majorly contributed to the interpretation and analysis of data.

1.24 Introduction

As illustrated in Chapter 2 and Chapter 3, we have been successful in developing a cascade protocol involving a C(sp^2)–H insertion of a carbenoid, derived from an α-diazocarbonyl compound **4.2**, followed by an annulation step onto a pendant electrophile to generate various cyclic products **4.4** (Scheme 4.1A). Outside of our contributions, the field of research devoted to trapping carbene insertion intermediates (such as **4.3**) with electrophiles has steadily been growing over the last decade. In fact, as discussed in Chapter 1 (Scheme 1.8), it was highlighted how many different types of electrophiles have been utilized to trap the carbene insertion intermediate to form various substituted heterocycles. Surprisingly, among this extensive list of compatible electrophiles, esters, which have the potential to undergo Dieckmann condensation with enolate nucleophiles, have remained unexplored (Scheme 4.1B). In continuation of our interest in cascade reactions based on a carbene insertion/annulation protocol, we hypothesized that carbene insertion on arene **4.5** would generate intermediate **4.7**, which can be trapped intramolecularly by a tethered ester electrophile *via* Dieckmann condensation, for the synthesis of phenolic scaffold **4.9**. Although both individual transformations, intermolecular C(sp^2)–H carbene insertion and Dieckmann condensation are well established, there was no report in the literature to utilize both in a cascade fashion. Importantly, through the development of this reaction, it is envisioned that upon etherification, phenol **4.9** could serve as a vital synthetic intermediate for the construction of various structurally similar pyrano[3,2-*a*]carbazole scaffolds **4.10**. Moreover, pyranocarbazoles represent a highly desirable structural motif found in natural products such as those obtained from the *Murray Koenigii* (Figure 4.1).[1]

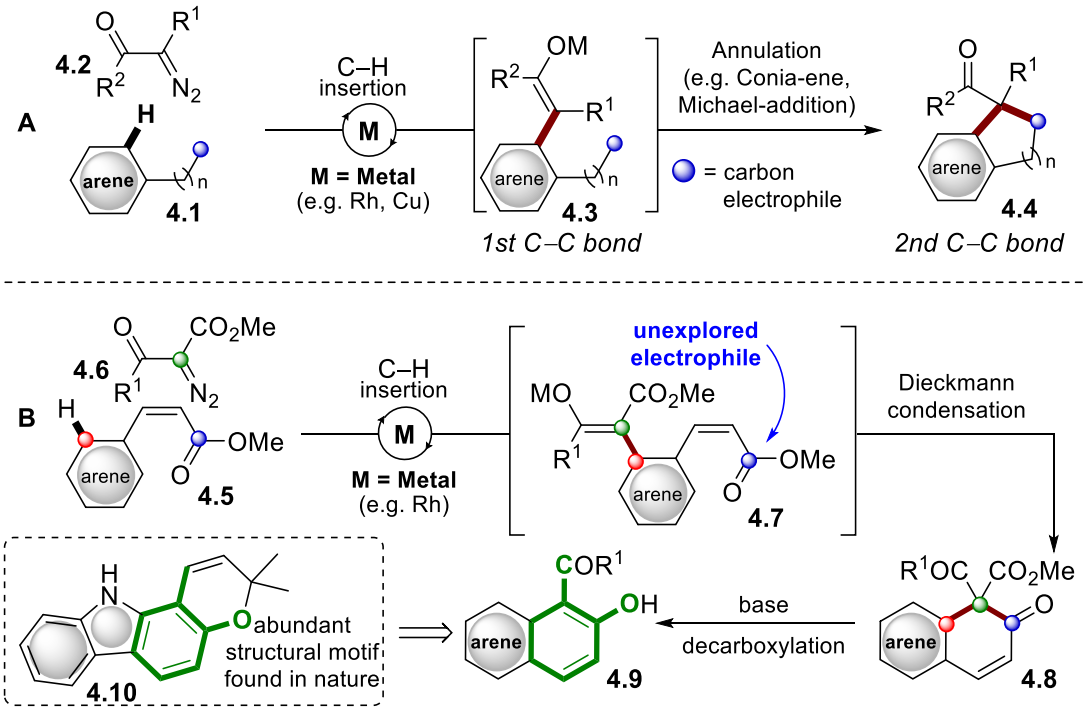

Scheme 0.1: (**A**) Previous work on C–H insertion/annulation cascade reaction protocol: (**B**): Proposed synthesis of phenolic framework **4.9** *via* C–H insertion/Dieckmann condensation.

Murraya Koenigii (*Linn.*) Spreng (Family: *Rutaceae*) is a tropical to subtropical tree found in Southeast Asia. It is commonly used in culinary spices due to its aromatic smell. Various parts of this edible plant have been used in conventional and folk medicine for the treatment of rheumatism, traumatic injury, influenza, and other diseases.[1] *Murraya Koenigii* is known to be the richest source of carbazole alkaloids.[2] Many bioactive compounds are present in *M. koenigii* and some of the pyranocarbazole alkaloids include mahanine **4.12**, murrayamine A **4.13**, murrayamine I **4.14**, koenimbine **4.15**, murrayacine **4.16** and girinimbine **4.17** (Figure 4.1).

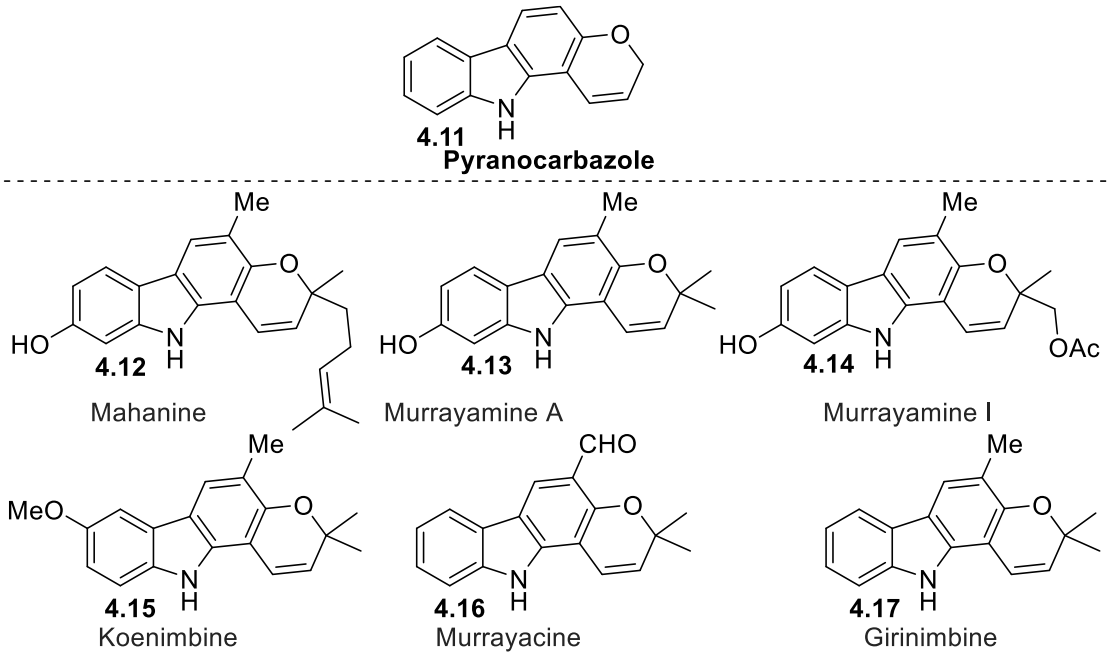

Figure 0.1: Notable examples of pyranocarbazoles from Murraya *K*oenigii.

Among the natural products obtained from *Murraya Koenigii*, mahanine **4.12** is the hallmark member in terms of bioactivities. Mahanine **4.12** has shown range of biological activities including cytotoxicity against human leukemia cells (HL60),10 (U937),[11] antimicrobial activity against *Bacillus cereus* and *Staphylococcus aureus*.[10a] Mahanine **4.12** is a potent anticancer molecule against various cancers including the inhibition of growth of prostate cancer cells.[12] Recently it was also found to be a potential antileishmanial agent.[13] In contrast, girinimbine **4.17**, the structurally least complex natural product of the family members, has shown anticancer properties involving free radical scavenging and apoptosis.[4a,5] Additionally, this compound inhibits cyclooxygenase activity, demonstrating antiplatelet properties.[6] Girinimbine was also reported to be cytotoxic against various cell lines, causing cell death by inducing apoptosis. It also exhibits anti-trichomonal,[7] anti-bacterial,[8] and anti-tumor activities. Furthermore, due to the structural simplicity of girinimbine **4.17** this was the initial target to test for C–H insertion/Dieckmann condensation reaction manifold. If successful, this strategy could be applied to all other related

family members or non-natural analogs of girinimbine. Moreover, we realized that the indole framework, which is a backbone structure of girinimbine, can be used as a starting point or a retrosynthon to devise a route for the total synthesis of girinimbine.

1.25 Hypothesis

From a retrosynthetic standpoint it was envisioned that the pyran ring of girinimbine **4.17** could be constructed through a late-stage annulation of allylic alcohol **4.18**, which itself could come from Grignard type addition to aldehyde **4.19** (Scheme 4.2). Aldehyde **4.19** can be obtained from the reduction of ester **4.20**, which itself can be synthesized through the decarboxylation of diester carbazole **4.21**. The synthesis of diester carbazole **4.21** can be achieved *via* the proposed tandem C–H insertion/Dieckmann condensation between indole ester **4.23** and *α*-diazocarbonyl **4.22**. Indole ester **4.23** can be obtained through olefination of commercially available indole-3-carboxaldehyde **4.24**.

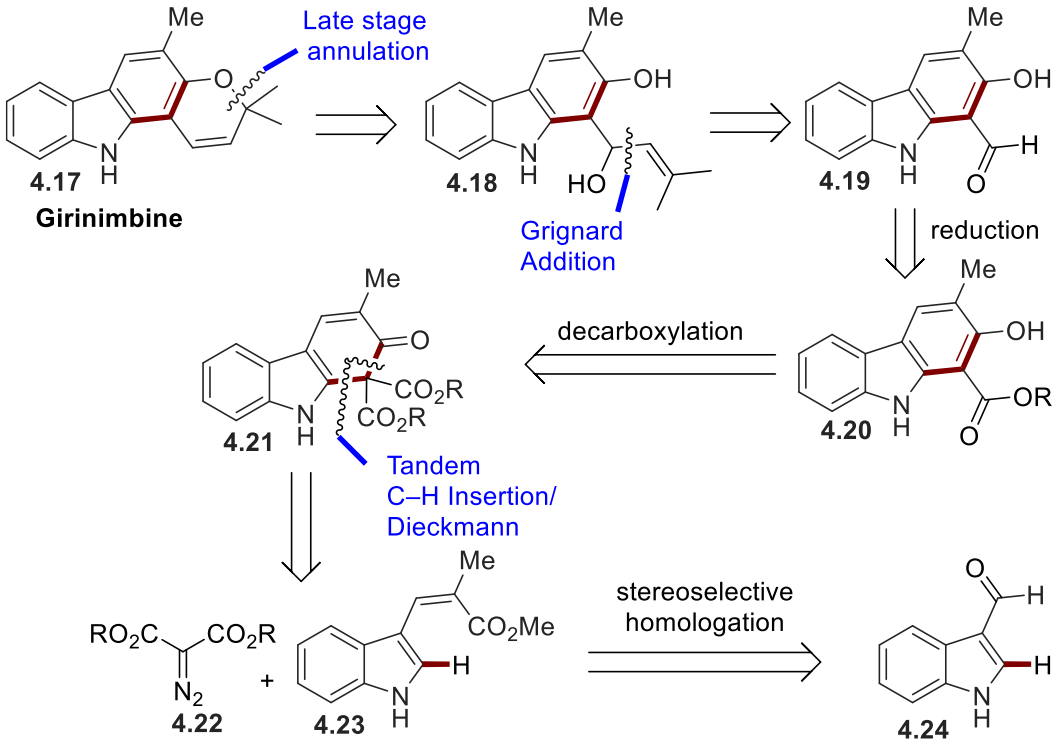

Scheme 0.2: Retrosynthesis of Girinimbine **4.17**.

1.26 Results and Discussion

The synthesis began with preparation of indole 3-carboxyldehyde **4.24** from indole **4.25** through Vilsmeier-Haack reaction in 89% yield (Scheme 4.3A).[14] Next, we synthesized the *α*-methyl-substituted phosphonoacetate reagent **4.29** needed to install the *Z*-*α,β*-unsaturated ester required for our tandem insertion/annulation strategy (Scheme 4.3B).[15] Finally, Horner–Wadsworth–Emmons (HWE) reaction of aldehyde **4.24** and HWE reagent **4.29** in THF and NaH conditions afforded a 1:7 *E/Z* mixture of methyl ester **4.23** in 76% yield (Scheme 4.3C).[16]

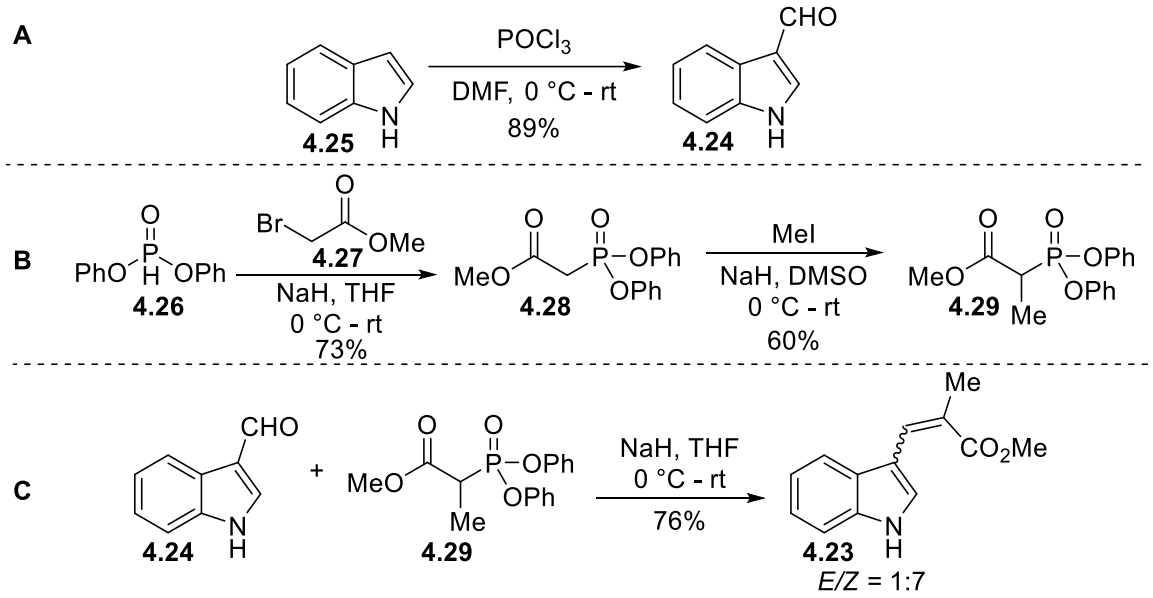

Scheme 0.3: (**A**) Synthesis of indole 3-carboxyldehyde **4.24**, (**B**) Synthesis of HWE reagent **4.29** (**C**) Synthesis of *Z*-*α,β*-unsaturated ester **4.23**.

1.26.1 Attempted Rh(II)-catalyzed insertion/Dieckmann condensation between substituted indole ester 4.23 and dimethyl diazomalonate 4.30

The initial attempt toward the synthesis of annulation product **4.32** was made by treating indole ester **4.23** with dimethyl diazomalonate **4.30** in CH_2Cl_2 under $Rh_2(OAc)_4$ conditions (Scheme 4.4). Unfortunately, intermediate C2 insertion product **4.31** did not form, although some

competing C5, C6 benzenoid insertions were observed through NMR analysis. This result parallels observations made in our previous work when exploring various C3 substituted indoles in diazo coupling reactions (see Chapter 2, Section 2.5.1). Perhaps, due to the pyrrole ring being conjugated with the electron-withdrawing ester group **4.33**, which ultimately could decrease the nucleophilicity of the ring, renders the desired C–C coupling ineffective with this starting material. It should be noted that several other catalysts including $Rh_2(tfa)_4$, $Rh_2(oct)_4$ and $Cu(tfacac)_2$ were explored in this reaction, but all were unsuccessful in forming the desired C–C bond.

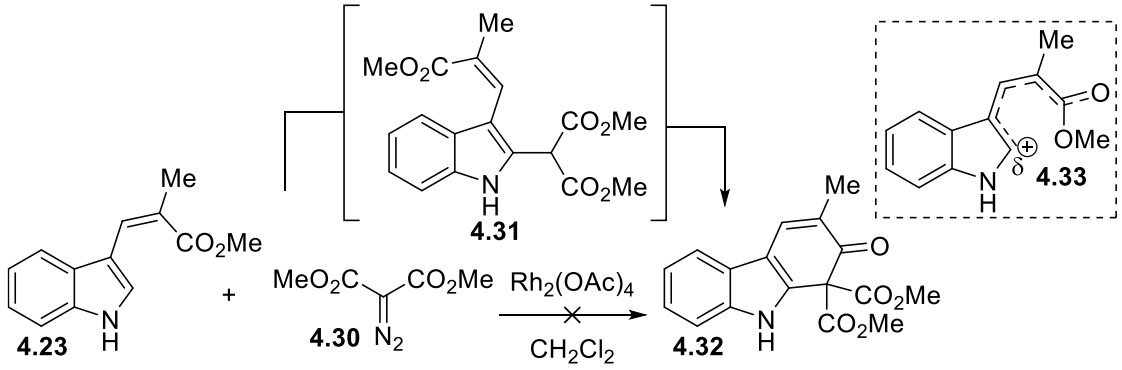

Scheme 0.4: Attempted Rh(II)-catalyzed tandem insertion/Dieckmann condensation.

1.26.2 Revised Strategy

Driven by the lack of success forming the desired C–H insertion product **4.31** under Rh(II) catalysis, an alternative approach based on a directing-group-enabled C–H activation/migratory carbene insertion was considered to forge the desired C–C bond between substituted indole **4.41** and α-diazocarbonyl **4.42** under Rh(III) catalysis (Scheme 4.5B). In this strategy the assistance of a directing group (DG) on an indole substrate **4.35** will direct a metal catalyst into the proximity of C2 position on indole, leading to its selective activation and generation of organometallic intermediate **4.36** (Scheme 4.5A). This intermediate **4.36**, when subjected to a reaction with diazocarbonyl **4.37**, results in the generation of metal carbene **4.38** and subsequent migratory insertion forms the C–C bond in **4.39**. To test this approach indole **4.41** was synthesized. The

synthesis began with treating indole 3-carboxyldehyde **4.24** with 2-chloropyrimidine under NaH in DMF conditions to obtain **4.40** in 74% yield (Scheme 4.5B). Horner–Wadsworth–Emmons olefination of aldehyde with phosphonate reagent **4.29** provided *α,β*-unsaturated ester **4.41** as 1:7 *E/Z* mixture in 63% yield. With **4.41** in hand, we next focused on the key C–C bond forming reaction. Ester **4.41** was treated with dimethyl diazomalonate **4.42** in DCE under Rh(III) conditions. To our satisfaction, this reaction led to the formation of the C-2 insertion product **4.43** in a 75% yield. Unfortunately, the subsequent annulation process to generate **4.44** did not take place under these specific conditions.

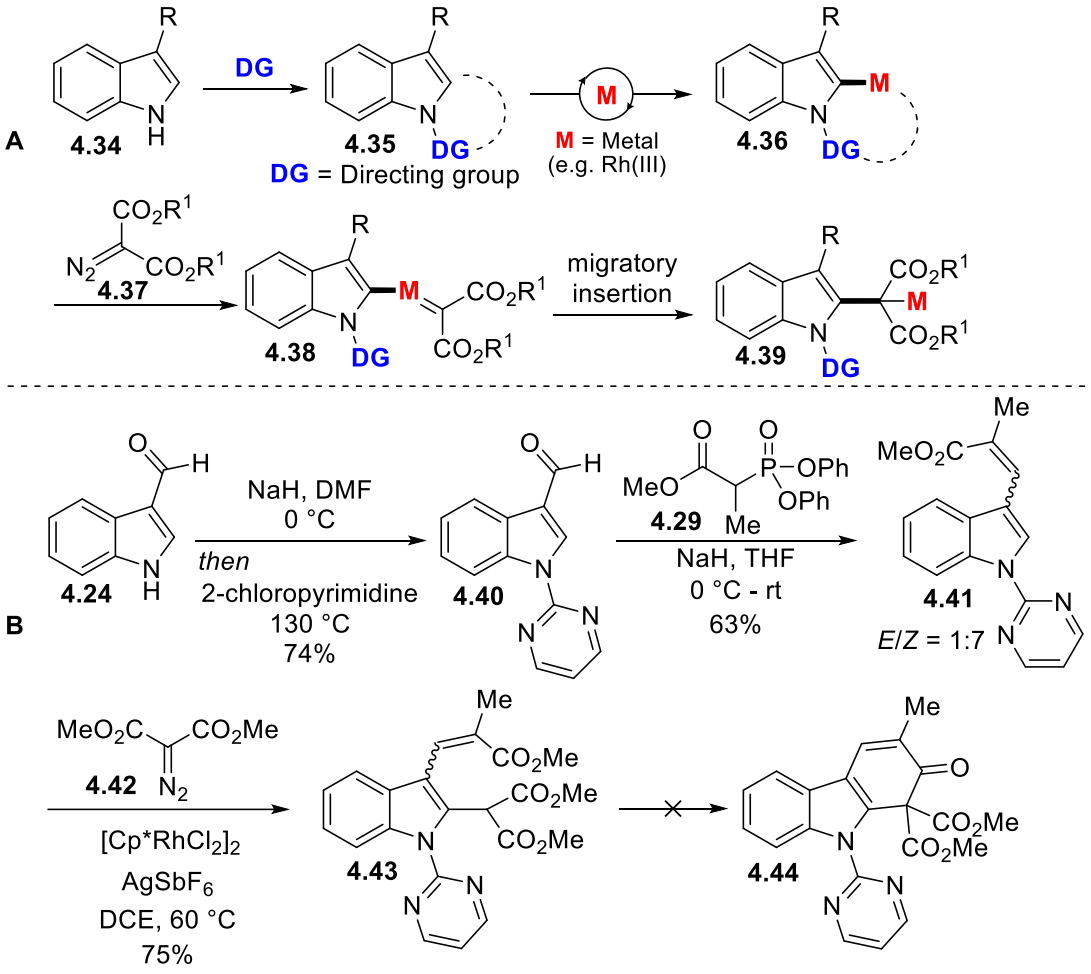

Scheme 0.5: (**A**) Plausible mechanism of directed C–H activation/migratory carbene insertion under Rh(III) catalysis. (**B**) Attempted synthesis of phenolic framework **4.44**.

The rationale for the unsuccessful annulation can be understood from the mechanism of Dieckmann condensation in which all the steps are reversible from **4.45** → **4.48** (Scheme 4.6A). For a Dieckmann condensation reaction to be successful, the cyclic *β*-keto ester **4.48** formed upon condensation (**4.47** → **4.48**) is required to contain an acidic alpha hydrogen. It is the presence of this proton that makes Dieckmann reaction possible since it is removed in an irreversible acid-base step which is the driving force that shifts the equilibrium in favor of the condensation product **4.50**. Based on the understanding of mechanism it was necessary to remove one of the esters of **4.43**, prior to the annulation event, to overcome the reversibility problem. To this end C2 insertion product **4.43** was subjected to dealkoxycarbonylation under Krapcho conditions (Scheme 4.6B). Unfortunately, selective removal of ester from **4.43** proved difficult in our hands.

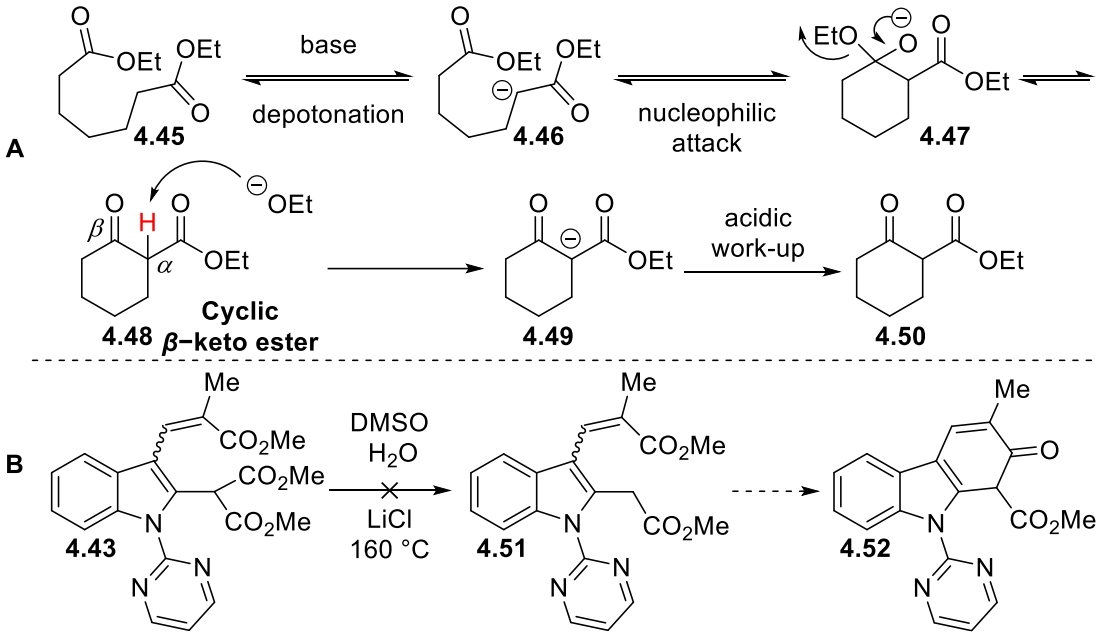

Scheme 0.6: (**A**) Mechanism of Dieckmann condensation showing importance of acidic hydrogen in ß-keto ester **4.48** (**B**) Attempted Krapcho dealkoxycarbonylation.

While facing difficulty in the removal of one ester moiety under Krapcho dealkoxycarbonylation conditions we came across a reported reaction manifold in which an

α-diazocarbonyl **4.54**, derived from Meldrum's acid, underwent a selective C–H insertion and subsequent decarboxylation reaction under Rh(III) conditions (Scheme 4.7A).[17] Utilizing this chemistry, we treated ester **4.41** with Meldrum's diazo **4.54** in ethanol under Rh(III) conditions (Scheme 4.7B). To our delight, the desired 2-acetate substituted indole **4.56** was obtained in 86% yield *via* a C2–H selective insertion and subsequent decarboxylation process in one-pot. Upon treating the insertion product **4.56** with NaOEt in ethanol at 40 °C, carbazole **4.57** was obtained in a 98% yield.

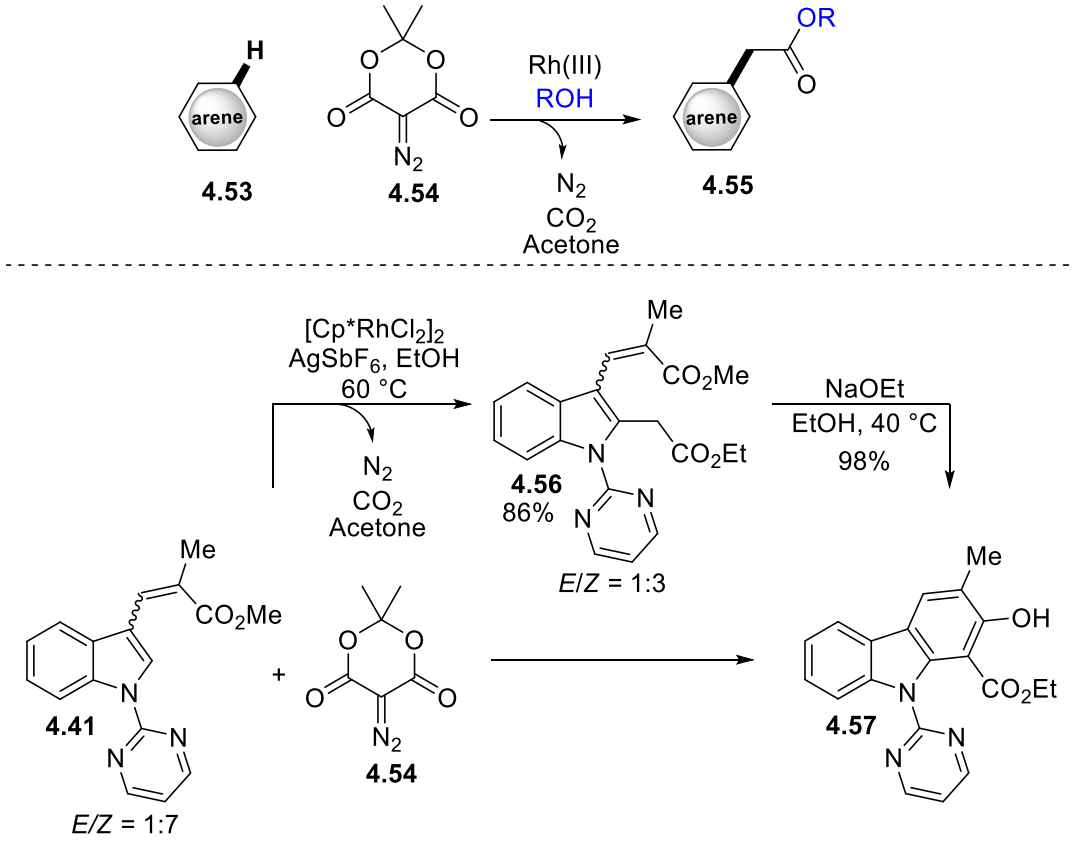

Scheme 0.7: (**A**) Reaction of Meldrum's diazo **4.54** under Rh(III) conditions, (**B**) Rh(III)-catalyzed two-step protocol for the synthesis of carbazole **4.57**.

It is important to note from the above results that the *E/Z* isomer ratio changes significantly from 1:7 to 1:3 during the insertion step **4.41** → **4.56**. Initially, it was believed that this erosion in

olefin geometry would be detrimental in the desired annulation step as it was hypothesized that only the isomer with the *Z*-configuration, (*Z*)-**4.56**, could undergo the Dieckmann condensation to deliver **4.57** (Scheme 4.8). However, not only did the expected (*Z*)-isomer **4.58** undergo condensation under base-mediated reaction conditions, but so did the (*E*)-isomer **4.60**, resulting in a near quantitative yield of **4.57**. While the (*E*)-isomer **4.60** does not have the correct configuration to undergo Dieckmann condensation it is likely that upon deprotonation, **4.59** can undergo an alkene isomerization, leading to the (*Z*)-isomer **4.60** → **4.58** which undergoes the desired annulation to form carbazole **4.57** (Scheme 4.8).

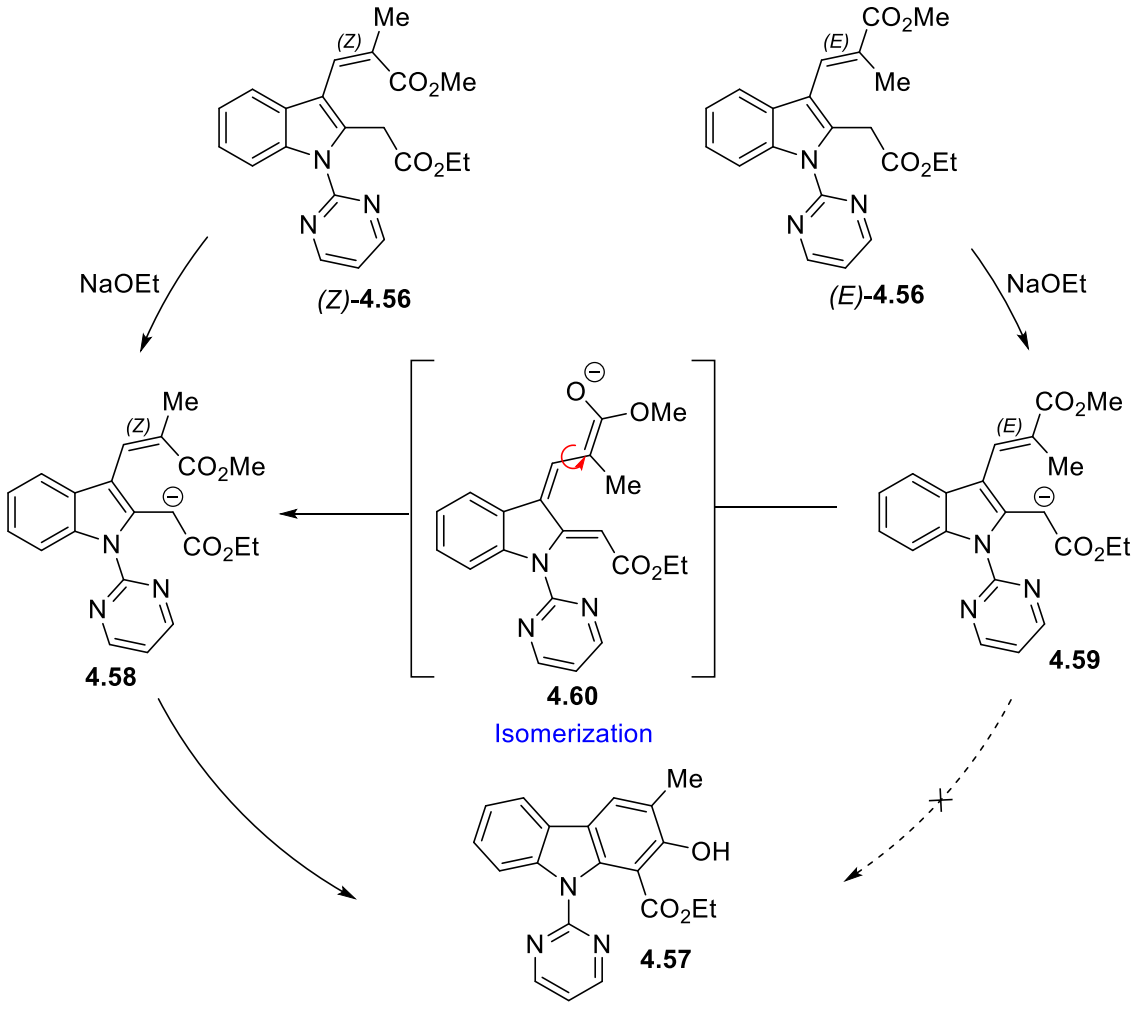

Scheme 0.8: Plausible explanation of conversion of (*E*)-isomer **4.60** to the carbazole **4.57**.

1.27 Summary and Future Work

Overall, the key cascade reaction involving Rh(III)-catalyzed C–H activation, migratory carbene insertion, and decarboxylation of Meldrum's diazo **4.54** in one-pot has been an important milestone in this project. Upon base-mediated annulation, carbazole **4.57** was constructed in high overall yields. Compound **4.57** represents a key carbazole intermediate with a functional handle to further explore the synthesis of pyranocarbazole natural products.

Future work on this project includes completing the synthesis of the girinimbine **4.17** by first reducing an ester **4.57** to the corresponding aldehyde **4.63** (Scheme 4.9). With aldehyde **4.63** in hand, Grignard addition with **4.64** would provide allylic alcohol **4.65**, which under protic acid conditions could undergo annulation to form pyran **4.66**. The final removal of directing group[18] would furnish girinimbine **4.17** and complete the synthetic efforts to the first member of the *Murraya Koenigii* pyranocarbazole family.

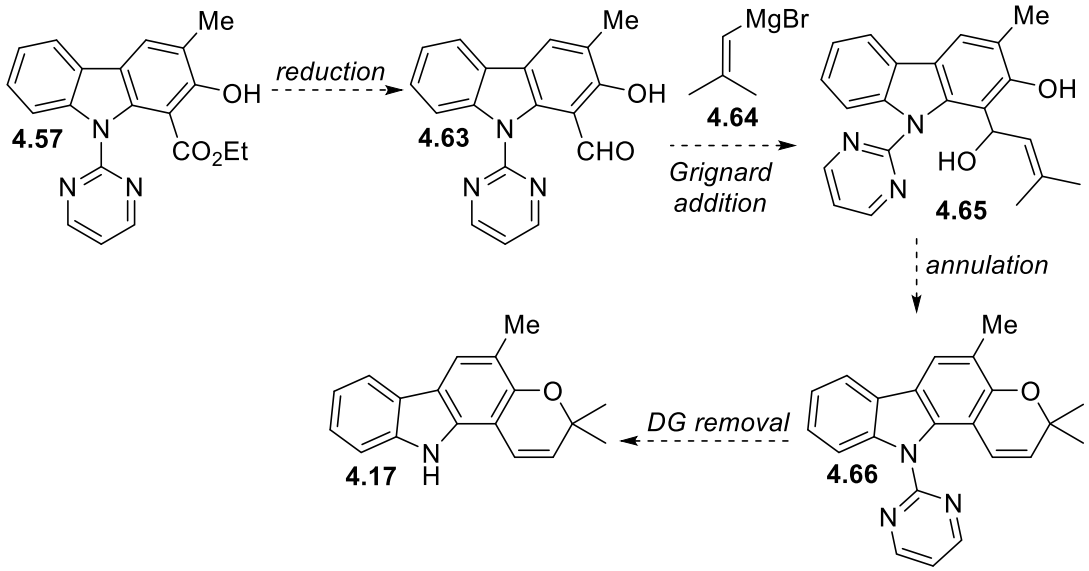

Scheme 0.9: Future work towards synthesis of girinimbine **4.17**.

1.28 Experimental

General Procedures

Unless stated otherwise, all reactions were performed in flame-dried glassware under an atmosphere of dry nitrogen. Dry trifluorotoluene ($PhCF_3$) and *N*,*N*-dimethylformamide (DMF) were obtained from Sigma Aldrich SureSeal™ bottles. Dry methyl *tert*-butyl ether (MTBE) was obtained from Alfa Aesar™. All other reagents were used as received from commercial sources unless stated otherwise. When indicated, solvents or reagents were degassed by sparging with nitrogen for 10 min in an ultrasound bath at 25 °C. For reactions conducted above room temperature, oil bath heating was used as the heat source. Reactions were monitored by thin layer chromatography (TLC) on Silicycle Siliaplate™ glass-backed TLC plates (250 μm thickness, 60 Å porosity, F-254 indicator) and visualized by UV irradiation or development with an anisaldehyde. Volatile solvents were removed under reduced pressure with a rotary evaporator. All flash column chromatography was performed using Silicycle SiliaFlash® F60, 230-400 mesh silica gel (40-63 μm). ^{1}H NMR and ^{13}C NMR spectra were recorded with Bruker AV, spectrometers operating at 300 or 500 MHz for ^{1}H (75 or 125 MHz for ^{13}C) in $CDCl_3$ or acetone-D_6. Except when noted otherwise, chemical shifts are reported relative to the residual solvent signal (^{1}H NMR: δ = 7.26 ($CDCl_3$), δ = 2.05 (acetone-D_6); ^{13}C NMR: δ = 77.16 ($CDCl_3$)). NMR data are reported as follows: chemical shift (multiplicity, coupling constants where applicable, number of hydrogens). Splitting is reported with the following symbols: s = singlet, bs = broad singlet, d = doublet, t = triplet, app t = apparent triplet, dd = doublet of doublets, ddd = doublet of doublet of doublets, dddd = doublet of doublet of doublet of doublets, m = multiplet.

Note: In adherence to ethical principles of transparency and academic integrity, it is essential to emphasize that this project is at an early stage of research. Consequently, only a limited amount of characterization data has been collected and analyzed thus far. This disclosure is made to avoid any potential misinterpretation or misrepresentation of the findings and to acknowledge the incomplete nature of the current research endeavor. It is imperative for researchers and readers to recognize the preliminary status of the project, and any conclusions drawn, or implications made must be approached with caution and subject to further scrutiny as the investigation progresses and more comprehensive data is obtained.

Synthesis and Characterization of Substituted Indole Starting Materials

Scheme 4.9: Synthesis of methyl (2*Z*)-3-(1*H*-indol-3-yl)-2-methylprop-2-enoate (**4.23**)

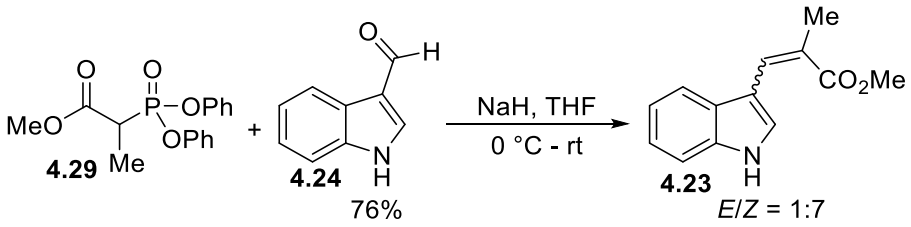

To a solution of methyl 2-(diphenylphosphono)propionate **4.29** (796 mg, 2.48 mmol, 1.2 equiv) in THF (12 mL) was added NaH (107 mg, 2.69 mmol, 1.3 equiv) in one portion at 0 ºC. The reaction was then stirred for 30 min at the same temperature before the adding the solution of **4.24** (0.300 g, 2.07 mmol, 1.0 equiv) in THF. The mixture was stirred at room temperature for another 2 h before quenching with water. The mixture was extracted with EtOAc (×2). The organic layers were combined, washed with brine, dried over $MgSO_4$, and concentrated *in vacuo*. The residue was purified by a column chromatography (5 - 40% EtOAc in hexanes) to afford 1:7 *E/Z* mixture methyl ester **4.23** (338 mg, 1.57 mmol, 76%) as light brown oil: R_f = 0.30, 35% EtOAc in hexanes. ^{1}H NMR (300 MHz, $CDCl_3$) δ 8.40 (s, 1H). 8.31 (d, *J* = 2.7 Hz, 1H), 7.75 – 7.66 (m, 1H),

7.42 – 7.32 (m, 1H), 7.24 – 7.17 (m, 1H), 7.12 (s, 1H), 3.77 (s, 3H), 2.18 (d, *J* = 1.4 Hz, 3H), 1.57 (s, 1H).

Scheme 4.10: Synthesis of 1-(pyrimidin-2-yl)-1*H*-indole-3-carbaldehyde (**4.40**)

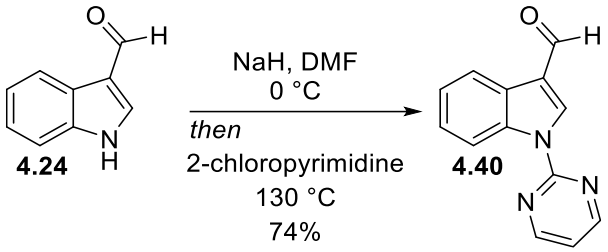

To a solution of indole 3-carboxyldehyde **4.24** (2.00 g, 17.1 mmol, 1.0 equiv.) in DMF (42 mL) was added sodium hydride (60% wt. in mineral oil, 751 mg, 18.8 mmol, 1.1 equiv.) portion-wise. The reaction mixture was allowed to stir at room temperature for 1 h. To the solution was added 2-chloropyrimidine (2.30 g, 20.5 mmol, 1.2 equiv.) and the reaction mixture was heated to 150 °C overnight. When the reaction was considered complete as determined by TLC analysis, the reaction mixture was cooled to r.t and quenched with H_2O, extracted three times with ethyl acetate, washed twice with H_2O, washed once with brine, dried over anhydrous Na_2SO_4, and concentrated *in vacuo*. The resulting residue was purified by silica gel column chromatography using a hexanes/EtOAc gradient (0 – 40%) to yield 1-(pyrimidin-2-yl)-1*H*-indole-3-carbaldehyde **4.40** as a beige color solid in 74% yield.^{1}H NMR (300 MHz, $CDCl_3$) δ 10.14 (s, 1H), 8.90 (s, 1H), 8.80 – 8.74 (m, 3H), 8.34 (d, *J* = 7.4 Hz, 1H), 7.46 – 7.35 (m, 2H), 7.19 (t, *J* = 4.8 Hz, 1H). ^{13}C NMR (75 MHz, $CDCl_3$) δ 185.97, 158.50, 157.10, 136.89, 136.42, 126.96, 125.64, 124.39, 122.12, 121.34, 118.03, 116.51.

Scheme 4.11: Synthesis of methyl 2-methyl-3-[1-(pyrimidin-2-yl)-1H-indol-3-yl]prop-2-enoate (**4.41**)

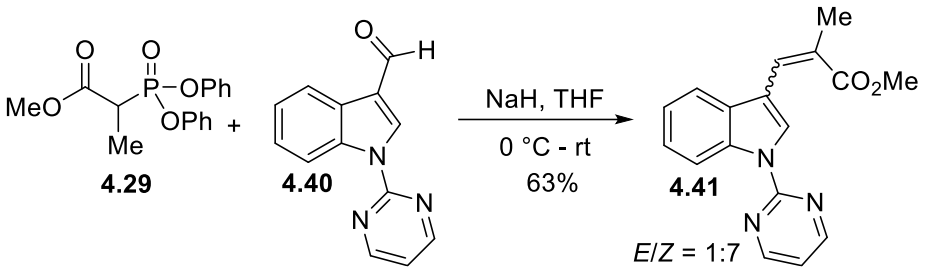

To a solution of methyl 2-diphenylphosphonopropionate **4.29** (862 mg, 2.69 mmol, 1.2 equiv) in THF (15 mL) was added NaH (116 mg, 2.91 mmol, 1.3 equiv) in one portion at 0 ºC. The reaction was then stirred for 30 min at the same temperature before the addition of a pre-dissolved solution of **4.40** (0.500 g, 2.24 mmol, 1.0 equiv) in THF. The mixture was stirred at room temperature for another 2 h before quenching with water. The mixture was extracted with EtOAc, organic layer was washed with brine, dried over $MgSO_4$, and concentrated *in vacuo*. The resulting residue was purified by silica gel column chromatography using a hexanes/EtOAc gradient (0 - 25%) to afford 1:7 *E/Z* mixture methyl ester **4.41** (486 mg, 1.66 mmol, 63%) as clear colorless oil: R_f = 0.30, 30% EtOAc in hexanes.^{1}H NMR (300 MHz, $CDCl_3$) δ 9.00 (s, 1H), 8.82 – 8.77 (m, 1H), 8.70 (s, 1H), 8.68 (s, 1H), 7.67 – 7.60 (m, 1H), 7.41 – 7.25 (m, 2H), 7.03 (t, *J* = 4.8 Hz, 1H), 7.00 – 6.98 (m, 1H), 3.77 (s, 3H), 2.20 (d, *J* = 1.4 Hz, 3H). ^{13}C NMR (75 MHz, $CDCl_3$) δ 169.13, 158.25, 135.13, 131.24, 127.94, 127.46, 126.25, 124.08, 122.46, 118.35, 116.54, 116.47, 115.01, 51.76, 22.29.

Synthesis and Characterization of Insertion Products

Scheme 4.12: Synthesis of methyl 3-[2-(2-ethoxy-2-oxoethyl)-1-(pyrimidin-2-yl)-1*H*-indol-3-yl]-2-methylprop-2-enoate (**4.56**)

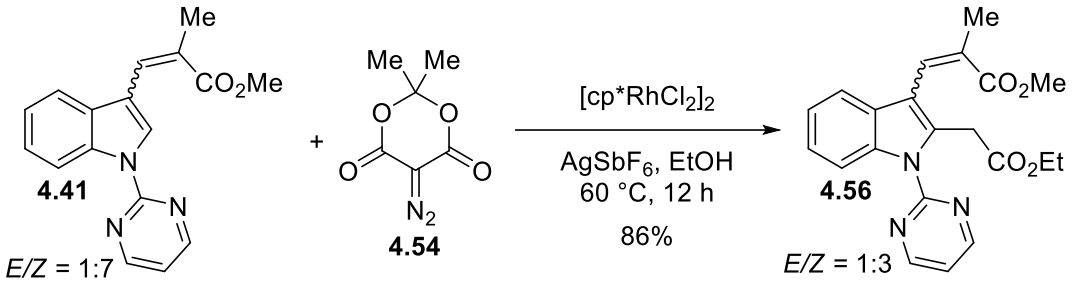

To a solution of indole starting material **4.41** (0.050 g, 0.17 mmol, 1.0 equiv) in DCE (1.5 mL) under N_2 atmosphere was added $[cp^*RhCl_2]_2$ (2.0 mg, 0.0030 mmol, 2 mol %), followed by $AgSbF_6$ (5.9 mg, 0.017 mmol, 10 mol %) and the vessel was evacuated (quickly) and backfilled with N_2. A pre-dissolved solution of diazo reagent **4.42** (44 mg, 0.26 mmol, 1.5 equiv) in DCE was added. The reaction mixture was then heated to 80 °C and stirred at this temperature for 12 h. The reaction progress was monitored by TLC analysis and considered complete upon consumption of diazo reagent. Upon completion, the reaction was cooled to room temperature, and then directly loaded, and purified by silica gel flash column chromatography (hexanes/EtOAc gradient) to yield pyrroloindole **4.43** in 86% yield (0.0560 g, 0.144 mmol). ^{1}H NMR (300 MHz, $CDCl_3$) δ 8.73 (s, 1H), 8.71 (s, 1H), 8.58 – 8.52 (m, 1H), 7.77 (d, *J* = 1.4 Hz, 1H), 7.48 – 7.41 (m, 1H), 7.36 – 7.29 (m, 1H), 7.29 – 7.23 (m, 1H), 7.11 (t, *J* = 4.8 Hz, 1H), 4.13 (s, 2H), 4.07 – 3.99 (m, 2H), 3.86 (s, 3H), 1.95 (d, *J* = 1.4 Hz, 3H), 1.09 (t, *J* = 6.4 Hz, 3H).

Scheme 4.13: Synthesis of ethyl 2-hydroxy-3-methyl-9-(pyrimidin-2-yl)-9*H*-carbazole-1-carboxylate (**4.57**)

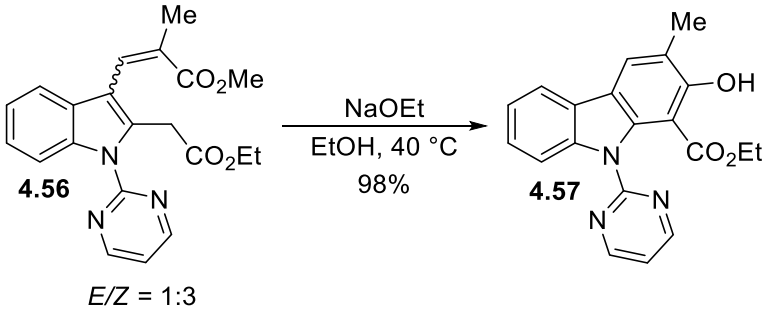

To a solution of indole starting material **4.56** (55 mg, 0.14 mmol, 1.0 equiv) in EtOH (1.5 mL) under N_2 atmosphere was added NaOEt (11 mg, 0.17 mmol, 1.2 equiv). The reaction mixture was then heated to 40 °C and stirred at this temperature for 3 h. The reaction progress was monitored by TLC analysis. Upon completion, the reaction was cooled to room temperature, and diluted with H_2O, extracted with EtOAc, organic layer was dried over $MgSO_4$, concentrated to dryness under reduced pressure. The crude was purified by silica gel flash column chromatography (hexanes/EtOAc gradient) to yield **4.57** in 98 % yield (42 mg, 0.12 mmol).^{1}H NMR (500 MHz, $CDCl_3$) δ 10.60 (s, 1H), 8.78 (d, *J* = 4.8 Hz, 2H), 8.44 (d, *J* = 8.2 Hz, 1H), 7.96 (s, 1H), 7.92 (d, *J* = 6.9 Hz, 1H), 7.40 – 7.31 (m, 2H), 7.16 (t, *J* = 4.8 Hz, 1H), 3.80 (q, *J* = 7.2 Hz, 2H), 2.43 (s, 3H), 0.88 (t, *J* = 7.2 Hz, 3H).

1.29 References

1. Abeysinghe, D. T.; Alwis, D. D. D. H.; Kumara, K. A. H.; Chandrika, U. G. *Evidence-based Complementary and Alternative Medicine: eCAM* **2021**, *2021*, 5523252.
2. Knolker, H. J.; Reddy, K. R. *Chem. Rev.* **2002**, *102*, 4303. (b) Knolker, H. J.; Reddy, K. R. *Alkaloids Chem. Biol.* **2008**, *65*, 181. (c) Schmidt, A. W.; Reddy, K. R.; Knolker, H. J. *Chem. Rev.* **2012**, *112*, 3193.
3. (a) Syam, S.; Abdul, A. B.; Sukari, M. A.; Mohan, S.; Abdelwahab, S. I.; Wah, T. S. **2011**, *16*, 7155-7170. (b) Aniqa, A.; Kaur, S.; Sadwal, S. *Nutrition and Cancer*, **2022**, *74*, 12.
4. (a) Cui, C. B.; Yan, S. Y.; Cai, B.; Yao, X. S. *J. Asian Nat. Prod. Res.* **2002**, *4*, 233. (b) Knölker, H.-J. *Top. Curr. Chem.* **2005**, 244, 115.
5. Wang, S. L.; Cai, B.; Cui, C. *Chinese Traditional and Herbal Drugs*. **2007**, *38*, 1677.
6. Feng-Nien, K.; Yi-San, L.; Tian-Shung, W.; Che-Ming, T. *Biochemical pharmacology*, **1994**, *48*, 353.
7. Adebajo, A. C.; Ayoola, O. F.; Iwalewa, E. O.; Akindahunsi, A. A.; Omisore, N. O. A.; Adewunmi, C. O.; Adenowo, T. K. *Phytomedicine*, **2006**, *13*, 246.
8. Thevissen, K.; Marchand, A.; Chaltin, P.; Meert, E. M.; Cammue, B. *Current medicinal chemistry*, **2009**, *16*, 2205.
9. (a) Nakahara, K.; Trakoontivakorn, G.; Alzoreky, N. S.; Ono, H.; Onishi-Kameyama, M.; Yoshida, M. *J. Agric. Food. Chem.* **2002**, *50*, 4796. (b) Roy, M. K.; Thalang, V. N.; Trakoontivakorn, G.; Nakahara, K. *Biochem. Pharmacol.* **2004**, *67*, 41. (c) Ito, C.; Itoigawa, M.; Nakao, K.; Murata, T.; Tsuboi, M.; Kaneda, N.; Furukawa, H. *Phytomedicine* **2006**, *13*, 359.

10. (a) Narasimhan, N.S.; Paradkar, M.V.; Gokhale, A. M. *Tetrahedron Lett.* **1970**, *19*, 1665. (b) Oikawa, Y.; Yonemitsu, O. *Heterocycles* **1976**, *5*, 233. (c) Knolker, H.-J.; Hofmann, C. *Tetrahedron Lett.* **1996**, *37*, 7947. (d) Hesse, R.; Gruner, K. K.; Kataeva, O.; Schmidt, A.W.; Knolker, H.-J. Chem. Eur J. **2013**, *19*, 14098. (e) Gruner, K. K.; Knolker, H.-J. *Org. Biomol. Chem.* **2008**, *6*, 3902. (f) Gruner, K. K.; Hopfmann, T.; Matsumoto, K.; Jaeger, A.; Katsuki, T.; Knolker, H.-*J. Org. Biomol. Chem.* **2011**, *9*, 2057. (g) Dai, J.; Ma, D.; Fu, C.; Ma, S. *Eur. J. Org. Chem.* **2015**, *2015*, 5655. (h) Zang, Y.; Song, X.; Li, C.; Ma, J.; Chu, S.; Liu, D.; Ren, Q.; Li, Y.; Chen, N.; Zhang, D. *Eur. J. Med. Chem.* **2018**, *143*, 438. (i) Chakraborti, G.; Paladhi, S.; Mandal, T.; Dash, J.; Jyotirmayee, D. *J. Org. Chem.* **2018**, *83*, 7347. (j) Mandal, T.; Chakraborti, G.; Karmakar, S.; Dash, J. *Org. Lett*. **2018**, *20*, 4759. (k) Polley, A.; Varalaxmi, K.; Nandi, A.; Jana, R.; *Asian J. Org. Chem.* **2021**, *10*, 1207.

11. Roy, M. K.; Thalang, V. N.; Trakoontivakorn, G.; Nakahara, K. *Br. J. Pharmacol.* **2005**, *145*, 145.

12. Jagadeesh, S.; Sinha, S.; Pal, B. C.; Bhattacharya, S.; Banerjee, P. P. *Biochem. Biophys. Res. Commun.* **2007**, *362*, 212.

13. Roy, S.; Dutta, D.; Satyavarapu, E. M.; Yadav, P. K.; Mandal, C.; Kar, S.; Mandal, C. *Scientific reports,* **2017**, *7*, 1.

14. Natalie, N.; Till, O. *J. Org. Chem.* **2016**, *81*, 1723.

15. Akwaboah, D. C.; Wu, D.; Forsyth, C. J. *Org. Lett.* **2017**, *19*, 1180.

16. Jin, G.; Lee, S.; Choi, M.; Son, S.; Kim, G. W.; Oh, J. W.; Lee, K. *Eur. J. Med. Chem.* **2014**, *75*, 413.

17. Shi, J.; Yan, Y.; Li, Q.; Xu, H. E.; Yi, W. *Chem. Commun.* **2014**, *50*, 6483.

18. Jiang, H.; Gao, S.; Xu, J.; Wu, X.; Lin, A.; Yao, H. *Adv. Synth. Catal.* **2016**, *358*, 188.

1.30 Appendix 3

^{1}H, ^{13}C NMR Spectra for Chapter 4

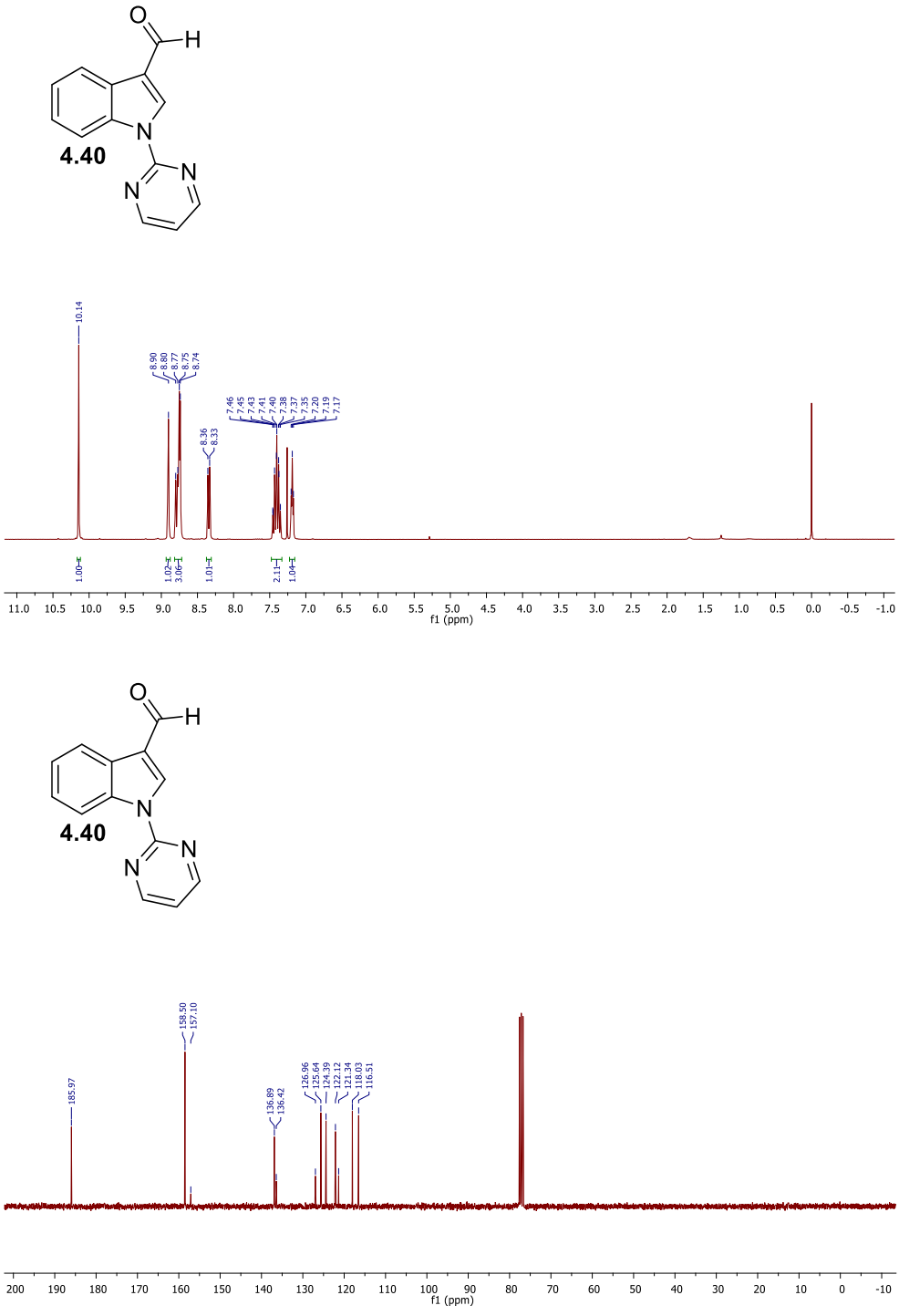

^{1}H NMR (300 MHz, $CDCl_3$) and ^{13}C NMR (75 MHz, $CDCl_3$) of compound **4.40**

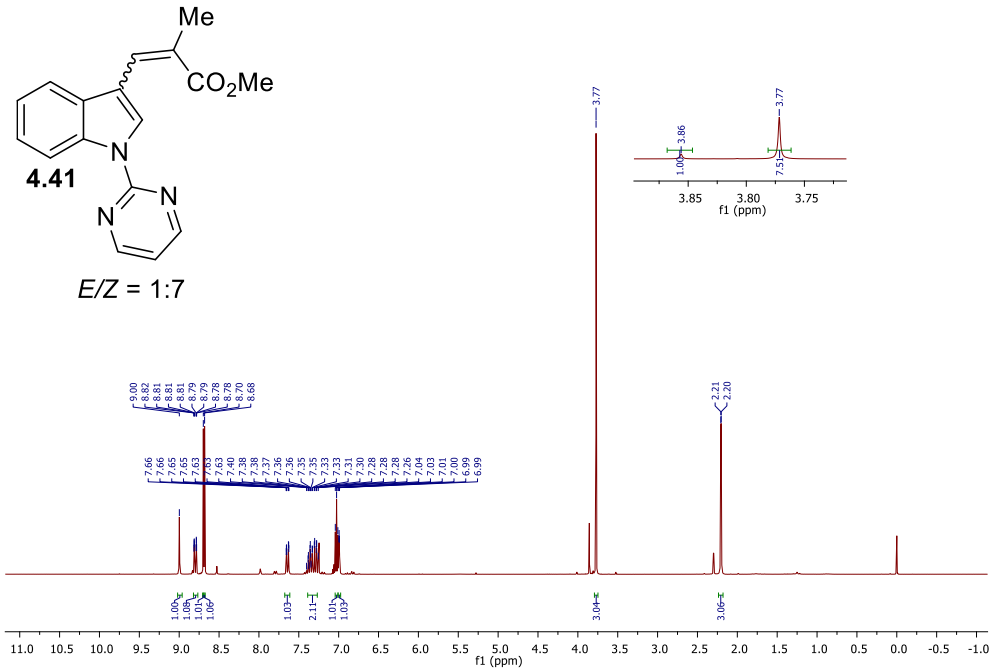

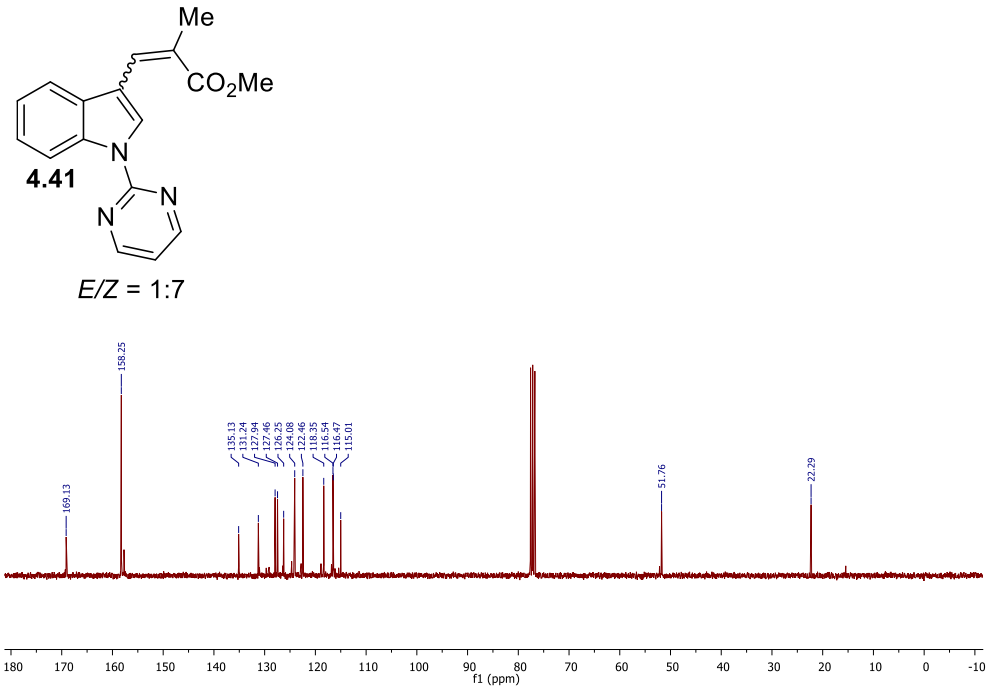

^{1}H NMR (300 MHz, $CDCl_3$) and ^{13}C NMR (75 MHz, $CDCl_3$) of compound **4.41**

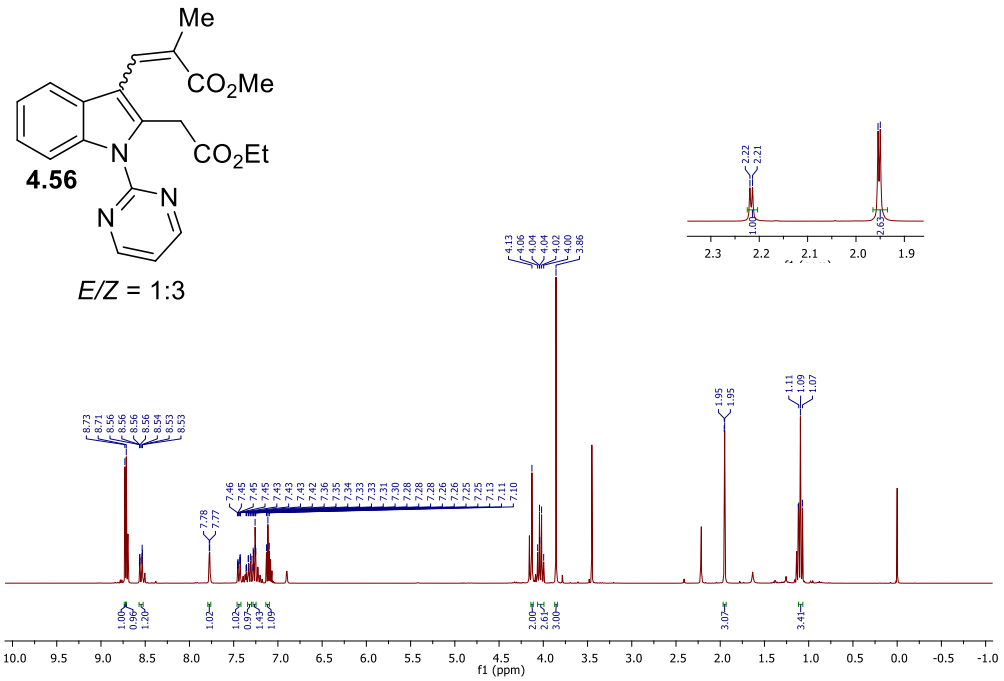

^{1}H NMR (300 MHz, $CDCl_3$) of compound **4.56**

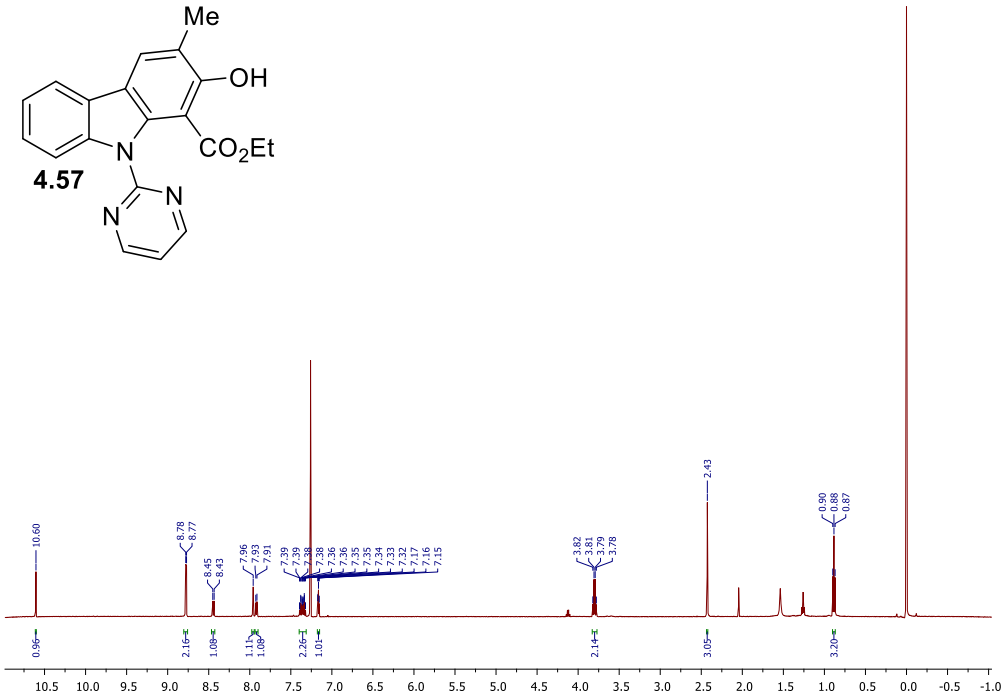

^{1}H NMR (300 MHz, $CDCl_3$) of compound **4.57**

Chapter 5: Biomimetic Domino Knoevenagel/Cycloisomerization Strategy for the Synthesis of Citridone A and Derivatives.

With the publisher's permission, this chapter was adapted from the original manuscript: Aabid H. Bhat, Gastón N. Quiroga, Agustina La-Venia, Huck K. Grover,* and Martín J. Riveira* *J. Org. Chem.* **2021**, *86*, 12226−12236.

Statement of Co-Authorship

Aabid H. Bhat (listed as 1st author): Performed the synthetic work, data collection, data analysis, and contributed to the preparation of the supporting information for the total synthesis of two natural products **5.1** and **5.3**.

Gastón N. Quiroga: Performed the synthetic work for the synthesis of a library of all non-natural products, data collection, data analysis, and contributed significantly to the preparation of the manuscript and supporting information.

Agustina La-Venia: Performed the synthetic work, data collection, data analysis, and contributed to the preparation of the supporting information.

Huck K. Grover: Principal investigator (PI) of the total synthesis work, who led the project and majorly contributed to the interpretation/analysis of data and writing of the manuscript.

Martín J. Riveira: Principal investigator (PI) of the work, who led the project and majorly contributed to the interpretation/analysis of data and writing of the manuscript.

1.31 Introduction

As illustrated in Chapter 1 Section 1.1, domino reactions are a fascinating branch of organic chemistry. The utility of a domino reaction depends on three factors: first, the number of bonds formed in a sequence of intermediate steps; second, the level of molecular complexity reached; and third, its application in the synthesis of pharmaceuticals, agrochemicals, and the design of new drug candidates. Domino reactions frequently occur in nature, utilizing the chirality embedded within enzymes to biosynthesize stereoselective natural products.[1] In contrast to biosynthesis, laboratory synthesis of complex organic molecules, such as natural products, is very challenging in terms of step-economy and stereoselectivity. The development of domino reactions in chemistry is a continuous effort to create molecular complexity with selective sequential transformations. Additionally, domino reactions on an industrial scale can lower costs for labor, waste management, energy, and chemical use. It is therefore an eco-friendly process as it uses fewer resources and helps the environment. In this chapter, a domino reaction that has been employed, in collaboration with Rivera Group, for the total synthesis of citridone A **5.1** and tersone D **5.3** *via* Knoevenagel-type condensation/bicyclization between a 1,3-dicarbonyl substrate and an $\alpha,\beta,\gamma,\delta$-unsaturated aldehyde, will be discussed.

Citridone A **5.1** is a naturally occurring phenylfuropyridone originally isolated from the fungal culture broth of *Penicillium sp.* FKI-1938 by Nobel Laureate S. Ōmura and co-workers (Figure 5.1).[2] Structurally related analogs of citridone A **5.1** were identified as potentiators of antifungal miconazole activity towards *Candida albicans.* citridones (75 μM) potentiate the miconazole activity against *Candida albicans*, decreasing the IC_{50} value of miconazole from 14.5 nM to 3.5~6.3 nM.[3] Moreover, it has also been shown to inhibit the biosynthesis of a key virulence factor *staphyloxanthin,* in methicillin-resistant *Staphylococcus aureus* (MRSA), which makes it a

potential antibiotic lead with a new mode of action.[4] The unique biological activity of citridone A arises from its polycyclic phenylfuropyridine chemical structure containing a phenyl-substituted tricyclic [6.5.5] ring system. The [6.5.5]cyclopenta[*b*]furopyridone is unique in nature, present in only some simple natural pyridone derivatives, including citridone A **5.1**.[2–4] However, the tricyclic scaffold is also present in recently developed synthetic antitumor clinical candidate eFT226 (zotatifin) **5.2** (Figure 5.1),[5] an eIF4A1 inhibitor which is also currently a promising anti-COVID-19 drug candidate.[6] Structurally related tersone D **5.3** and its natural analogs were isolated in 2019 from the FS441 strains of fungus *Phomopsis tersa*, which was collected from the deep-sea sediment at a depth of 3000 m (Figure 5.1). Moreover, phenylfuropyridone racemates, including phenylpyridone racemate (±)-tersone D, have been evaluated for *in vitro* antimicrobial and cytotoxic activity.[7]

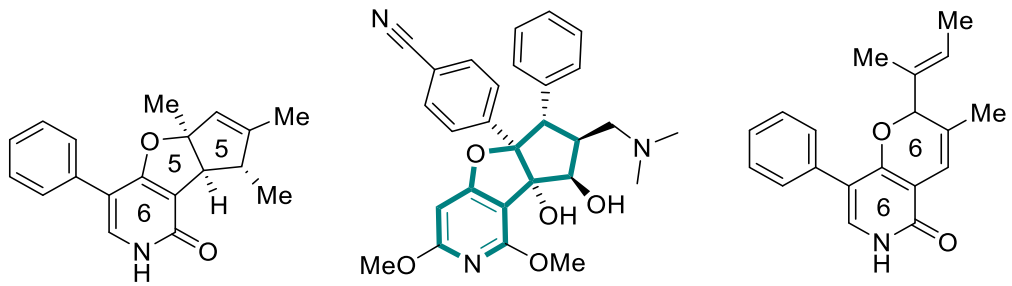

Figure 5.1: Structures of Citridone A **5.1**, synthetic antitumor clinical candidate eFT226 **5.2** and tersone D **5.3**.

Owing to their diverse bioactivities, the development of efficient synthetic strategies toward functionalized phenylfuropyridones is essential to promote further biological studies and to explore their application as pharmaceuticals. One approach to the construction of these phenylfuropyridone skeletons was highlighted by Ōmura and Nagamitsu in the first total synthesis of citridone A in 2011 (Scheme 5.1).[8] Starting from (+)-pulegone **5.4** the total synthesis was achieved over 24 steps in 3.2% overall yield. Their synthesis began with the preparation of *trans*-

isopropylidenecyclopentane **5.5** from (+)-pulegone **5.4** in 60% yield over 5 steps, with purification only required in the final step. Cyclopentane **5.5** was converted to a key intermediate **5.6** (required for the allylic alkylation) over 12 steps in 34% yield. Intermediate **5.6** was treated with nucleophile **5.7** (obtained from *trans*-cinnamic acid in 55% yield over 7 steps), resulting in coupling product **5.8** in 99% yield. Heating of the coupling product **5.8** in diphenyl ether at 210 °C provided advanced intermediate pyridine **5.9** in 66% yield. Next, a regioselective intramolecular iodocyclization of **5.9** furnished the key intermediate **5.10** in 67% yield. Finally, from intermediate **5.10**, citridone A **5.1** was obtained in 48% yield over 5 steps.

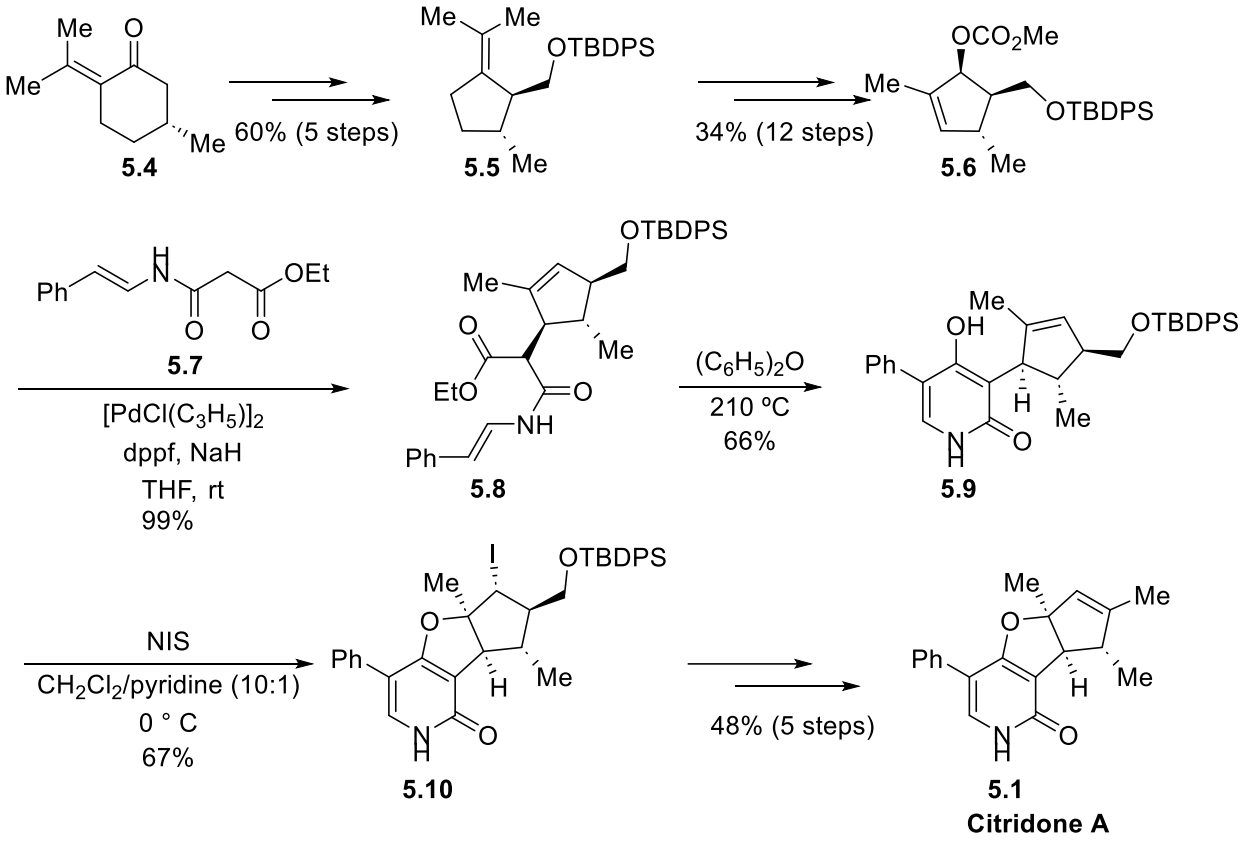

Scheme 0.1: Total synthesis of Citridone A **5.1** by Ōmura and Nagamitsu.

Shortly after Ōmura's initial synthesis, the Zografos group, also in 2011, reported the convergent synthesis of citridone A.[9] Their synthetic plan commenced with the construction of the aldehyde **5.12** over 6 steps (19%), starting from ethyl tiglate **5.11** (Scheme 5.2). Then they

synthesized the key coupling partner pyridone **5.15** from malonyl chloride **5.13** and phenylacetonitrile **5.14** (56% over 2 steps). Next, the coupling of aldehyde **5.12** with 4-hydroxy-5-phenylpyridone **5.15** provided a complex mixture of isomers **5.16**. Finally, a bismuth triflate promoted carbocyclization provided citridone A **5.1** in 40% yield. Although **5.1** has been elegantly prepared *via* the total synthesis in both enantioselective and racemic fashion as described above, to date, there are no reports of the synthesis of tersone D **5.3**. Furthermore, operationally simple, and straightforward synthetic methodologies toward cyclopenta[*b*]furopyridones are lacking.[10]

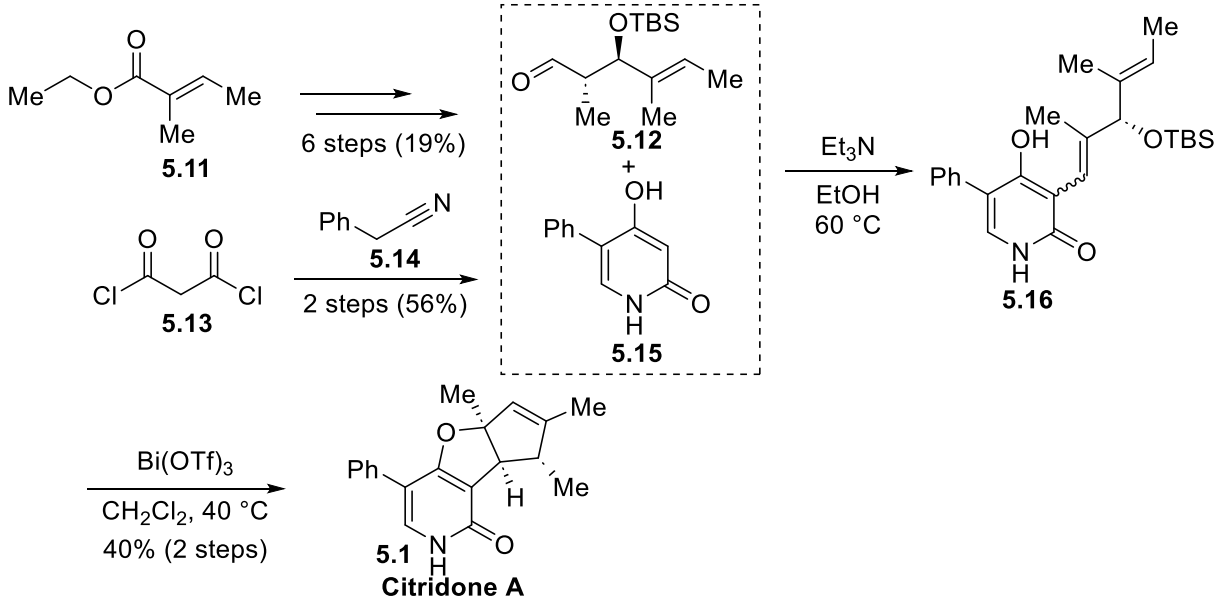

Scheme 0.2: Total synthesis of Citridone A **5.1** by the Zografos group.

1.32 Hypothesis

Over the past several years, the Rivera group has been interested in developing Knoevenagel initiated cascade processes involving the coupling of 1,3-dicarbonyl molecules **5.17** with *α,β,γ,δ*-unsaturated aldehydes **5.18** (Scheme 5.3A).[11] This method combines a classic aldol-type condensation between dimedone **5.17** and **5.18**, followed by a spontaneous metal-free cycloisomerization, a process which was initially developed for the stereoselective synthesis of

cyclopenta[*b*]furan-type derivatives **5.19** (Scheme 5.3A). Later, the same group extended this reaction manifold to include 2,4-quinolinediol **5.20**, as the 1,3-dicarbonyl source, for the synthesis of novel heterocycles **5.22** (Scheme 5.3B).[12] Based on their expertise in the synthesis of cyclopenta[*b*]dihydrofurans and our interest in developing cascade protocols, we entered into a collaboration for the synthesis of the natural product citridone A. We hypothesized that subjecting 1,3-dicarbonyl compound **5.15** and unsaturated aldehyde **5.23** to ethylenediammonium diacetate (EDDA) conditions could promote a domino Knoevenagel condensation/cycloisomerization sequence to synthesize natural product citridone A **5.1** (Scheme 5.3C).

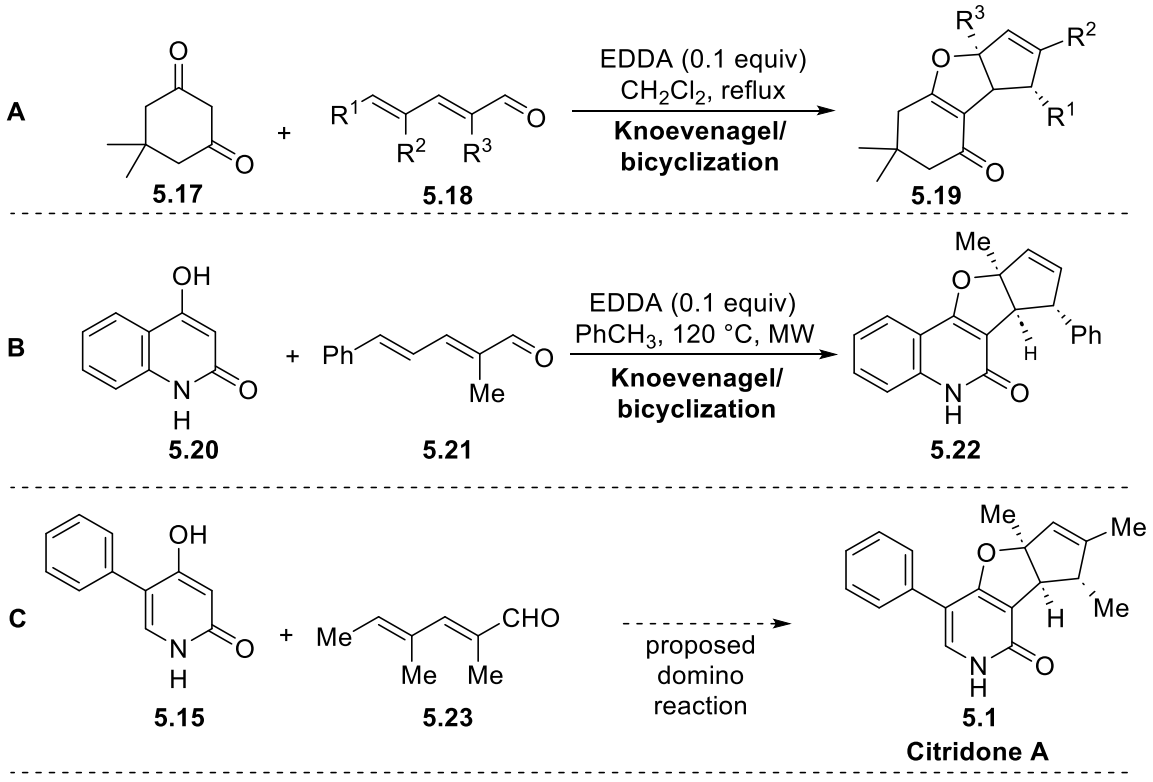

Scheme 0.3: (**A**) Domino Knoevenagel/bicyclization for the synthesis of cyclopenta[b]furan-type derivatives **5.19** (**B**) Domino Knoevenagel/bicyclization for the synthesis of cyclopenta[b]furans **5.22** (**C**) Proposed synthetic route for the synthesis of **5.1**.

1.33 Results and Discussion — Synthesis of Starting Materials

1.33.1 Attempted Synthesis of Pyridone Substrate (5.15)

At the outset of our work, we attempted to synthesize pyridone substrate **5.15** through a known literature procedure.[13] Phenylacetonitrile **5.24** was subjected to condensation with malonyl chloride **5.13** for 4 d at r.t (Scheme 5.4). Unfortunately, upon analysis of the crude reaction product using ^{1}H NMR spectroscopy, only trace quantities of the desired chloropyridone product **5.25** were detected. Consequently, the subsequent step of hydrogenation was not pursued. Considering the unsatisfactory yield of **5.25** and recognizing the potential hazards associated with malonyl chloride **5.13**, an alternate pathway was chosen to synthesize the desired compound **5.15**.

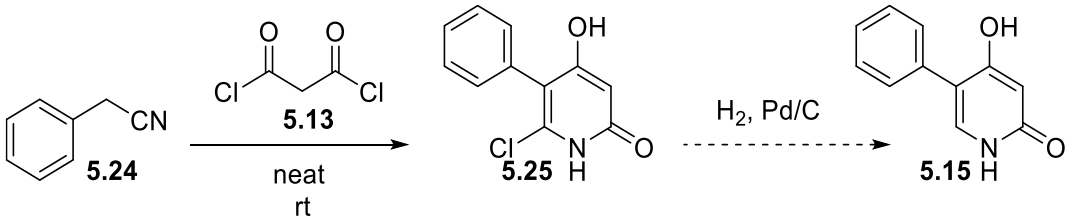

Scheme 0.4: Attempted synthesis of 4-hydroxy-5-phenyl-2(1*H*)-pyridone (**5.15**).

1.33.2 Revised Strategy for the Synthesis of Pyridone Substrate (5.15)

In an alternative route,[14] phenylacetyl chloride **5.26** was subjected to refluxing conditions in EtOH to obtain ethyl phenylacetate **5.27** in 67% yield (Scheme 5.5). **5.27** was treated with ethylformate and NaH in THF to obtain enol product **5.28** in 72% yield, which was converted to enamine **5.29** upon refluxing with NH_4OH in THF. The enamine **5.29** was condensed with diethylmalonate **5.30** in the presence of freshly prepared sodium ethoxide in EtOH to afford pyridone-3-carboxyate **5.31** in 88% yield as a white solid.

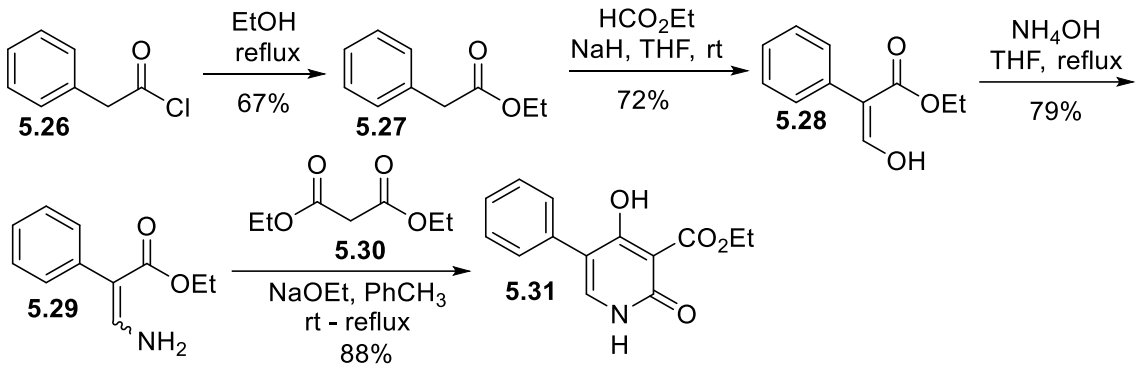

Scheme 0.5: Synthesis of 2,4-dihydroxy-3-ethoxycarbonyl-5-phenylpyridine (**5.31**).

The final stage in the synthesis of the pyridone starting material required the removal of the C-3 ester functionality of **5.31**. Initially, an acid-catalyzed decarboxylation reaction was attempted using 1 M HCl at reflux conditions. Regrettably, this reaction did not yield the desired product, pyridone **5.15**; moreover, starting material did not dissolve under these conditions (Scheme 5.6). However, when the same reaction mixture was transferred to a pressure tube and subjected to stirring at an elevated temperature for an extended period, a clear light-yellow solution was observed. After neutralization with an aqueous NaOH solution, pyridone **5.15** precipitated out as a white solid in 88% yield.

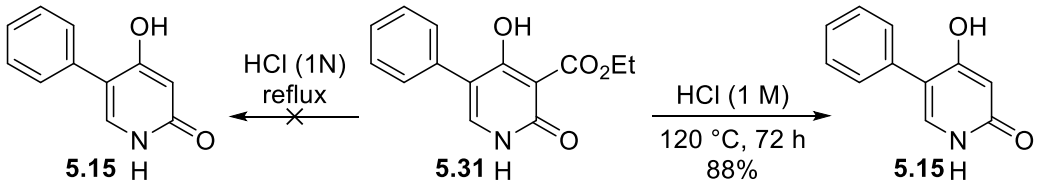

Scheme 0.6: Acid-catalyzed decarboxylation for the synthesis of **5.15**.

1.33.3 Synthesis of (2*E*,4*E*)-2,4-dimethyl-2,4-hexadienal (5.23)

The enal substrate **5.23** was synthesized from commercially available tiglic aldehyde **5.33** through a known literature procedure (Scheme 5.7).[15] Triethyl-2- phosphonopropionate **5.32** was treated with the freshly prepared sodium ethoxide solution in ethanol followed by the addition of aldehyde **5.33** to form the ester product **5.34** in a 57 % yield. Next, ester **5.34** was reduced with

$LiAlH_4$ in diethyl ether to the corresponding alcohol **5.35**, which was then oxidized using MnO_2 to afford (2*E*,4*E*)-2,4-dimethylhexa-2,4-dienal **5.23** in 65% yield over 2 steps.

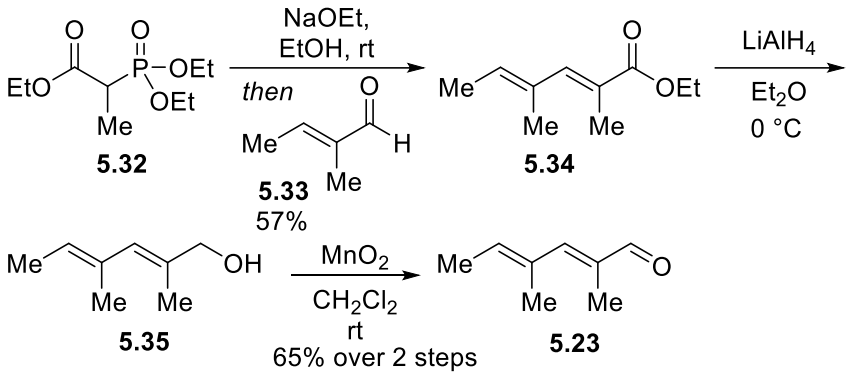

Scheme 0.7: Synthesis of unsaturated enal substrate **5.23**.

1.33.4 Synthesis of Ethylenediamine Diacetate (EDDA) (5.37)

Next, we focused on the synthesis of the catalyst ethylenediamine diacetate (EDDA). Treatment of ethylenediamine **5.36** with glacial acetic acid in diethyl ether overnight resulted in the formation of yellow crystals (Scheme 5.8).[16] The crude product was washed multiple times with cold ether and then recrystallized in methanol to obtain ethylenediammonium diacetate (EDDA) **5.37** as white crystals in a 79% yield.

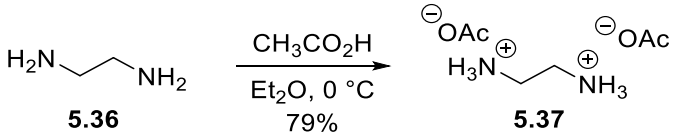

Scheme 0.8: Synthesis of ethylenediamine diacetate **5.37**.

Toward the synthesis of citridone A **5.1** (Scheme 5.9), pyridone **5.15** and (2*E*,4*E*)-2,4-dimethylhexa-2,4-dienal **5.23** were subjected to domino Knoevenagel/bicyclization reaction conditions using 20 mol% ethylenediamine diacetate (EDDA) in toluene at 120 °C in a microwave reactor. To our delight, after chromatographic purification and ^{1}H NMR analysis, racemic citridone A **5.1** was identified based on comparing with the reported characterization of isolated citridone

A.[2] However, the material isolated upon purification was contaminated with an impurity in a 12:1 ratio. We believe this minor impurity is the rearranged isomer **5.40** which possibly comes from the ring-opening process of citridone A to form the intermediate **5.38**, which upon double [1,2]-H shift followed by ring-closure leads to the formation of rearranged product **5.40**. It should be noted that a similar rearrangement had been previously reported for some cyclopenta[*b*]furans.[ref] Unfortunately, changing reaction conditions (varying temperature and catalyst loading) did not stop the formation of rearranged product **5.40**. Additionally, attempts to purify this mixture of isomers, by recrystallization and preparative TLC were not successful in our hands. Other reaction conditions were also tried, including the use of the polar solvent ethanol to increase the solubility of the starting material, which unfortunately resulted in a significant increase in unwanted isomer formation at a ratio of 1.6:1.

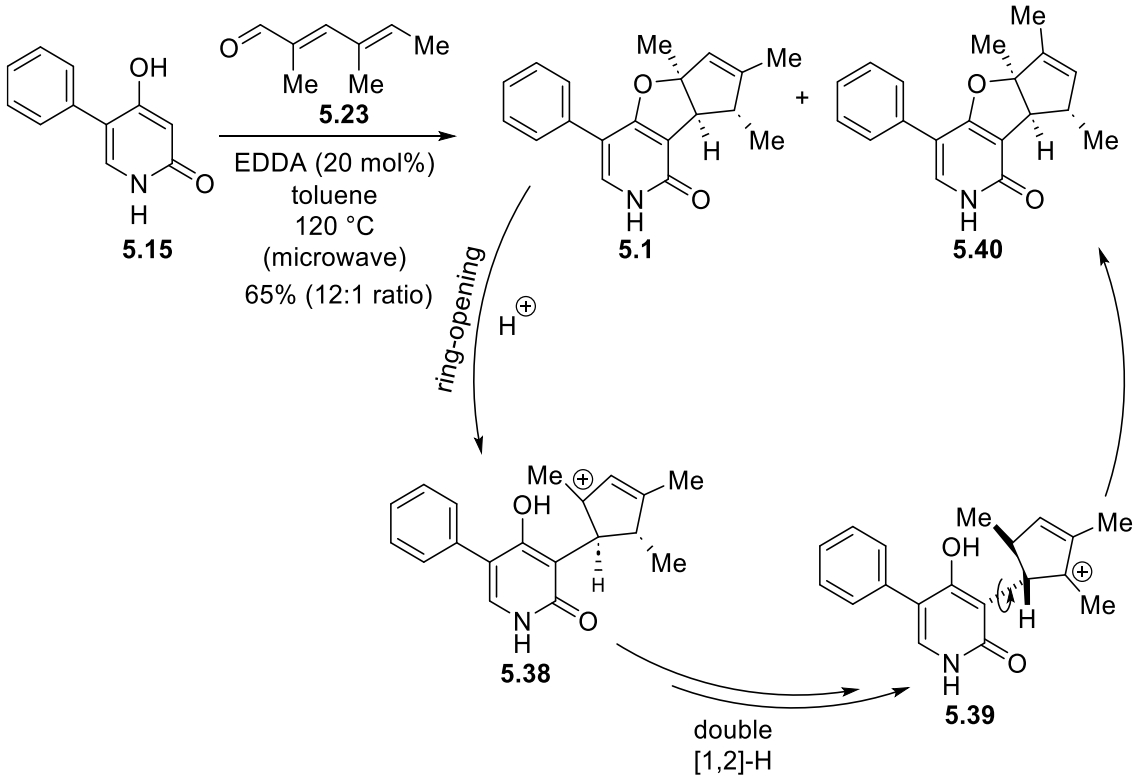

Scheme 0.9: Domino Knoevenagel/bicyclization reaction for synthesizing **5.1** and a possible mechanism for forming rearranged side product **5.40**.

To solve the problem of undesired isomer formation, we undertook a thorough review of the existing literature related to Knoevenagel condensations of dienals with 1,3-dicarbonyl compounds. Our search led us to a study conducted by the Mischne group in 2012, where they demonstrated that when dienals **5.42** and 4-hydroxy-1-methyl-2(1*H*)-quinolone **5.41** were subjected to catalytic EDDA in dichloromethane under reflux conditions, a domino Knoevenagel/oxa-6π electrocyclic ring-closure sequence resulted in the formation of 2*H*-pyran **5.43** (Scheme 5.10A).[12] Notably, this reaction did not produce any cyclopenta[*b*]furan under the specified reaction conditions. Drawing inspiration from this literature finding, we devised a two-step strategy. We were intrigued whether we would also be able to generate the pyran intermediate (*via* Knoevenagel/oxa-6π electrocyclization) as described by the Mischne group (Scheme 5.10 B). Upon the formation of this intermediate, a possible cycloisomerization in a non-polar solvent without the use of EDDA could lead to the formation of the desired natural product **5.1** free from the minor isomer **5.40**. Importantly, the desired intermediate, if successfully formed in our case, corresponds to a natural product known as tersone D **5.3**, thus presenting the possibility of targeting two natural products within the same synthetic sequence.

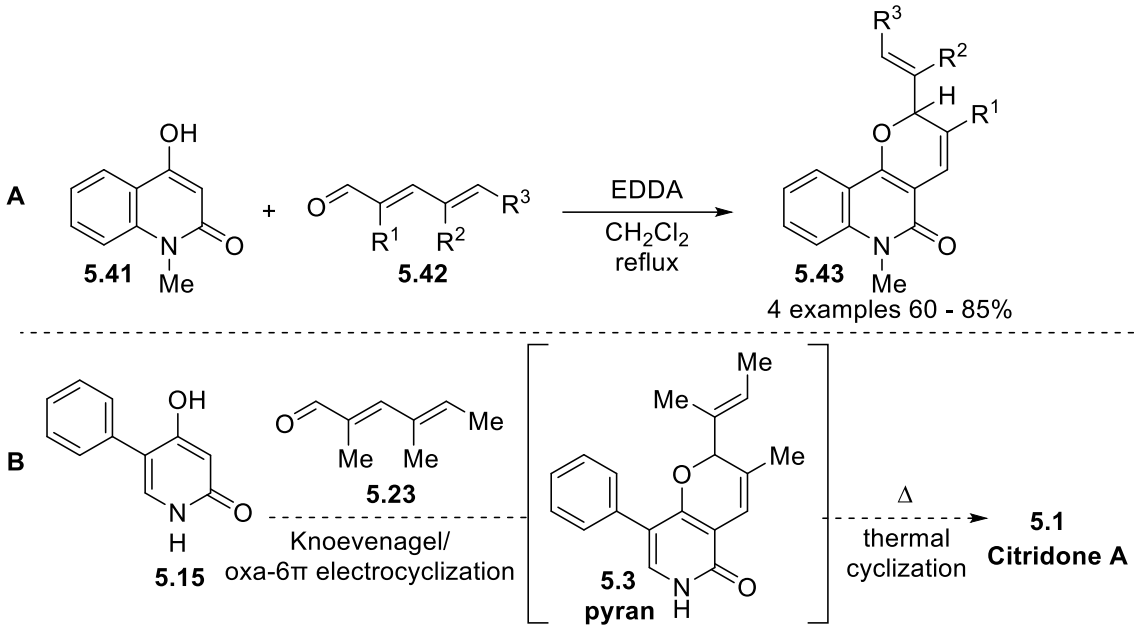

Scheme 0.10: (**A**) Synthesis of pyran **5.43** by Mischne group. (**B**) Proposed two step strategy for the synthesis of Citridone A **5.1**.

With the aforementioned promising strategy in mind, a mixture of pyridone **5.15** and dienal **5.23** in dichloromethane was subjected to refluxing conditions in the presence of catalytic EDDA. As a result, the proposed intermediate tersone D **5.3** was successfully generated (Scheme 5.11). In order to assess the thermal cycloisomerization event of our two-step strategy, the crude intermediate mixture was concentrated *in vacuo* and subsequently subjected to solvent switch to toluene. Upon further heating, the desired product citridone A **5.1** was obtained as the sole isolable compound, with an overall yield of 48%. The physical and spectroscopic data of the synthetic sample matched those reported in the literature for **5.1**.[2a]

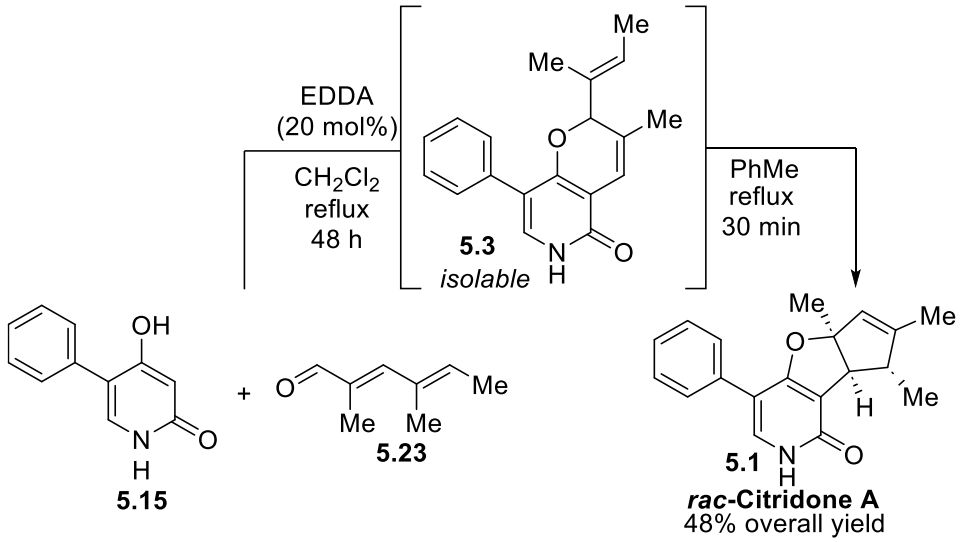

Scheme 0.11: Two-step approach for the synthesis of citridone A **5.1**.

To achieve the first synthesis of natural product tersone D **5.3**, the EDDA-catalyzed condensation between **5.15** and **5.23** in dichloromethane under reflux was repeated (Scheme 5.12) under similar conditions as described in Scheme 5.11. Purification *via* column chromatography afforded 68% yield of tersone D **5.3**; however, a minor amount of intermediate **5.3** converted to citridone A **5.1** was also observed in a 5:1 ratio. Separation of the two natural products by preparative TLC allowed the characterization of **5.3**, with all the spectral data matching those reported for the natural sample.[7]

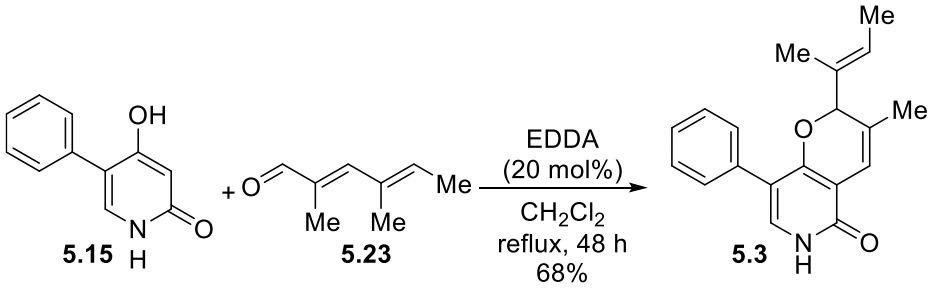

Scheme 0.12: Synthesis of tersone D **5.43**.

A plausible mechanism for the synthesis of citridone A was proposed (Scheme 5.13). The formation of compound **5.1** from the initial condensation product **5.44** can be explained by two

distinct pathways: ionic and pericyclic-based. In the ionic pathway (path a), the ketone **5.44** is activated by an acid catalyst, leading to the formation of a pentadienyl cation intermediate **5.45**. This intermediate then undergoes a Nazarov-type 4π electrocyclization to generate intermediate **5.46**. Finally, intermediate **5.46** can further undergo electrocyclization to produce the furan product **5.1**. On the other hand, in path b, the condensation product **5.44** can undergo oxa-6π electrocyclic ring-closure, resulting in the formation of pyran intermediate **5.3**. This intermediate can subsequently isomerize to (Z)-intermediate **5.47** through a 6π electrocyclic ring-opening. Finally, intermediate **5.47** can undergo an intramolecular cycloaddition [π4a + π4s] to form furan product **5.3**.

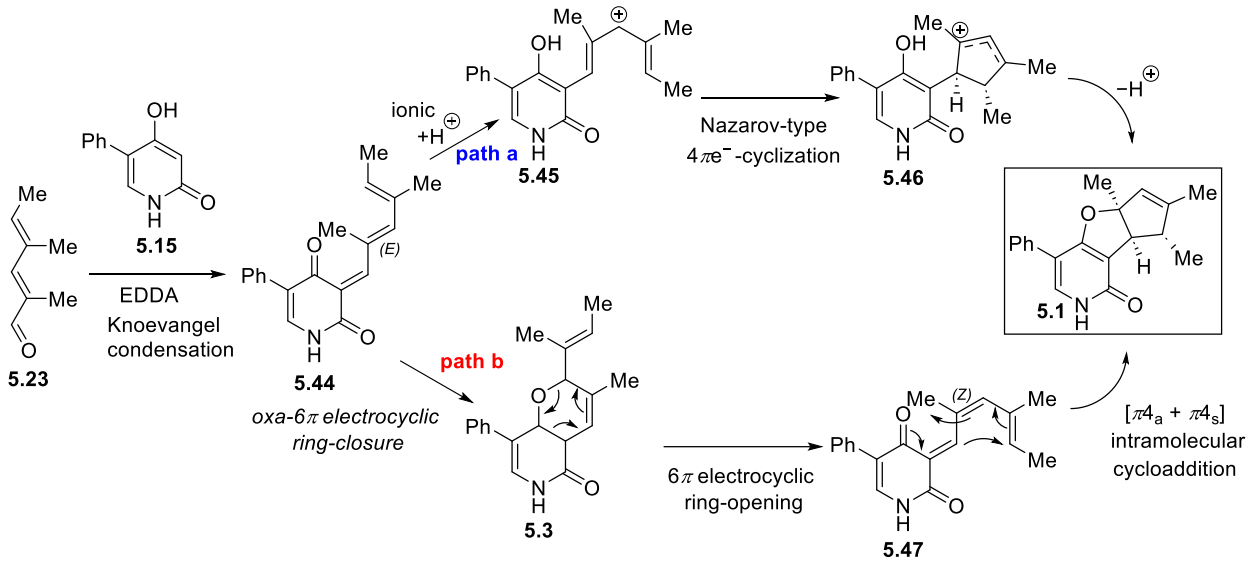

Scheme 0.13: Plausible mechanism for the synthesis of citridone A **5.1**.

1.34 Summary

In summary, we have developed the first synthetic preparation of the natural product tersone D *via* a one-pot Knoevenagel condensation/cycloisomerization process between (2*E*,4*E*)-2,4-dimethylhexa-2,4-dienal and pyridone substrate. This domino transformation also allowed us to synthesize the natural product citridone A in racemic form. We also demonstrated our efforts in the improved synthesis of the 4-hydroxy-2-pyridone, a heteroaromatic core abundant in natural alkaloids. We have also successfully addressed the challenge of avoiding the rearrangement common in cyclopenta[*b*]furans. In future the same domino route may be applicable in targeting other natural analogs of tersone D.

1.35 Experimental Section

General Procedures

Unless stated otherwise, all reactions were performed in flame-dried glassware under an atmosphere of dry nitrogen. Dry trifluorotoluene ($PhCF_3$) and *N*,*N*-dimethylformamide (DMF) were obtained from Sigma Aldrich SureSeal™ bottles. Dry methyl *tert*-butyl ether (MTBE) was obtained from Alfa Aesar™. All other reagents were used as received from commercial sources unless stated otherwise. When indicated, solvents or reagents were degassed by sparging with Nitrogen for 10 min in an ultrasound bath at 25 °C. For reactions conducted above room temperature, oil bath heating was used as the heat source. Reactions were monitored by thin layer chromatography (TLC) on Silicycle Siliaplate™ glass-backed TLC plates (250 μm thickness, 60 Å porosity, F-254 indicator) and visualized by UV irradiation or development with an anisaldehyde. Volatile solvents were removed under reduced pressure with a rotary evaporator. All flash column chromatography was performed using Silicycle SiliaFlash® F60, 230-400 mesh silica gel (40-63 μm). ^{1}H NMR and ^{13}C NMR spectra were recorded with Bruker AV,

spectrometers operating at 300 or 500 MHz for ^{1}H (75 or 125 MHz for ^{13}C) in $CDCl_3$ or acetone-D_6. Except when noted otherwise, chemical shifts are reported relative to the residual solvent signal (^{1}H NMR: δ = 7.26 ($CDCl_3$), δ = 2.05 (acetone-D_6); ^{13}C NMR: δ = 77.16 ($CDCl_3$)). NMR data are reported as follows: chemical shift (multiplicity, coupling constants where applicable, number of hydrogens). Splitting is reported with the following symbols: s = singlet, bs = broad singlet, d = doublet, t = triplet, app t = apparent triplet, dd = doublet of doublets, ddd = doublet of doublet of doublets, dddd = doublet of doublet of doublet of doublets, m = multiplet. Infrared (IR) spectra were recorded using neat samples on a Bruker Alpha spectrometer. High resolution mass spectrometry (HRMS) data were obtained using an Agilent 6200 series instrument employing a TOF mass analyzer. Melting points (M.P.) were obtained on an OptiMelt instrument (a digital apparatus) produced by Stanford Research Systems by scanning temperature ranges from 40 - 150 °C at a rate of 3 °C/s.

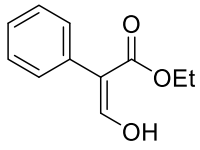

5.28

Sodium hydride (60% dispersion in mineral oil, 3.50 g, 87.6 mmol, 3.0 equiv) was added slowly to a solution of freshly prepared ethyl phenylacetate **5.27** (4.80 g, 29.2 mmol, and 1.0 equiv) and ethylformate (50.0 mL, 0.613 mol, 21.0 equiv) in anhydrous THF (74 mL). The reaction mixture was stirred overnight at room temperature. After completion of the reaction, as determined by TLC analysis, the mixture was cooled to 0 °C, and an aqueous solution of 2 M HCl (50 mL) was added dropwise. The reaction mixture was then extracted with Et_2O (3 x 70 mL), and the organic layers were combined, dried over Na_2SO_4, filtered, and concentrated *in vacuo*. The resulting yellow oil was purified by column chromatography (8-10 % EtOAc in hexanes) to give **5.28** (4.06 g, 72%) as a colorless oil. R_f = 0.50, 20% EtOAc in hexanes. ^{1}H NMR (300 MHz, $CDCl_3$): δ 12.14 (d, *J* = 12.7 Hz, 1H), 7.35 – 7.23 (m, 6H), 4.28 (q, *J* = 7.1 Hz, 2H), 1.27 (t, *J* = 7.2 Hz, 3H). ^{13}C NMR (75 MHz, $CDCl_3$): 171.7,

163.5, 134.2, 129.5, 128.2, 127.0, 108.7, 61.0, 14.2. IR (neat): 2985, 1732, 1688, 1200, 1175, 1014, 691 cm^{-1}. HRMS (APPI+): calc'd for $C_{11}H_{13}O_3$ $[M+H]^+$ 193.0859, found 193.0858.

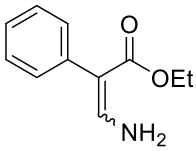
5.29

To a solution of hydroxyacrylate **5.28** (4.06 g, 21.12 mmol, 1.0 equiv) in THF (100 mL) was added 4 mL of NH_4OH. The reaction mixture was stirred at reflux temperature (oil bath heating) for 45 min. The mixture was then cooled to r.t, THF was removed *in vacuo* and the residual was extracted with Et_2O (3 x 20 mL). The combined organic layers were dried over Na_2SO_4, filtered and concentrated *in vacuo*, and the resulting yellow mixture was purified by column chromatography (12-15 % EtOAc in hexanes) to give **5.29** (3.20 g, 79%) as thick light-yellow oil. R_f = 0.55, 30% EtOAc in hexanes. ^{1}H NMR (300 MHz, $CDCl_3$): δ 7.29 – 7.16 (m, 5H), 6.92 (t, *J* = 10.9 Hz, 1H), 4.20 (q, *J* = 7.1 Hz, 2H), 1.26 (t, *J* = 7.1 Hz, 3H) *Note: the two exchangeable NH_2 protons are missing*. ^{13}C NMR (75 MHz, $CDCl_3$): 169.4, 149.6, 138.6, 129.4, 127.9, 125.6, 101.0, 59.4, 14.6. IR (neat): 3477, 3340, 2926, 1665, 1627, 1372, 1202, 1028, 700 cm^{-1}. HRMS (APPI+): calc'd for $C_{11}H_{14}NO_2$ $[M+H]^+$ 192.1019, found 192.1017.

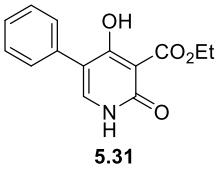
5.31

Sodium metal (240.0 mg, 10.45 mmol, 2.0 equiv) was added to a round-bottom flask containing anhydrous EtOH (3.7 mL). Upon complete consumption of the sodium metal, a solution of diethyl malonate (1.60 mL, 10.5 mmol, 2.0 equiv) in toluene (0.58 mL) was added. The resulting solution was stirred at room temperature for 1 h, followed by the addition of **5.29** (1.00 g, 5.23 mmol, 1.0 equiv) in toluene (1.6 mL). The solution was then heated at reflux for 18 h, during which a yellow precipitate formed, providing a cloudy yellow suspension. The solution was cooled to 0 °C, diluted with water (50 mL), and stirred for 30 min. The phases were separated, and the aqueous layer was washed with toluene (50 mL). Ethanol was removed from the aqueous layer *in vacuo*, and the remainder was acidified with aqueous HCl (conc.). The precipitate obtained was filtered, washed with water, and dried to

provide a yellow solid which was purified by recrystallization in MeOH to give **5.31** (544 mg, 40%) as a shiny yellow crystalline solid. M. P. = 219-221 °C. ^{1}H NMR (300 MHz, DMSO-*d6*): δ 13.69 (s, 1H), 11.73 (s, 1H), 7.60 (s, 1H), 7.47 – 7.32 (m, 5H), 4.34 (q, *J* = 7.1 Hz, 2H), 1.31 (t, *J* = 7.1 Hz, 3H). ^{13}C NMR (75 MHz, DMSO-*d6*): 172.7, 172.4, 159.7, 140.8, 133.7, 129.5, 128.7, 127.6, 112.0, 98.8, 61.7, 14.6. IR (neat): 2972, 1636, 1416, 1328, 1199, 1072, 885, 809, 767, 693 cm^{-1}. HRMS (APPI+): calc'd for $C_{14}H_{14}NO_4$ $[M+H]^+$ 260.0918, found 260.0920.

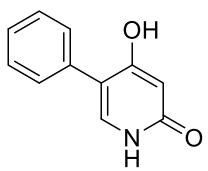

5.15

A 35 mL pressure tube equipped with a magnetic stirrer was charged with pyridone-3-carboxylate **5.31** (490 mg, 1.89 mmol). An aqueous solution of 1 M HCl (25 mL) was added to the reaction vessel and sealed. The heterogeneous mixture was stirred at 120 °C (oil bath heating) for 72 h, during which the solid starting material completely dissolved to provide a light yellow solution. The reaction mixture was cooled and then transferred to a 50 mL beaker and neutralized with an aqueous NaOH solution until pH 4. The precipitate obtained was filtered, washed with water, and dried to yield **5.15 (**310 mg, 88%) as a white solid. M.P. = 286-289 °C. ^{1}H NMR (300 MHz, DMSO-*d6*): δ 11.21 (s, 1H), 10.86 (s, 1H), 7.44 – 7.24 (m, 5H), 5.70 (s, 1H), 2.50 (dt, J = 3.5, 1.7 Hz, 1H). ^{13}C NMR (75 MHz, DMSO-*d6*): δ 165.7, 163.8, 135.3, 135.0, 129.2, 128.5, 127.0, 113.3, 99.1. IR (neat): 2789, 1605, 1436, 1367, 1217, 880, 846, 763, 695 cm^{-1}. HRMS (APPI+): calc'd for $C_{11}H_9NO_2$ $[M]^+$ 187.0633, found 187.0627.

To a suspension of pyridone **5.15** (70 mg, 0.37 mmol, 1.0 equiv) and toluene (3.7 mL) in a 10 mL micro-reaction vessel was added ethylenediamine diacetate (EDDA) (13 mg, 0.072 mmol, 20 mol%) and (*E*,*E*)-2,4-dimethylhexa-2,4-dienal **5.23** (46 mg, 0.37 mmol, 1.0 equiv) subsequently. The reaction vessel was sealed, and the heterogenous mixture was heated at 120 °C (microwave heating) for 45 min. Toluene was then removed for the homogenous solution *in vacuo*, and the

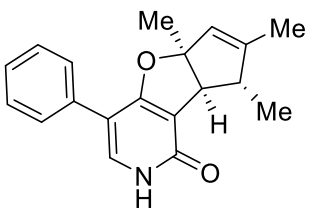

5.1

crude reaction mixture was purified by column chromatography (3-7 % MeOH in CH_2Cl_2), to give a 12:1 mixture of citridone A **5.1**: isomer **5.40** (70 mg, 65%) as light yellow crystalline solid. Pure citridone A was obtained by the following two step procedure.

Scheme 5.14: Two-step approach for the synthesis of *rac*-citridone A **5.1.**

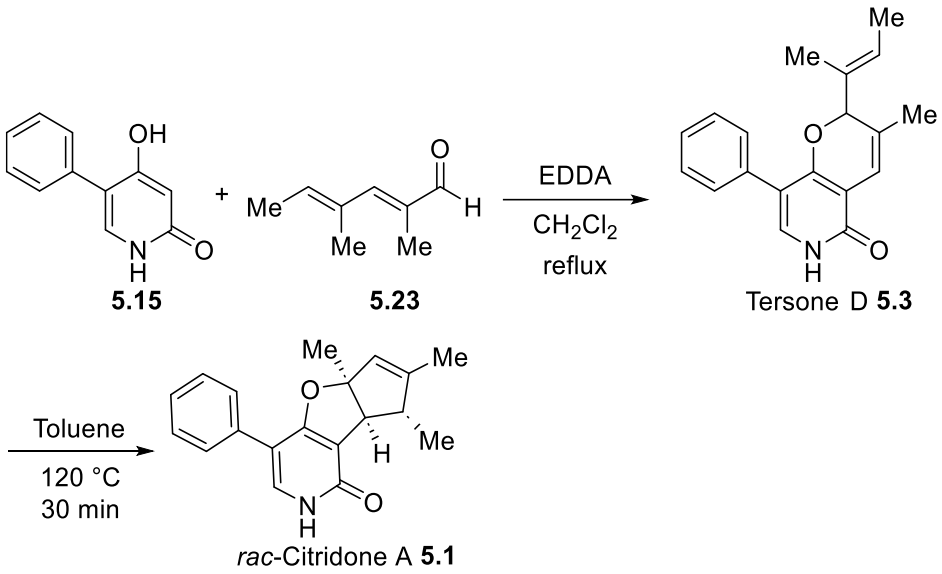

Step 1: To a suspension of pyridone **5.15** (0.200 g, 1.07 mmol, 1.0 equiv) and CH_2Cl_2 (5.4 mL) in a 100 mL round-bottom flask was added ethylenediamine diacetate (EDDA) (38 mg, 0.21 mmol, 20 mol%) followed by (*E*,*E*)-2,4-Dimethylhexa-2,4-dienal **5.23** (133 mg, 1.07 mmol, 1.0 equiv). The heterogenous mixture was heated at reflux (oil bath heating) for 48 h. Solvent was then removed on *vacuo*, and the mixture was flushed through a plug of silica using 10 % MeOH in CH_2Cl_2, to give a 5:1 mixture of tersone D **5.3**: citridone A **5.1** (242 mg, 77% overall yield) as light-yellow solid foam which was subjected to next step without any further purification. *NOTE:* tersone D was separated by preparative TLC (5% hexanes in EtOAc, developed three times sequentially) for characterization. R_f = 0.05, 5% hexanes in EtOAc. ^{1}H NMR (300 MHz, $CDCl_3$):

δ 7.38 – 7.28 (5H, m), 7.24 (1H, s), 6.58 (1H, s), 5.56 (1H, q, *J* = 6.5 Hz), 5.16 (1H, s), 1.71 (3H, s), 1.66 – 1.62 (6H, m). ^{13}C NMR (75 MHz, $CDCl_3$): δ 162.4, 159.2, 133.9, 132.6 (2C), 129.0, 128.4, 127.9, 127.4, 125.0, 114.9, 114.6, 107.2, 86.3, 19.6, 13.4, 11.9. IR (neat): 2931, 2252, 1639, 1426, 1214, 951, 867, 766, 700 cm^{-1}. HRMS (APPI+): calc'd for $C_{19}H_{19}NO_2$ $[M]^+$ 293.1416, found 293.1435.

Step 2: The product mixture from step 1 was dissolved in toluene (4.1 mL) and the resulting yellow solution was transferred to sealed reaction vial and heated at 120 °C (oil bath heating) for 30 min. After a change in color from yellow solution to dark orange, toluene was then removed *in vacuo*, the crude reaction mixture was purified by column chromatography (3-7 % MeOH in CH_2Cl_2), to give a pure citridone A **5.1** (150 mg, 48%) as light-yellow crystalline solid. R_f = 0.50, 10% MeOH in CH_2Cl_2. M.P. = 169 – 171 °C. ^{1}H NMR (300 MHz, $CDCl_3$): δ 7.53 – 7.51 (2H, m), 7.44 (1H, s), 7.39 – 7.36 (2H, m), 7.30 – 7.27 (1H, m), 5.38 (1H, t, *J* = 1.5 Hz), 3.26 (1H, d, *J* = 1.9 Hz), 2.90 (1H, bq, *J* = 7.2 Hz), 1.72 (3H, bs), 1.65 (3H, s), 1.29 (3H, d, *J* = 7.2 Hz). ^{13}C NMR (75 MHz, $CDCl_3$): δ 164.9, 163.1, 150.4, 134.0, 133.6, 128.5, 127.5, 127.1, 126.3, 113.4, 111.1, 103.8, 56.6, 49.0, 26.3, 20.3, 14.8 (Note: for this compound, the reference signal was set to 77.0 ppm). IR (neat): 2961, 1645, 2240, 1210, 1028, 1389, 824, 760, 696 cm^{-1}. HRMS (APPI+): calc'd for $C_{19}H_{20}NO_2$ $[M+H]^+$ 294.1488, found 294.1489.

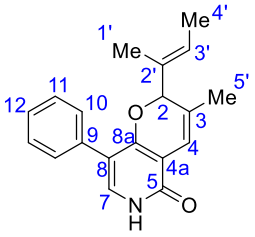

Tersone D **5.3**

	Isolated (CD_3OD)[1]	**Biosynthesized (Lit.) ($CDCl_3$)[2]**	**Synthetic (this work) ($CDCl_3$)**
C-2	87.3	86.3	86.3
C-3	129.7	127.9	127.9
C-4	115.1	114.6	114.6
C-4a	108.3	107.2	107.2
C-5	162.5	162.4	162.4
C-7	134.5	132.6	132.6
C-8	116.6	114.9	114.9
C-8a	160.8	159.2	159.2
C-9	134.9	134.0	133.9
C-10	129.3	129.0	129.0
C-11	130.0	128.4	128.4
C-12	128.5	127.4	127.4
C-1'	11.7	11.9	11.9
C-2'	133.9	132.6	132.6
C-3'	126.2	125.0	125.0
C-4'	13.3	13.4	13.4
C-5'	19.6	19.6	19.6

^{1}H chemical shifts (ppm)

	Isolated (CD_3OD)[1]	**Biosynthesized (Lit.) ($CDCl_3$)[2]**	**Synthetic (this work) ($CDCl_3$)**
C-2	5.23 (1H, s)	5.15 (1H, s)	5.16 (1H, s)
C-4	6.50 (1H, s)	6.58 (1H, s)	6.58 (1H, s)
C-7	7.21 (1H, s)	7.23 (1H, s)	7.24 (1H, s)
C-10	7.36 (2H, overlapped)	7.37 (2H, m)	δ 7.38 – 7.28 (5H, m)
C-11	7.36 (2H, overlapped)	7.37 (2H, m)	
C-12	7.30 (1H, t, *J* = 7.5)	7.30 (1H, m)	
C-1'	1.64 (3H, overlapped)	1.65 (3H, s)	1.64 (3H, overlapped)
C-3'	5.61 (1H, q, *J* = 6.2)	5.5 (1H, q, *J* = 6.4)	5.56 (1H, q, *J* = 6.5 Hz)
C-4'	1.64 (3H, overlapped)	1.63 (3H, d, *J* = 6.8)	1.64 (3H, overlapped)
C-5'	1.72 (3H, s)	1.70 (3H, s)	1.71 (3H, s)

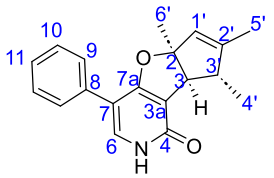

rac-Citridone A **5.1**

^{13}C chemical shifts (ppm) ($CDCl_3$)

	Isolated[3]	Synthetic (this work)	Synthetic (Lit.)[4]
C-2	104.1	103.8	103.8
C-3	56.4	56.6	56.7
C-3a	113.5	113.4	113.4
C-4	162.4	163.1	163.1
C-6	133.8	133.6	133.6
C-7	111.7	111.1	111.1
C-7a	165.2	164.9	164.9
C-8	133.2	134.0	133.9
C-9	127.5	127.5	127.6
C-10	128.5	128.5	128.5
C-11	127.3	127.1	127.2
C-1'	126.2	126.3	126.3
C-2'	150.5	150.4	150.5
C-3'	49.0	49.0	49.0
C-4'	20.2	20.3	20.3
C-5'	14.7	14.8	14.8
C-6'	26.2	26.3	26.3

Note: *The reference signal for ^{13}C NMR of the natural product was set to 77.0*

^{1}H chemical shifts (ppm) ($CDCl_3$)

	Isolated[3]	Synthetic (this work)	Synthetic (Lit.)[4]
C-3	3.26 (1H, d, *J* = 2.0 Hz)	3.26 (1H, d, *J* = 1.9 Hz)	3.27 (d, J = 1.7 Hz, 1H),
C-6	7.45 (1H, s)	7.44 (1H, s)	7.45 (s, 1H)
C-9	7.52 (2H, m)	7.53-7.51 (2H, m)	7.55-7.51 (m, 2H)
C-10	7.38 (2H, m)	7.39-7.36 (2H, m)	7.42-7.36 (m, 2H)
C-11	7.29 (1H, m)	7.30-7.27 (1H, m)	7.33-7.27 (m, 1H)
C-1'	5.38 (1H, t, *J* = 1.5 Hz)	5.38 (1H, t, *J* = 1.5 Hz)	5.39 (dq, J = 1.7 Hz, 1H),
C-3'	2.90 (1H, dq, *J* = 2.0, 7.0 Hz)	2.90 (1H, bq, *J* = 7.3 Hz)	2.91 (bq, J = 7.2 Hz, 1H)
C-4'	1.29 (3H, d, *J* = 7.0 Hz)	1.29 (3H, d, *J* = 7.2 Hz)	1.30 (d, J = 7.9 Hz, 3H)
C-5'	1.72 (3H, br.s)	1.72 (3H, bs)	1.73 (s, 3H)
C-6'	1.65 (3H, s)	1.65 (3H, s)	1.65 (s, 3H)

1.36 References

1. (a) Eschenbrenner-Lux, V.; Waldmann, H.; Kumar, K. *Domino reactions in library synthesis*. In Domino reactions: Concept for efficient organic synthesis; Tietze, L. F., Ed.; Wiley: Hoboken, NJ, 2014; pp 497– 522. (b) Duefert, S.-C.; Hierold, J.; Tietze, L. F *Domino reactions in total synthesis of Natural Products*. In Domino reactions: Concept for efficient organic synthesis; Tietze, L. F., Ed.; Wiley: Hoboken, NJ, 2014; pp 523– 578.
2. (a) Fukuda, T.; Tomoda, H.; Õmura, S. *J. Antibiot.* **2005**, *58*, 315. (b) Fukuda, T.; Yamaguchi, Y.; Masuma, R.; Tomoda, H.; Õmura, S. *J. Antibiot.* **2005**, *58*, 309.
3. Fukuda, T.; Shimoyama, K.; Nagamitsu, T.; Tomoda, H. *J. Antibiot.* **2014**, *67*, 445.
4. Yan, T.; Ding, W.; Liu, H.; Wang, P.-M.; Zheng, D.; Xu, J. *Tetrahedron Lett.* **2020**, *61*, 151843.
5. Ernst, J. T.; Thompson, P. A.; Nilewski, C.; Sprengeler, P. A.; Sperry, S.; Packard, G.; Michels, T.; Xiang, A.; Tran, C.; Wegerski, C. J.; Eam, B.; Young, N. P.; Fish, S.; Chen, J.; Howard, H.; Staunton, J.; Molter, J.; Clarine, J.; Nevarez, A.; Chiang, G. G.; Appleman, J. R.; Webster, K. R.; Reich, S. H. Design of development candidate eFT226, a first in class inhibitor of eukaryotic initiation factor 4A RNA helicase. *J. Med. Chem.* **2020**, *63*, 5879.
6. Gordon, D. E.; Jang, G. M.; Bouhaddou, M.; Xu, J.; Obernier, K.; White, K. M.; O'Meara, M. J.; Rezelj, V. V.; Guo, J. Z.; Swaney, D. L.; Tummino, T. A.; Hüttenhain, R.; Kaake, R. M.; Richards, A. L.; Tutuncuoglu, B.; Foussard, H.; Batra, J.; Haas, K.; Modak, M.; Kim, M.; Haas, P.; Polacco, B. J.; Braberg, H.; Fabius, J. M.; Eckhardt, M.; Soucheray, M.; Bennett, M. J.; Cakir, M.; McGregor, M. J.; Li, Q.; Meyer, B.; Roesch, F.; Vallet, T.; Mac Kain, A.; Miorin, L.; Moreno, E.; Naing, Z. Z. C.; Zhou, Y.; Peng, S.; Shi, Y.; Zhang, Z.; Shen, W.; Kirby, I. T.; Melnyk, J. E.; Chorba, J. S.; Lou, K.; Dai, S. A.;

BarrioHernandez, I.; Memon, D.; Hernandez-Armenta, C.; Lyu, J.; Mathy, C. J. P.; Perica, T.; Pilla, K. B.; Ganesan, S. J.; Saltzberg, D. J.; Rakesh, R.; Liu, X.; Rosenthal, S. B.; Calviello, L.; Venkataramanan, S.; LiboyLugo, J.; Lin, Y.; Huang, X.-P.; Liu, Y.; Wankowicz, S. A.; Bohn, M.; Safari, M.; Ugur, F. S.; Koh, C.; Savar, N. S.; Tran, Q. D.; Shengjuler, D.; Fletcher, S. J.; O'Neal, M. C.; Cai, Y.; Chang, J. C. J.; Broadhurst, D. J.; Klippsten, S.; Sharp, P. P.; Wenzell, N. A.; Kuzuoglu-Ozturk, D.; Wang, H.-Y.; Trenker, R.; Young, J. M.; Cavero, D. A.; Hiatt, J.; Roth, T. L.; Rathore, U.; Subramanian, A.; Noack, J.; Hubert, M.; Stroud, R. M.; Frankel, A. D.; Rosenberg, O. S.; Verba, K. A.; Agard, D. A.; Ott, M.; Emerman, M.; Jura, N.; von Zastrow, M.; Verdin, E.; Ashworth, A.; Schwartz, O.; d'Enfert, C.; Mukherjee, S.; Jacobson, M.; Malik, H. S.; Fujimori, D. G.; Ideker, T.; Craik, C. S.; Floor, S. N.; Fraser, J. S.; Gross, J. D.; Sali, A.; Roth, B. L.; Ruggero, D.; Taunton, J.; Kortemme, T.; Beltrao, P.; Vignuzzi, M.; García-Sastre, A.; Shokat, K. M.; Shoichet, B. K.; Krogan, N. J. A SARS-CoV-2 protein interaction map reveals targets for drug repurposing. *Nature* **2020**, *583*, 459.

7. Chen, S.-C.; Liu, Z.-M.; Tan, H.-B.; Chen, Y.-C.; Li, S.-N.; Li, H.-H.; Guo, H.; Zhu, S.; Liu, H.-X.; Zhang, W.-M. *Mar. Drugs* **2019**, *17*, 394.
8. Miyagawa, T.; Nagai, K.; Yamada, A.; Sugihara, Y.; Fukuda, T.; Fukuda, T.; Uchida, R.; Tomoda, H.; Õ mura, S.; Nagamitsu, T. *Org. Lett.* **2011**, *13*, 1158.
9. Fotiadou, A. D.; Zografos, A. L. *Org. Lett.* **2011**, *13*, 4592.
10. For two developed methodologies to access cyclopenta[*b*]furopyridine derivatives, see: (a) Nilewski, C.; Michels, T. D.; Xiang, A. X.; Packard, G. K.; Sprengeler, P. A.; Eam, B.; Fish, S.; Thompson, P. A.; Wegerski, C. J.; Ernst, J. T.; Reich, S. H. *Org. Lett.* **2020**, *22*, 6257. (b) Katsina, T.; Papoulidou, K. E.; Zografos, A. L. *Org. Lett.* **2019**, *21*, 8110.

11. Riveira, M. J.; Marsili, L. A.; Mischne, M. P. *Org. Biomol. Chem.* **2017**, *15*, 9255. (b) Riveira, M. J.; Gayathri, C.; Navarro-Vázquez, A.; Tsarevsky, N. V.; Gil, R. R.; Mischne, M. P. *Org. Biomol. Chem.* **2011**, *9*, 3170.
12. Riveira, M. J.; Mischne, M. P. *Chem. Eur. J.* **2012**, *18*, 2382.
13. Snider, B. B.; Lu, Q. *J. Org. Chem.* **1996**, *61*, 2839.
14. Streef, J. W.; Den Hertog, H. J.; van der Plas, H. C. *J. Heterocycl. Chem.* **1985**, *22*, 985.
15. Fotiadou, A. D.; Zografos, A. L. *Org. Lett.* **2012**, *14*, 5664.
16. Riveira, M.J.; Mischne, M.P. *Synth. Commun.* **2013**, *43*, 208.
17. Riveira, M. J.; Mischne, M. P. *J. Org. Chem.* **2014**, *79*, 8244.

1.37 Appendix 4

^{1}H, ^{13}C NMR Spectra for Chapter 5

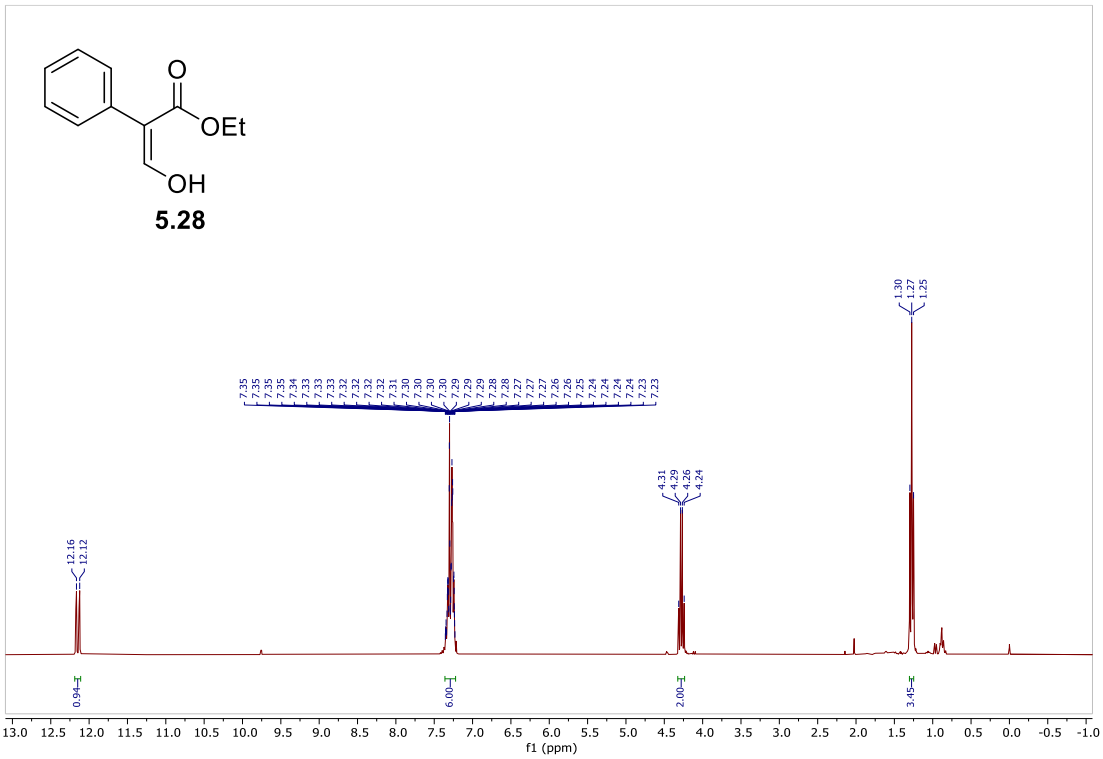

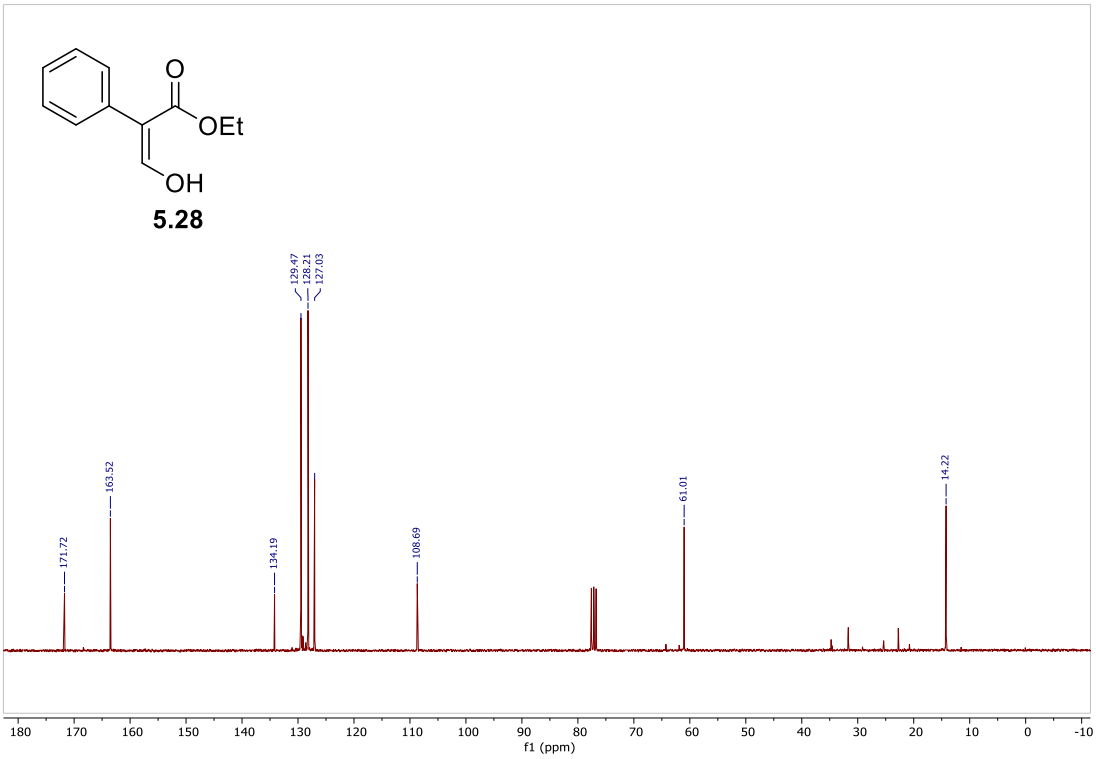

^{1}H NMR (300 MHz, $CDCl_3$) and ^{13}C NMR (75 MHz, $CDCl_3$) of compound **5.28**

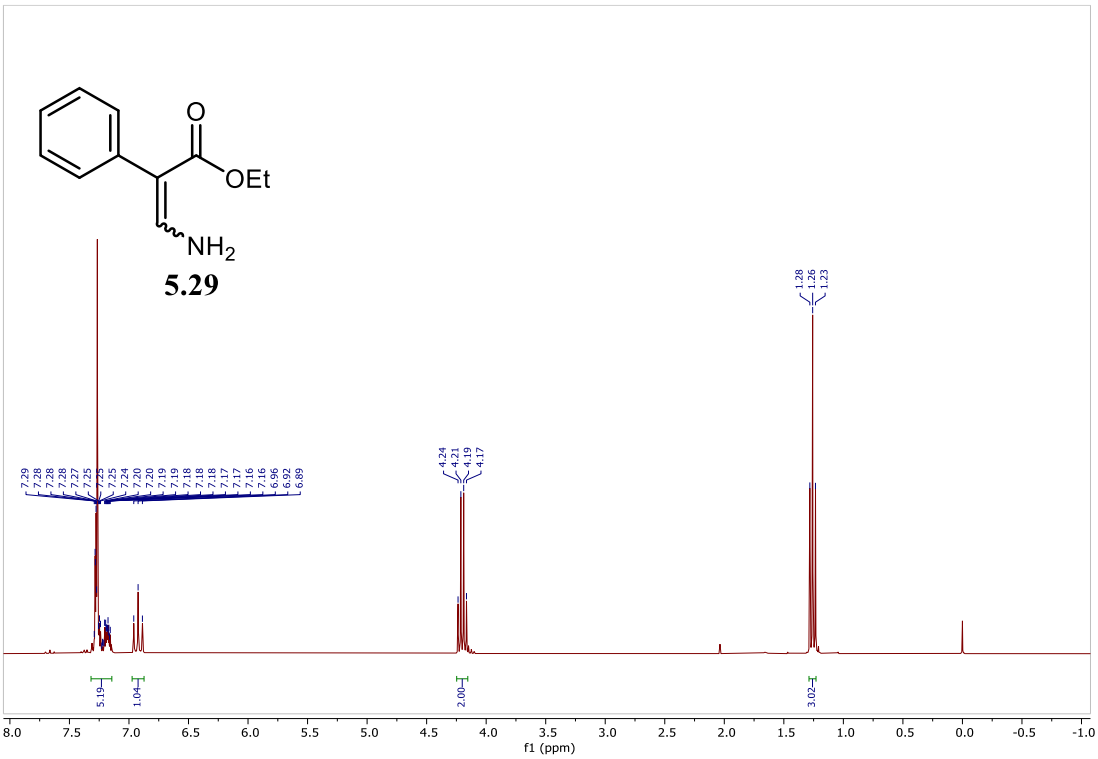

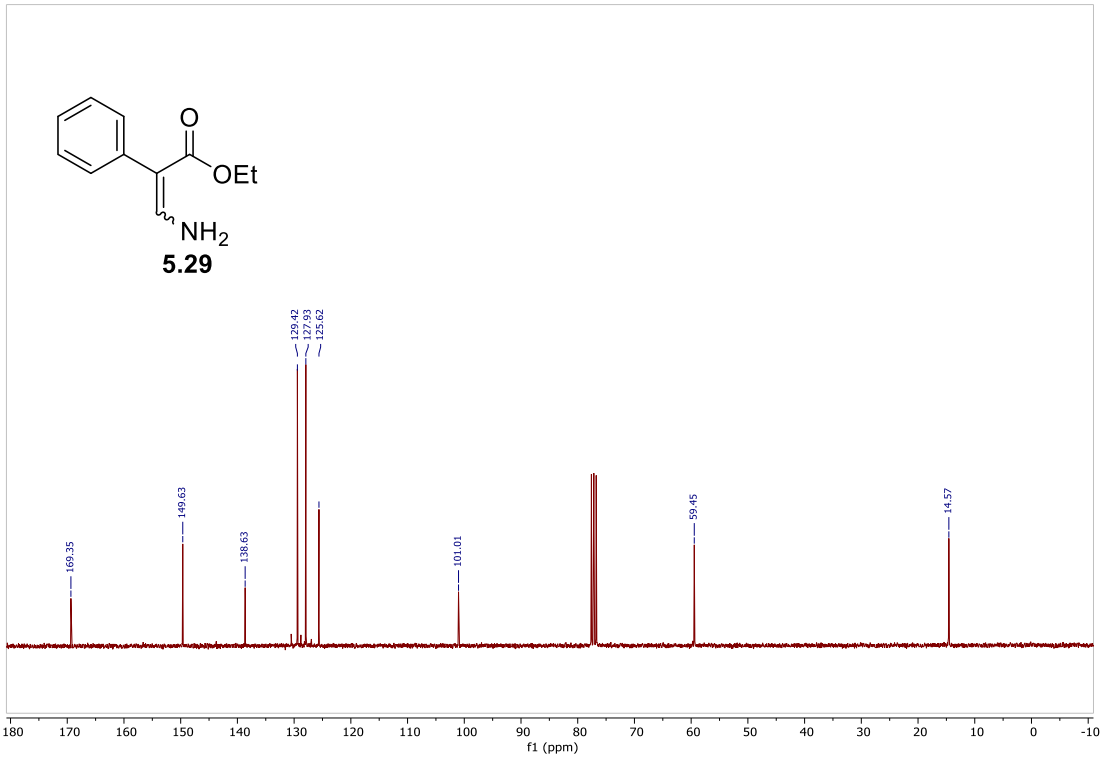

^{1}H NMR (300 MHz, $CDCl_3$) and ^{13}C NMR (75 MHz, $CDCl_3$) of compound **5.29**

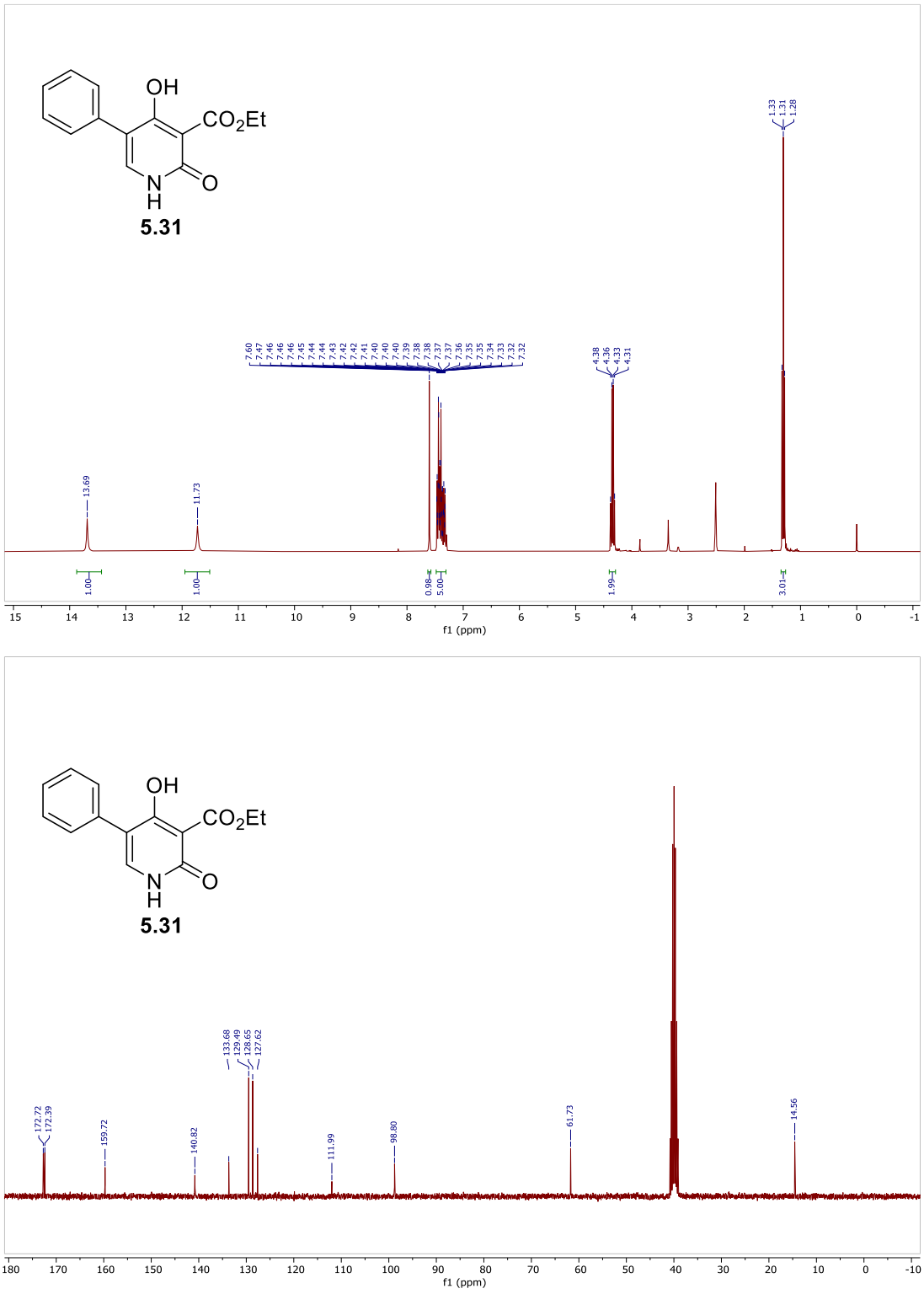

^{1}H NMR (300 MHz, $CDCl_3$) and ^{13}C NMR (75 MHz, $CDCl_3$) of compound **5.31**

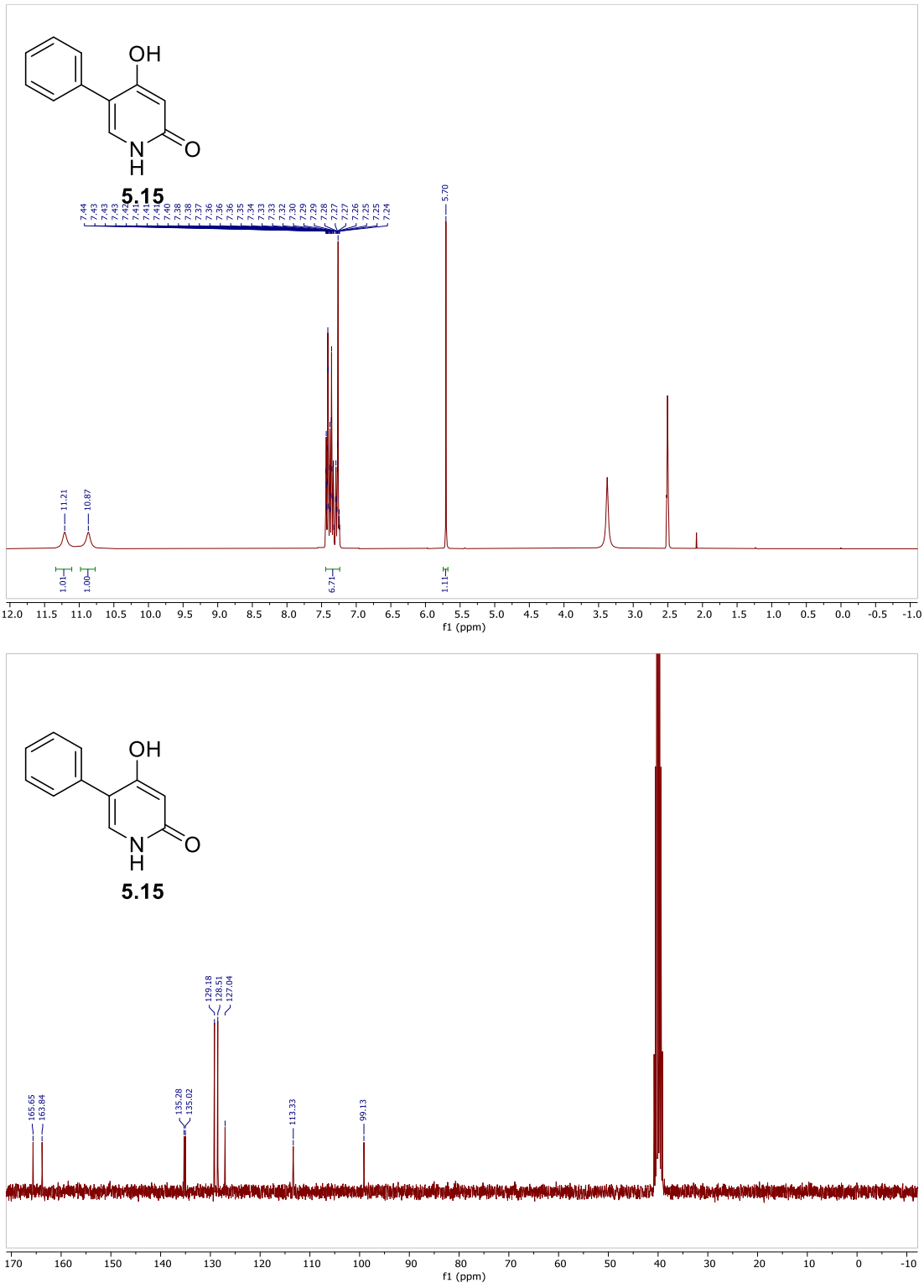

^{1}H NMR (300 MHz, $CDCl_3$) and ^{13}C NMR (75 MHz, $CDCl_3$) of compound **5.15**

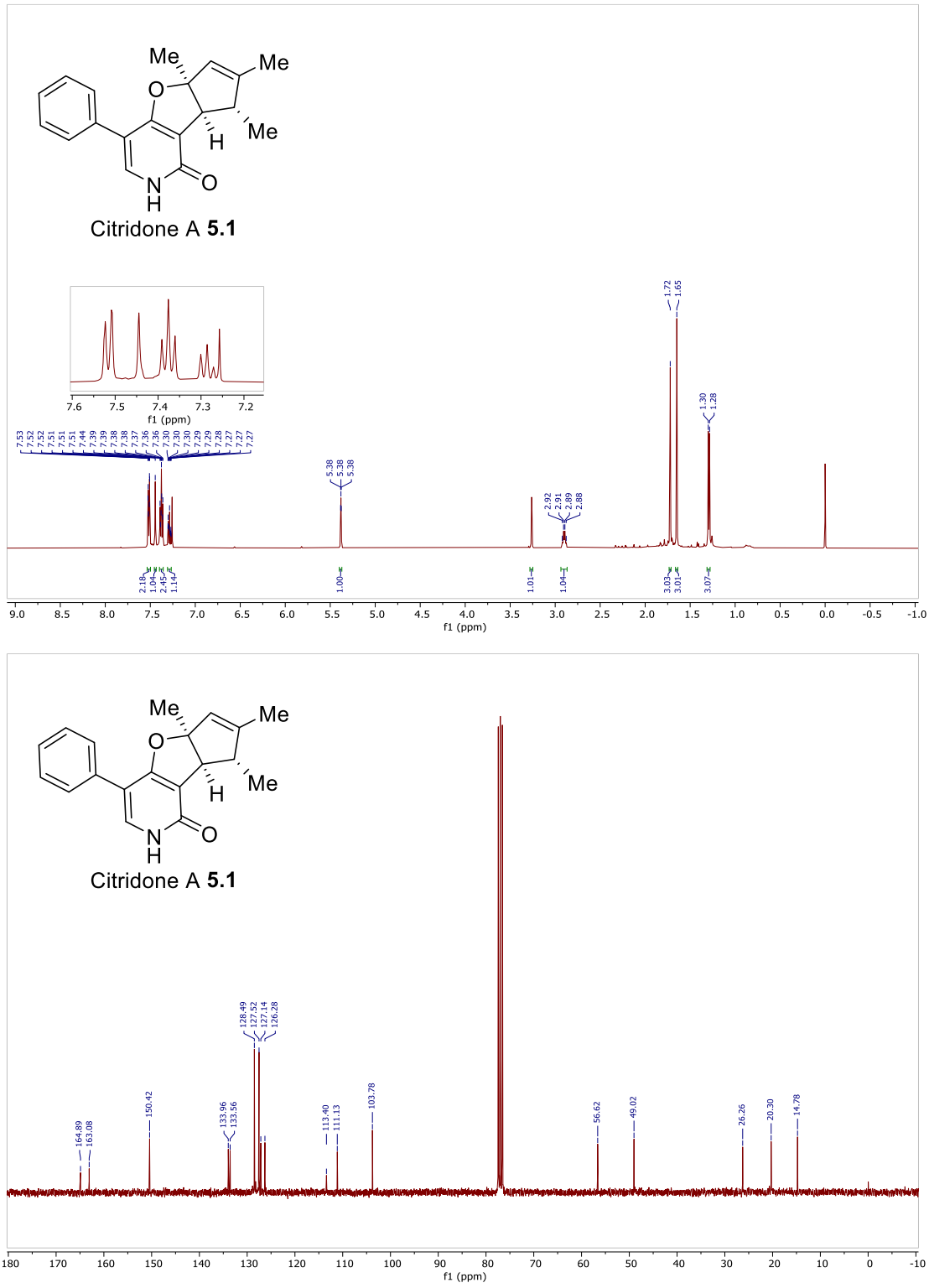

^{1}H NMR (300 MHz, $CDCl_3$) and ^{13}C NMR (75 MHz, $CDCl_3$) of compound **5.1**